

# Hydrocarbyl Ligand Transformations on Heterobimetallic Complexes

Vincent Ritleng and Michael J. Chetcuti\*

Laboratoire de Chimie Organométallique Appliquée, UMR CNRS 7509, ECPM, Université Louis Pasteur, 25 rue Becquerel, 67087 Strasbourg Cédex 2, France

Received July 31, 2006

## Contents

1. Introduction	798	3.1.1. Alkyl–Carbonyl Coupling without External CO Addition	809
1.1. General Introduction and Layout: What Is Covered and What Is Not	798	3.1.2. Alkyl–Carbonyl Coupling with External CO Addition	810
1.2. Pertinent Review Articles	799	3.1.3. Couplings of Metallacyclic Groups with Carbonyl Ligands	814
1.3. Manuscript Organization	799	3.1.4. Alkyl–Isocyanide and –Cyanide Coupling	814
2. Hydrocarbyl Bond Formation or Cleavage Accompanied by Heterobimetallic Complex Formation	800	3.1.5. Other Hydrocarbyl Group Couplings with Carbonyl Groups	816
2.1. Carbon–Carbon Coupling Reactions Accompanied by Heterobimetallic Complex Formation	800	3.2. Carbyne–Ligand Coupling	817
2.1.1. Carbyne–Carbonyl Coupling	800	3.2.1. Carbyne–Carbyne Coupling	817
2.1.2. Carbyne–Alkyl Coupling	801	3.2.2. Carbyne–Alkyl Coupling	817
2.1.3. Carbyne–Carbene Coupling	801	3.2.3. Carbyne–Carbonyl Coupling	817
2.1.4. Alkyne–Carbonyl Coupling	801	3.2.4. Carbyne–Carbene Coupling	818
2.1.5. Alkyne–Alkyne Coupling	802	3.2.5. Carbyne–Alkyne Coupling	819
2.1.6. Alkyl–Carbonyl Coupling	803	3.2.6. Carbyne–Alkene Coupling	821
2.1.7. Multiple Carbene–Carbonyl Coupling	803	3.3. Carbene– and Vinylidene–Ligand Coupling	821
2.2. Carbon–Carbon Bond Cleavage Reactions Accompanied by Heterobimetallic Complex Formation	804	3.3.1. Carbene–Carbonyl Coupling	821
2.3. Carbon–Hydrogen Bond Formation	804	3.3.2. Carbene–Carbene Coupling	821
2.3.1. Hydrogen–Alkyl Coupling	804	3.3.3. Carbene–Alkyne Coupling	822
2.3.2. Hydrogen–Alkene Coupling	805	3.3.4. Carbene–Alkene and –Allene Coupling	823
2.3.3. Hydrogen–Vinylidene Coupling	805	3.3.5. Vinylidene–Alkyl Coupling	824
2.3.4. Hydrogen–Carbyne Coupling	806	3.4. Alkyne–Ligand Coupling	824
2.3.5. Hydrogen–Alkenyl Coupling	806	3.4.1. Alkyne–Carbonyl Coupling	824
2.3.6. Hydrogen–Alkynyl Coupling	806	3.4.2. Alkyne–Acyl Coupling	825
2.3.7. Hydrogen– $\pi$ -Allyl Coupling	806	3.4.3. Alkyne–Alkyl Coupling	826
2.4. Carbon–Hydrogen Bond Cleavage (C–H Activation) Accompanied by Heterobimetallic Complex Formation	807	3.4.4. Alkyne–Alkyne Coupling	826
2.4.1. Cleavage of Carbon(sp)– and Carbon(sp <sup>2</sup> )–Hydrogen Bonds of Coordinated Alkenes and Alkynes	807	3.4.5. Alkyne–Vinyl Coupling	828
2.4.2. Cleavage of Carbon(sp <sup>2</sup> )–Hydrogen Bonds of Phenyl and Cyclopentadienyl Groups	807	3.4.6. Alkyne–Alkene Coupling	828
2.4.3. Cleavage of Carbon(sp <sup>3</sup> )–Hydrogen Bonds	807	3.5. Alkene–Ligand Coupling	830
3. Carbon–Carbon Bond Formation on Preformed Heterobimetallic Frameworks	808	3.5.1. Alkene–Carbonyl Coupling	830
3.1. Alkyl–Carbonyl (“CO Insertion”), –Isocyanide, and –Cyanide Coupling	808	3.5.2. Alkene–Acyl Coupling	830
		3.5.3. Alkene–Alkyl Coupling	830
		3.5.4. Alkene–Alkene Coupling	830
		3.6. Other Miscellaneous Carbon–Carbon Coupling	831
		4. Carbon–Carbon Bond Cleavage on Preformed Heterobimetallic Frameworks	832
		4.1. Carbon–Carbon Bond Cleavage by Metallacyclic Complex Decarbonylation	833
		4.2. Carbon–Carbon Bond Cleavage by Other Decarbonylation Reactions	833
		5. Carbon–Hydrogen Bond Coupling on Preformed Heterobimetallic Frameworks	834
		5.1. Protonation (H <sup>+</sup> Addition) Reactions	834
		5.1.1. Proton Addition to Carbynes	834
		5.1.2. Proton Addition to Carbenes	834
		5.1.3. Proton Addition to Vinylidenes	836

\* Corresponding author. E-mail: chetcuti@chimie.u-strasbg.fr. Tel: +33 3 90 24 26 31. Fax: +33 3 90 24 26 39.

5.1.4. Proton Addition to Alkynes	836	9. Acknowledgment	854
5.1.5. Proton Addition to Alkynyls	836	10. Addendum	854
5.1.6. Proton Addition to Alkenyls	837	11. References	855
5.1.7. Proton Addition to Alkyls and Acyls	838		
5.1.8. Proton Addition To Generate Heterometal-Bound Carbocations	838		
5.1.9. Other Protonations of Hydrocarbyl Ligands	839		
5.2. Hydride (H <sup>-</sup> ) Addition Reactions	840		
5.2.1. Hydride Addition to Carbynes	840		
5.2.2. Hydride Addition to Alkenyls and Alkynyls	840		
5.2.3. Hydride Addition to Alkenes	841		
5.2.4. Hydride Addition to Carbocations	841		
5.2.5. Other Hydride Additions Leading to Carbon-Hydrogen Bond Formation	841		
5.3. Metal Hydride (M-H) Additions to Hydrocarbyl Ligands	842		
5.3.1. Metal Hydride Additions to Alkynes and Allenes	842		
5.3.2. Metal Hydride Additions to Alkenes and Dienes	844		
5.3.3. Metal Hydride Additions to Alkyls	845		
5.4. Molecular Hydrogen Addition to Hydrocarbyl Ligands	846		
5.4.1. Hydrogen Addition to Alkyls and Acyls	846		
5.4.2. Hydrogen Addition to Alkenes	846		
6. Carbon-Hydrogen Bond Cleavage on Preformed Heterobimetallic Frameworks	847		
6.1. Carbon-Hydrogen Bond Cleavage by Formal Proton (H <sup>+</sup> ) Abstraction	847		
6.1.1. Proton Abstraction from Carbenes	847		
6.1.2. Proton Abstraction from Carbynes	847		
6.1.3. Proton Abstraction from Alkenes	847		
6.1.4. Proton Abstraction from Methyl Groups in Ligands	847		
6.1.5. Proton Abstraction from $\mu$ -dppm Ligands	848		
6.1.6. Proton Abstraction from a $\pi$ -Allylic Group	849		
6.2. Carbon- $\beta$ -Hydrogen Bond Cleavage by Metal-Hydrogen Abstraction	849		
6.3. Carbon-Hydrogen Activation by Heterobimetallic Complexes	849		
6.3.1. Carbon-Hydrogen Activation of C(sp)-H Bonds	849		
6.3.2. Carbon-Hydrogen Activation of C(sp <sup>2</sup> )-H Bonds	849		
6.3.3. Carbon-Hydrogen Activation of C(sp <sup>3</sup> )-H Bonds	850		
6.4. Hydrocarbyl Rearrangement Reactions That Lead to Carbon-Hydrogen Bond Cleavage and Concomitant Carbon-Hydrogen Bond Formation	851		
6.4.1. Hydrocarbyl Rearrangements That Lead to Vinylidenes	851		
6.4.2. Hydrocarbyl Rearrangements That Lead to Alkenyls	851		
6.4.3. Hydrocarbyl Rearrangements That Lead to Carbenes	852		
6.4.4. Hydrogen Scrambling and Hydrogen Exchange Reactions	852		
6.4.5. Other Hydrocarbyl Rearrangements	852		
6.5. Other Carbon-Hydrogen Cleavage Reactions	853		
7. Conclusion	853		
8. List of Abbreviations	854		

## 1. Introduction

### 1.1. General Introduction and Layout: What Is Covered and What Is Not

The advantages of using two different metals to enhance some desired property has been recognized by different cultures dating from around 1500 BC in Europe to much earlier (as early as 4000 or 4500 BC) in Asia. While the various independent discoveries of alloying copper and tin to form bronze remain ill-defined in time, the achievements are considered a milestone in human history, as they globally mark the generally accepted transformation of *Homo sapiens* from the Stone Age to the Bronze Age. The current goal of synthetic chemists to enhance certain properties by combining two different metals remains somewhat similar to the probably serendipitous discoveries of more than four thousand years ago, though the level of sophistication has improved.

Heterobimetallic complexes form a large subset of bimetallic complexes, and their chemistry has been developed with the idea of exploiting synergistic effects between the two metal centers. The coordination of hydrocarbyl ligands and their activation and reactivity toward carbon-hydrogen and carbon-carbon bond formation and cleavage has clear implications for stoichiometric and catalytic chemistry. It has long been established, for example, that heterogeneous catalysts, made up of a combination of two or more metals, often have significantly enhanced catalytic properties.<sup>1,2</sup> The driving force behind much research in heterobimetallic chemistry has been molecular activation, especially activation that is unique to heterobimetallic complexes.<sup>3,4</sup> Owing to their asymmetry, their polarity, and the different electronic and steric requirements of the two metal centers, heterobimetallic complexes are usually more reactive than their homobimetallic congeners. Early-late transition metal combinations, in particular, are expected to enhance reactivity differences between the metals and have been subjected to much study, because chemical reactivity differences in hard-soft character and in coordination number and electronic requirements are more significant. Many groups have attempted to take advantage of the oxophilicity of the early metal for oxygen abstraction reactions or for stabilizing acyl complexes.

This review targets the transformation and reactions of hydrocarbyl ligands on transition metal heterobimetallic templates, though some transition metal-main group metal heterometallic bonds on which these transformations take place are also targeted. It covers carbon-carbon and carbon-hydrogen bond formation or bond rupture mediated by these heterobimetallic complexes. When possible, reactions effected by heterobimetallic species are compared and contrasted with those of related homobimetallic species, though often such data are lacking. Simple hydrocarbyl or alkyl ligand migrations from one metal to another are not discussed here, since they do not involve the creation or the breakage of C-C or C-H bonds. Nor, in most cases, are P-C, P-H or Si-H, N-H, or O-H activation reactions included, unless carbon or hydrogen atoms are transferred to a hydrocarbyl ligand. The syntheses of heterobimetallic complexes are not explicitly covered, except when a hydrocarbyl ligand also



Dr. Ritteng was born in Strasbourg, France, in 1974. He received his Ph.D. from the Université Louis Pasteur (Strasbourg) in 2001 under the supervision of Dr. Michel Pfeffer. He then joined the Massachusetts Institute of Technology (Cambridge, MA) where he was a postdoctoral associate of Prof. Richard R. Schrock (2001–2003). After a second postdoctoral stay in a joint team with Prof. Ben L. Feringa and Prof. Johannes G. De Vries at the Rijksuniversiteit Groningen (The Netherlands) in 2004, he was appointed Maître de Conférences at the Ecole Européenne de Chimie, Polymères et Matériaux of the Université Louis Pasteur where he works in the group of Prof. Chetcuti. His current Research interests involve the activation of small molecules by heterobimetallic complexes.



Professor Chetcuti graduated with a Ph.D. at the University of Bristol (U.K.) with Professor F. Gordon A. Stone FRS in 1980 and then spent 3 years with Professor Malcolm H. Chisholm, at Indiana University, as a postdoctoral researcher. He accepted a position of Assistant Professor at the University of Notre Dame (Indiana) in 1984. There he established his own group and carried out research on the reactions of small ligands with heterobimetallic complexes. After promotion and tenure in 1991, and a sabbatical year at the University of California, Berkeley, Professor Chetcuti moved to France in 1999. Since 2002, he has been a professor of chemistry at the European School of Chemistry, Polymers and Materials (ECPM), which is part of the Université Louis Pasteur, in Strasbourg, France. He has authored two chapters in the multivolume *Comprehensive Organometallic Chemistry II*, on Nickel  $\pi$ -Complexes and on Heterobimetallic Complexes.

undergoes a transformation during such a synthesis. Reactions that involve heteropolynuclear molecules (metal clusters) are omitted. In addition, hydrocarbyl transformations on heterobimetallic species in which there is no metal–metal bonding or no other obvious interactions between the two metals are not discussed comprehensively, though when a clear, though indirect, activation effect of one metal on the other is noted, these reactions are mentioned. This topic has never been reviewed this way before, so coverage starts from around 1980 to 2005, though a handful of earlier articles are also discussed when pertinent to later work. Catalytic reactions are not discussed because discussion is focused on

molecular activation and transformations. In addition, in many cases, proof of the intermediacy of a heterobimetallic complex in a catalytic cycle is lacking.

## 1.2. Pertinent Review Articles

Various aspects of the chemistry of heterobimetallic complexes have been surveyed, and this information is summarized here. General reviews of heterobimetallic complexes include some early articles by Bruce<sup>5,6</sup> and by one of the authors of this article.<sup>7</sup> Early–late heterobimetallic complexes are specifically covered in other reviews.<sup>3,4,8</sup> More specialized articles on certain heterobimetallics are available, on Mn–Mo  $\mu$ -(diarylphosphino)cyclopentadienyl species<sup>9</sup> and on Ru–Zr complexes.<sup>10</sup> Other review articles on bimetallic complexes that are ligand based and that sometimes include both homo- and heterobimetallic compounds are accounts on bimetallic silicon chemistry,<sup>11</sup> dppm in binuclear complexes,<sup>12</sup> and group 6–group 10 complexes with sulfur ligands<sup>13</sup> and an article on short bite ligands that support homo- and heterodinuclear complexes.<sup>14</sup> Two reviews exist on metal methylene complexes; one contains useful information but is now dated,<sup>15</sup> while a more recent one focuses on  $\mu$ -methylene complexes lacking metal–metal bonds.<sup>16</sup> Review articles that target hydrocarbyl ligands, often on di- and polynuclear centers, include dinuclear and trinuclear allenyl complexes,<sup>17</sup> complexes with bridging four-electron donor unsaturated hydrocarbons, metal-stabilized cations,<sup>18,19</sup> and the organometallic chemistry of vinylidenes and unsaturated carbenes.<sup>20</sup> Reviews that specifically target hydrocarbon and hydrocarbyl ligands include one that focuses on binuclear complexes of these species<sup>21</sup> and another that covers hydrocarbyl ligands in mixed-metal systems.<sup>22</sup> The rich chemistry of metal carbyne complexes and metal–metal multiple bonds as ligands was presented by Stone.<sup>23</sup>

## 1.3. Manuscript Organization

This review starts (section 2) with a discussion of reactions in which a hydrocarbyl ligand is modified when two monometallic fragments are brought together to form a heterobimetallic complex. The four basic reactions, carbon–carbon bond formation and bond breakage, followed by carbon–hydrogen bond formation and bond breakage, are discussed in subsections in section 2 since fewer examples exist. Sections 3–6 discuss the same reactions in the same sequential order but on preformed heterobimetallic complexes, with each section devoted to one class of reactions. Each section is subdivided further, as necessary, depending on the number and kinds of observed reactions. The way each section is subdivided depends on the reported reactions in the literature: bond-forming and bond-breaking reactions are not always complementary or equally well represented.

When representing the formulas of complexes, clarity is the main objective. The metals in heterobimetallic complexes are usually given in alphabetical order, and the ligands are written to show (as much as possible) to which metal they are bonded. The metal is given first, followed by neutral ligands and then anionic ligands, but this order is often not followed if it is not clear what is bonded to what. If no metal–metal bond is shown in a particular complex, it is presumably absent, has not been described in the relevant publication, or both. The two metals A and B bonded together in a heterobimetallic complex are denoted as “metal

A–metal B” while the metals in such a complex without an A–B bond are designated as “metal A/metal B”. Note that the terms carbene and alkylidene, alkylidyne and carbyne, vinyl and alkenyl, and vinylidene and alkenylidene are sometimes used interchangeably for convenience, even though they are not always strictly equivalent.

Within a subsection, reactions are often grouped together based on their similarity, and thus, the order of presentation is not always chronological.

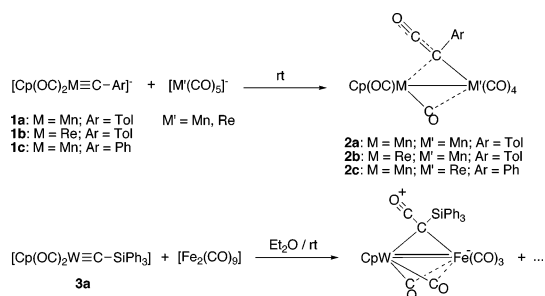
## 2. Hydrocarbyl Bond Formation or Cleavage Accompanied by Heterobimetallic Complex Formation

### 2.1. Carbon–Carbon Coupling Reactions Accompanied by Heterobimetallic Complex Formation

#### 2.1.1. Carbyne–Carbonyl Coupling

Mononuclear alkylidyne complexes have been used to prepare a variety of homo- and heterobimetallic  $\mu_2$ -carbyne complexes by addition of 14 or 16 electron complexes to the mononuclear alkylidyne complex, in a vast body of work pioneered by Stone and his group. When similar reactions are attempted between cationic alkylidyne complexes and carbonyl metalates, there are, in addition, CO–C<sub>carbyne</sub> coupling reactions. More than 25 years ago, Stone’s group discovered that the mononuclear group 7 cationic carbyne complexes  $[\text{Cp}(\text{OC})_2\text{M}\equiv\text{CTol}]^+$  (**1a**, M = Mn; **1b**, M = Re) react with the anion  $[\text{Mn}(\text{CO})_5]^-$  to yield bimetallic species **2a,b**, in which a CO ligand has coupled with the carbyne carbon to give a  $\mu$ -ketenyl ligand.<sup>24</sup> A similar reaction leading to product **2c** was almost simultaneously reported by Fischer and his group, who established the structure of the Mn–Re complex by a single-crystal X-ray diffraction study (Scheme 1).<sup>25</sup>

**Scheme 1. Formation of  $\mu$ -Ketenyl Complexes by Carbyne–Carbonyl Coupling**

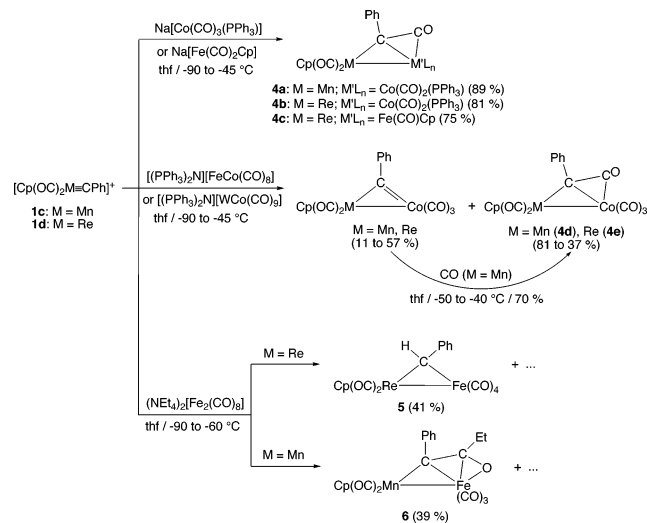


The triphenylsilyl carbyne complex  $[\text{Cp}(\text{OC})_2\text{W}\equiv\text{C}\text{SiPh}_3]$ , **3a** (which is isoelectronic with the group 7 carbyne complexes **1**), undergoes a related reaction with  $[\text{Fe}_2(\text{CO})_9]$ . The product is also a  $\mu$ -ketenyl species, but the authors prefer to regard the compound as existing predominantly in its acylium resonance form, in accord with the short formal Fe=C bond of 2.516(1) Å.<sup>26</sup> Surprisingly, the SiPh<sub>3</sub> substituent on the carbyne is required: no ketenyl formation is observed with the Tol-substituted analog  $[\text{Cp}(\text{OC})_2\text{W}\equiv\text{CTol}]$ , **3b**. These coupling reactions are shown in Scheme 1.

More recently, these reactions have been followed up and extended by Chen and his group,<sup>27–29</sup> who have explored the reactions of the cationic carbyne complexes  $[\text{Cp}(\text{OC})_2\text{M}\equiv\text{CPh}]^+$  (**1c**, M = Mn; **1d**, M = Re) with a wide variety of

carbonyl metalates. This research has also been reviewed.<sup>30</sup> In a typical reaction of this type, complexes **1c** and **1d** reacted with  $[\text{Co}(\text{CO})_3(\text{PPh}_3)]^-$  to afford  $[\text{Cp}(\text{OC})_2\text{M}\{\mu\text{-}\eta^1, \eta^2\text{-C}(\text{CO})\text{-Ph}\}\text{Co}(\text{CO})_2(\text{PPh}_3)]$  (Co–M, M = Mn, Re) complexes **4a,b** in high yields (Scheme 2). An X-ray diffraction study for the Co–Re species **4b** established that the PPh<sub>3</sub> ligand is *trans* to the Re–Co bond (Re–Co–P = 161°).<sup>29</sup>

**Scheme 2. Reactions of Group 7 Carbyne Complexes with Various Metal Carbonyl Anions**



The reactions of the manganese and rhenium cationic carbyne complexes **1c** and **1d** with bimetallic anions almost invariably give dimetallic products and not metal clusters. One metal is preferentially incorporated into the bimetallic complex. Thus the iron–cobalt anion  $[(\text{OC})_4\text{Co}-\text{Fe}(\text{CO})_4]^-$  reacts with **1c** and **1d** to afford compounds with Mn–Co or Re–Co bonds, but none with Mn–Fe or Re–Fe bonds. The same Mn–Co or Re–Co species are also recovered from reactions of the  $[(\text{OC})_4\text{Co}-\text{W}(\text{CO})_5]^-$  (Co–W) anion with cations **1c** and **1d**. In each case (except for the reaction of **1d** with the cobalt–tungsten anion), the major products are unsaturated M–Co (M = Mn, Re) carbene complexes. Only a small quantity of the ketenyl complex is formed initially, but the unsaturated carbyne complexes add CO to give the corresponding ketenyl complexes **4d** and **4e** in high yields (Scheme 2).<sup>28</sup>

These ketenyl products are similar to those reported by Stone and Fischer, but there are stronger interactions of the CO carbon atom of the bridging ketenyl ligand with the added metal, and the products may also be described as  $\eta^1, \eta^2$ -substituted ketene complexes. They are obtained in remarkably high yields. Occasionally, there are differences in reactivity among metals belonging to the same periodic group. Thus, **1d** (M = Re) reacts with  $[\text{Fe}(\text{CO})_2\text{Cp}]^-$  to afford **4c**, but **1c** (M = Mn) does not (Scheme 2).

Two possible mechanisms are envisaged for these reactions. A CO transfer may take place from a carbene intermediate of the type  $[\text{Cp}(\text{OC})_2\text{M}=\text{C}(\text{Ar})(\text{M}'\text{L}_n)]$  to the carbene carbon. Alternatively, there may be direct CO transfer from the  $\text{ML}_n$  anionic fragment to the metal–carbyne center.

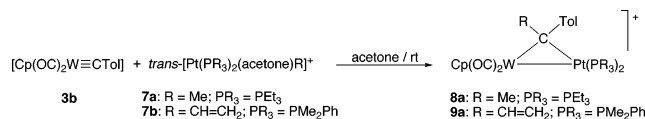
The reactions of complexes **1c** and **1d** with iron carbonyl anions do not afford the same ketenyl species. When M = Re, the products isolated after workup are the monometallic rhenium carbene complex  $[\text{Cp}(\text{OC})_2\text{Re}=\text{C}(\text{OEt})(\text{Ph})]$  and the  $\mu$ -carbene species **5**. The same products are isolated irrespec-

tive of whether the anion is  $[\text{Fe}(\text{CO})_4]^{2-}$ ,  $[\text{Fe}_2(\text{CO})_8]^{2-}$ , or  $[\text{Fe}_3(\text{CO})_{11}]^{2-}$ .<sup>31</sup> However, the products obtained when  $(\text{NEt}_4)_2[\text{Fe}_2(\text{CO})_8]$  is reacted with the Mn cationic carbyne include  $[\text{Mn}(\text{CO})_3\text{Cp}]$ , a tetrametallic bicarbene ( $\text{Mn}=\text{C}-\text{Fe}-\text{Fe}-\text{C}=\text{Mn}$ ) species, and the unexpected acyl carbene species **6**. The structures of the last two compounds were established by X-ray diffraction.<sup>32</sup> The unusual acyl carbene ligand  $[\mu\text{-CPh}-\text{C}(\text{O})\text{Et}]$  in **6** interacts with the Fe atom [ $\text{Fe}-\text{C}_{\text{COEt}} = 2.134(5) \text{ \AA}$ ;  $\text{Fe}-\text{O} = 2.004(3) \text{ \AA}$ ], and this is borne out by IR data [ $\nu(\text{CO}) = 1595 \text{ cm}^{-1}$  for this ligand's C=O group]. The source of the Et group of the  $\mu$ -carbene ligand is not the  $[\text{NEt}_4]^+$  cation, since **6** is also obtained with the salt  $\text{Na}_2\text{Fe}(\text{CO})_4$  with **1c**. The likely source of the Et group is  $\text{BBr}_2(\text{OEt})$ , which is a byproduct in the synthesis of the **1c**.<sup>32</sup> Scheme 2 summarizes all these reactions.

### 2.1.2. Carbyne–Alkyl Coupling

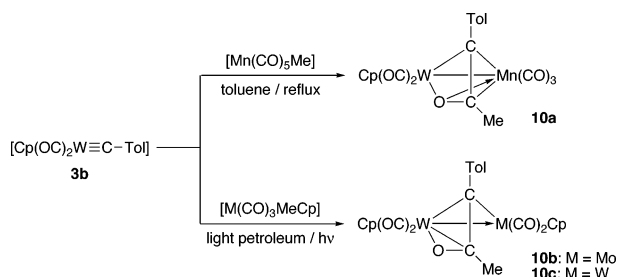
The Fischer carbyne  $[\text{Cp}(\text{OC})_2\text{M}\equiv\text{CTol}]$ , **3b**, reacts with the platinum methyl complex **7a** to give the cationic alkylidene complex **8a**, shown in Scheme 3. The reaction of **3b** with the vinylic species **7b** is similar, but the product **9a** has a  $\pi$ -interaction between the vinylic C=C bond and the tungsten atom.<sup>33</sup>

### Scheme 3. Carbyne–Alkyl Coupling To Afford $\mu$ -Carbene Complexes



When the tungsten alkylidyne complex **3b** is refluxed with  $[\text{Mn}(\text{CO})_5\text{Me}]$ , the product is a Mn–W complex **10a** with a short Mn–W bond of 2.696(1) Å, in which an acetyl group has coupled to the carbyne carbon (Scheme 4).<sup>34</sup> **3b** also reacts with the group 6 complexes  $[\text{M}(\text{CO})_3\text{MeCp}]$  (M = Mo, W) under photolytic conditions to generate complexes **10b** and **10c** that have a similar coupled organic framework. However, the acyl oxygen atoms in **10b,c** are not bonded to both metals. These reactions are believed to proceed via unsaturated acyl intermediates, which then coordinate to the  $\text{W}\equiv\text{C}$  triple bonds. If so, these reactions are really examples of acyl–alkylidyne couplings.

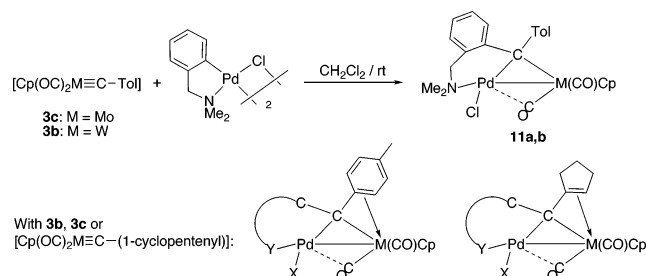
### Scheme 4. Reactions of a Tungsten–Carbyne Complex with Metal–Alkyl Complexes



The molybdenum and tungsten carbyne complexes **3b** and **3c** react analogously to alkynes and insert into the Pd–C bonds of a series of palladium metallacycles to give the  $\mu$ -carbene species **11** shown in Scheme 5: a Pd–M bond is formed simultaneously. The reactions go through intermediates in which the tungsten-bonded carbyne ligand shows a bonding interaction with the palladium atom, prior to the C–C coupling reaction.<sup>35</sup> Similar reactions were reported when a cobalt-based tripodal phosphonate ligand replaced

the Cp group on the group 6 metal.<sup>36</sup> Further research showed that the products obtained either with **3b**, with **3c**, or with the 1-cyclopentenyl carbyne complexes  $[\text{Cp}(\text{OC})_2\text{M}\equiv\text{C}(1\text{-cyclopentenyl})]$  (M = Mo, W), all contain  $\eta^2$ -arene or  $\eta^2$ -cyclopentenyl group interactions with the group 6 metal in solution (Scheme 5). The  $\pi$ -donation allows the group 6 metal atoms, in each case, to attain 18-electron configurations. Evidence for this bonding mode was deduced from detailed 2D NMR studies (<sup>1</sup>H nuclear Overhauser effect spectroscopy (NOESY), long-range and conventional <sup>13</sup>C–<sup>1</sup>H inverse correlation, and <sup>1</sup>H–<sup>183</sup>W correlation spectroscopy) for some of the palladium–tungsten complexes.<sup>37,38</sup> A number of the products have been characterized structurally.<sup>35,36,38,39</sup>

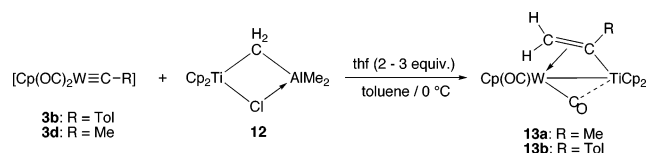
### Scheme 5. The Insertion of Alkylidyne Complexes into Palladium–Carbon Bonds of Palladacycles



### 2.1.3. Carbyne–Carbene Coupling

The carbyne complex **3b** and its methyl analog **3d** (Scheme 6) react with Tebbe's reagent **12** to afford complexes **13** with contain  $\mu\text{-}\eta^1(\text{Ti}), \eta^2(\text{W})\text{-C}(\text{R})=\text{CH}_2$  alkenyl ligands that straddle the two metals. The methylene group has coupled with the carbyne carbon atom. Complexes **13** contain rare Ti–W bonds [of length 3.082(2) Å for **13b**].<sup>40</sup>

### Scheme 6. Reaction of Tebbe's Reagent with Tungsten–Carbyne Complexes

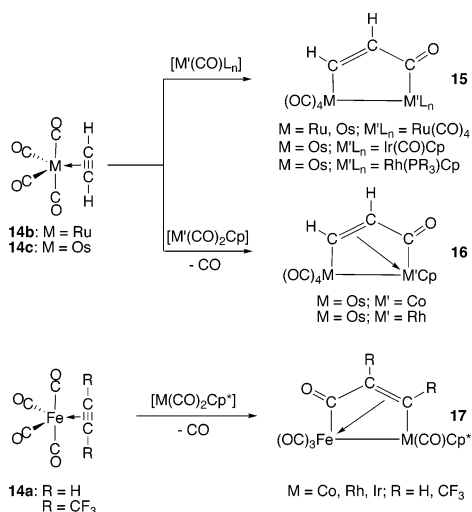


### 2.1.4. Alkyne–Carbonyl Coupling

While the coupling of alkynes with CO has been observed on heterobimetallic centers (section 3.4.1), this reaction also takes place when coordinated CO ligands of a metal–carbonyl complex are reacted with a mononuclear alkyne complex. A demonstration of this reaction is provided by the ruthenium and osmium ethyne species  $[\text{M}(\text{CO})_4(\eta^2\text{-HC}\equiv\text{CH})]$  (**14b**, M = Ru; **14c**, M = Os), which react with  $[\text{Ru}(\text{CO})_5]$  to give complexes **15** with dimetallacyclopentenone cores (Scheme 7). However, the reaction of **14c** with  $[\text{Os}(\text{CO})_5]$  leads to the  $\mu\text{-}\eta^1, \eta^1\text{-HC}\equiv\text{CH}$  species  $\text{Os}_2(\text{CO})_8(\mu\text{-}\eta^1, \eta^1\text{-HC}\equiv\text{CH})$  (no C–C coupling). Products **16** with a  $\text{M}'\text{-C}(\text{O})\text{-C}(\text{H})\text{-C}(\text{H})\text{-M}$  core similar to those of **15** are found when the group 9 complexes  $[\text{M}'(\text{CO})_2\text{Cp}]$  (M = Co, Rh) are reacted with **14c**. Carbon monoxide loss takes place in these cases. However, with the complex  $[\text{Ir}(\text{CO})_2\text{Cp}]$ , no CO loss was observed, and thus the bonding mode of the  $\text{C}(\text{O})\text{-C}(\text{H})\text{-C}(\text{H})$  linkage to the Ir ( $\eta^1$  in **15**) is slightly different from that of its lighter Co and Rh congeners ( $\eta^1, \eta^2$  in **16**).<sup>41</sup> Similar reactions take place with the rhodium phosphine complexes  $[\text{Rh}(\text{CO})(\text{PR}_3)\text{Cp}]$  ( $\text{PR}_3 = \text{PMe}_2\text{Ph}, \text{PMePh}_2$ ) to

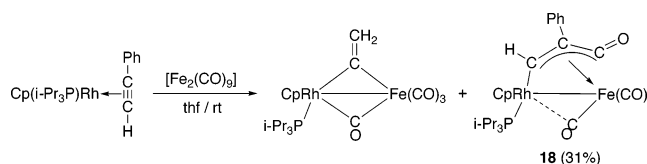
give complexes of type **15**<sup>42</sup>. Later work showed that **14a** (M = Fe) and its CF<sub>3</sub> analog react similarly with the group 9 complexes [M(CO)<sub>2</sub>Cp\*] (M = Co, Rh, Ir).<sup>43</sup> All these reactions are highly stereospecific, and only one metallacycle isomer is obtained in each case. For the iron reactions, complexes **17** are obtained. These complexes are structurally different from complexes **15** and **16** as the acyl groups are now  $\sigma$ -bonded to the iron atom and not to the group 9 metal. A kinetic and mechanistic study of these reactions has been published.<sup>44</sup>

#### Scheme 7. Reactions of Group 8 $\eta^2$ -Alkyne Complexes with Metal Carbonyl Complexes



Another example of alkyne–carbonyl coupling accompanied by M–M' bond formation comes from the group of Werner. The reaction of the rhodium  $\eta^2$ -phenylacetylene complex [Rh( $\eta^2$ -PhC≡CH)(P-*i*-Pr<sub>3</sub>)Cp] with [Fe<sub>2</sub>(CO)<sub>9</sub>] affords a  $\mu$ -vinylidene species and complex **18** best represented as shown in Scheme 8, on the basis of an X-ray diffraction structural study. This complex contains an  $\eta^3$ -metalloallyl-like ligand in which a CO ligand has coupled with the alkyne.<sup>45</sup>

#### Scheme 8. Alkyne–Carbonyl Coupling and Synthesis of an Iron–Rhodium Complex

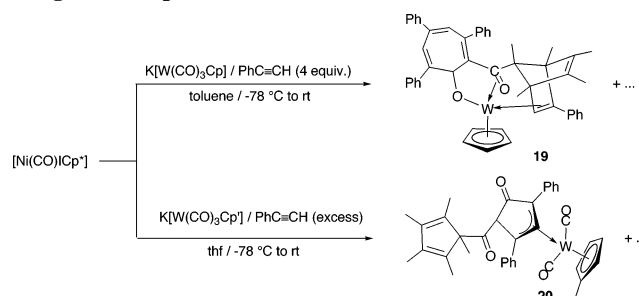


The coupling of alkynes with CO ligands on a preformed Ni–W platform is discussed later (section 3.4.1). However, the monometallic precursors to a Ni–W complex react with PhC≡H in situ to give complicated products that result from multiple alkyne couplings with CO. While some products contain no Ni–W bond, these complex organic coupling reactions require the presence of both metals and have never been obtained with various combinations of ligands and single monometallic complexes, and they merit discussion here.

When [Ni(CO)ICp\*] is reacted with [W(CO)<sub>3</sub>Cp]<sup>−</sup>, the mixture of complexes obtained includes the metallacycles and the  $\mu$ -alkyne complexes that are harvested from the reaction of a Ni–W complex with PhC≡CH (section 3.4.1).<sup>46</sup> In addition, smaller quantities of more complex products are

obtained. The remarkable 16-electron tungsten side-bonded ketone complex **19** [WCp( $\eta^2$ -R(C=O)R')], shown in Scheme 9, was isolated in moderate yield from this reaction. The “R” group of the ketone is the enol form of a triphenyl-tropone ligand, formed by the head-to-tail coupling of three PhC≡CH groups with a CO group. This portion of the ligand binds to the tungsten atom via its enol oxygen. The other group of the ketone (R') is an alkyl ligand formed by a Diels–Alder addition of PhC≡CH to a C<sub>5</sub>Me<sub>5</sub> ligand that has migrated off the nickel atom. Eight new carbon–carbon bonds are formed regioselectively at −78 °C in this synthesis.<sup>47</sup>

#### Scheme 9. Isolation of Tungsten Ketone Complexes from the Reaction of PhC≡CH with a Mixture of Nickel and Tungsten Complexes



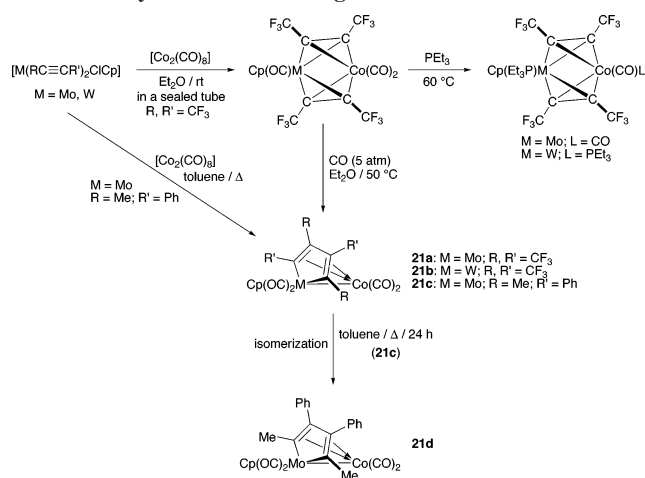
Another alkyne–CO coupled product **20** was isolated from the very similar reaction of [Ni(CO)ICp\*] with the tungsten Cp' anion [W(CO)<sub>3</sub>Cp']<sup>−</sup> as shown in Scheme 9. A ketone ligand, formed by the coupling of two CO groups with two phenylacetylene groups, is present in **20**. One of the CO groups forms the C=O group of the ketone, while the other is part of a five-membered ring that is  $\eta^3$ -allylically coordinated to the tungsten atom. Complex **20** (with a Cp rather than a Cp' ligand) may be a precursor to **19**.<sup>48</sup>

#### 2.1.5. Alkyne–Alkyne Coupling

A large number of C–C coupling reactions on heterobimetallic complexes involve alkynes. In many cases, these reactions take place on a preformed bimetallic alkyne complex. Reactions in which both starting products are monometallic are discussed here, even though it is likely that the coupling reactions take place on an intermediate heterobimetallic alkyne species and even if, in few cases, a heterobimetallic alkyne complex is indeed observed.

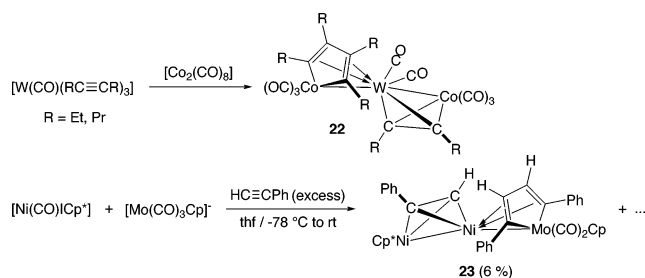
The HFB units in the monometallic complexes [M(CF<sub>3</sub>C≡CCF<sub>3</sub>)<sub>2</sub>ClCp] (M = Mo, W) adopt bridging positions when these complexes are reacted with [Co<sub>2</sub>(CO)<sub>8</sub>] in a sealed tube to yield the complexes [(OC)<sub>2</sub>Co( $\mu$ -HFB)<sub>2</sub>M-(CO)Cp] (Co–M, M = Mo, W). The alkynes in these species (Scheme 10) were induced to couple with each other to give **21a** and **21b** when these molecules were treated with 5 atm of CO at 50 °C. In contrast, PEt<sub>3</sub> addition simply resulted in PEt<sub>3</sub>-for-CO substitution.<sup>49,50</sup> When treated with [Co<sub>2</sub>(CO)<sub>8</sub>], the PhC≡CMe complex [Mo(PhC≡CMe)<sub>2</sub>ClCp] afforded the coupled alkyne product directly. A regioselective head-to-tail alkyne coupling reaction has ensued to give the molybdenacyclopentadiene product complex **21c**, which is the kinetic isomer of this reaction. When heated in toluene for 24 h, **21c** isomerized to the thermodynamically more stable head-to-tail coupled product **21d**.<sup>51</sup> (Co–Mo coupled alkyne complexes **21** are also accessible from the reactions of Co–Mo species with alkynes. These reactions are discussed later in section 3.4.4).<sup>52,53</sup>

### Scheme 10. Alkyne Dimerization Coupled with Cobalt–Molybdenum or –Tungsten Bond Formation



The tris(alkyne) tungsten carbonyl complex  $[W(CO)(RC\equiv CR)_3]$  reacts with  $[Co_2(CO)_8]$  to afford a metallacyclopentadiene, which is part of a Co–W–Co skeleton, but in this case, a cobaltacycle **22** is formed. The coupled product also contains a  $\mu$ -alkyne spanning the other Co–W bond (Scheme 11). The trimetallic complex formed with hex-3-yne was structurally characterized by an X-ray study.<sup>54,55</sup>

### Scheme 11. Alkyne Coupling Accompanied by Nickel–Molybdenum or Cobalt–Tungsten Bond Formation



The trimetallic complex **23** somewhat similar to that just described was observed when the  $[Mo(CO)_3Cp]^-$  anion was reacted with the nickel complex  $[Ni(CO)ICp^*]$  at  $-78\text{ }^\circ C$  in the presence of phenylacetylene and the mixture was warmed to ambient temperature. The Mo–Ni–Ni trimetallic chain complex was characterized crystallographically.<sup>56</sup> It shows the same tail-to-tail ( $-CPh-CH-CH-CPh-$ ) organic connectivity that is observed in an Fe–Rh-coupled phenylacetylene complex<sup>57</sup> and contains a molybdenacycle of the type found in complexes **21**.<sup>47,48</sup> (See section 3.4.4 for more alkyne–CO coupling on nickel–molybdenum bonds).

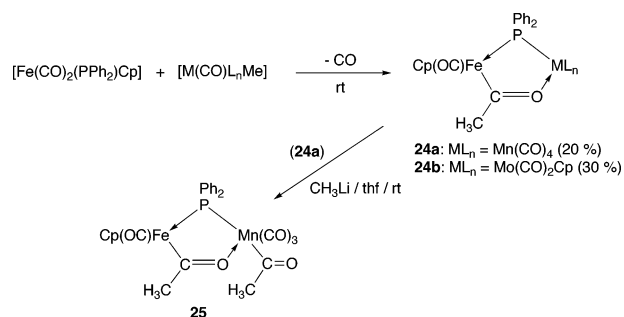
#### 2.1.6. Alkyl–Carbonyl Coupling

In the classic “CO insertion” reaction, an alkyl ligand migrates from one site onto a neighboring CO group that is bonded to the same metal. In the reactions discussed in this section, the alkyl group migrates onto a CO ligand of another metal at the same time as a heterobimetallic complex (with M–M’ not necessarily present) is formed. The acyl group that forms often bridges the two metals, and in the reactions hitherto reported, one of the metallic groups involved in these reactions is a  $M(CO)_2Cp$  ( $M = Fe$  or  $Ru$ ) group.

An early example is provided by the reaction of the complex  $[Mn(CO)_5Me]$  and the diphenylphosphido species

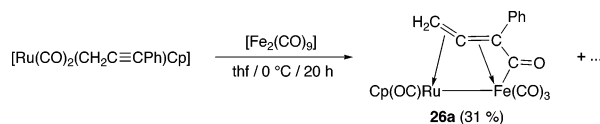
$[Fe(CO)_2(PPh_2)Cp]$ .<sup>58</sup> The product, obtained in a moderate 20% yield, is complex **24a**, which contains a bridging acyl ligand that is  $\sigma$ -bonded to the iron atom via its carbonyl carbon and linked to the manganese via the acyl oxygen atom. The mechanism of formation of the product is discussed in the article. It is noteworthy that the acyl CO carbon is carbene-like (based on its low-field  $^{13}C$  NMR chemical shift of 319.3 ppm) and no  $\nu(CO)$  stretch was observed for this group in the IR. The addition of MeLi to this Fe–Mn acyl leads to **25** in which one of the manganese-bonded carbonyl ligands has now been methylated to afford a second acyl ligand, which is  $\eta^1$ -bonded to the manganese.<sup>58</sup> The related reaction of  $[Fe(CO)_2(PPh_2)Cp]$  with  $[Mo(CO)_3(Me)Cp]$  yielded a similar complex **24b** in which a  $\mu$ -acyl ligand is  $\sigma$ -bonded, via the carbon atom, to the iron atom and interacting, via the oxygen, to the molybdenum. No M–M’ bonds are present in any of these complexes (Scheme 12).<sup>59</sup>

### Scheme 12. Coupling of Metal–Methyl Complexes with an Iron–Carbonyl Complex To Generate Acyl Species



When the complex  $[Ru(CO)_2(CH_2C\equiv CPh)Cp]$  is reacted with  $[Fe_2(CO)_9]$ , the major products are the Fe–Ru allenyl–acyl complex **26a** (formed in 31% yield) and a  $Fe_2Ru$  cluster. A diiron allylic acyl species was also isolated. Since the acyl ligand is  $\sigma$ -bonded to the iron atom, the reaction is believed to involve an alkyl group migration onto the iron atom CO group (Scheme 13).<sup>60</sup>

### Scheme 13. Formation of an Allenyl–Acyl Ligand That Spans an Iron–Ruthenium Bond

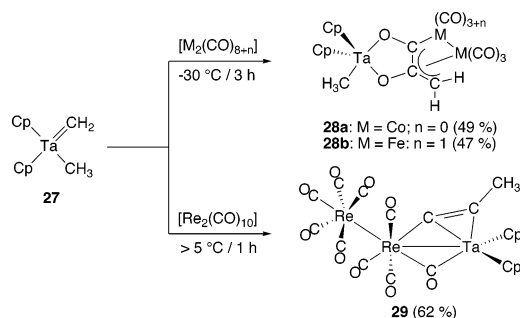


#### 2.1.7. Multiple Carbene–Carbonyl Coupling

Complex **27**,  $[Cp_2Ta(=CH_2)Me]$ , reacts with many metal binuclear carbonyl complexes to afford new products in which the alkyl and the methylene group of **27** have coupled either with each other or with the CO groups of the metal carbonyl.<sup>61</sup> It is believed that all these reactions are initiated by a cycloaddition reaction between the  $Ta=CH_2$  group and a CO ligand of the dinuclear metal carbonyl complex. With  $[Co_2(CO)_8]$  and with  $[Fe_2(CO)_9]$ , the structures of the products **28a** and **28b** (established by X-ray diffraction studies) both contain  $C_3H_2O_2$  ligands that bridge three metal centers. These reactions are shown in Scheme 14. However, the reaction of **27** with  $[Re_2(CO)_{10}]$  yields a different product, **29**, whose structure was also determined by an X-ray diffraction study. These reactions all provide new examples of transformation processes in which CO ligands are coupled to each other and to  $CH_2$  groups: the reaction with  $[Re_2-$

(CO)<sub>10</sub>] also cleaves a CO bond and is accompanied by hydrogen migration reactions. The relative rapidity of these reactions even at low temperatures “appears to be a direct result of the interaction of two metal complexes in which the metal centers have very different electronic properties.”<sup>61</sup>

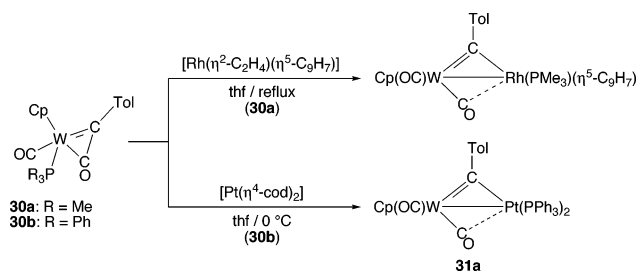
#### Scheme 14. Reactions of a Tantalum Alkylidene with Bimetallic Carbonyl Complexes



## 2.2. Carbon–Carbon Bond Cleavage Reactions Accompanied by Heterobimetallic Complex Formation

Reactions in this class are rare, and few examples are known to us. The reaction of the tungsten ketylenyl complex **30a** (PR<sub>3</sub> = PMe<sub>3</sub>) with the indenyl–rhodium synthon [Rh(η<sup>2</sup>-C<sub>2</sub>H<sub>4</sub>)<sub>2</sub>(η<sup>5</sup>-C<sub>9</sub>H<sub>7</sub>)] affords the Rh–W bridging carbyne complex [Cp(OC)<sub>2</sub>W(μ-C(Tol))Rh(PMe<sub>3</sub>)(η<sup>5</sup>-C<sub>9</sub>H<sub>7</sub>)], in which the carbyne ligand is formally double bonded to the tungsten atom. There is also a simultaneous PMe<sub>3</sub> ligand migration (W ⇒ Rh). The reaction of **30b** (PR<sub>3</sub> = PPh<sub>3</sub>) with [Pt(η<sup>4</sup>-1,5-cod)<sub>2</sub>] leads to cleavage of the (Tol)C–CO bond and to the formation of the Pt–W μ-carbyne complex **31a** as depicted in Scheme 15. However, this reaction is quite sensitive to the nature of the phosphine ligand, and the C–C bond is not broken in the reaction of [Pt(η<sup>4</sup>-1,5-cod)<sub>2</sub>] with **30a**, **30c** (PR<sub>3</sub> = PMePh<sub>2</sub>), **30d** (PMe<sub>2</sub>Ph), or **30e** (R = PMe<sub>2</sub>-Bz).<sup>62</sup>

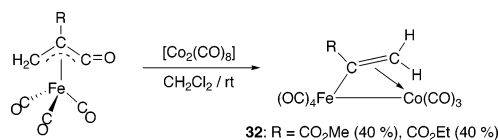
#### Scheme 15. Reactions of Tungsten Ketylenyl Complexes with Platinum(0) and Rhodium(I) Synthons



Heterobimetallic Co–Fe complexes with bridging alkenyl ligands have been isolated from the reaction of [Co<sub>2</sub>(CO)<sub>8</sub>] with the η<sup>3</sup>-allyl-like species [(η<sup>3</sup>-CH<sub>2</sub>–CR–CO)Fe(CO)<sub>3</sub>] (R = CO<sub>2</sub>Me or CO<sub>2</sub>Et). In the resulting alkenyl species **32**, the ligand is σ-bonded to the iron atom and π-coordinated to the cobalt atom (Scheme 16): the CR–CO bond has been cleaved.<sup>63</sup>

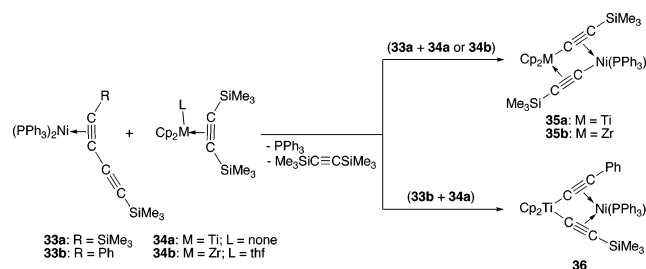
When the η<sup>2</sup>-buta-1,3-diyne complex [Ni(PPh<sub>3</sub>)<sub>2</sub>(η<sup>2</sup>-Me<sub>3</sub>-SiC≡C–C≡CR)], **33a** (R = SiMe<sub>3</sub>) and the titanocene alkyne complex [Cp<sub>2</sub>Ti(η<sup>2</sup>-Me<sub>3</sub>SiC≡CSiMe<sub>3</sub>)] **34a** are reacted, loss of Me<sub>3</sub>SiC≡CSiMe<sub>3</sub> ensues and the product is the heterobimetallic diacetylide **35a**, resulting from formal C–C bond cleavage of Me<sub>3</sub>SiC≡C–C≡CSiMe<sub>3</sub>.<sup>64</sup> The reaction of **33a** with the zirconocene complex **34b** yields

#### Scheme 16. Reaction of Iron Complexes with [Co<sub>2</sub>(CO)<sub>8</sub>] To Generate Heterobimetallic μ-Alkenyls



the analogous nickel zirconium complex **35b** (Scheme 17). The long Ni–M distances observed [Ni···Ti = 2.7277(10) Å; Ni···Zr = 2.8295(13)] suggest that a metal–metal bond is absent; the diamagnetism of these complexes is attributed to antiferromagnetic interactions between the two metals or else to electronic coupling via the μ-C≡CSiMe<sub>3</sub> groups. The product of the reaction of unsymmetrical diyne complex **33b** (R = Ph) with **34a** is different. A formally Ti(IV)/Ni(0) mixed diacetylide species **36** is obtained here, in which the –C≡CSiMe<sub>3</sub> and –C≡CPh groups are σ-bonded to the Ti and π-bonded to the nickel atom. The presence of two different metals seems to be crucial since the reaction of excess **34a** with free dialkyne Me<sub>3</sub>SiC≡C–C≡CSiMe did not lead to C≡C bond rupture.<sup>64</sup>

#### Scheme 17. C–C Cleavage in Reactions of Nickel(0) Diyne Complexes with Group 4 Synthons



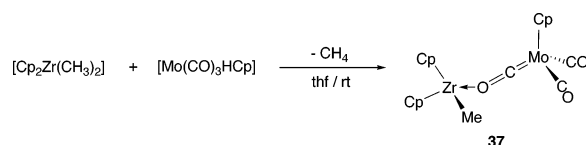
## 2.3. Carbon–Hydrogen Bond Formation

When a metal hydride reacts with a metal alkyl, a bimetallic reductive elimination reaction often follows and an alkane is eliminated; a bimetallic species is formed simultaneously. Occasionally, a bonded hydrogen atom on one metal combines with an unsaturated hydrocarbyl ligand on another, the new organic ligand remains bonded to the metal, and the products are now heterobimetallic complexes. Both kinds of coupling reactions are common and are known for many metal combinations.

### 2.3.1. Hydrogen–Alkyl Coupling

An early example of alkane elimination and formation of a bimetallic complex reaction is the reaction of the complex [ZrMe<sub>2</sub>Cp<sub>2</sub>] with [Mo(CO)<sub>3</sub>HCp], first reported in 1978,<sup>65</sup> which leads to the elimination of CH<sub>4</sub> and to the formation of the Mo, Zr species **37** shown in Scheme 18 (with an isocarbonyl–OC bridge and no C–C bond).<sup>66,67</sup> It is noteworthy that all CO groups undergo site exchange at room temperature on the <sup>13</sup>C NMR time scale. (Further reactions of **37** are discussed in Scheme 46, section 3.1.2).

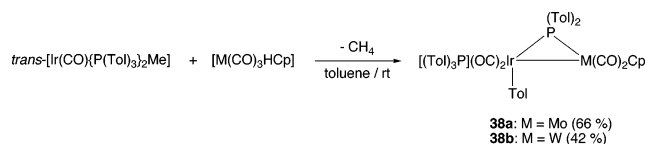
#### Scheme 18. Formation of a Molybdenum/Zirconium Heterobimetallic Complex by Reductive Elimination of CH<sub>4</sub>





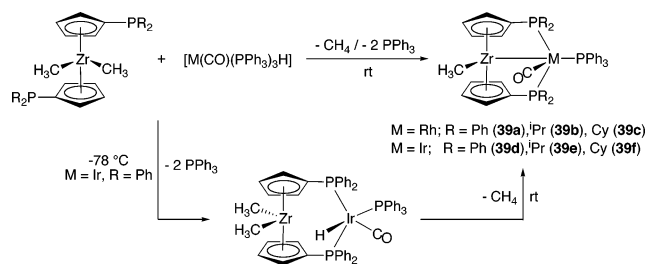
The reactions of the methyl iridium complex *trans*-[Ir(CO)(PTol<sub>3</sub>)<sub>2</sub>Me] with the group 6 hydride complexes [M(CO)<sub>3</sub>HCP] (M = Mo, W) liberate CH<sub>4</sub>. However, the bimetallic products are not the expected [(OC)(Tol<sub>3</sub>P)<sub>2</sub>Ir–M(CO)<sub>3</sub>Cp] (Ir–M, M = Mo, W) complexes. Instead, a C–P oxidative addition reaction takes place (Scheme 19) to give complexes **38**. These species are isomers of the “expected” products in which the two metals attain an 18-electron configuration.<sup>68</sup>

#### Scheme 19. Reductive Elimination of CH<sub>4</sub> Followed by a P–C Cleavage Reaction



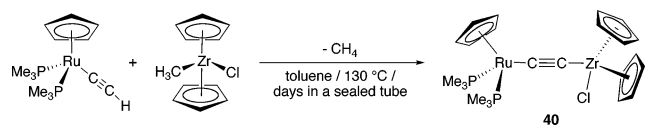
The dimethylzirconium complex [ZrMe<sub>2</sub>(η-C<sub>5</sub>H<sub>4</sub>PPh<sub>2</sub>)<sub>2</sub>] reacts with [Ir(CO)(PPh<sub>3</sub>)<sub>3</sub>H] at –78 °C to form a spectroscopically observed bimetallic species in which the phosphorus atoms of the η-C<sub>5</sub>H<sub>4</sub>PPh<sub>2</sub> ligands ligate to the iridium (Scheme 20). This methyl hydride complex reductively eliminates an equivalent of CH<sub>4</sub> when warmed and forms the “early–late” Zr–Ir-bonded complex **39d**.<sup>69</sup> Other combinations of [ZrMe<sub>2</sub>(η-C<sub>5</sub>H<sub>4</sub>PR<sub>2</sub>)<sub>2</sub>] (R = *i*-Pr, Cy, or Ph) complexes with [M(CO)(PPh<sub>3</sub>)<sub>3</sub>H] (M = Rh, Ir), give complexes **39** directly.<sup>69–71</sup> Addition of isopropanol or water to the Rh–Zr complex **39a** leads to the liberation of another equivalent of CH<sub>4</sub> and yields isopropoxy- or hydroxy-zirconium complexes respectively.<sup>69</sup> Complexes **39a–c** react with CO to give acyl species (section 3.1.1).<sup>71</sup>

#### Scheme 20. Reductive Elimination of CH<sub>4</sub> and Formation of Iridium– and Rhodium–Zirconium Bonded Complexes from Monometallic Precursors



Another example of methane elimination, which also involves a zirconium complex, is shown in Scheme 21. When the alkynyl complex [Ru(PMe<sub>3</sub>)<sub>2</sub>(C≡CH)Cp] is reacted with [ZrClMeCp<sub>2</sub>], the dimetalla-alkyne (or a dimetalladiyne) complex **40** forms, together with the liberation of CH<sub>4</sub>.<sup>72</sup>

#### Scheme 21. Formation of a Heterobimetallic Dimetalla-alkyne Complex by Reductive Elimination of CH<sub>4</sub>

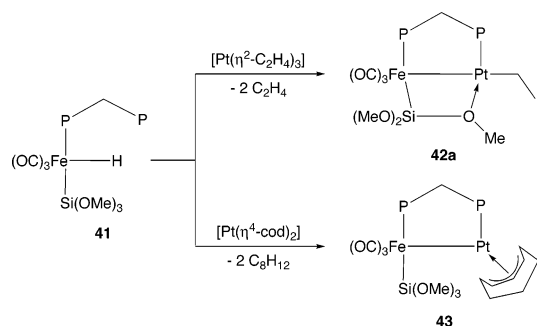


### 2.3.2. Hydrogen–Alkene Coupling

The monocoordinated dpmm iron hydride species **41** shown in Scheme 22 reacts with the Pt(0) olefin complexes [Pt(η<sup>2</sup>-C<sub>2</sub>H<sub>4</sub>)<sub>3</sub>] or [Pt(η<sup>4</sup>-cod)<sub>2</sub>] to afford **42a** and **43** in which the hydrogen has added to an olefinic double bond. The reaction is believed to take place via initial coordination of the dpmm

to the platinum atom and partial olefin loss. It is likely that an intermediate platinum olefin hydride complex is formed, whose structure is analogous to that of an isolated, closely related species in which a PPh<sub>3</sub> group substitutes the olefin ligand.<sup>73</sup> A reverse β-hydrogen elimination reaction then follows to give the final ethyl (**42a**) or cyclooctenyl (**43**) complexes.<sup>74</sup>

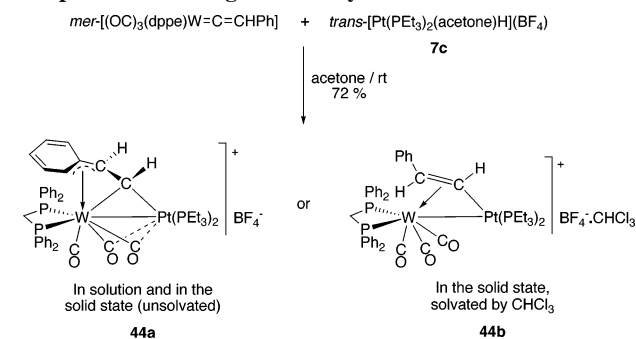
#### Scheme 22. Additions of an Iron Hydride to Platinum(0) Olefin Complexes



### 2.3.3. Hydrogen–Vinylidene Coupling

Reactions of platinum hydrides with mononuclear vinylidene (alkenylidene) complexes can, in principle, give rise to either μ-alkenyl complexes (following α-hydrogen addition to the vinylidene ligand) or to μ-carbyne complexes (if β-addition takes place). When the tungsten vinylidene complex *mer*-[(OC)<sub>3</sub>(dppe)W=C=CHPh] is reacted with *trans*-[Pt(PEt<sub>3</sub>)<sub>2</sub>(acetone)H]<sup>+</sup> **7c**, the product is the cationic μ-carbene species **44a** (Scheme 23). The bridging carbene is in fact a μ-η<sup>1</sup>,η<sup>4</sup>-styryl ligand. The structure of this complex, which is dynamic on the NMR time scale, was established by detailed solution NMR studies using <sup>13</sup>C and <sup>2</sup>H specifically labeled compounds. This structure is believed to be adopted in the solid state without solvent of crystallization. However, a single-crystal X-ray diffraction study of the solvated solid **44b** BF<sub>4</sub><sup>–</sup>·CHCl<sub>3</sub> revealed a different ligand coordination mode, in which the bridging group is now best considered to be a μ-η<sup>1</sup>,η<sup>2</sup>-styryl ligand. The reaction and geometries of the two structural isomers of **44** are shown in Scheme 23.<sup>75</sup>

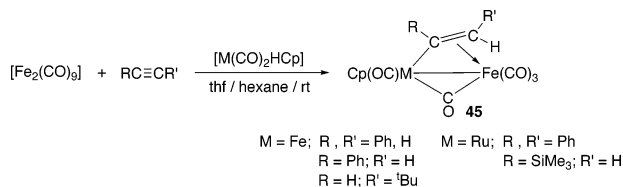
#### Scheme 23. Reaction of a Cationic Platinum(II) Hydride Complex with a Tungsten Alkenylidene



When the complexes [M(CO)<sub>2</sub>HCP] (M = Fe, Ru), [Fe<sub>2</sub>(CO)<sub>9</sub>] and free alkynes are all reacted together, homo- or heterobimetallic μ-η<sup>1</sup>,η<sup>2</sup>-alkenyl complexes **45** are formed (Scheme 24).<sup>76</sup> The reaction is regioselective with terminal alkynes, but the isomers obtained depend on the alkyne and not on the nature of M. Substituent groups such as SiMe<sub>3</sub> or Ph on a terminal alkyne RC≡CH might be stabilized by

$\pi$ -interactions with the organic backbone, and thus these groups lead to geminal alkenyls, in which the SiMe<sub>3</sub> or Ph groups are on the  $\alpha$ -carbon atom of the alkenyl. The intermediates in this reaction were assumed to be [Fe(CO)<sub>4</sub>-( $\eta^2$ -RC<sub>2</sub>R')] complexes of type **14**; such species were indeed subsequently reported.<sup>43</sup>

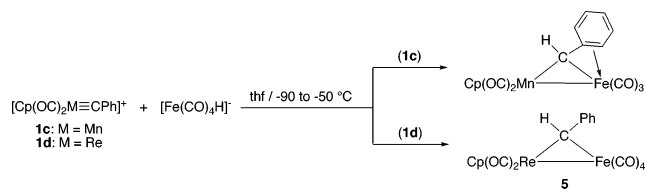
#### Scheme 24. Formation of Bimetallic Alkenyl Complexes from Metal Hydride Addition to Intermediate Monometallic Alkyne Complexes



#### 2.3.4. Hydrogen–Carbyne Coupling

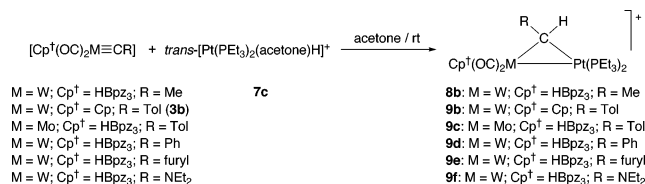
Reactions of metal carbonyl anions with the group 7 cationic carbyne complexes [Cp(OC)<sub>2</sub>M≡CPh]<sup>+</sup> **1** to afford ketene or ketyl complexes have already been discussed (section 2.1.1, Scheme 2). No carbyne–carbonyl coupling results when the iron carbonyl hydride [Fe(CO)<sub>4</sub>H]<sup>−</sup> is reacted with complexes **1c** or **1d**; instead,  $\mu$ -carbene complexes are obtained (Scheme 25). In the Fe–Mn complex [(OC)<sub>3</sub>Fe( $\mu$ -CHPh)Mn(CO)<sub>2</sub>Cp] (Fe–Mn) there is an  $\eta^2$ -olefin interaction from the Ph to the iron atom. This is absent in the Fe–Re complex **5** since the iron atom is electronically saturated here.<sup>77</sup>

#### Scheme 25. Metal Hydride Addition to Cationic Group 7 Carbynes To Give $\mu$ -Carbene Species



In a series of reactions that historically preceded the above example, the tungsten carbyne complex **3b** [Cp(OC)<sub>2</sub>W≡CTol] reacted with *trans*-[Pt(PEt<sub>3</sub>)<sub>2</sub>H(acetone)]<sup>+</sup> **7c** to afford a bridging  $\mu$ -carbene complex, **9b**, in which the  $\mu$ -CHTol ligand is also donating electron density to the tungsten atom via one of the aromatic carbon–carbon bonds.<sup>78</sup> The reaction with **7c** has been extended to molybdenum and to a variety of other tungsten carbyne complexes of type [Cp<sup>†</sup>(OC)<sub>2</sub>M≡CR] (Scheme 26). Complexes **9** with electron donation from the ligand R to the group 6 metal are obtained in all cases except for the methyl complex **8b**.<sup>33</sup>

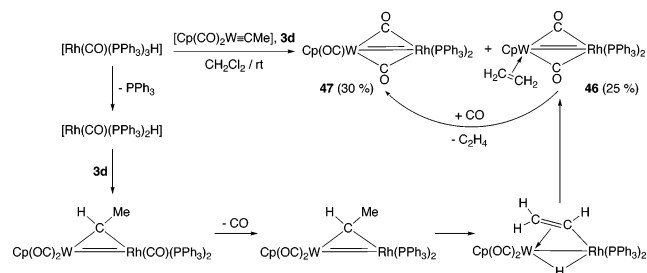
#### Scheme 26. Formation of $\mu$ -Carbene Complexes by Metal Hydride Insertion across M≡C Bonds



The reaction of the tungsten complex **3d**, [Cp(OC)<sub>2</sub>W≡Me], with the rhodium hydride [Rh(CO)(PPh<sub>3</sub>)<sub>3</sub>H] surprisingly affords the  $\eta^2$ -CH<sub>2</sub>=CH<sub>2</sub> complex **46**. The reaction is believed to proceed via formation of a  $\mu$ -CHMe species,

which then rearranges to an olefin complex via an intermediate  $\mu$ -vinyl  $\mu$ -hydrido species. The unsaturated Rh=W complex **47** that results from ethylene loss from **46** is also observed (Scheme 27).<sup>79</sup>

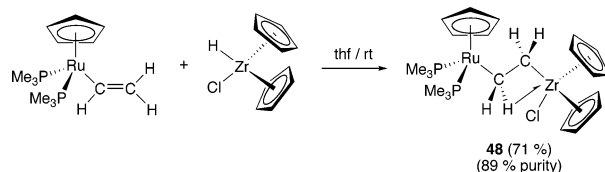
#### Scheme 27. Transformation of a Tungsten Ethylidyne Complex into a ( $\eta$ -C<sub>2</sub>H<sub>4</sub>)Rhodium–Tungsten Species



#### 2.3.5. Hydrogen–Alkenyl Coupling

The reaction of the electron-rich ruthenium vinyl complex [Ru(PMe<sub>3</sub>)<sub>2</sub>(CH=CH<sub>2</sub>)Cp] with [ZrHCICp<sub>2</sub>] leads to the formation of complex **48**, which can be considered to be a 1,2-dimetalla-ethane species (Scheme 28). The structure of **48** was established by an X-ray diffraction study. Both structural and NMR spectroscopic evidence suggest that an agostic interaction exists between a C–H bond  $\alpha$  to the ruthenium atom and the zirconium atom.<sup>72</sup>

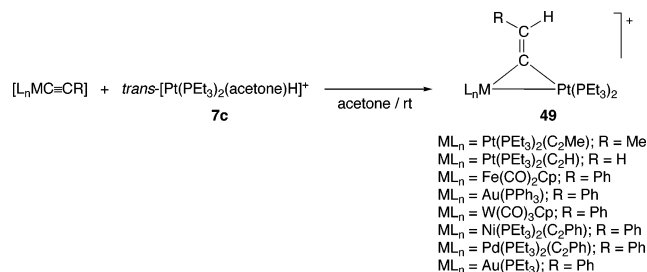
#### Scheme 28. Formation of a 1,2-Dimetalla-ethane Complex by Reaction of a Ruthenium Vinyl Complex with a Zirconium Hydride



#### 2.3.6. Hydrogen–Alkynyl Coupling

The formal addition of Pt–H bonds of the cationic complex **7c** across the C≡C bonds of various alkynyl ligands in a series of monometallic alkynyl complexes of W, Fe, Ni, Pd, Pt, and Au afforded the cationic  $\mu$ -vinylidene complexes **49**. In all these reactions, metal–metal bond formation accompanied the C–H bond formation (Scheme 29).<sup>80</sup>

#### Scheme 29. Synthesis of Vinylidene Complexes by Pt–H Addition to Alkynyl Ligands

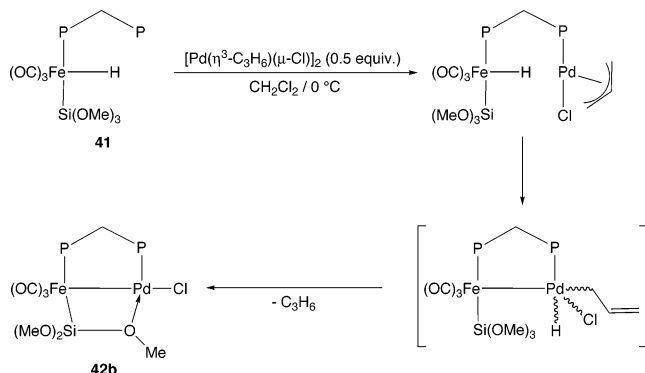


#### 2.3.7. Hydrogen– $\pi$ -Allyl Coupling

When the octahedral iron complex **41** is reacted with [Pd( $\eta^3$ -C<sub>3</sub>H<sub>5</sub>)( $\mu$ -Cl)]<sub>2</sub>, propene is evolved and the iron–palladium complex **42b** shown in Scheme 30 is formed. The reaction is believed to proceed via the intermediacy of an iron–palladium  $\mu$ -dppm intermediate, followed by bimetallic

reductive elimination of propene from what is formally a Pd(IV) center.<sup>81</sup>

**Scheme 30. Reductive Elimination of Propene from the Reaction of an Iron Hydride with a Palladium  $\pi$ -Allyl Species**

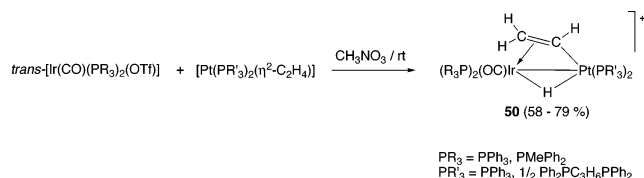


**2.4. Carbon–Hydrogen Bond Cleavage (C–H Activation) Accompanied by Heterobimetallic Complex Formation**

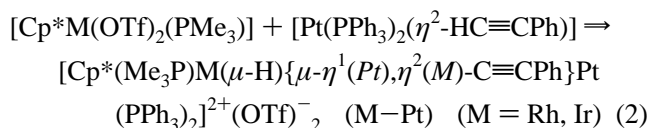
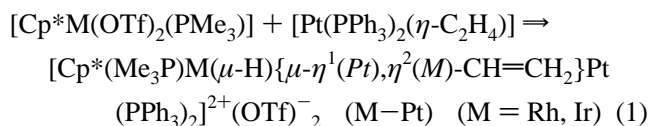
**2.4.1. Cleavage of Carbon(sp)– and Carbon(sp<sup>2</sup>)–Hydrogen Bonds of Coordinated Alkenes and Alkynes**

The addition of 16-electron Pt(0) alkene or alkyne complexes to a variety of Rh and Ir complexes leads to new cationic complexes with Pt–M (M = Rh, Ir) bonds and to the concomitant activation of an olefinic or acetylenic C–H bond.<sup>82–85</sup> The products of this reaction are cationic species with a bridging hydride and a  $\mu$ - $\eta^1$ (Pt),  $\eta^2$ (M)-alkenyl or -alkynyl ligand. Examples of alkenyls **50** are shown in Scheme 31.

**Scheme 31. C–H Activation of a Platinum-Bonded  $\eta^2$ -Alkene on Reaction with Iridium(I) Species**



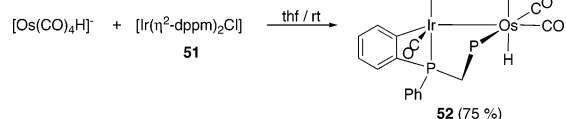
Related reactions, which give products very similar to those shown in this scheme are summarized in eqs 1 and 2.<sup>84,85</sup>



**2.4.2. Cleavage of Carbon(sp<sup>2</sup>)–Hydrogen Bonds of Phenyl and Cyclopentadienyl Groups**

The reaction of  $[\text{Os}(\text{CO})_4\text{H}]^-$  with  $[\text{Ir}(\eta^2\text{-dppm})_2\text{Cl}]$  **51** resulted in the formation of a heterobimetallic hydride complex **52**, which contains an Ir–Os bond and a cyclometalated dppm phenyl ring. Its structure is shown in Scheme 32.<sup>86</sup>

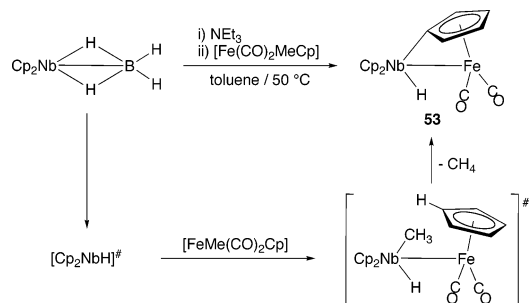
**Scheme 32. Cyclometalation of a Phenyl Group of a dppm Ligand Leading to an Iridium–Osmium Complex**



A number of groups have reported the activation of a coordinated  $\eta^5$ -cyclopentadienyl group on reaction with another metallic species, leading to new  $\mu$ - $\eta^1, \eta^5$ -C<sub>5</sub>H<sub>4</sub> MM' hydride species. Examples of this kind of reaction have long been known.

Both Mn–Mo- and Mn–Re-bonded complexes are obtained from the reaction of  $[\text{Cp}_2\text{MoH}_2]$  or  $[\text{Cp}_2\text{ReH}]$  with  $[\text{Mn}(\text{CO})_5\text{Me}]$ . The entropically favored elimination of CH<sub>4</sub> drives these reactions.<sup>87</sup> The reaction of the iron methyl species  $[\text{FeMe}(\text{CO})_2\text{Cp}]$  with in situ generated  $[\text{NbCp}_2\text{H}]$  proceeds similarly. There is bimetallic reductive elimination of CH<sub>4</sub> and the formation of  $[\text{Cp}_2\text{Nb}(\text{H})\{\mu\text{-}\eta^1(\text{Nb}), \eta^5(\text{Fe})\text{-C}_5\text{H}_4\}]\text{Fe}(\text{CO})_2$ , **53** (Scheme 33). The presumed intermediate contains a Nb–CH<sub>3</sub> bond.<sup>88</sup>

**Scheme 33. Reaction of a Metallocene Hydride with a Metal Alkyl Leads to a Heterobimetallic Complex with an  $\eta^1, \eta^5$ - $\mu$ -C<sub>5</sub>H<sub>4</sub> Ligand**

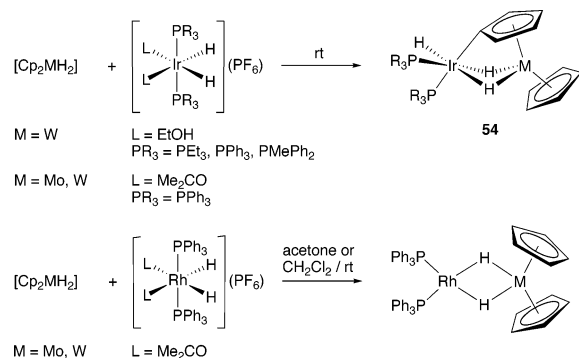


The reactions of  $[\text{Cp}_2\text{MH}_2]$  (M = Mo, W) with Ir(III) octahedral cationic species also lead to C–H activation reactions. The iridium species  $[\text{Ir}(\text{cis-L})_2(\text{cis-H}_2)(\text{trans-PR}_3)_2]^+$  (L = C<sub>2</sub>H<sub>5</sub>OH, PR<sub>3</sub> = PET<sub>3</sub>, PMePh<sub>2</sub>, PPh<sub>3</sub>,<sup>89</sup> L = Me<sub>2</sub>CO, PR<sub>3</sub> = PPh<sub>3</sub>)<sup>90</sup> have all been reacted with either one or both of these metallocene dihydrides. The products are trihydrido heterobimetallic complexes **54** in which one of the group 6 metal's cyclopentadienyl groups has been transformed into a  $\mu$ - $\eta^1, \eta^5$ -C<sub>5</sub>H<sub>4</sub> ligand and in which two hydrido ligands are bridging. Interestingly, the reaction follows a different pathway with the analogous Rh species  $[\text{Rh}(\text{cis-Me}_2\text{CO})_2(\text{cis-H}_2)(\text{trans-PPh}_3)_2]$ , and no C–H activation is observed here (Scheme 34).<sup>90</sup>

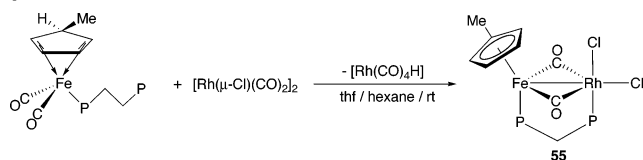
**2.4.3. Cleavage of Carbon(sp<sup>3</sup>)–Hydrogen Bonds**

As might be expected, these reactions are less common and require more-reactive metals. The examples listed below have the formation of an early (group 5)–late (group 9 or 10) heterobimetallic species in conjunction with the C–H activation reaction in common.

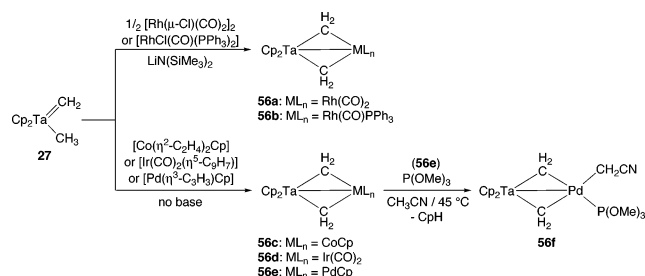
The sp<sup>3</sup>-hybridized C–H bond of the  $\eta^4$ -methylcyclopentadiene is cleaved when the complex  $[\text{Fe}(\eta^4\text{-C}_5\text{H}_5\text{Me})(\text{CO})_2(\eta^1\text{-dppm})]$  is reacted with  $[\text{Rh}(\mu\text{-Cl})(\text{CO})_2]_2$ .<sup>91</sup> The product **55** contains an  $\eta^5$ -methylcyclopentadienyl (C<sub>5</sub>H<sub>4</sub>Me) ligand (Scheme 35) and a now bridging dppm ligand. The proposed reaction mechanism invokes attack on the rhodium

**Scheme 34. Reactions of Group 6 Metallocene Dihydrides with Rhodium(III) and Iridium(III) Cations**


center, electron-transfer reactions, and metal–metal bond formation as the last step.

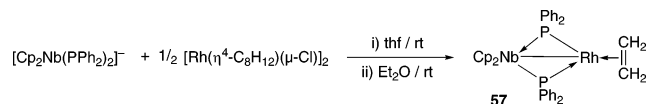
**Scheme 35. C–H Activation of an Olefinic Methylcyclopentadiene Hydrogen Atom Leading to an  $\eta^5$ -C<sub>5</sub>H<sub>4</sub>Me Heterobimetallic Complex**


Activation of the  $\text{sp}^3$ -hybridized C–H bond in the complex  $[\text{Cp}_2\text{Ta}(\text{=CH}_2)\text{Me}]$ , **27**, is seen together with metal–metal bond formation when the tantalum alkyl–alkylidene species is reacted with various group 9 complexes (Scheme 36) to give products **56**.<sup>92–94</sup> With rhodium complexes, the terminal  $\text{CH}_2$  group becomes a bridging ligand and the  $\text{CH}_3$  group of **27** is transformed into a  $\mu\text{-CH}_2$  group by the abstraction of one hydrogen atom with the base  $\text{LiN}(\text{SiMe}_3)_2$ .<sup>95</sup> Base addition is unnecessary when the complex  $[\text{Ir}(\text{CO})_2(\eta^5\text{-C}_5\text{H}_7)]$  is used (the indenyl ligand becomes the hydrogen acceptor here)<sup>93</sup> or when **27** is reacted with  $[\text{Co}(\eta\text{-C}_3\text{H}_4)_2\text{Cp}]$ .<sup>92</sup> Ethene is liberated in the reaction with the cobalt complex.

**Scheme 36. Methyl Group C–H Activation and  $\mu\text{-CH}_2$  Formation Following the Reaction of  $[\text{Cp}_2\text{Ta}(\text{=CH}_2)\text{Me}]$  with Cobalt, Rhodium, Iridium, and Palladium Complexes**


The reaction of **27** with  $[\text{Pd}(\eta^3\text{-C}_3\text{H}_3)\text{Cp}]$  evolves propene and affords a similar bis( $\mu\text{-CH}_2$ ) species, **56e**, in which the methylene ligands straddle the Pd–Ta bond.<sup>95,96</sup> The proposed mechanism is similar to that of the Ir–Ta reaction.<sup>93</sup> The palladium-bonded Cp ligand in **56e** is readily displaced to give a Ta–PdL<sub>2</sub> species (L = PR<sub>3</sub> ligands) and a free Cp<sup>−</sup> anion; in  $\text{CH}_2\text{Cl}_2$ , the molecule  $\text{CpCH}_2\text{Cp}$  is obtained. When **56e** is treated with  $\text{P}(\text{OMe})_3$  in  $\text{CH}_3\text{CN}$ , the Cp<sup>−</sup> anion that is formed activates acetonitrile to give complex **56f** (Scheme 36). The reaction leading to a Cp<sup>−</sup> anion has been investigated mechanistically.<sup>96</sup>

When the anionic niobium complex  $[\text{Cp}_2\text{Nb}(\text{PPh}_2)_2]^- \text{Li}^+$  was reacted with  $[\text{Rh}(\mu\text{-Cl})(\text{cod})]_2$ , the product was a surprising Nb–Rh complex **57** that contains an ethylene ligand  $\eta^2$ -linked to the rhodium atom. This unusual product, whose structure was established crystallographically, could only be isolated when the reaction solvent was  $\text{Et}_2\text{O}$ , and hence, the  $\text{C}_2\text{H}_4$  is believed to originate from this solvent (Scheme 37).<sup>97</sup> It is likely that many uncharacterized “decomposition” products in organometallic chemistry contain products resulting from C–H activation reactions with the solvent, but such products are rarely characterized.

**Scheme 37. Activation of  $\text{Et}_2\text{O}$  and Formation of a Heterobimetallic  $\eta^2$ -Ethene Complex**

**3. Carbon–Carbon Bond Formation on Preformed Heterobimetallic Frameworks**
**3.1. Alkyl–Carbonyl (“CO Insertion”), –Isocyanide, and –Cyanide Coupling**

These reactions are often alkyl group migrations onto a CO ligand (“CO insertion reactions”). The alkyl group is sometimes provided externally (frequently as a masked carbanion in the form of a lithium alkyl). Subsequent electrophilic addition to acyl groups frequently leads to Fischer carbene complexes. While there are fewer examples with heterobimetallic complexes than there are in monometallic chemistry, this section is still relatively large. It is conveniently divided in two parts, depending on whether carbon monoxide is pre-coordinated onto a heterobimetallic complex as a carbonyl ligand or whether it is introduced as a free CO ligand. No mechanistic classification is implied by this subdivision, and the reactions are in most cases probably mechanistically similar since they are frequently induced by an added nucleophile (CO or a general ligand, L). In this particular section, the term alkyl is used in a very general sense and includes alkenyl and alkynyl groups. Note that various hydrocarbyl–carbonyl ligand couplings on different monometallic fragments have already been discussed (sections 2.1.1, 2.1.4, 2.1.6, and 2.1.7).

There are many examples of alkyl migration reactions on heterobimetallic frameworks induced by added CO ligands. In addition, many transition metal combinations are represented. In most cases, the two metal centers are anchored together by ligands, frequently of the 1,2-bis(diarylphosphine)alkane type, that stabilize the bimetallic system. Migratory insertion reactions generate acyl complexes that are  $\sigma$ -bonded via the carbonyl carbon atom to one metal. If a second metal can also bond to the acyl group through the oxygen atom of the RCO group, the acyl will be stabilized. Many bimetallic acyls, especially those formed with an oxophilic early transition metal, show this kind of interaction with the oxygen atom of the  $\mu\text{-}(\text{O},\text{C})$ -acyl-bonded to the early transition metal. Recently, examples of this bonding mode with late transition metals have also been observed.

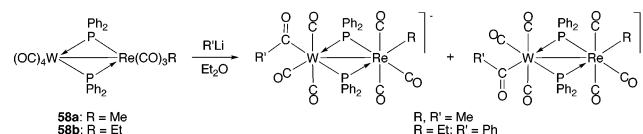
Some examples of alkyl–isocyanide coupling reactions (isocyanide insertion reactions) are known, but they are much less common than alkyl–carbonyl coupling reactions. As in mononuclear chemistry, isocyanide ligands show a larger propensity toward multiple insertions. Alkyl–cyanide cou-

pling remains quite rare, and only a handful of examples are known.

### 3.1.1. Alkyl–Carbonyl Coupling without External CO Addition

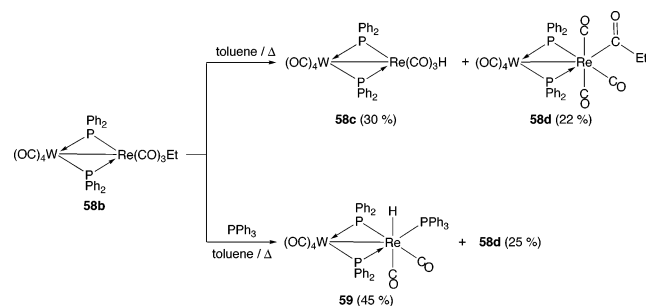
Early examples of these reactions were those of the alkylrhenium–tungsten complexes **58a** and **58b**, which contain  $\mu$ -phosphido ligands that anchor the two metals together, with alkyllithium reagents. The reaction led to a mixture of anionic acyl stereoisomers, in which the new acyl groups are in a *cisoid* or *transoid* conformation relative to the alkyl groups on the rhenium atom (Scheme 38).<sup>98</sup> (Another example of acyl formation was referred to earlier in Scheme 12).<sup>58</sup>

#### Scheme 38. Formation of a Bimetallic Acyl by Nucleophilic Attack on a Coordinated CO Group



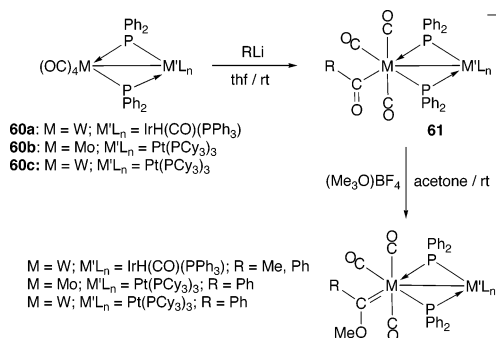
Simply heating the ethyl complex **58b** (Scheme 38) on its own in toluene leads to two different products: a  $\beta$ -hydride elimination reaction affords a hydride complex **58c**, while an ethyl migration yields acyl complex **58d** (Scheme 39) in slightly lower yield. When **58b** is heated in toluene with  $PPh_3$ , the acyl species **58d** was again obtained, but the *cis*-triphenylphosphine hydride complex **59** was also formed.<sup>98</sup>

#### Scheme 39. Thermally Induced Ethyl Group Migration on a Rhenium–Tungsten Complex



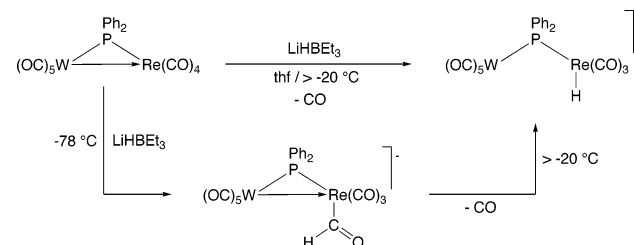
Reactions of the iridium–tungsten complex **60a**, shown in Scheme 40, with methyl- or phenyllithium give group 6 metal-bonded anionic acyl species **61**, which can be isolated in high yields (>90%).<sup>99,100</sup> The acyl can be alkylated with  $Me_3O^+BF_4^-$  to give the corresponding Fischer carbene complexes. The carbene ligand is not bridging but is terminally bonded to tungsten, as was established by a single-crystal X-ray diffraction study for the phenyl(methoxy)-tungsten–iridium species.<sup>99,100</sup> The Pt–Mo and –W complexes **60b** and **60c** behave similarly with phenyllithium (Scheme 40).<sup>101,102</sup> The latter examples contrast sharply with the behavior of  $ArLi$  species with either  $[cis-M(CO)_4L_2]$  ( $M = Cr, Mo, W$ ) or  $[(OC)_4W(\mu-PPh_2)_2ZrCp_2]$ , where no reaction is observed in each case. The acyl complex stereochemistry is different from that “expected” and, according to a Hückel MO study, stems from the higher electron density present in the equatorial CO groups in the Mo–Pt or W–Pt species. The results provide “an unusually clear illustration of the way in which cooperativity...can occur.”<sup>101,102</sup>

#### Scheme 40. Acyl and Fischer Carbene Formation in a Heterobimetallic Complex



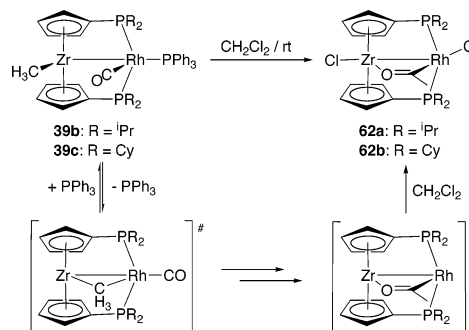
The rhenium–tungsten complex  $[(OC)_4Re(\mu-PPh_2)W(CO)_5]$  ( $Re-W$ ), in which there is a weak donor–acceptor bond of 3.111(1) Å, reacts with  $LiHBEt_3$  at  $-78^\circ C$  (Scheme 41) to give a spectroscopically observed rhenium-bonded formyl anion. However, this complex decarbonylates on heating and affords a rhenium terminal hydride species.<sup>103</sup>

#### Scheme 41. Formation of a Thermally Unstable Formyl Complex by Hydride Attack on a Coordinated CO Ligand



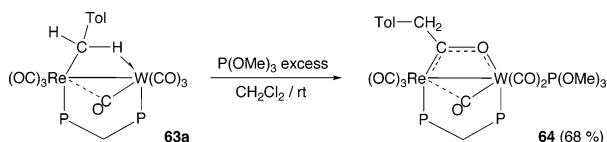
The Rh–Zr species **39b** and **39c** shown in Scheme 42 undergo formal intramolecular CO insertion into their Rh–Me bonds and chlorine atom abstraction (from the solvent) to give complexes **62** in which there are  $\mu-O(Zr),C(Rh)-CH_3CO$  ligands. The structures of complexes **62a** ( $R = i-Pr$ ) and **62b** ( $R = Cy$ ) were both determined.<sup>71</sup>

#### Scheme 42. Bridging Acyl Formation in Rhodium–Zirconium Alkyl Complexes



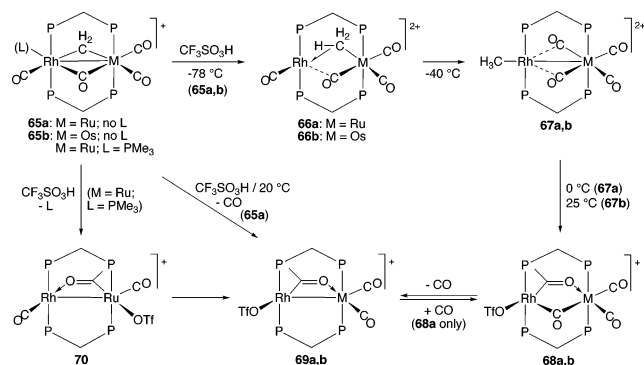
Alkyl groups in which there are agostic bridging interactions to a second metal have been shown to undergo formal CO insertions. The substituted benzyl ligand in the Re–W complex **63a** is transformed into a  $\mu(O,C)$ -acyl ligand by addition of  $P(OMe)_3$ . The phosphite ligand formally replaces a tungsten carbonyl that now presumably forms part of the acyl ligand (Scheme 43). The structure of the  $\mu$ -acyl species **64** was determined by an X-ray diffraction study. A Re–W bond of 3.155(1) Å is present.<sup>104,105</sup>

Bridging  $\mu(O,C)$ -acyl complexes have been isolated as the end result of a low-temperature protonation of cationic Rh–

**Scheme 43. A P(OMe)<sub>3</sub>-Induced Benzylic Group Migration To Afford a  $\mu$ -Acyl Ligand**


Ru or Rh–Os  $\mu$ -CH<sub>2</sub> complexes. These late transition metals are not generally considered to be oxophilic, but nevertheless, examples of the oxygen atom of the acyl being bonded to Rh, to Ru, and to Os are described in the two papers discussed here.

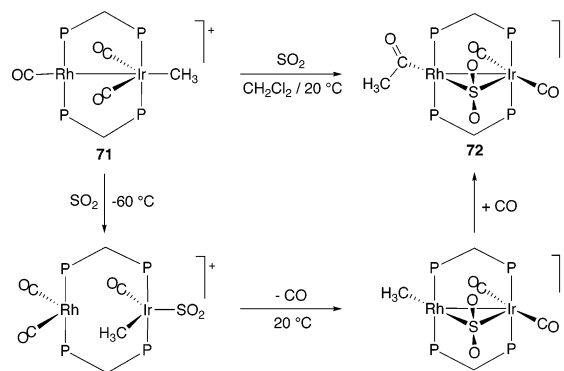
Treatment of cations **65a,b** with CF<sub>3</sub>SO<sub>3</sub>H at –78 °C led to dicationic  $\mu$ -CH<sub>3</sub> species **66**. The methyl groups in each complex are  $\sigma$ -bonded to the group 8 metals and undergo an agostic C–H interaction with the rhodium. When these dications are warmed to –40 °C, the methyl group migrates completely onto the rhodium atom to give **67**. The Rh–Ru complex **67a** is transformed into a  $\mu$ -acyl species **68a** at 0 °C, while the CF<sub>3</sub>SO<sub>3</sub><sup>–</sup> ligand simultaneously coordinates to the rhodium atom. In this complex, the acyl O-atom is bonded to ruthenium and the acyl carbon is rhodium-bonded. The Rh···Ru distance of 3.3992(4) Å is a nonbonded distance. Finally,  $\mu$ -acyl **68a** reversibly decarbonylates to give a new metal–metal-bonded [Rh–Ru = 2.6953(4)]  $\mu$ -acyl species **69a** with no bridging CO groups and with the same acyl-to-metal bonds (O–Ru, C–Rh).<sup>106</sup> The Rh–Os cation **65b** behaves similarly to the Rh–Ru system **65a**. The principal differences are (i) the need for a somewhat higher temperature for acyl formation and (ii) the decarbonylation of **68b** to **69b** is not reversible.<sup>107</sup> These complex transformations are detailed in Scheme 44.

**Scheme 44. Formation of  $\mu$ -(O,C) Acyl Complexes Spanning Rhodium–Ruthenium and –Osmium Bonds**


When the same reaction sequence is attempted on the rhodium-bonded PMe<sub>3</sub> adduct of **65a**, the first acyl product isolated, after loss of PMe<sub>3</sub> is **70**, which is an isomer of **69a**. In complex **70**, the  $\mu$ -CH<sub>3</sub>C(O) ligand is O-bonded to the rhodium and C-bonded to the ruthenium. However this isomer converts to **69a** within a few hours (Scheme 44).<sup>106</sup>

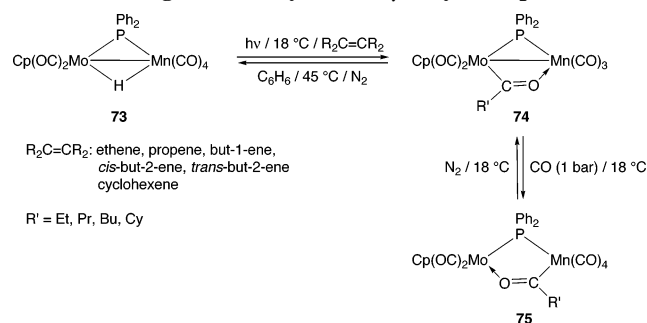
The iridium-bonded methyl group in the dppm-bridged cationic complex [(OC)Rh( $\mu$ -dppm)<sub>2</sub>Ir(CH<sub>3</sub>)(CO)<sub>2</sub>]<sup>+</sup> (Rh–Ir, **71**) undergoes a migration to form a rhodium-bonded acetyl ligand when treated with SO<sub>2</sub>. The  $\mu$ -SO<sub>2</sub>-bridged cation [(MeC(O)Rh( $\mu$ -dppm)<sub>2</sub>( $\mu$ -SO<sub>2</sub>)Ir(CO)<sub>2</sub>]<sup>+</sup> **72** (Scheme 45) is formed. The metal–metal bond is retained. A mechanism was proposed, based on spectroscopically observed low-temperature intermediates in this reaction. It involves the initial formation of a terminal (Ir-bonded) SO<sub>2</sub> ligand, followed by a methyl migration to the rhodium atom

accompanied by CO loss, and finally, addition of CO and migration of the methyl group onto a carbonyl ligand.<sup>108</sup>

**Scheme 45. An SO<sub>2</sub>-Induced Migratory CO Insertion on an Iridium–Rhodium Framework**


The reaction of a metal carbonyl hydride with an alkene may generate an acyl. These species probably arise through initial addition of the alkene to the hydride to give a metal alkyl intermediate, which then migrates onto a neighboring coordinated CO ligand. These are key steps of the hydroformylation reaction.

When the Mn–Mo hydride species [(OC)<sub>4</sub>Mn( $\mu$ -PPh<sub>2</sub>)( $\mu$ -H)Mo(CO)<sub>2</sub>Cp] (Mn–Mo) **73** reacts with a variety of alkenes under photolytic conditions, the products are  $\mu$ (O,C)-acyl species **74** that are O-bonded to the Mn and C-bonded to the Mo atoms. They contain Mn–Mo bonds. However, when **74** are treated with CO, the Mn–Mo bond cleaves and the acyl ligand flips to become C-bonded to Mn and O-bonded to Mo. Both reactions are readily reversible under the conditions outlined in Scheme 46. Representative structures of **74** and **75** were obtained by X-ray diffraction.<sup>109</sup>

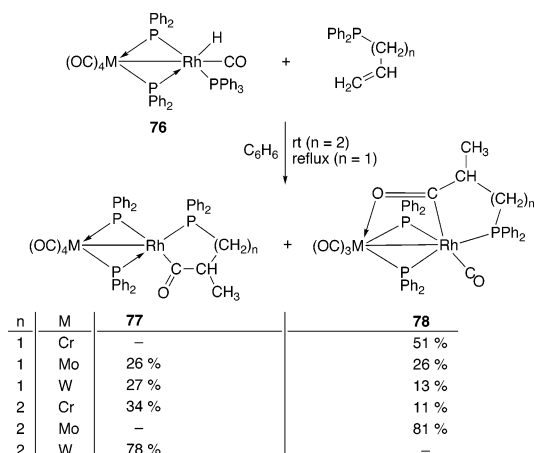
**Scheme 46. Reversible Formation and Alternative Binding Modes of Manganese–Molybdenum  $\mu$ -Acyl Complexes**


Reactions of the mixed-metal complexes [(OC)<sub>4</sub>M( $\mu$ -PPh<sub>2</sub>)<sub>2</sub>RhH(CO)PPh<sub>3</sub>] (Rh–M, M = Cr, Mo, W) **76** were investigated with phospho-alkenes, PPh<sub>2</sub>(CH<sub>2</sub>)<sub>n</sub>CH=CH<sub>2</sub> (*n* = 1, 2). These ligands were chosen to chelate, and thus stabilize, organometallic species that mimic or represent intermediates in the catalytic hydroformylation reaction. The reaction products were, in general, two acyl species, **77** and **78**, whose yields were quite sensitive to the nature of M and to the length of the phosphine chain, *n*. The products and their yields as a function of the metal and the phosphine ligand are summarized in Scheme 47.<sup>110</sup>

**3.1.2. Alkyl–Carbonyl Coupling with External CO Addition**

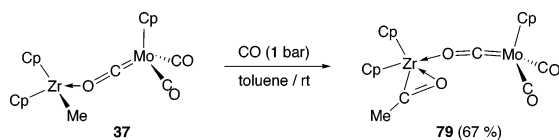
A long known example of alkyl–CO (external) coupling is shown in Scheme 48.<sup>66</sup> The molybdenum/zirconium

**Scheme 47. Formation of Acyl Complexes as a Function of the Phosphaalkene and the Metal in [(OC)<sub>4</sub>M(μ-PPh<sub>2</sub>)<sub>2</sub>RhH(CO)PPh<sub>3</sub>] (Rh–M, M = Cr, Mo, W) Complexes**



methyl complex **37** reacts with CO to give the  $\pi$ -acetyl product **79**, which is carbon- and oxygen-bonded to the oxophilic zirconium (as established by a subsequent single-crystal X-ray diffraction study).<sup>67</sup> The metals in **79** are not directly bonded but are held together by a linear  $\mu$ -CO that is O-coordinated to the zirconium atom. Labeling experiments with <sup>13</sup>CO-enriched **37** unambiguously establish that the CO group in the  $\pi$ -CH<sub>3</sub>CO group arises from the added CO.<sup>66</sup> The reaction is not readily reversible (yields  $\leq 4\%$ ). Complex **79** reacts with protic sources (H<sub>2</sub>O or CF<sub>3</sub>CO<sub>2</sub>H) to give acetaldehyde.

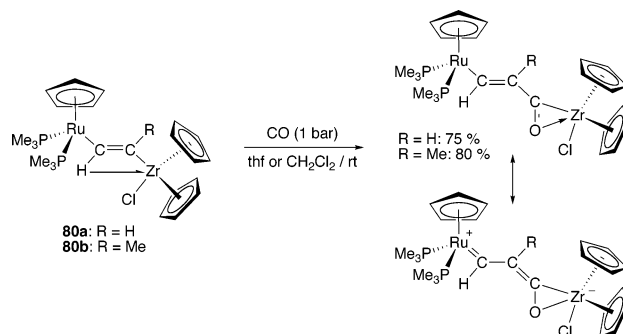
**Scheme 48. CO Insertion into a Molybdenum/Zirconium Methyl Complex**



Another example with the metal zirconium now associated with ruthenium is seen in the dimetalla-ethene complexes **80a** and **80b**. These complexes, in which there is an agostic interaction between the C–H group  $\alpha$  to the ruthenium atom toward the zirconium, react with CO to give the  $\eta^2$ -acyl insertion products (Scheme 49). The structure of these species, characterized by X-ray diffraction, has considerable contributions from the zwitterionic form shown in the scheme and two others (not shown). Evidence for these zwitterionic contributions is manifested in structural data and spectroscopically. For example in the IR spectrum of the R = H complex,  $\nu(\text{CO})_{\text{acyl}} = 1443 \text{ cm}^{-1}$ , and in the <sup>13</sup>C NMR spectrum of this species, the ruthenium-bonded carbon atom, which now has carbenoid character, appears at  $\delta(\text{C}) = 246.5 \text{ ppm}$ .<sup>72</sup>

Cowie and his co-workers have published a vast body of work, which is ongoing, on the reactions of heterobimetallic complexes with small organic molecules, and not surprisingly, “CO insertion” reactions have been observed frequently. The reported examples contain two common parameters: (1) a heavier group 9 metal (Rh or Ir) as one of the two metals in the heterobimetallic complex and (2)  $\mu$ -dppm ligands that lock the two metals together. Occasionally there are differences in reactivity between Rh–M and Ir–M complexes. While even non-oxophilic metals oc-

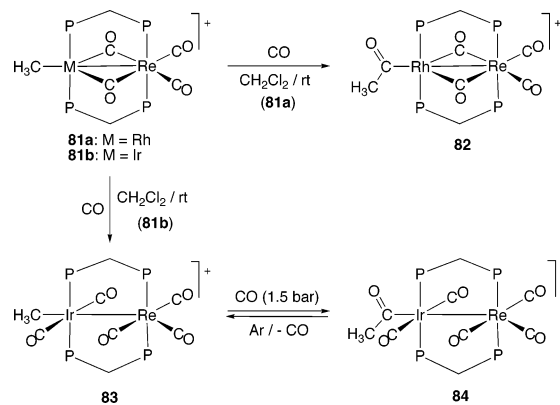
**Scheme 49. CO Insertion into the Zirconium–Carbon Bond of a Ruthenium/Zirconium Dimetalla-ethene Complex**



asionally bind to acyl oxygen atoms, the acyl ligands that are produced in these reactions are terminally bonded via their RC(=O)– carbon atom and the acyl oxygen atom is not involved in bonding to any metal.

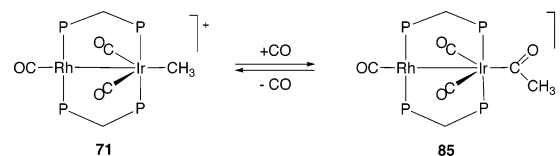
The reaction of the Rh–Re cation **81a** with CO converts the rhodium-bonded methyl group into a rhodium-bonded acetyl group and generates the acyl cation **82** (Scheme 50). The reaction with the analogous Ir–Re cation **81b** proceeds somewhat differently, as the CO addition product is a simple CO adduct (**83**) and not the corresponding acyl cation. All five CO ligands in **83** are terminal. The Ir–Re acyl cation **84** can be obtained under slight CO pressure, but **84** is in equilibrium with the alkyl cation **83**, and it decarbonylates rapidly under an argon purge.<sup>111</sup>

**Scheme 50. Different Reactivities of Isostructural Rhodium- and Iridium-Rhenium Cations with CO**



Many acyl complexes form reversibly, and this is the case when the bis( $\mu$ -dppm) Rh–Ir complex **71** is reacted with CO to give **85** (Scheme 51); the reaction of the Ir<sub>2</sub> analog of **71** proceeds similarly.<sup>112</sup>

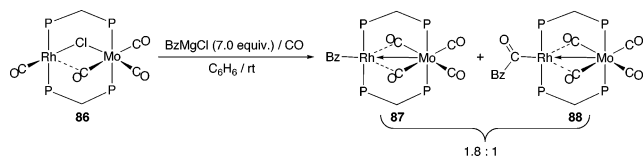
**Scheme 51. Addition of CO to an Iridium–Rhodium Complex To Generate an Acetyl Species**



The reaction of BzMgCl with the Mo–Rh complex **86** (Scheme 52) gives a 1.8:1 mixture of the benzyl complex **87** and the corresponding acyl **88**. The alkyl or acyl group in each case is bonded to rhodium. Both the alkylation and acylation require CO (no alkylation products are obtained in its absence), and pentacarbonyl species are likely inter-

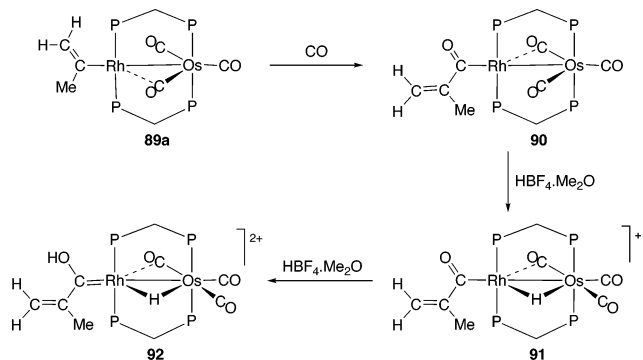
mediates. The reaction is specific to BzMgCl as only metal alkyls (no acyls) are obtained with other Grignards, RMgX, where R = vinyl, allyl, Me, or Ph.<sup>113</sup>

#### Scheme 52. Formation of an Acyl and a Benzyl Complex under Mild CO Pressure



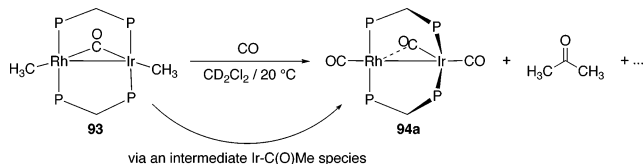
In general, it is more difficult to carry out “CO insertions” with alkenyl ligands. Nevertheless, the Rh–Os  $\sigma$ -bonded propenyl complex **89a** does undergo a CO insertion when reacted with CO. Protonation of the resultant acyl species **90** with HBF<sub>4</sub>·Me<sub>2</sub>O yields a cationic bridging hydride complex **91**, which in turn may be further protonated to the hydroxycarbene dication **92**. This series of reactions is shown in Scheme 53.<sup>114</sup>

#### Scheme 53. Formation of a Rhodium–Osmium Acyl and Its Conversion to a Hydroxycarbene Dication



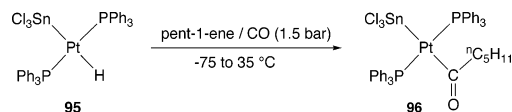
Acyl complexes that are formed via alkyl–carbonyl coupling are sometimes not isolated but are observed as intermediates. The reaction of the A-frame complex [RhMe( $\mu$ -CO)( $\mu$ -dppm)<sub>2</sub>IrMe] (Ir–Rh) **93** with CO leads to the absorption of three molar equivalents of CO per mole of complex. This reaction, shown in Scheme 54, generates an intermediate acetyl species that undergoes reductive elimination with C–C coupling to give acetone. This intermediate was not clearly identified, but the single acyl carbonyl resonance observed in the <sup>13</sup>C NMR spectrum did not show rhodium coupling, strongly suggesting that the acyl is iridium bonded. The final metallic product is **94a**.<sup>115</sup>

#### Scheme 54. Generation of Acetone via an Intermediate Iridium–C(O)Me Species



Migratory CO insertion reactions have also been observed in complexes with platinum–tin bonds. The platinum–tin hydride complex **95** undergoes an olefin insertion (i.e., a reverse  $\beta$ -hydrogen elimination), followed by a CO insertion reaction when treated with pent-1-ene and CO (1.5 bar). The product is the acyl complex **96** *trans*–[(Ph<sub>3</sub>P)<sub>2</sub>Pt(COC<sub>5</sub>H<sub>11</sub>)–SnCl<sub>3</sub>] as shown in Scheme 55.<sup>116</sup>

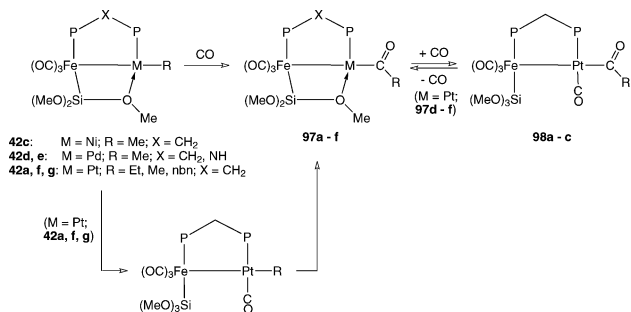
#### Scheme 55. Acyl Formation from a Tin–Platinum Hydride, Pentene, and Carbon Monoxide



Many examples of alkyl migration reactions are observed in bimetallic Fe–M systems (M = usually Pd, sometimes Ni, Pt). These reactions take advantage of hemilabile  $\mu$ -Si(OMe)<sub>3</sub> groups, which are bonded via their silicon atoms to the iron and via one of the methoxy oxygen atoms to the group 10 metal atom. These reversible interactions protect the electronically unsaturated group 10 metal when necessary.

The Fe–Pd and Fe–Pt systems **42** (Scheme 56) add on CO in a series of migratory insertion reactions to give palladium- or platinum-bonded acetyl complexes **97**.<sup>74,117</sup> Multiple insertions of CO and alkenes such as norbornadiene ensue if these ligands are subsequently added to the Fe–Pd system (section 3.5.2). For the Fe–Pt system, intermediates could be spectroscopically characterized, but no multiple insertions were observed. Instead, two acyl complexes (**97** and **98**) were accessible as a function of the CO pressure (Scheme 56).<sup>74</sup> Addition of *t*-BuNC to the Fe–Pt alkyl complex led to simple addition of the isocyanide (and not to formal isocyanide insertion). A Fe–Pt acyl does form when this species is treated with CO, but the reaction is very slow.<sup>74</sup>

#### Scheme 56. Migratory Insertion on Iron–Group 10 Metal Frameworks



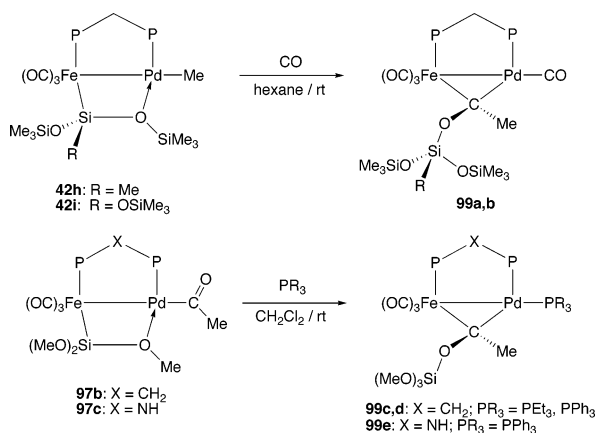
This reaction has been extended to related systems. It is observed when the  $\mu$ -dppm ligand in the Fe–Pd system is replaced by a  $\mu$ -Ph<sub>2</sub>P–NH–PPh<sub>2</sub> group.<sup>118</sup> Migratory insertion reaction to give Fe–Ni(COMe) species is also seen when a nickel atom replaces the palladium or platinum in the Fe–Ni equivalents of **42** (Scheme 56).<sup>119</sup> The hemilabile trialkoxysilyl groups are not always required: the Fe–Pd complex [(OC)<sub>4</sub>Fe( $\mu$ -dppm)PdCl(Me)] (Fe–Pd) forms the Pd-bonded acetyl species [(OC)<sub>4</sub>Fe( $\mu$ -dppm)PdCl(COMe)] (Fe–Pd) when treated with CO.<sup>120</sup>

When a Si(OSiMe<sub>3</sub>)<sub>2</sub>R (R = Me, **42h**; R = OSiMe<sub>3</sub>, **42i**) group replaces the Si(OMe)<sub>3</sub> group in the Fe–Pd systems shown in Scheme 56, the reaction proceeds further and the final products of the migratory insertions are the  $\mu$ -siloxy-carbene complexes **99** (Scheme 57). Labeling experiments with <sup>13</sup>CO indicate that the label is incorporated into the carbenoid carbon as well as onto the Pd-bonded CO group. The contrasting behavior between the Si(OMe)<sub>3</sub> and the Si(OSiMe<sub>3</sub>)<sub>2</sub>R derivatives may be assigned to the more electropositive character of the central silicon atom in the case of complexes **42h** and **42i** as OSiMe<sub>3</sub> substituents are less electron donating than OMe groups.<sup>121</sup> Thus,  $\mu$ -siloxy-



carbenes of type **99** are obtained from  $\text{Si}(\text{OMe})_3$  acyl complexes **97** when stronger donor ligands ( $\text{PEt}_3$  or even  $\text{PPh}_3$ ) are added.<sup>118</sup>

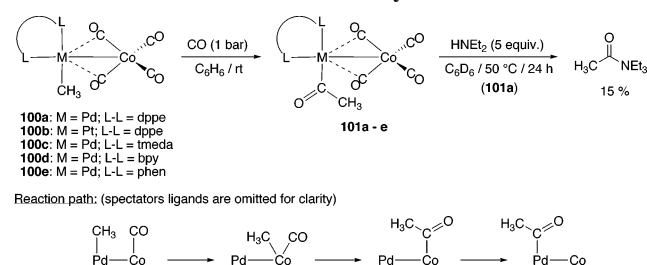
### Scheme 57. Migratory Insertion Reactions Leading to $\mu$ -Siloxycarbenes on Iron–Palladium Systems



The observations of Braunstein and co-workers concerning the lower reactivity of M–Pt versus M–Pd systems (and thus greater stability of intermediates for the M–Pt systems) are paralleled by Komiya and his group who, in a series of papers, studied the reactivity of palladium and platinum heterobimetallic complexes. The addition of CO to the Co–Pd complex  $[(\text{OC})_4\text{Co}-\text{Pd}(\text{Me})(\text{dppe})]$  **100a** in benzene at ambient temperature afforded the corresponding acyl  $[(\text{OC})_4\text{Co}-\text{Pd}(\text{COMe})(\text{dppe})]$  **101a** in high yield (85%). This complex liberates the amide  $\text{MeC}(\text{O})\text{NEt}_2$  in low yield when treated with excess diethylamine.<sup>122</sup> Time–yield curves show that the reaction of the corresponding Co–Pt complex **100b** is much slower and that of the monometallic  $[\text{Pd}(\text{dppe})(\text{Me})(\text{Cl})]$  is even slower (initial rates  $\sim 1/80$  that of the Co–Pd species **100a**). Monometallic  $[\text{Pt}(\text{dppe})(\text{Me})(\text{Cl})]$  does not even react, indicating that CO insertion is enhanced when the  $\text{Co}(\text{CO})_4$  group is attached to the methylpalladium or -platinum group.<sup>122,123</sup>

The reaction has been extended to other  $[(\text{OC})_4\text{Co}-\text{Pd}(\text{Me})\text{L}_2]$  complexes **100** ( $\text{L}_2 = \text{tmeda}$ ,  $\text{bipy}$ ,  $\text{phen}$ ).<sup>124</sup> The mechanism of these reactions was studied by analyzing the fast reaction rates, by a <sup>13</sup>CO labeling study, and by hybrid density function calculations (B3LYP) on the model complex  $[(\text{OC})_4\text{Co}-\text{Pd}(\text{Me})(\text{H}_2\text{PC}_2\text{H}_4\text{PH}_2)]$ .<sup>123</sup> These results (Scheme 58) collectively suggest that methyl group migration from the palladium to the cobalt takes place, followed by a methyl migration onto a Co-bonded CO ligand followed by an acyl migration from the cobalt atom onto the palladium.<sup>122–124</sup>

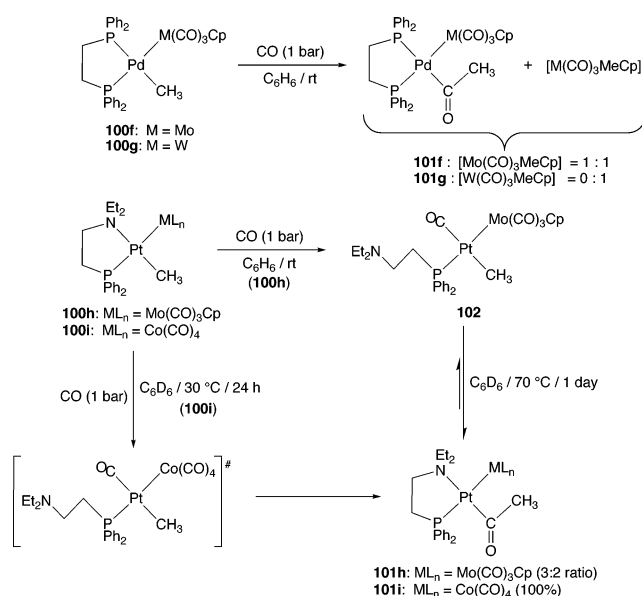
### Scheme 58. Migratory Insertion Reactions on Cobalt–Palladium and –Platinum Systems



Similar migratory insertion reactions have been observed in palladium–molybdenum and –tungsten systems, but the reaction is much less efficient. When the Pd–Mo complex

$[\text{Cp}(\text{OC})_3\text{Mo}-\text{PdMe}(\text{dppe})]$  (Mo–Pd, **100f**) was treated with CO, a mixture consisting of the bimetallic acyl  $[\text{Cp}(\text{OC})_3\text{Mo}-\text{Pd}(\text{COMe})(\text{dppe})]$  (Mo–Pd) **101f** and its reductive elimination product  $[\text{Mo}(\text{CO})_3\text{MeCp}]$  was obtained in approximately a 1:1 ratio. However, the analogous W–Pd complex **100g** did not afford the corresponding acyl complex and only gave  $[\text{W}(\text{CO})_3\text{MeCp}]$ . A theoretical study suggested that the more electron-rich tungsten fragment strengthens the CO bonds significantly through back-donation and cannot stabilize the Pd–W bond; the outcome is simple alkyl transfer to the tungsten atom, followed by reductive elimination (Scheme 59).<sup>122,123</sup>

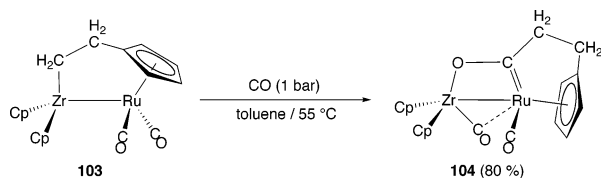
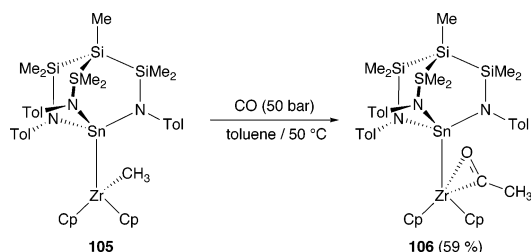
### Scheme 59. Migratory Insertion Reactions on Mixed-Metal Frameworks with Chelating Ligands on Palladium or Platinum



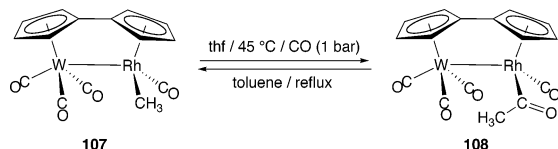
The alkyl complex **100h**, formed by formal replacement of the Pd(dppe) unit in **100f** by a  $\text{Pt}(\text{Et}_2\text{NC}_2\text{H}_4\text{PPh}_2)$  group, could be induced to form the acetyl complex **101h** (Scheme 59). This acyl exists in equilibrium with the phosphorus-bonded monodentate  $\text{Et}_2\text{NC}_2\text{H}_4\text{PPh}_2$  alkyl species **102**: the two species are present in a 3:2 ratio at 70 °C. The analogous complex **100i**  $[(\text{OC})_4\text{Co}-\text{Pt}(\text{Et}_2\text{NC}_2\text{H}_4\text{PPh}_2)\text{Me}]$  affords the corresponding acyl **101i** much more quickly. The reaction goes to completion via an alkyl carbonyl intermediate that is structurally similar to **102**.<sup>125</sup>

Many bimetallic migratory insertion reactions have been reported in which one of the two metals is zirconium. The oxophilic metal is able to stabilize the resulting acyl by O-coordination. The reaction of the Ru–Zr complex **103** with CO at 55 °C and 1 atm pressure affords an acyl complex **104** (Scheme 60) that is best considered to be an oxycarbene complex. The structure of **104** was determined by X-ray diffraction, and this revealed that the Ru–Zr bond was retained. Evidence that supports a carbene description of this species comes from IR spectroscopy [ $\nu(\text{CO}_{\text{acyl}}) = 1380 \text{ cm}^{-1}$ ] and from the very low field chemical shift of the acyl CO in the <sup>13</sup>C NMR spectrum ( $\delta = 279 \text{ ppm}$ ). The carbene is ligated to the zirconium via its oxygen atom.<sup>10,126</sup>

The tin–methylzirconocene complex **105** reacts with CO under pressure (50 bar) to afford the C,O-coordinated acetyl **106** shown in Scheme 61, whose structure was established crystallographically. The Sn–Zr bond is retained in the product, but there are no acyl–tin interactions.<sup>127</sup>

**Scheme 60.** The Reaction of a Ruthenium–Zirconium Complex with CO Leads to an Oxycarbene**Scheme 61.** The Reaction of a Tin–Zirconium Complex with CO

The Rh–W fulvalene-bridged heterobimetallic species **107** shown in Scheme 62 forms the acetyl complex **108** when treated with CO. The reaction is reversible, and the acyl decarbonylates and is reconverted to the methyl species **107** when heated. The structure of the acyl species **108** was determined crystallographically. A  $^{13}\text{C}$ O labeling study established that the migratory insertion involves a coordinated CO ligand.<sup>128</sup>

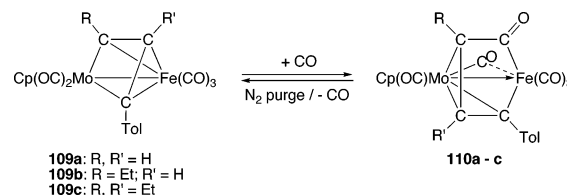
**Scheme 62.** The Reaction of a Rhodium–Tungsten Fulvalene Bridged Complex with CO

The iron–tungsten anion  $[\text{Me}(\text{CO})_4\text{Fe}-\text{W}(\text{CO})_5]^-$  (Fe–W, Me *cis* to Fe–W bond) reacts with CO to form the anionic iron acyl  $[\text{Fe}(\text{CO})_4(\text{COMe})]^-$ . This species, rather than a heterobimetallic complex, is obtained quickly and quantitatively. The migratory insertion can also be induced by adding excess  $\text{PPh}_3$  and leads to the acyl  $[\text{Fe}(\text{CO})_3(\text{PPh}_3)(\text{COMe})]^-$ .<sup>129</sup>

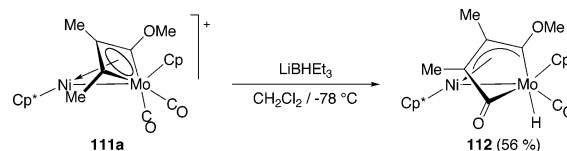
### 3.1.3. Couplings of Metallacyclic Groups with Carbonyl Ligands

A few examples of CO insertion into a metallacycle are known. The Fe–Mo metallacyclic complexes **109**, which can be considered to contain molybdenacyclobutadienyl ligands bonded to iron, shown in Scheme 63, undergo CO addition when the complexes are exposed to an atmosphere of carbon monoxide. Ring expansion reactions to give five-membered ferracyclopentenone species **110** follow. However, the rings now contain iron and not molybdenum, so the ring expansion reactions are accompanied by ring flips. The reactions may be reversed when the products are exposed to  $\text{N}_2$ .<sup>130</sup>

A similar “CO insertion” reaction is seen with the Ni–Mo metallacycle **111a** (Scheme 64),<sup>131</sup> but this ring expansion reaction is induced by addition of the nucleophile  $\text{HBET}_3^-$  to the mixed-metal metallacycle and not by CO addition. Unlike the Fe–Mo example just cited, the new five-membered ring complex **112**, characterized spectroscopically,

**Scheme 63.** Reversible Ring CO Insertion into a  $\text{MoC}_3$  Metallacycle Leads to Acyl Formation and Ring Flip To Give a  $\text{FeC}_4$  Ring

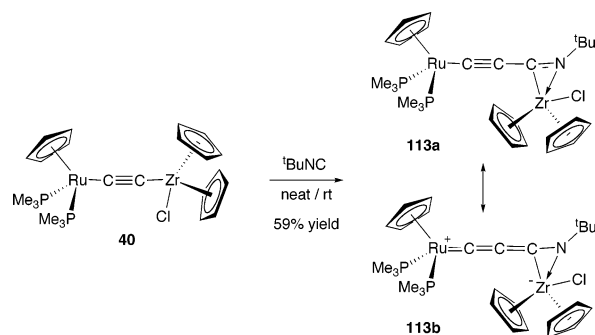
is still a molybdenacycle (a ring flip to form a molybdenacycle from an initial nickelacycle occurs at an earlier stage).<sup>131</sup>

**Scheme 64.**  $[\text{BHEt}_3]^-$  Induces a CO Migratory Insertion into a  $\text{MoC}_3$  Metallacycle and Generates a Five-Membered Ring

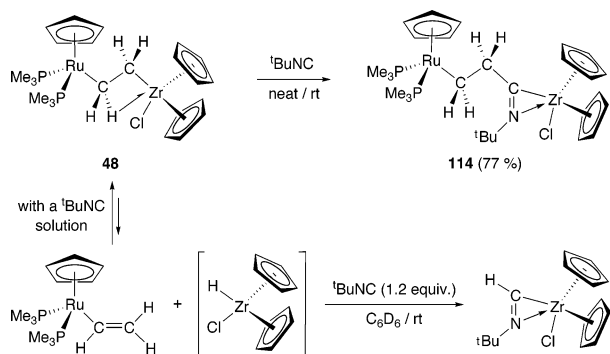
### 3.1.4. Alkyl–Isocyanide and –Cyanide Coupling

Fewer examples of these reactions have been reported than for CO insertion reactions. Many complexes that insert RNC ligands also insert CO ligands. One major difference between alkyl migratory insertion reactions onto isocyanide ligands and onto carbonyl ligands is that with isocyanide ligands, multiple insertions are frequently observed. Most known examples of multiple isocyanide insertions come from the reactions of monometallic alkyls, but examples are known in heterobimetallic chemistry. Some initial examples come from complexes without metal–metal bonds but in which the metals are bridged by various  $\text{C}_2$  ligands.

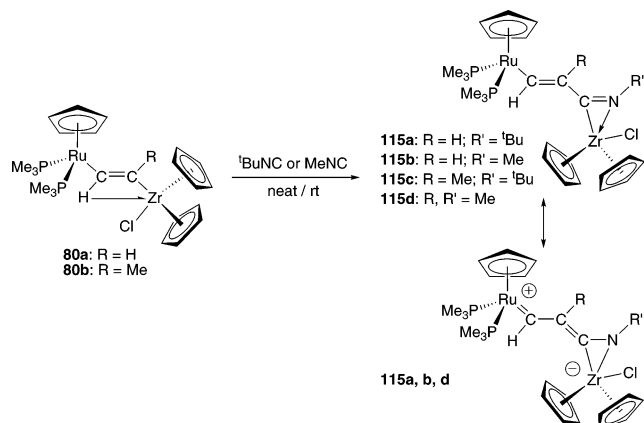
The ruthenium/zirconium dimetalla-alkyne complex **40** reacts with *t*-BuNC to give the  $\eta^2$ -iminoacyl complex **113**. This reaction is interesting as the insertion of isocyanides (and of carbon monoxide) into M–C alkynyl bonds is rarely observed. IR and NMR data suggest that the zwitterionic resonance form (**113b**) shown in Scheme 65 is a moderate contributor to the structure.<sup>132</sup>

**Scheme 65.** Addition of *t*-BuNC to a Ruthenium/Zirconium Dimetalla-alkyne Complex

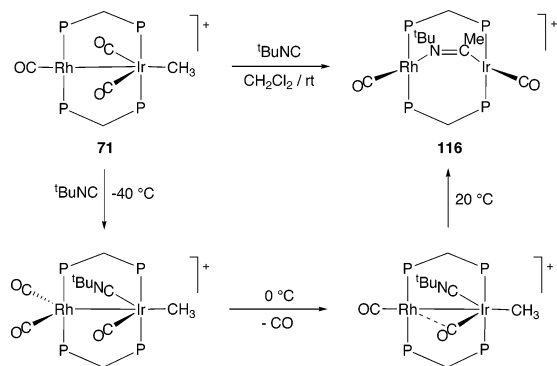
A similar reaction, described in the same article as in the previous paragraph, occurs when the dimetalla-alkane complex **48** (which contains an agostic interaction) is dissolved in neat *t*-BuNC. The  $\eta^2$ -iminoacyl product **114** is solely obtained under these reaction conditions. However, if a lower concentration of isocyanide is used,  $\beta$ -elimination competes with isocyanide insertion, as shown in Scheme 66.<sup>132</sup>

**Scheme 66. Addition of *t*-BuNC to a Ruthenium/Zirconium Dimetalla-alkane Complex**


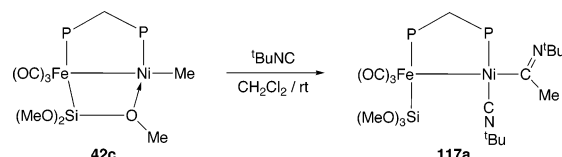
Related complexes **80** also insert both MeNC and *t*-BuNC to give  $\eta^2$ -iminoacyl species **115** as shown in Scheme 67. The reaction of **80a** with *t*-BuNC proceeds via the formation of a kinetic isomer (not shown), which transforms, following first-order reaction kinetics, into the final thermodynamic product **115a**. Evaluation of the spectroscopic and structural data of the  $\eta^2$ -iminoacyl complexes **115** show that the zwitterionic resonance contribution shown in the scheme is important for complexes **115a,b,d**, but not for complex **115c**.

**Scheme 67. Formation of  $\eta^2$ -Iminoacyl Complexes from Isocyanide Addition to Ruthenium/Zirconium Dimetalla-alkene Complexes**


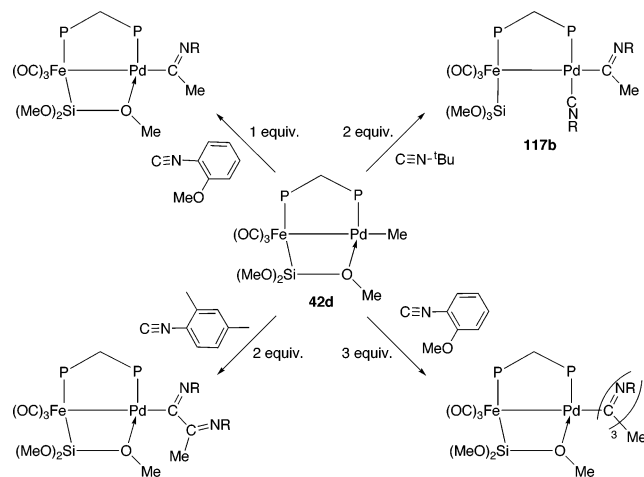
Complex **71** undergoes a migratory insertion reaction with CO, which was discussed earlier (Scheme 51).<sup>112</sup> It also reacts with *t*-BuNC, as shown in Scheme 68. There is no metal–metal bond in the final product **116**, and both metals are in a 16-electron configuration.<sup>108</sup>

**Scheme 68. Alkyl Migration onto an Isocyanide Ligand in a Rhodium–Iridium Complex**


Many Fe–M (M = group 10 metal) complexes of type **42**, previously presented in Schemes 56 and 57, undergo isocyanide “insertion” reactions. In many cases, the products are analogous to those obtained in the corresponding CO reactions. For example, the Fe–Ni complex **42c** formally inserts *t*-BuNC into the Ni–Me bond to give **117a** as shown in Scheme 69.<sup>119</sup> A  $\mu$ -Si(OR) group is not always necessary as the related complex [(OC)<sub>4</sub>Fe( $\mu$ -Ph<sub>2</sub>PNHPPH<sub>2</sub>)PdClMe] (Fe–Pd) forms the Pd-bonded species [(OC)<sub>4</sub>Fe( $\mu$ -Ph<sub>2</sub>-PNHPPH<sub>2</sub>)-PdCl{C(NR)Me}] (Fe–Pd) when treated with RNC (R = Bz, 2,4-Me<sub>2</sub>C<sub>6</sub>H<sub>3</sub>).<sup>120</sup>

**Scheme 69. Isocyanide Insertion into an Iron–Nickel Methyl Complex**


The Fe–Pd complex **42d** (Scheme 56) undergoes multiple isocyanide insertions with various isocyanide ligands. Depending on the nature of the R group in RNC and the molar excess of ligand added, single (R = *t*-Bu, **117b**; 2-MeOC<sub>6</sub>H<sub>4</sub>), double (R = 2,4-Me<sub>2</sub>C<sub>6</sub>H<sub>3</sub>), or triple (R = 2-MeOC<sub>6</sub>H<sub>4</sub>) isocyanide insertions have been observed. These interesting reactions are summarized in Scheme 70.<sup>117</sup>

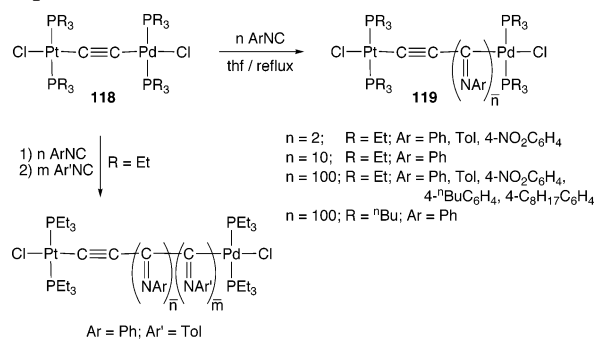
**Scheme 70. Single and Multiple RNC Insertions into a Palladium–Methyl Bond on an Iron–Palladium Framework**


Multiple isocyanide insertions have also been observed in dipalladium and palladium/platinum dialkynyl complexes. The mixed Pd/Pt complexes **118** (R = Et) react with 2 molar equiv of various aryl isocyanides in refluxing thf to afford complexes **119** in which two aryl isocyanides have regioselectively inserted into the palladium alkynyl bond.<sup>133</sup> At room temperature or in refluxing dichloromethane, simple isocyanide-for-chloride substitution occurs. This contrasts to the equivalent reaction on the Pd/Pd dialkynyl complex, which undergoes insertion at room temperature.<sup>134,135</sup>

When a large excess of aryl isocyanide is present, complexes **118** readily undergo multiple insertions. Thus with 10 molar equiv of ArNC, complexes **119** with an average value of  $n = 10$  can be isolated. The system is believed to be an example of living polymerization as various experiments are in accord with this observation. Thus, large numbers of isocyanide ligands can be inserted sequentially to give high molecular weight polymers. Block copolymers can be isolated by adding  $n$  molar equiv of one aryl

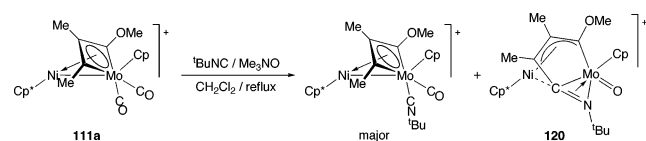
isocyanide ( $\text{ArNC}$ ) followed by  $m$  molar equiv of a second one ( $\text{Ar}'\text{NC}$ ). These results are summarized in Scheme 71.<sup>133</sup>

**Scheme 71. Multiple Aryl Isocyanide Insertions into a Palladium–Alkynyl Bond of a Palladium/Platinum Dialkynyl Complex**



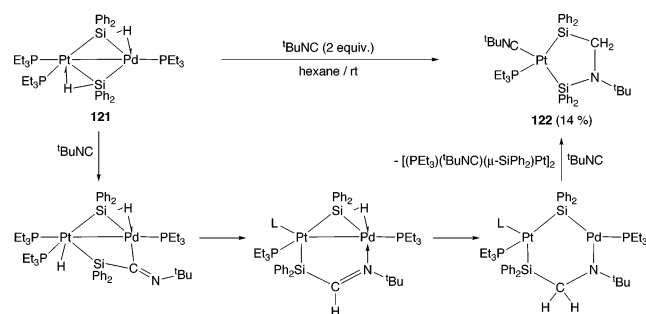
When  $t\text{-BuNC}$  and  $\text{Me}_3\text{NO}$  were added to the cationic metallacycle **111a** (shown previously in Scheme 64), the expected CO substitution product shown in Scheme 72 was the major (but not isolated) product. Another product, **120**, formed in lower yield, resulted from the insertion of  $t\text{-BuNC}$  into a Mo–C bond of the molybdenacycle ring. This product, which was characterized by an X-ray diffraction study, also contains a Mo=O bond, and the modified organic group is still ligated to both metals. The Ni $\cdots$ Mo interaction is too long to be considered a single bond [Ni $\cdots$ Mo = 3.0625(9) Å], but the metals are close enough that there may be some bonding electron density between them. Presumably,  $\text{Me}_3\text{-NO}$  acts as the oxidant in this reaction and delivers the oxo group to the molybdenum atom.<sup>131</sup>

**Scheme 72. Oxidative Insertion of  $t\text{-BuNC}$  into a Molybdenum–Carbon Bond**



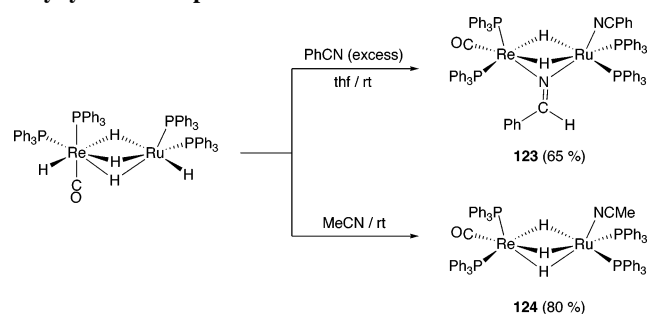
The Pd–Pt complex  $[(\text{Et}_3\text{P})\text{Pd}(\mu\text{-SiPh}_2\text{H})_2\text{Pt}(\text{PEt}_3)_2]$  (Pd–Pt) **121** contains agostic-like Si–H–M interactions to both the Pd and the Pt atoms. This complex reacts in an unusual way with  $t\text{-BuNC}$ : this ligand is believed to insert into a Si–Pd bond. Hydrogen transfer reactions follow, and after the elimination of  $[(\text{Et}_3\text{P})(t\text{-BuNC})\text{Pt}(\mu\text{-SiPh}_2)_2\text{Pt}(t\text{-BuNC})(\text{PEt}_3)]$  and of uncharacterized palladium isocyanide complexes, the platinumacycle species **122** shown in Scheme 73 was isolated. This molecule was characterized by X-ray diffraction, and the presumed reaction scheme is outlined here.<sup>136</sup>

**Scheme 73. Insertion of  $t\text{-BuNC}$  into a Palladium–Silicon Bond and Subsequent Reactions**



A rare example of a cyanide insertion reaction has been reported on a heterobimetallic template. When the Re–Ru pentahydride complex  $[(\text{Ph}_3\text{P})_2(\text{OC})\text{HRe}(\mu\text{-H})_3\text{RuH}(\text{PPh}_3)_2]$  (Scheme 74) is reacted with excess benzonitrile, the ligand formally inserts into one of the  $\mu\text{-H-M}$  bonds and affords complex **123**, which contains a bridging benzylideneimido ligand. This complex is an unsaturated 32-electron species, but the Re–Ru bond of 2.654(1) Å is not particularly short. The second PhCN group in **123** has replaced two hydride ligands. The reaction follows a different pathway with acetonitrile: there is no nitrile insertion, and the acetonitrile ligand simply coordinates to the ruthenium atom in complex **124**.<sup>137</sup>

**Scheme 74. Nitrile Insertion into a Rhodium–Ruthenium Polyhydride Complex**

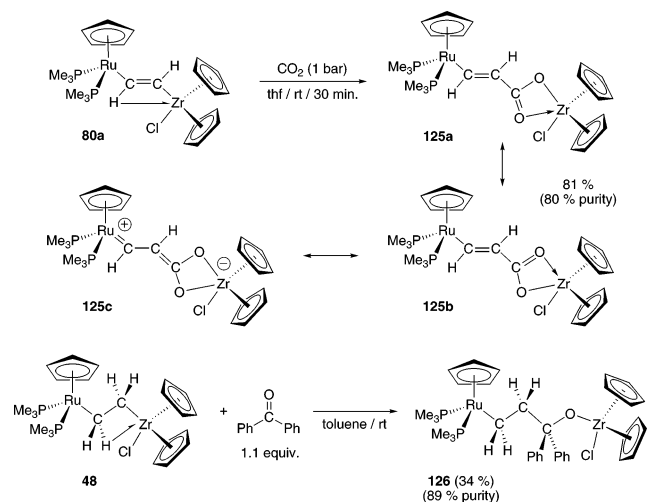


**3.1.5 Other Hydrocarbonyl Group Couplings with Carbonyl Groups**

This section covers the coupling reactions of C=O groups with alkyl (in the most general sense of the term) ligands. Examples of ketone and carbon dioxide couplings with alkyl ligands are presented.

The complex **80a** incorporates  $\text{CO}_2$  when exposed to 1 bar of this gas to give the  $\eta^2$ -bonded carboxylate complex **125**. Spectroscopic evidence exists that there is a modest contribution of the zwitterionic resonance structure **125c** to the two other hybrids **125a** and **125b**, as shown in Scheme 75.<sup>132</sup> The related complex **48** reacts with benzophenone to give **126**.  $\beta$ -Elimination from **48** competes with the reaction that leads to **126** to give a 5:2 mixture of the latter and the vinylic species  $[\text{Ru}(\text{PMe}_3)_2(\text{CH}=\text{CH}_2)\text{Cp}]$ . These two separate reactions are treated for convenience in the same

**Scheme 75. Addition Reactions of C=O Bonds to Ruthenium/Zirconium Complexes**



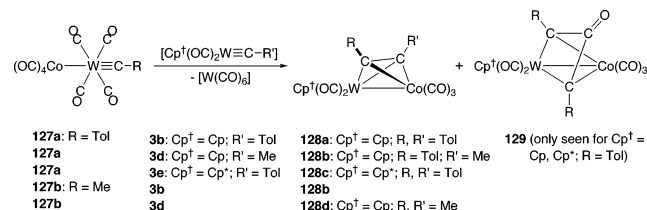
scheme. Note that neither **125** nor **126** could be structurally characterized.<sup>132</sup>

## 3.2. Carbyne–Ligand Coupling

### 3.2.1. Carbyne–Carbyne Coupling

The reactions of the cobalt–tungsten alkyldiene complexes **127** with the Fischer carbyne complexes **3b**, **3d**, or  $[\text{Cp}^*-(\text{OC})_2\text{W}\equiv\text{C}\text{Tol}]$ , **3e** (Scheme 76), yield heterobimetallic

**Scheme 76. Carbyne–Carbyne Coupling Reactions Resulting in Heterobimetallic Complexes**



species in which the carbyne carbon atoms have coupled with each other, or with a CO ligand. Two cobalt–tungsten heterobimetallic complexes are obtained:  $\mu\text{-RC}\equiv\text{CR}'$  species **128** (for all combinations of **127** and **3** attempted) and complexes **129** (formed in the reactions of **127a** with **3b** and **3e** only), in which there are bridging CTol–CO–CTol groups as summarized in the scheme.<sup>138</sup>

### 3.2.2. Carbyne–Alkyl Coupling

These coupling reactions take place either by nucleophilic addition of R<sup>−</sup> or by the electrophilic addition of R<sup>+</sup> to the carbyne carbon atom of  $\mu$ -carbyne complexes. When the electrophilic alkyl group additions are successful, H<sup>+</sup> additions are also attempted. However, these protonation reactions lead to C–H bond formation, and they are discussed later in section 5.1.1.

#### 3.2.2.1. Nucleophilic (Carbanion) Addition to Carbynes.

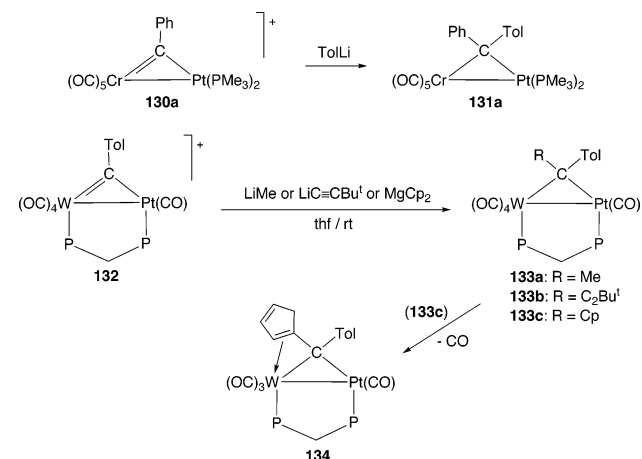
An early example of C–C bond formation via carbanion attack on a cationic carbyne complex was observed with the Cr–Pt species  $[(\text{OC})_5\text{Cr}(\mu\text{-CPh})\text{Pt}(\text{PMe}_3)_2]^+$  (Cr–Pt, **130a**). Addition of tolyllithium yielded the neutral  $\mu$ -diaryl alkyldiene complex  $[(\text{OC})_5\text{Cr}\{\mu\text{-C}(\text{Ph})(\text{Tol})\}\text{Pt}(\text{PMe}_3)_2]$  (Cr–Pt, **131a**).<sup>139</sup>

Cationic Pt–W carbyne complexes behave similarly. The cation  $[(\text{OC})_4\text{W}(\mu\text{-dppm})(\mu\text{-CTol})\text{Pt}(\text{CO})]^+$  (Pt–W, **132**) reacts with MeLi, *t*-BuC≡CLi, or MgCp<sub>2</sub> to give  $\mu$ -alkyldiene complexes **133**. A Pt–W derivative with a  $\mu\text{-C}(\text{Tol})\text{-Cp}$  ligand can be isolated with one CO ligand less than the others; in this complex **134**, the Cp group is  $\eta^2$ -bonded to the tungsten atom via an olefinic C=C bond, as shown in Scheme 77.<sup>140</sup>

#### 3.2.2.2. Electrophilic (Carbocation) Addition to Carbynes.

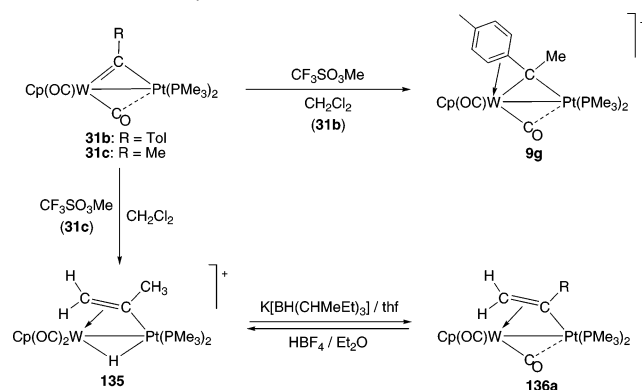
Platinum–tungsten carbyne complexes react with electrophilic alkyls. The addition of Me<sup>+</sup> as methyl triflate to  $[(\text{Me}_3\text{P})_2\text{Pt}(\mu\text{-CTol})\text{W}(\text{CO})_2\text{Cp}]$  (Pt–W, **31b**) led to the  $\mu$ -alkyldiene complex **9g** shown in Scheme 78, in which the electron deficiency at the tungsten center is relieved by  $\eta^2$ -coordination from the tolyl ring.<sup>141,142</sup> (Olefinic  $\eta^2$ -coordination has also been observed on other electron-deficient Pt–W complexes as shown in Schemes 3 and 77.)<sup>33,140</sup> This olefinic interaction cannot happen when the ethyldiene complex **31c** is alkylated with methyl triflate, so the product instead is the cationic  $\mu$ -alkenyl  $\mu$ -hydrido complex **135** (Scheme 78). The hydride ligand in **135** can be abstracted with potassium

**Scheme 77. Nucleophilic Attack on the Alkyldiene Carbon Atom of Cationic  $\mu$ -Carbyne Complexes To Give  $\mu$ -Alkyldiene Species**



selectride,  $\text{K}^+[\text{BH}(\text{CHMeEt})_3]^-$ , to give the neutral alkenyl complex **136a**.<sup>143,144</sup>

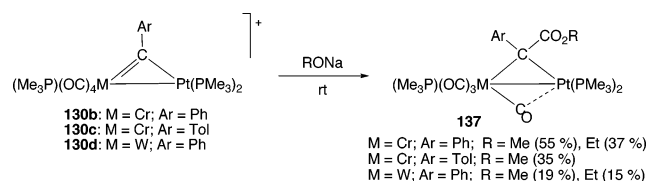
**Scheme 78. Electrophilic Attack on the Alkyldiene Carbon Atom of Cationic  $\mu$ -Carbynes**



### 3.2.3. Carbyne–Carbonyl Coupling

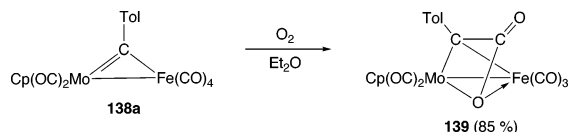
A possible example of this kind of reaction was reported long ago by Stone and co-workers. When the platinum–chromium and –tungsten cationic carbyne complexes **130b–d** shown in Scheme 79 were reacted with methoxide or ethoxide anions, the products were bimetallic complexes **137**, which contained bridging C(Ar)(CO<sub>2</sub>R) carbene ligands (Ar = Ph, Tol; R = Me, Et). These products are consistent with a mechanism that involves alkoxide-induced metal-assisted CO transfer to the  $\mu\text{-CAr}$  ligands and alkoxide attack on the carbyne-bonded CO ligand. However it is possible that there is initial alkoxide attack on a metal-bonded CO ligand, followed by migration of the ester group to the  $\mu\text{-CAr}$  carbon atom. The structures of the starting complexes **130**, unlike those of some of the products, have not been established by X-ray crystallography.<sup>139,145</sup>

**Scheme 79. Reactions That May Involve Carbyne–Carbonyl Coupling on a Heterobimetallic Center**



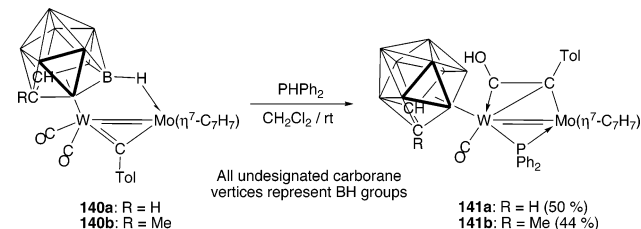
When the  $\mu$ -carbyne complex **138a** (Scheme 80) is exposed to  $O_2$ , an unusual coupling reaction ensues between the carbyne carbon, a CO ligand, and an oxygen atom. The structure of the product **139**, obtained in 85% yield, is shown in the scheme.<sup>146</sup>

#### Scheme 80. Carbyne–CO–Oxygen Coupling in an Iron–Molybdenum $\mu$ -Carbyne Complex



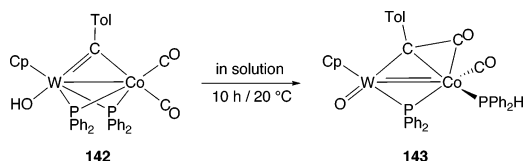
The unsaturated Mo=W carborane complexes **140** shown in Scheme 81 contain a formal Mo=W double bond, a  $\mu$ -C(tolyl) ligand, and an agostic-like B–H interaction from the tungsten-bonded carborane bridging to the molybdenum atom. Complexes **140** undergo a phosphine-induced CO insertion reaction when treated with  $PPh_2H$ . It is proposed that this ligand oxidatively adds to the dimetal center forming  $\mu$ -PPh<sub>2</sub> and  $\mu$ -H groups. The hydrogen then adds onto the ketyl intermediate. The final isolated products are the protonated  $\mu$ -ketyl complexes **141** shown in the scheme; the structure of one of these complexes was established via X-ray diffraction.<sup>147</sup>

#### Scheme 81. Formation of Protonated $\mu$ -Ketyl Derivatives by $PPh_2H$ Addition to Unsaturated Mo=W Carbyne Complexes



A ketyl complex is also formed when the Co–W  $\mu$ -alkylidyne complex **142** shown in Scheme 82 is maintained in solution.<sup>148</sup> The tungsten-bonded hydroxy group is transformed into an oxo group, and a hydrogen migration ensues onto a  $\mu$ -PPh<sub>2</sub> group to give a Co-bonded PPh<sub>2</sub>H ligand. Simultaneously, there is a coupling reaction between the  $\mu$ -CTol group and a carbonyl ligand to give complex **143**. The structures of **142** and **143** were established by single-crystal X-ray diffraction studies; surprisingly the two complexes have practically the same Co–W bond lengths despite the formal difference in bond multiplicities [2.594(1) and 2.584(1) Å, respectively, for the initial and final products].

#### Scheme 82. Carbyne–Carbonyl Coupling on a Cobalt–Tungsten Framework



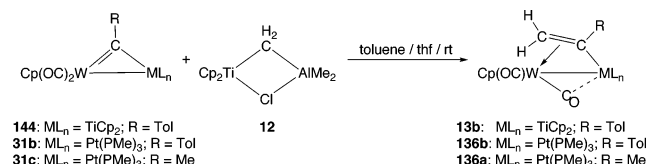
### 3.2.4. Carbyne–Carbene Coupling

To date, the only examples of these reactions stem from Stone's group; the carbene (or strictly alkylidene) in question is  $CH_2$ , and it is chemically bonded either as Tebbe's reagent,  $[Cp_2Ti(\mu-CH_2)(\mu-Cl)AlMe_2]$ , **12**, or as diazomethane,  $CH_2N_2$ .

The products of a single methylene addition are alkenyl complexes, but multiple methylene insertions are sometimes observed.

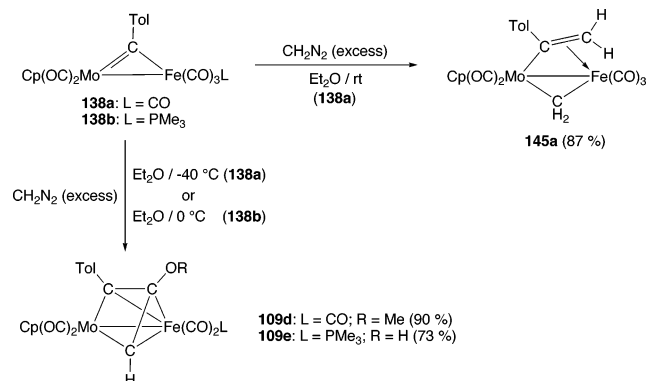
Early examples of this type of reaction were provided by the reactions of  $\mu$ -carbyne species with complex **12**. Both the Ti–W complex **144** and the Pt–W complexes **31b** and **31c** react with **12**.<sup>149</sup> These reactions (Scheme 83) yield the heterobimetallic alkenyl complexes **13b**, **136b**, and **136a**, respectively; in each case, the  $\mu$ - $\eta^1, \eta^2$ -CR=CH<sub>2</sub> is ligated to both metals via the CR carbon atom and to the tungsten atom via the CH<sub>2</sub> carbon atom.<sup>40</sup>

#### Scheme 83. Reactions of $\mu$ -Carbyne Complexes with Tebbe's Reagent To Give $\mu$ -Alkenyl Species



Methylene addition can be induced by diazomethane. When  $CH_2N_2$  is added to the iron–molybdenum  $\mu$ -alkylidyne complexes **138**, alkenyl complexes may be obtained. Other products can be isolated if reaction conditions are carefully controlled. Thus, room temperature addition of excess  $CH_2N_2$  to **138a** yielded the  $\mu$ -alkenyl  $\mu$ -CH<sub>2</sub> complex  $[(OC)_3Fe(\mu-\eta^1, \eta^2-CTol=CH_2)(\mu-CH_2)Mo(CO)_2Cp]$  (Fe–Mo, **145a**), which is a product of sequential  $CH_2$  addition, in high yield (87%).<sup>146</sup> The same reaction carried out at  $-40$  °C afforded the molybdenacycle complex **109d** almost quantitatively (Scheme 84). It is speculated that complex **109d** forms from initial  $CH_2$  addition, which induces CTol–CO coupling. This is followed by a  $CH_2$ –(CO–CTol) coupling reaction, a hydrogen transfer reaction, and finally O-alkylation of the resulting CH–COH–CTol group by another  $CH_2$  moiety to give **109d**. The final oxygen alkylation does not take place when the PMe<sub>3</sub>-substituted complex **138b** is reacted with  $CH_2N_2$ .<sup>150</sup>

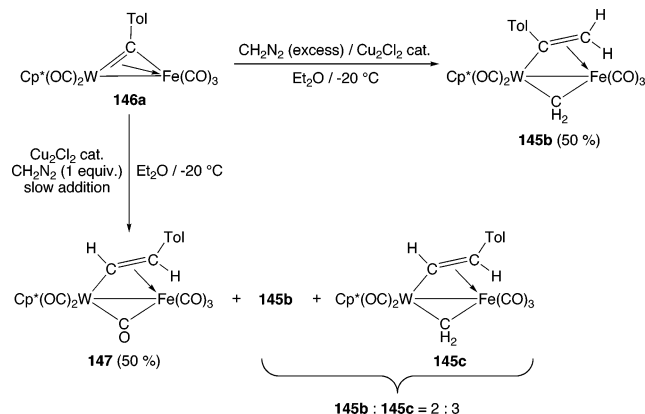
#### Scheme 84. Multiple $CH_2$ Addition to Iron–Molybdenum $\mu$ -Alkylidyne Complexes



Mechanistic information was gleaned from isotopic studies using specifically labeled <sup>2</sup>H and <sup>13</sup>C reagents. By using the labeled complex  $[(O^{13}C)_4Fe(\mu-CTol)Mo(^{13}CO)_2Cp]$  (Fe–Mo, **138a-<sup>13</sup>C<sub>6</sub>**) it was shown that the C(OMe) group of the metallacycle product **109d** comes from the bonded CO ligands. Dideuterodiazomethane afforded  $[(OC)_3Fe(\mu-\eta^1, \eta^2-CTol=CD_2)(\mu-CD_2)Mo(CO)_2Cp]$  (Fe–Mo, **145a-d<sub>4</sub>**) or the metallacycle **109d-d<sub>4</sub>**, in which there is a CD–C(OCD<sub>3</sub>)–CTol group.<sup>150</sup>

The iron–tungsten versions of complexes **138** are unstable. However the unsaturated Cp\* iron tricarbonyl complex [(OC)<sub>3</sub>Fe( $\mu$ -CTol)W(CO)<sub>2</sub>Cp\*] (Fe–W, **146a**) has greater stability, and diazomethane reactions have been investigated with this species. Single or double CH<sub>2</sub> addition products are observed, and they are accompanied by proton migration reactions on the alkenyl unit.<sup>151,152</sup> Excess CH<sub>2</sub>N<sub>2</sub> addition to **146a** at low temperature in the presence of a copper(I) chloride catalyst led to formation of [(OC)<sub>3</sub>Fe( $\mu$ - $\eta^1, \eta^2$ -CTol=CH<sub>2</sub>)( $\mu$ -CH<sub>2</sub>)W(CO)<sub>2</sub>Cp\*] (Fe–W) **145b**, which is closely related to the isostructural MoCp analog **145a** (Scheme 84). However slow room temperature addition of a molar equivalent of CH<sub>2</sub>N<sub>2</sub> yielded primarily the monoaddition product **147**, together with smaller quantities of **145b** and its regioisomer **145c**, both of which result from double methylene addition to **146a**. The *trans* stereochemistry found in the alkenyl protons of **145c** and **147** was established by <sup>1</sup>H NMR spectroscopy and is the result of proton migration reactions. Scheme 85 summarizes these transformations.<sup>151,152</sup>

### Scheme 85. Alkylidyne–Methylene Coupling Reactions on an Iron–Tungsten Framework



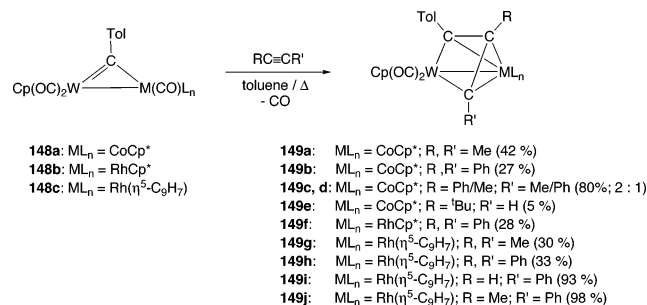
### 3.2.5. Carbyne–Alkyne Coupling

This class of reactions is richly represented. Almost all examples come from the group of Stone and co-workers. Most alkyne–alkylidyne couplings take place on a hetero-bimetallic complex in which at least one metal is Mo or W. The reactions are often accompanied by additional or concurrent CO–C(R) and CO–alkyne coupling reactions and usually proceed in relatively high yield and in high stereospecificity. In most cases, further reactions, usually protonations, have been carried out on the products. These protonation reactions are discussed under C–H formation reactions (section 5.1).

The alkylidyne carbyne atoms in the tungsten–cobalt and –rhodium  $\mu$ -methyltolylidyne complexes **148** react with free alkynes to give complexes **149**, which contain  $\mu$ - $\eta^2, \eta^3$ -C(R)–C(R′)–C(R′′) ligands, analogous to those observed in complexes **109** and **110**. In complexes **149**, these ligands are allylically bonded to the group 9 metal (Scheme 86).<sup>141,153–155</sup> The <sup>13</sup>C NMR chemical shifts for these three carbon atoms all fall in the range of  $\delta = 90$ –120 ppm. This indicates that they have no carbyne character. The products can alternatively be regarded as substituted tungstacyclobutadiene rings interacting with a CoCp\*, RhCp\*, or Rh( $\eta^5$ -C<sub>9</sub>H<sub>7</sub>) fragment. Viewed this way, the products are isolobally analogous to the well-known [M( $\eta^4$ -C<sub>4</sub>R<sub>4</sub>)( $\eta^5$ -C<sub>5</sub>R<sub>5</sub>)] complexes (M = Co, Rh). Terminal alkynes give highly regioselective products that have a C(Tol)–C(R)–C(H)

connectivity for the W–CoCp\* complexes (see complex **149e**) and a C(Tol)–C(H)–C(R) linkage in W–Rh( $\eta^5$ -C<sub>9</sub>H<sub>7</sub>) systems (see complex **149i**).

### Scheme 86. Coupling Reactions of Carbynes and Alkynes on Tungsten–Cobalt and –Rhodium Templates



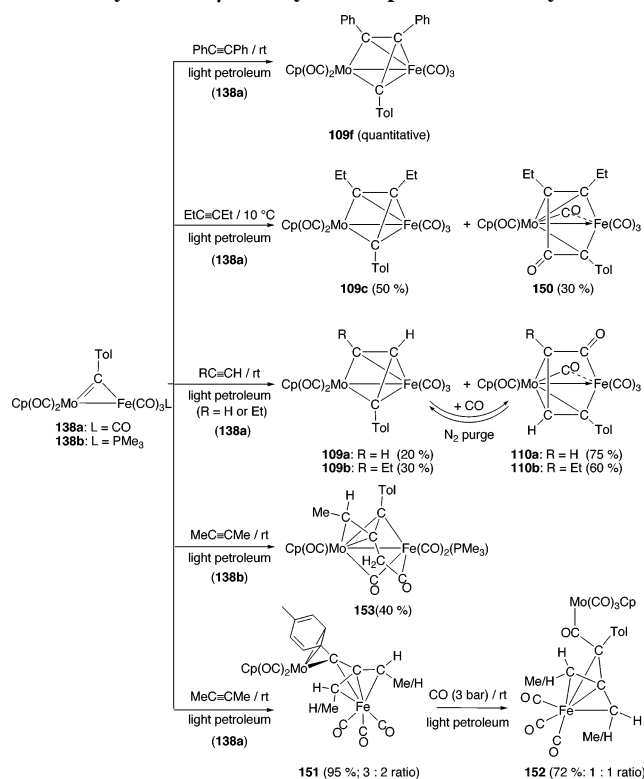
The reaction of PhC≡CPh with the W–RhCp\* **148b** species requires somewhat forceful conditions (refluxing toluene, up to 5 days).<sup>155</sup> However, reactions with the Rh( $\eta^5$ -C<sub>9</sub>H<sub>7</sub>) complex **148c** are more rapid. This difference is attributed to the “indenyl effect”, the facile creation of a vacant coordination site by  $\eta^5$ - to  $\eta^3$ -ring slippage of the indenyl ligand. In some cases, the rhodium complexes also afford trimetallic Rh<sub>2</sub>W  $\mu_3$ -tolylidyne clusters. Monometallic Rh species such as cyclopentadienone complexes are formed with more prolonged reaction times. Evidence suggests that complexes **149** are not formed by cluster fragmentation reactions.

The iron–molybdenum  $\mu$ -alkylidyne complexes **138** react with acetylenes, but the products of these reactions are very alkyne dependent (Scheme 87). In some cases, the organic ligands are similar to those found in complexes **149**. This is the case when diphenylacetylene reacts with complex **138a** to give **109f**, Scheme 87.<sup>156,157</sup> Hex-3-yne gives the similar species **109c**, but a byproduct of the reaction, **150**, contains an alkyne–CO–carbyne linkage and can be considered to be a ferracyclopentenone complex, that is, an isomer of **110c** (see Scheme 63).<sup>130,156</sup> Terminal alkynes afford ferracyclopentenone species of type **110** with alkylidyne–alkyne–CO rather than alkyne–CO–alkylidyne linkages. Both classes of complexes (**109**, molybdenacyclobutadienyl, or ferracyclopentenone species **110**) are obtained with ethyne or but-1-yne. These can be interconverted by adding CO to the dienyl complex (see Scheme 63) or by subjecting the enone species to a nitrogen purge.<sup>130</sup>

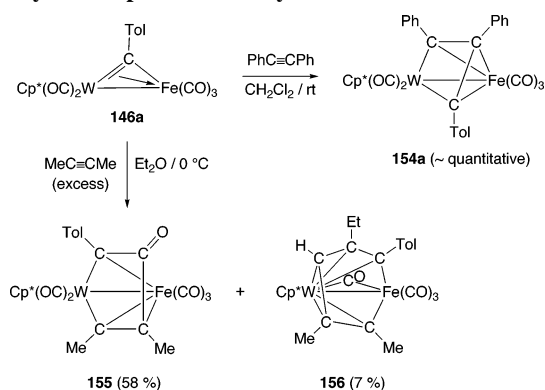
More complex products are obtained when 2-butyne is reacted with complex **138a**. Products **151** contain molybdenum-substituted “trimethylenemethane” moieties and exist as a 3:2 mixture of isomers in solution. There are no Fe–Mo bonds in these species as attested by the X-ray crystal structure of one of the isomers (Fe···Mo = 4.027 Å).<sup>156,157</sup> Isomeric mixture **151** undergoes a formal CO insertion to give a new 1:1 mixture of the molybdenum acyl trimethylenemethane products **152** shown in Scheme 87.<sup>157</sup>

In contrast, the reaction product of but-2-yne with **138b** is a C<sub>5</sub> fragment **153** ligated to both metals. This fragment is derived from the tolylmethylidyne group, a 2-butyne molecule, and a CO ligand. A metal–metal bond is present.<sup>156,157</sup> All these spectacular transformations and couplings are summarized in the very busy Scheme 87.

The reaction of the Fe–WCp\* complex **146a** with diphenylacetylene yielded complex **154a**, which is the WCp\* equivalent of the MoCp species **109f**. An alkyne–CO–CTol

**Scheme 87. Complex Coupling Reactions of Iron–Molybdenum  $\mu$ -Carbyne Complexes with Alkynes**


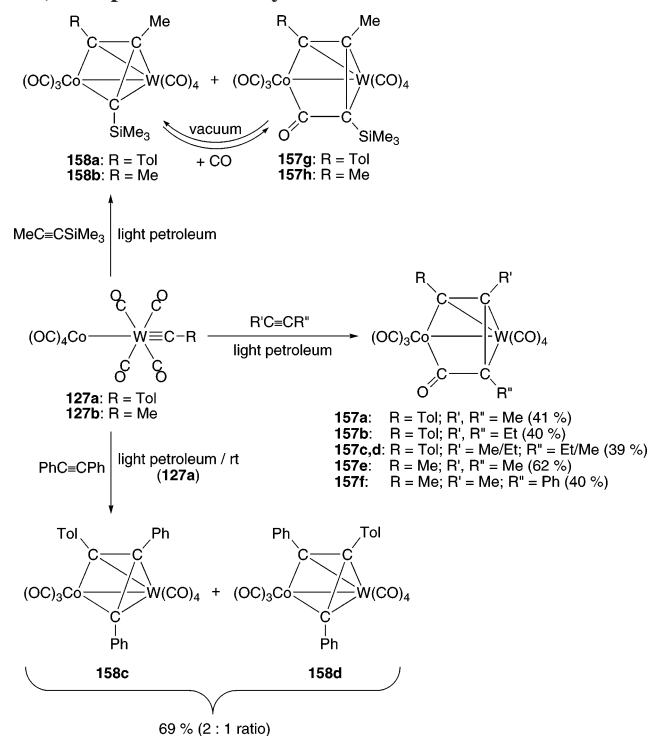
coupled complex **155** is obtained with but-2-yne. The organic linkage in metallacyclic complex **155** is similar to what is found in complex **150**, described in Scheme 87, but complex **150** is a ferracyclopentenone species, while **155** is a tungstacyclopentenone. Another more complex product, **156**, is derived from the coupling of 2 equiv of the alkyne with the alkylidyne carbon, followed by H-shift reactions. These reactions are all collected in Scheme 88.<sup>158</sup>

**Scheme 88. Reactions of an Unsaturated Iron–Tungsten  $\mu$ -Carbyne Complex with Acetylenes**


Alkyne coupling reactions with carbyne ligands can also take place if the dimetallic system contains a terminal carbyne ligand. Such reactions were attempted on complexes [L<sub>n</sub>M–W(CO)<sub>4</sub>≡CR] [ML<sub>n</sub> = Co(CO)<sub>4</sub> or Mo(CO)<sub>3</sub>Cp] in which the carbyne is ligated solely to the tungsten atom.

The [(OC)<sub>4</sub>Co–W(CO)<sub>4</sub>≡CR] (R = Me, Tol) systems **127**<sup>159,160</sup> react with disubstituted alkynes to give cobaltacyclopentenone complexes **157** that are  $\eta^3$ -coordinated to the tungsten atom. The coupling is regiospecific (alkylidyne carbon–alkyne–CO) and is the same as is found in the

ferracyclopentenone species **110**. Pent-2-yne yielded a mixture of isomers **157c** and **157d**, when the alkyne was reacted with **127a**. These isomers differ in the linkage of the alkyne to the other organic fragment. However only one isomer, **157f**, was obtained in the reaction of **127b** with PhC≡CMe.<sup>159</sup> The metallacycles **158** (structurally similar to metallacycles **109**, **149**, and **154**) are obtained regiospecifically with the unsymmetrical alkyne MeC<sub>2</sub>SiMe<sub>3</sub>.<sup>160</sup> Complexes **158a** and **158b** undergo reversible CO addition to give the cobaltacyclopentenone addition products **157g** and **157h**, respectively, as shown in Scheme 89. This CO insertion reaction, which is believed to occur in the last step mechanistically, seems to be favored when the end carbon of the C<sub>3</sub> unit carries an alkyl substituent.

**Scheme 89. Reactions of [(OC)<sub>4</sub>Co–W(CO)<sub>4</sub>≡CR] (R = Me, Tol) Complexes with Alkynes**


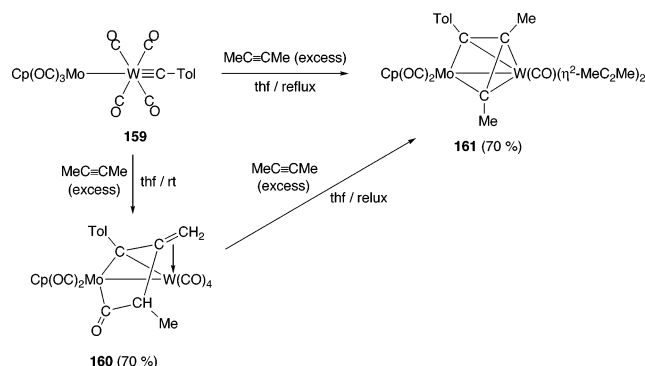
Indeed, no cobaltacyclopentenone species are obtained in the reaction of **127a** with PhC≡CPh. An isomeric mixture of the cobaltacyclobutadiene species **158c** and **158d** is obtained instead.<sup>160</sup> One isomer has a CTol–CPh–CPh linkage, while the other has a CPh–CTol–CPh connectivity. This remarkable result demonstrates that the alkyne has been cleaved into its constituent CPh fragments in this reaction. The migratory CO insertion reaction can also be induced by adding PPh<sub>3</sub> to the four-membered metallacycle.<sup>160</sup>

The Mo–W complex [Cp(OC)<sub>3</sub>Mo–W(CO)<sub>4</sub>≡CTol] **159** also exhibits a rich alkyne chemistry. The addition of but-2-yne to **159** at ambient temperature gave **160**, a product that results from alkylidyne–alkyne–CO coupling, together with H-shift reactions and multiple bond migrations (Scheme 90). All the tungsten-bonded CO ligands are still present. However the same reaction takes a different turn when conducted in refluxing thf. Product **161** is now a substituted molybdenacyclobutadiene ligand coordinated to a tungsten atom (similar to complexes **158**). In this new complex, all but one of the tungsten-bonded CO ligands have been replaced, and even the last remaining one may be displaced by the addition of PMe<sub>3</sub>. When heated with but-2-yne, **160**



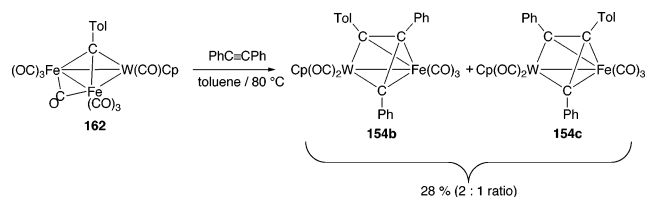
is converted to **161**; this shows that the H-migration reactions leading to complex **160** are easily reversed. Both **160** and **161** retain Mo–W bonds [of 3.131(1) and 2.971(1) Å, respectively].<sup>161</sup>

### Scheme 90. Addition of But-2-yne to a Molybdenum–Tungsten Terminal Carbyne Complex



Organic frameworks similar to those found in complexes **158c** and **158d** (Scheme 89) are obtained in a cluster degradation reaction. The  $\text{Fe}_2\text{W}$  cluster **162** reacts with  $\text{PhC}\equiv\text{CPh}$  to afford the isomers **154b** and **154c** (Scheme 91). In **154c**, the  $\text{C}\equiv\text{C}$  bond has been formally cleaved to afford a  $\mu\text{-}\eta^2\text{-}\eta^3\text{-CPh-CTol-CPh}$  ligand that spans the two metals as found in **158d**.<sup>153,154</sup>

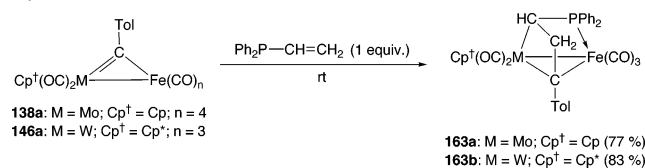
### Scheme 91. Alkyne $\text{C}\equiv\text{C}$ Scission on a Trimetal Center by Formal Insertion of a $\mu$ -Carbyne into the $\text{C}\equiv\text{C}$ Bond



### 3.2.6. Carbyne–Alkene Coupling

This remains a rare reaction. The only reported example appears to be that between vinyl-diphenylphosphine and the iron–molybdenum and –tungsten  $\mu$ -carbyne complexes **138a** and **146a**.<sup>162</sup> A coupling reaction ensues between the vinyl and the  $\mu\text{-CTol}$  groups to form a  $\text{Ph}_2\text{P-CH-CH}_2\text{-CTol}$  fragment, which bridges the dimetal center in the products **163** (Scheme 92).

### Scheme 92. A Carbyne–Alkene Coupling Reaction between a $\mu$ -CTol Group and $\text{PPh}_2(\text{CH}=\text{CH}_2)$

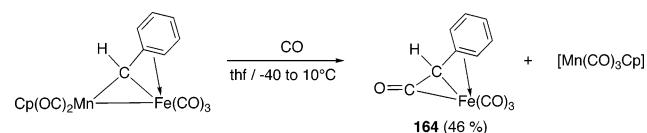


## 3.3. Carbene– and Vinylidene–Ligand Coupling

### 3.3.1. Carbene–Carbonyl Coupling

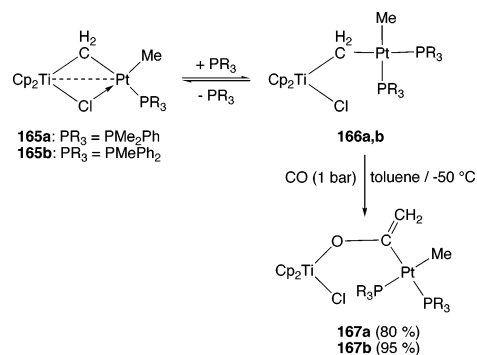
When the Fe–Mn  $\mu$ -carbene complex shown in Scheme 93 (see also Scheme 25) was treated with CO, the mono-metallic iron ketenyl complex **164** was isolated. The Ph group of the organic ligand is  $\eta^2$ -coordinated to the iron atom in both the starting heterobimetallic species and **164**.<sup>77</sup>

### Scheme 93. Elimination of an Iron Acyl from a Mixed Iron–Manganese $\mu$ -Carbene Species on CO Addition



Another example of a carbene–carbonyl coupling is provided by an early–late transition metal combination. The methylene-bridged complexes **165**,  $[\text{Cp}_2\text{Ti}(\mu\text{-CH}_2)(\mu\text{-Cl})\text{-PtMeL}]$  ( $\text{Ti-Pt}$ ;  $\text{L} = \text{PMe}_2\text{Ph}$  or  $\text{PMePh}_2$ ) react reversibly with more phosphine ligands to give the bis(phosphine) species  $[\text{Cp}_2\text{Ti}(\text{Cl})(\mu\text{-CH}_2)\text{PtMeL}_2]$ , species **166**. These species, which no longer contain a Ti–Pt bond, are in equilibrium with the monophosphine complexes **165** and free ligand. The equilibrium mixture exhibits reactivity with CO toward CO insertion (even at  $-50\text{ }^\circ\text{C}$ ) to give  $\mu\text{-}(C,O)$ -ketene complexes **167** in high yield and selectivity. The highly air-sensitive complexes **167** were not isolated pure but were unambiguously characterized spectroscopically (Scheme 94). The pure monophosphine complexes **165** and their  $\mu\text{-Me}$  derivatives  $[\text{Cp}_2\text{Ti}(\mu\text{-CH}_2)(\mu\text{-Me})\text{PtMe}(\text{L})]$  are inert to CO insertion.<sup>163</sup>

### Scheme 94. Addition of CO to a $\mu$ -Methylene Species Leads to Ketene Complex Formation

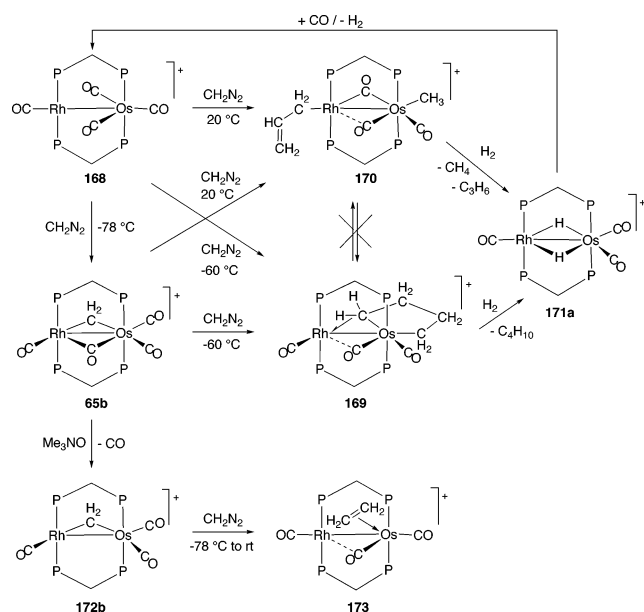


### 3.3.2. Carbene–Carbene Coupling

These reactions are relatively recent and so far have been restricted to heterobimetallic complexes formed between group 8 and group 9 metals. Bridging dppm ligands help anchor the two metals together. All cases to date involve methylene couplings, and multiple  $\text{CH}_2$  additions are often observed.

The first reaction of this type was reported on a cationic rhodium–osmium framework. The products of the reaction of complex **168** (Scheme 95) with diazomethane are critically dependent on the reaction conditions.<sup>164,165</sup> At  $-78\text{ }^\circ\text{C}$ , single methylene addition is observed to form the  $\mu\text{-CH}_2$  species, **65b**. Complex **65b**, (and also **168**) add on three more equivalents of  $\text{CH}_2\text{N}_2$  at  $-60\text{ }^\circ\text{C}$  to give a bimetallic osmacyclopentane species **169** in which there is an agostic C–H interaction to the rhodium atom. Both **168** and **65b** react with excess  $\text{CH}_2\text{N}_2$  at  $20\text{ }^\circ\text{C}$  to afford the  $\eta^1$ -allyl rhodium–osmium species **170** in which a net total of four  $\text{CH}_2$  units have been added. These reactions have been subjected to a mechanistic analysis by using isotopically labeled **65b**- $^{13}\text{C}_1$  and **65b**- $d_2$  made from isotopically labeled  $\text{CH}_2\text{N}_2$ .

Complexes **169** and **170** do not interconvert; they are apparently formed via different pathways. Both complexes react with molecular hydrogen to give the dihydride species

**Scheme 95. Methylene Coupling Reactions on a Rhodium–Osmium Platform**


**171a** and either *n*-butane (from **169**) or a mixture of propene and methane (from **170**). Complex **171a** regenerates **168** when treated with CO.<sup>166</sup> Complex **65b** can be decarbonylated with Me<sub>3</sub>NO to give the  $\mu$ -CH<sub>2</sub> tricarbonyl Rh–Os complex **172b**, which in turn reacts with CH<sub>2</sub>N<sub>2</sub> to give the ethylene complex **173**: there is no further CH<sub>2</sub> incorporation (Scheme 95).<sup>165</sup>

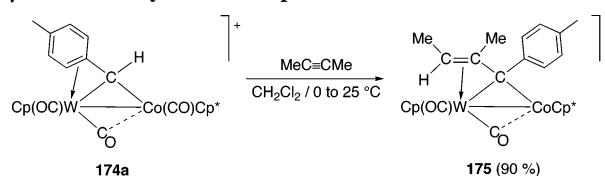
The Ir–Ru analog of **65** may also be reacted with Me<sub>3</sub>NO and then with diazomethane to give the iridium-bonded  $\eta$ -C<sub>2</sub>H<sub>4</sub> complex [Ir(CO)( $\eta$ -C<sub>2</sub>H<sub>4</sub>)( $\mu$ -CH<sub>2</sub>)( $\mu$ -dppm)<sub>2</sub>Ru(CO)<sub>2</sub>]<sup>+</sup> (Ir–Ru).<sup>167</sup> However in the absence of Me<sub>3</sub>NO, there are no multiple CH<sub>2</sub> coupling reactions here, nor in the Rh–Ru system,<sup>168</sup> and potential reasons for this are discussed.<sup>166</sup> These fascinating reactions and the interconversions of many of these complexes are collected in Scheme 95.<sup>164–167</sup>

### 3.3.3. Carbene–Alkyne Coupling

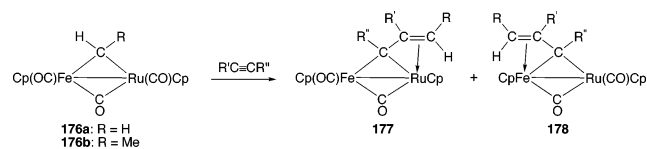
Most reactions have been carried out with “middle–late” and with “late–late” transition metal combinations. The usual products of alkyne additions to  $\mu$ -carbene or alkyldiene complexes are metalloallyl complexes or vinyl carbene complexes depending on how the organic framework bonds to the dimetal center. (Note that when the vinyl carbene is  $\eta^3$ -coordinated, it is not always easy to distinguish the two limiting forms). Dimetallacyclopentene species have also been observed. In many alkyne–methylene coupling reactions reported for “late–late” bimetallic centers, the metal–metal link is fortified by  $\mu$ -dppm ligands. These reactions are necessarily accompanied by C–M or C–H bond cleavage reactions as the alkene “inserts” into a C–H or C–M bond.

An early illustrative example of carbene–alkyne coupling is that of the cationic Co–W  $\mu$ -carbene complex **174a** (Scheme 96) with but-2-yne. The alkyne formally inserts into the C–H bond of the carbene and affords the  $\mu$ -alkenyl complex **175**. The reaction is regio- and stereospecific, and the two Me groups are mutually *cis*.<sup>141,169</sup>

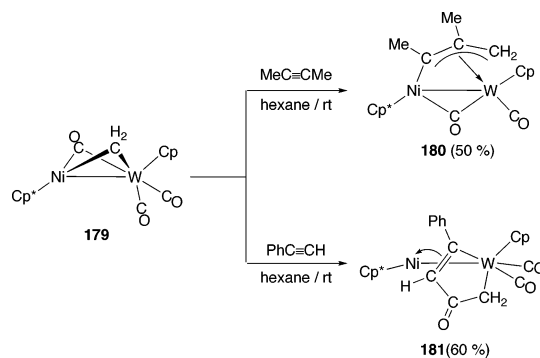
Similar products are obtained from reactions of alkynes with the Fe–Ru complexes **176a** and **176b**, but the reactions are less regioselective, as shown in Scheme 97, and the alkynes formally insert into the Fe– or Ru–C bond of the carbene. Isomers **177** and **178** in which the organic groups

**Scheme 96. Formal Alkyne Insertion into the C–H Bond of a  $\mu$ -CHTol Alkyldiene Complex**


are  $\eta^3$ -bonded either to the iron atom or to the ruthenium atom are obtained, since the differences between the two group 8 metal centers are much smaller than between metals from different periodic groups.<sup>170,171</sup>

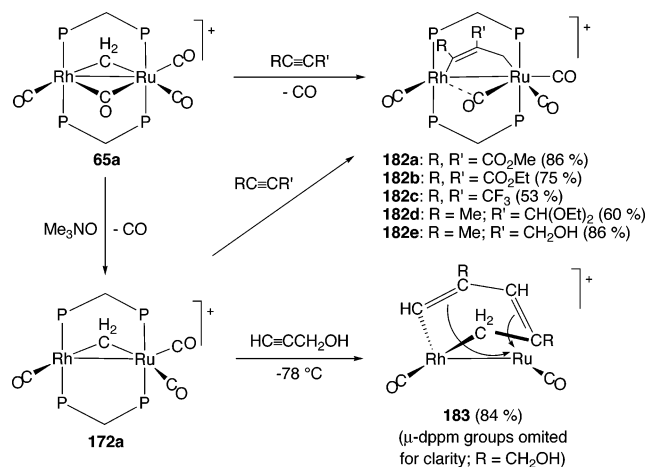
**Scheme 97. Carbene–Alkyne Coupling on an Iron–Ruthenium Framework**


The nickel–tungsten  $\mu$ -methylene complex [Cp\*<sub>2</sub>Ni( $\mu$ -CH<sub>2</sub>)( $\mu$ -CO)W(CO)<sub>2</sub>Cp] (Ni–W) **179** reacts with but-2-yne to give the metalloallyl species **180** in which the alkyne has formally inserted into the Ni–CH<sub>2</sub> bond.<sup>172</sup> Phenylacetylene induces CH<sub>2</sub>–CO–PhC<sub>2</sub>H coupling when reacted with **179** and affords a tungstenacycle complex **181** with the regio- and stereospecific connectivity W–CH<sub>2</sub>–CO–CH=CPh. This ligand is  $\pi$ -coordinated to the Cp\*<sub>2</sub>Ni unit via the CH=CPh double bond (Scheme 98).<sup>173</sup>

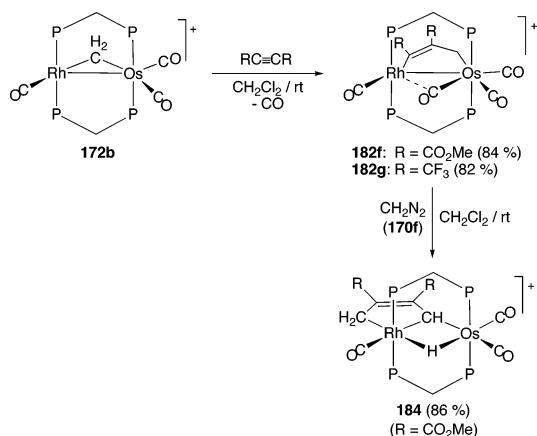
**Scheme 98. Reactions of a Nickel–Tungsten Methylene Complex with Some Alkynes**


Regioselective alkyne insertions into a rhodium–ruthenium  $\mu$ -CH<sub>2</sub> moiety lead to C<sub>3</sub>- and C<sub>5</sub>-bridged fragments. Both the saturated cationic species **65a** and its unsaturated congener **172a** react with a variety of alkynes to give the regioselective dimetallacyclopentene species **182** shown in Scheme 99, which result from formal alkyne insertion into the Rh–CH<sub>2</sub> bond. The structure of complex **182c** was established by a single-crystal X-ray diffraction study. The regiochemistry of unsymmetrical alkyne adducts **182d** and **182e** was established unambiguously by using 2D-NMR spectroscopy. The larger alkyne substituent was always found to be adjacent to the CH<sub>2</sub> group.<sup>174</sup>

Finally, the terminal alkyne propargyl alcohol reacts with the unsaturated cation **172a** to give a double insertion product. The stepwise coupling of 2 mol of the alkyne in a head-to-tail manner with the methylene group afforded the six-membered rhodacycle species **183**. This complex was stable to mild heating or mild oxidation and was characterized by X-ray diffraction.<sup>174</sup>

**Scheme 99. Reactions of Rhodium–Ruthenium Methylene Complexes with Alkynes**


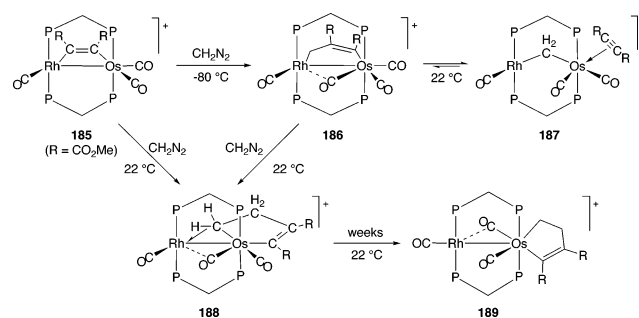
The results of alkyne additions to closely related  $\mu$ -CH<sub>2</sub> Rh–Os systems are identical to those observed with the Rh–Ru systems. When the Rh–Os cation **172b** is treated with DMAD or HFB, the alkynes also insert into the Rh–CH<sub>2</sub> bond yielding complexes **182f** and **182g** in which the Rh–Os bonds are maintained (Scheme 100). However, further addition of diazomethane converts the DMAD dimetallacyclopentene cation into a bridging rhodacyclopentene cation **184** with concomitant Os–Rh bond rupture and C–H activation of the Os-bonded methylene group by the rhodium atom.<sup>175</sup>

**Scheme 100. Reactions of Alkynes with a  $\mu$ -CH<sub>2</sub> Osmium–Rhodium Complex and Subsequent Additions of CH<sub>2</sub>N<sub>2</sub>**


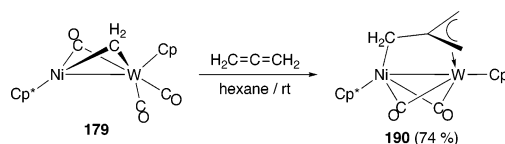
The coupling of alkynes with methylene groups has been attempted on the same Os–Rh metal framework but in reverse order, that is, by the addition of CH<sub>2</sub>N<sub>2</sub> to a preformed  $\mu$ -alkyne complex. The parallel-bridged  $\mu$ -alkyne complex [(CO)Rh( $\mu$ - $\eta^1, \eta^1$ -DMAD)( $\mu$ -dppm)<sub>2</sub>Os(CO)<sub>2</sub>]<sup>+</sup> (Os–Rh) **185** formally inserts CH<sub>2</sub>N<sub>2</sub> into the Rh–DMAD bond at –80 °C to yield complex **186**.<sup>175</sup> This complex resembles **182**, but the olefinic C=C bond is  $\beta$  to the rhodium in **186** and is  $\alpha$  to this metal in complexes **182**.

At room temperature, this insertion product becomes the minor component of an equilibrium mixture that favors the  $\mu$ -CH<sub>2</sub> terminal alkyne species **187** shown in Scheme 101. Room temperature addition of more CH<sub>2</sub>N<sub>2</sub> to this equilibrium mixture or to complex **185** gives the osmacyclopentene species **188** in which there is an agostic interaction with the

rhodium atom (see complex **169**, Scheme 95 for an osmacyclopentane analog of **188**). This species slowly rearranges to the (nonbridging) osmacyclopentene species **189** whose structure was determined by X-ray diffraction. Detailed labeling studies have established the sequence and regiochemistry of the methylene additions and have provided valuable mechanistic information.<sup>166,175</sup>

**Scheme 101. Methylene Insertion into Metal–Carbon Bonds of Osmium–Rhodium  $\mu$ -Alkyne Complexes**

**3.3.4. Carbene–Alkene and –Allene Coupling**

Carbene–alkene and –allene coupling reactions are less reported than carbene–alkyne couplings, but they are also known. Allene formally inserts into the W–CH<sub>2</sub> bond of the  $\mu$ -CH<sub>2</sub> complex **179** to give complex **190**, a rare example of a  $\mu$ -trimethylene–methane (TMM) species, as shown in Scheme 102. The structure of **190** was confirmed by a single-crystal X-ray diffraction study.<sup>173</sup> The question as to whether the allene inserts into the W–CH<sub>2</sub> bond is moot, because the molecule is fluxional at room temperature and effectively rotates in a helicopter-like motion, while remaining attached to its heterometallic skeleton. The fluxional behavior of **190** has been the subject of a theoretical study.<sup>176</sup>

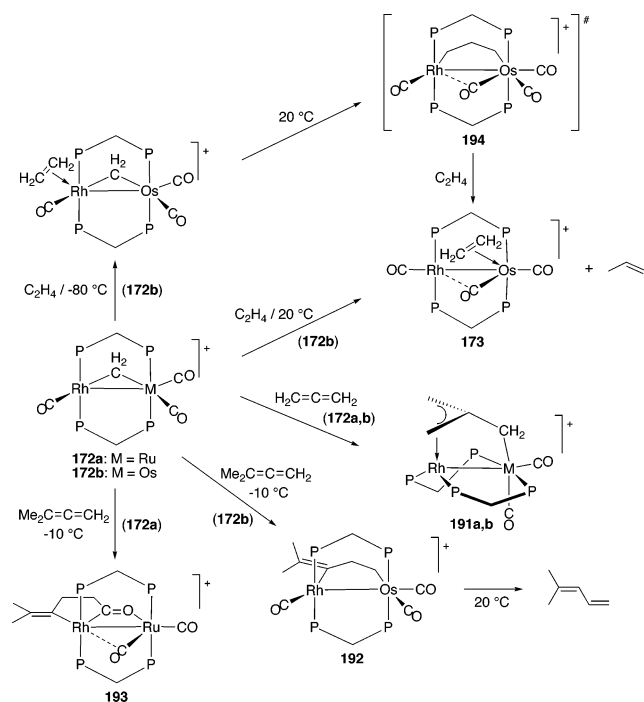
**Scheme 102. Insertion of Allene into a  $\mu$ -CH<sub>2</sub> Group of a Nickel–Tungsten Bond To Afford a  $\mu$ -Trimethylenemethane Complex**


A more recent example of methylene–allene coupling is seen in the Ru–Rh complex **172a** and its Os–Rh analog **172b**. Both species react with allene to give  $\mu$ -TMM species **191** (Scheme 103). In contrast with the bridging TMM ligand observed in **190** (Scheme 102),<sup>173</sup> the ligands in **191** complexes are not dynamic. By use of <sup>13</sup>C-enriched samples of methylene complexes **172**, it was shown that for both **191a** and **191b**, the cumulene inserts into the Rh–CH<sub>2</sub> bonds of each species.<sup>177</sup>

The reactions of **172a** and **172b** differ with 1,1-dimethylallene. At low temperature, the free ligand inserts into the Rh–CH<sub>2</sub> bond of the Rh–Os complex **172b** to afford a dimetallacyclopentane complex **192** (a saturated analog of complex **186**). This complex ejects 2-methyl-2,4-pentadiene at room temperature. However with **172a** 1,1-dimethylallene couples not just with the methylene group but simultaneously with a CO ligand to give complex **193**, whose structure was determined crystallographically.<sup>177</sup>

The Rh–Os cation **172b** also reacts with ethene at ambient temperature to form free propene and the  $\eta^2$ -C<sub>2</sub>H<sub>4</sub> species

### Scheme 103. Reactions of Rhodium–Ruthenium and –Osmium $\mu$ -Methylene Complexes with Ethylene and Cumulenes

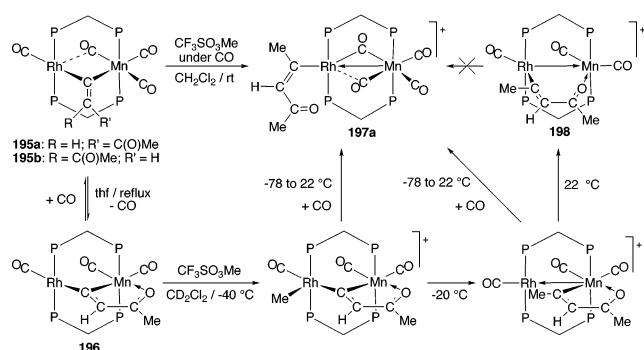


**173** (Scheme 103; see also Scheme 95). At  $-80\text{ }^{\circ}\text{C}$ , under an ethene atmosphere, an  $\eta\text{-C}_2\text{H}_4$  addition product can be observed, that rearranges to **173** at room temperature, with propene evolution, as shown in Scheme 103. The reaction presumably proceeds via a Rh–Os–(CH<sub>2</sub>)<sub>3</sub> five-membered ring intermediate **194** (a saturated analog of complex **186**).<sup>165,166</sup>

### 3.3.5. Vinylidene–Alkyl Coupling

The parallel-bridged alkyne complex [(OC)<sub>3</sub>Mn( $\mu$ -HC $\equiv$ CCOMe)( $\mu$ -dppm)<sub>2</sub>Rh(CO)] obtained at  $-40\text{ }^{\circ}\text{C}$  rearranges to an isomeric mixture of  $\mu$ -vinylidene complexes **195**. This isomeric mixture and its decarbonylated analog **196** (in which the ketone carbonyl ligand is also coordinated to the manganese atom) are both methylated with methyltriflate as shown in Scheme 104. Depending on the reaction conditions and on the starting vinylidene complex (**195** or **196**), two alkenyl complexes that are stable at room temperature may be isolated: the rhodium-bonded terminal alkenyl complex **197a** and the bridged alkenyl complex **198**.<sup>178</sup>

### Scheme 104. Synthesis of Alkenyl Complexes on a Manganese–Rhodium Framework



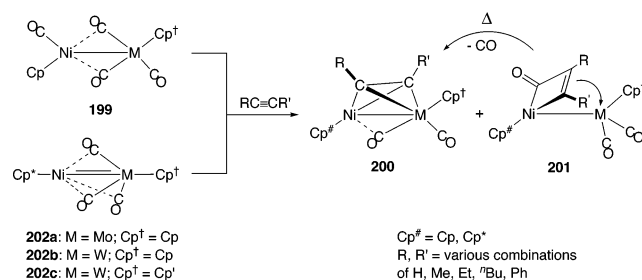
## 3.4. Alkyne–Ligand Coupling

### 3.4.1. Alkyne–Carbonyl Coupling

Many monometallic metal carbonyl complexes react with alkynes to afford a plethora of complexes. Some of these contain products that result from single or multiple carbonyl–alkyne coupling reactions. Such reactions have been less investigated for heterobimetallic carbonyl species, but among those reactions that have been studied, similar coupling products are often observed. Metallacyclobutenone or dimetallacyclopentenone species are common outcomes of such reactions.

Alkynes react with the group 6 metal–nickel complexes **199** to afford a mixture of both metallatetrahedrane-type  $\mu$ -alkyne complexes **200** and lesser quantities of metallacyclic species **201** (when M = W) in which a nickelacyclobutenone ring is present (Scheme 105).<sup>179,180</sup> Unsymmetric alkynes give a mixture of isomeric nickelacyclobutenone species **201** that differ in their linkage with the CO moiety (CO–CR=CR' or CO–CR'=CR). In each case, the formal C=C bond in the ring is  $\pi$ -coordinated to the group 6 metal. Other terminal alkynes such as HC $\equiv$ CCMe<sub>2</sub>(OMe) also afford mixtures of complexes **200** and **201** (and not of type **203** as reported earlier)<sup>181</sup> when reacted with the saturated species [Cp(OC)–Ni–M(CO)<sub>3</sub>Cp'] **199** (Ni–M, M = Mo, W).

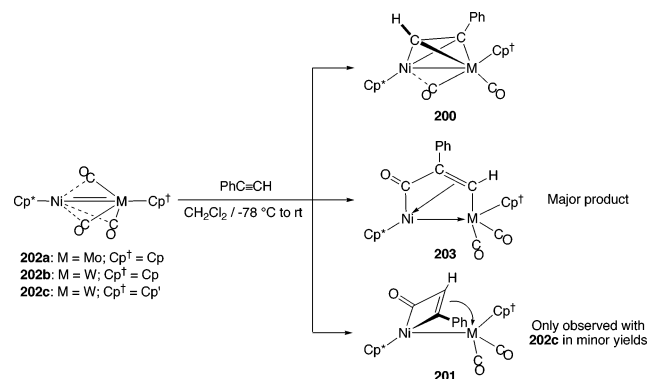
### Scheme 105. Reactions of Group 6 Metal–Nickel Complexes with Alkynes



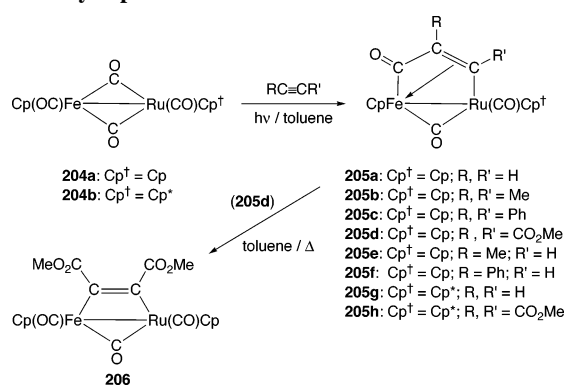
Complexes **201** all lose CO when heated (or in a mass spectrometer) to give **200**. However, a kinetic study shows that CO loss from metallacycles is not the primary pathway to the synthesis of the  $\mu$ -alkyne complexes.<sup>182</sup>

The replacement of a Cp ligand on the nickel atom by a Cp<sup>\*</sup> ligand allows the isolation of the highly reactive unsaturated complexes **202**, which can be considered to contain nickel–molybdenum or –tungsten double bonds.<sup>183</sup> These species react with disubstituted alkynes to give the nickelacyclobutenone products **201** with NiCp<sup>\*</sup> groups. However complexes **201** are stabilized by the Cp<sup>\*</sup> ligand, and they now form the major reaction products. These complexes are still decarbonylated when heated to give the corresponding  $\mu$ -alkyne species **200** (Scheme 105).<sup>131</sup>

The reaction of PhC $\equiv$ CH with **202c** yields two metallacycles and the corresponding dimetallatetrahedrane complex of type **200**. The metallacycles are a nickelacyclobutenone species **201** (with a Ni–CO–CH=CPh ring linkage) and complex **203**, in which there is a Ni–CO–CPh=CH–M dimetallacyclopentenone ring (Scheme 106),<sup>46</sup> similar to those found in complexes **15–17** (Scheme 7). The reactions of PhC $\equiv$ CH with **202a** and **202b** yield complexes of type **200** and **203** exclusively. [More complex reaction products that are obtained in minor yields when phenylacetylene is added to a mixture of [Cp<sup>\*</sup>Ni(CO)] and [W(CO)<sub>3</sub>Cp]<sup>–</sup> have already been discussed in Scheme 9 (section 2.1.4)]<sup>47,48</sup>

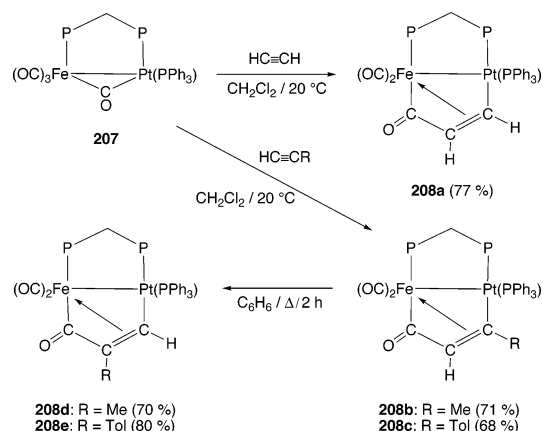
**Scheme 106. Reactions of Terminal Alkyne Complexes with Unsaturated Nickel–Molybdenum and –Tungsten Complexes**


Alkyne–carbonyl coupling is also observed when alkynes are irradiated with the iron–ruthenium cyclopentadienyl complex **204a**. Incidentally, these systems are isoelectronic with complexes **199** whose alkyne chemistry has just been discussed. In general, dimetallacyclopentenone complexes **205** are obtained, with a Fe–CO–CR–CR'–Ru linkage (Scheme 107), similar to what is found in complexes **203**.<sup>170,171</sup> Thermolysis of the DMAD metallacycle leads to decarbonylation and generates the parallel-bonded  $\mu$ -alkyne Fe–Ru complex **206**. The geometry of **206** contrasts with the dimetallatetrahedrane (perpendicular)  $\mu$ -alkyne species **200** obtained from thermolysis of the Ni–Mo and Ni–W metallacycles **201** (Scheme 105).<sup>46,131,180</sup> The related RuCp\* complex **204b** reacts similarly with the alkynes HC≡CH and DMAD (Scheme 107). Alkyne–alkyne coupling also takes place with HC≡CCMe<sub>2</sub>OH (Scheme 120).<sup>184</sup>

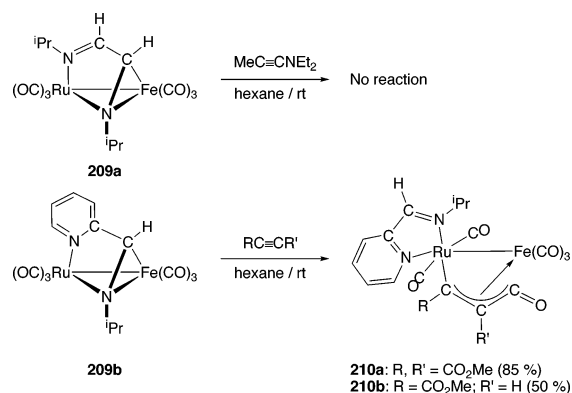
**Scheme 107. Alkyne–Carbonyl Coupling on Iron–Ruthenium Bonds Leading to Dimetallacyclopentenones**


Similar dimetallacyclopentenone rings found in complexes **208** were obtained in high yields when the Fe–Pt complex **207** was reacted with ethyne, propyne, or tolylacetylene (Scheme 108). The Fe–Pt bond distance barely changes during the course of this reaction [2.579(4) Å for the starting complex and 2.597(4) Å for the final product in the case of the ethyne reaction].<sup>185,186</sup> For asymmetric alkynes, the kinetic product (Pt–CR–CH–CO–Fe linkage) slowly isomerizes to the more thermodynamically stable final product (Pt–CH–CR–CO–Fe linkage) when heated in benzene. Reactions with other dppm-type ligands, such as Ph<sub>2</sub>P–C(=CH<sub>2</sub>)–PPh<sub>2</sub>, are also described.<sup>186</sup>

The iron–ruthenium  $\alpha$ -diimine complex **209a** shown in Scheme 109 does not react with MeC≡CNEt<sub>2</sub> at room

**Scheme 108. Alkyne–Carbonyl Coupling on Iron–Platinum Bonds Leading to Dimetallacyclopentenones**


temperature, and simple alkyne coordination is observed at 69 °C. This complex provides an unusual example of a heterobimetallic complex exhibiting less reactivity than its homobimetallic congeners because the corresponding Fe<sub>2</sub> and Ru<sub>2</sub> complexes both react (differently) with this alkyne at room temperature.<sup>187</sup> The closely related asymmetric iron–ruthenium  $\alpha$ -diimine complex **209b** (Scheme 109) does react with the alkynes DMAD and HC≡CCO<sub>2</sub>Me under these conditions to give the alkyne–CO coupled products **210**.<sup>188</sup>

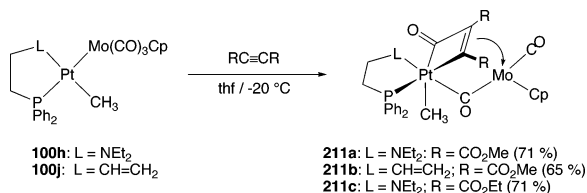
**Scheme 109. Alkyne–Carbonyl Coupling on an Asymmetric Iron–Ruthenium  $\alpha$ -Diimine Complex**


Molybdenum–platinum complexes in which an asymmetric bidentate ligand is coordinated to the platinum atom (**100h** and **100j**) react with DMAD and with its diethoxy analog EtO<sub>2</sub>CC≡CCO<sub>2</sub>Et with rupture of the Mo–Pt bond and the formation of platinumacyclobutenone complexes **211**, which are  $\pi$ -coordinated to the molybdenum atom (Scheme 110). However, this reaction requires a strongly electron-withdrawing alkyne and does not work with phenyl-, diphenyl-, or even ethylcarbomethoxyacetylene. Furthermore, no reaction is observed with the monometallic platinum complex [Pt(Et<sub>2</sub>NC<sub>2</sub>H<sub>4</sub>PPh<sub>2</sub>)(Me)Cl] or even with Mo–Pt species on which a dppe, tmeda, or MeSC<sub>2</sub>H<sub>4</sub>PPh<sub>2</sub> has replaced the ligands shown in complexes **100h** and **100j**. The bidentate ligand coordinated to the platinum atom must be capable of generating a vacant coordination site.<sup>189</sup>

**3.4.2. Alkyne–Acyl Coupling**

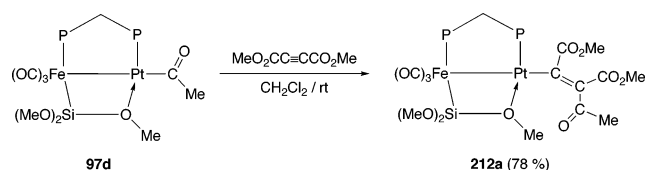
Few examples of these coupling reactions have been reported. However, the Fe–Pt  $\mu$ -dppm complex **97d**, in which there is a Pt-bonded acyl group, does react with DMAD. The alkyne inserts into the Pt–C(O)CH<sub>3</sub> bond to

**Scheme 110. Platinacyclobutenone Formation Following the Reaction of a Molybdenum–Platinum Complex with Electron-Withdrawing Alkynes**



give the Pt-bonded terminal alkenyl complex **212a** (Scheme 111). Terminal alkynes such as PhC≡CH, *n*-BuC≡CH, or *t*-BuC≡CH afford  $\mu$ -vinylidene complexes as the final products, but the reactions proceed via spectroscopically observed alkenyl intermediates whose structures are surmised to be similar to those of the structurally characterized DMAD complex.<sup>190</sup>

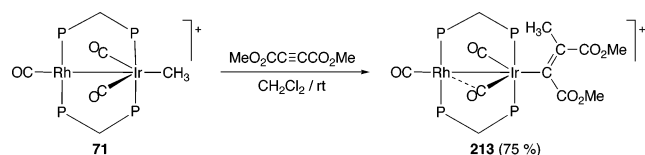
**Scheme 111. Alkyne Insertion into the Platinum–Acyl Bond of an Iron–Platinum Complex**



**3.4.3. Alkyne–Alkyne Coupling**

This reaction is rare on a heterobimetallic center, but it has been observed with the alkyne DMAD. This alkyne inserts into the Ir–Me bond of the Rh–Ir cation **71** shown in Scheme 112 to give the alkenyl complex **213**. The related  $\mu$ -CH<sub>2</sub> diiridium hydride reacts similarly but a (parallel) bridged DMAD hydride complex is a byproduct.<sup>191</sup>

**Scheme 112. Alkyne Insertion into an Iridium–Methyl Bond of an Iridium–Rhodium Complex**

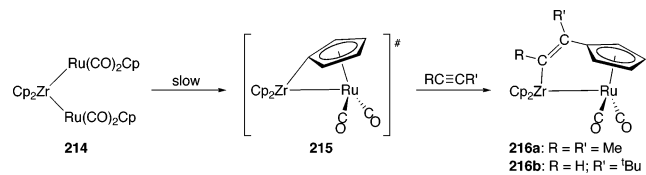


The early–late trimetallic chain complex Cp<sub>2</sub>Zr{Ru(CO)<sub>2</sub>Cp}<sub>2</sub> **214** undergoes a slow intramolecular C–H activation reaction to give the reactive species **215**, which is not isolable. A tilt angle of 34° was found in the isolated and structurally characterized Ru–Zr(CO) species [(OC)<sub>2</sub>Ru-( $\mu$ - $\eta^5$ (Ru), $\eta^1$ (Zr)-C<sub>5</sub>H<sub>4</sub>)Zr(CO)Cp<sub>2</sub>] (Ru–Zr),<sup>10</sup> and in **215**, the Zr–C  $\sigma$ -bond is also likely to be out of the plane of the C<sub>5</sub>H<sub>4</sub> ring. This significant angle strain explains the high reactivity of the Zr–C  $\sigma$ -bond in **215** toward insertion reactions.<sup>10</sup> The complex inserts both MeC≡CMe and *t*-BuC≡CH into its Zr–C bond (the latter regioselectively) to form less sterically strained bimetallic complexes **216** (Scheme 113).<sup>10,192</sup>

**3.4.4. Alkyne–Alkyne Coupling**

Alkyne coupling reactions on metals are very well-known and monometallic, homobimetallic, and heterobimetallic examples of this kind of reaction are well represented. These reactions can be complex, and frequently, in addition to alkyne–alkyne coupling, alkyne–carbonyl coupling is observed. Furthermore, the reaction is not necessarily limited

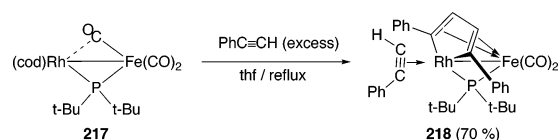
**Scheme 113. Alkyne Insertion into the Zirconium–Carbon  $\sigma$ -Bond of a Sterically Strained Early–Late Heterobimetallic Complex**



to the coupling of just two alkynes, and more complex alkyne oligomerizations can take place. Two alkynes may couple in a head-to-tail fashion or symmetrically (head-to-head or tail-to-tail). The products can be considered to be metallacyclopentadiene complexes. There are also rare, more complex couplings of two alkynes in which both C–C cleavage and C–C formation reactions occur. Three-alkyne couplings frequently give rise to “fly over”-type complexes. Alkyne–alkyne coupling reactions that arise from the reaction of two monometallic species have been discussed previously (section 2.1.5).

When asymmetric alkynes dimerize, their couplings are often highly stereospecific, especially when terminal alkynes are involved, owing to the large steric difference between the two ends of the alkyne. This is seen when the Fe–Rh phosphido-bridged complex **217** is treated with PhC≡CH. The head-to-head alkyne coupled product obtained, **218**, is a Rh–CPh–CH–CH–CPh rhodacycle that is  $\pi$ -( $\eta^4$ )-coordinated to the iron (Scheme 114).<sup>57</sup>

**Scheme 114. Head-to-Head Coupling of Alkynes on an Iron–Rhodium Framework**

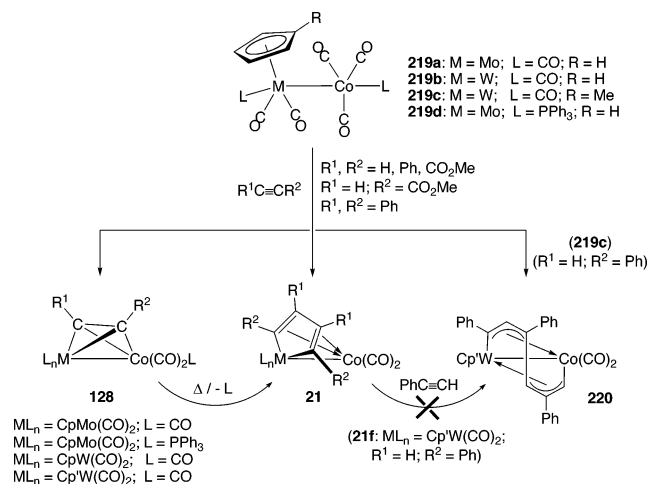


The alkynes shown in Scheme 115 react with cobalt–molybdenum and –tungsten complexes **219a** and **219b** in refluxing toluene to give metallacyclopentadienyl complexes **21** in which the group 6 metal forms part of the metallacycle. Massive decomposition ensues when more forceful conditions are used. However, under milder conditions, perpendicularly coordinated  $\mu$ -alkyne complexes **128** may be isolated, which themselves add on a molar equivalent of alkyne to give metallacycles **21**. Dissymmetric alkynes give only one metallacycle isomer of type **21**. An X-ray analysis of the bis(diphenylacetylene) complex **21e** (ML<sub>n</sub> = CpMo(CO)<sub>2</sub>; R<sup>1</sup> = R<sup>2</sup> = Ph) (Scheme 115) shows that the molybdenum–carbon  $\sigma$ -bonds in the metallacycle ring are equal. All C–C ring distances are also equivalent in the metallacycle, and a Co–Mo bond is present.<sup>52</sup>

These results were independently confirmed with the reaction of complex **219c** with excess PhC≡CH, which gave complexes **21f** (ML<sub>n</sub> = Cp'W(CO)<sub>2</sub>; R<sup>1</sup> = H; R<sup>2</sup> = Ph) and **128e** (ML<sub>n</sub> = Cp'W(CO)<sub>2</sub>; L = CO; R<sup>1</sup> = H; R<sup>2</sup> = Ph). Small quantities of the fly over complex **220** formed by head-to-tail coupling of three alkynes (as shown in Scheme 115) were also isolated in this reaction, and its structure was established spectroscopically.<sup>53</sup> The head-to-head coupled product **21f** has the same linkage as is seen in the Fe–Rh complex **218**<sup>57</sup> and does not react with more phenylacetylene to give the fly over complex.

The bis(triphenylphosphine)-substituted complex **219d** afforded the Co–Mo  $\mu$ -PhC≡CH complex **128f** (ML<sub>n</sub> =

## Scheme 115. Alkyne Coupling on Cobalt–Molybdenum and –Tungsten Bonds



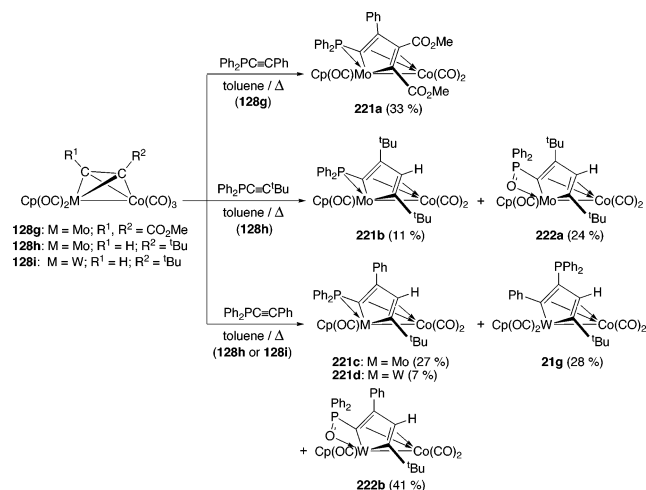
CpMo(CO)<sub>2</sub>; L = PPh<sub>3</sub>; R<sup>1</sup> = H; R<sup>2</sup> = Ph.<sup>193</sup> An intermediate complex in which the PPh<sub>3</sub> ligand was still coordinated on to the cobalt atom was isolated. The Co–Mo distance in **128f** of 2.698(1) Å<sup>193</sup> is marginally longer than the value of 2.6761(1) Å seen in the linked diphenylacetylene complex **21e**.<sup>52</sup> Scheme 115 summarizes these related reactions.

The coupling of diphenylphosphino-alkynes with other alkynes has also been carried out on these popular group 6–group 9 frameworks. Complexes **128g** and **128h** react with Ph<sub>2</sub>PC≡CR (R = Ph, *t*-Bu) but do not always give simple alkyne-coupled products, and carbon–phosphorus bond cleavage is a common theme of these reactions.<sup>194</sup> The  $\mu$ -DMAD complex **128g** couples regioselectively with Ph<sub>2</sub>PC≡CPh to afford the molybdenacyclopentadienyl species **221a**, which is similar to complexes **21** but in which there is additional phosphorus coordination to the molybdenum atom. The reaction of **128h** with Ph<sub>2</sub>PC≡C*t*-Bu similarly yields **221b**, but a phosphine oxide product **222a** that probably results from fortuitous oxygen is also isolated. X-ray diffraction studies of most of these molybdenacyclopentadienyl species were undertaken, and it was shown that they all contain normal Co–Mo bonds of around 2.70 ± 0.02 Å.<sup>195</sup>

The reactions of **128h** and **128i** with Ph<sub>2</sub>PC≡CPh differ. The Co–Mo complex **128h** gave only **221c**.<sup>195</sup> However, complex **128i** afforded three tungstenacyclic products (**221d**, **21g**, and **222b**), with structures shown in Scheme 116.<sup>196</sup> In each case, there is alkyne–phosphinoalkyne coupling, and all three molecules have a W–C–*t*-Bu–CH– linkage. However regio isomers with a W–C–*t*-Bu–CH–CPh–C(PPh<sub>2</sub>) and a W–C–*t*-Bu–CH–C(PPh<sub>2</sub>)–CPh connectivity are both obtained (in a 1:4 ratio). The third product **222b** is a phosphine oxide complex similar to **222a**.

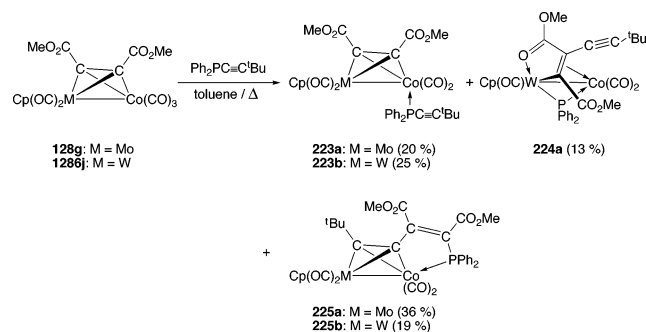
Reactions that involve  $\mu$ -DMAD complexes can yield more complex products because the DMAD ligand contains ester functionalities, which can also ligate to metals. This is observed in reactions of the DMAD complexes of **128g** (M = Mo) and **128j** (M = W) with Ph<sub>2</sub>PC≡C-*t*-Bu. Complexes are obtained in which the alkyne simply coordinates to the cobalt atom (**223**); another reaction pathway cleaves the Ph<sub>2</sub>P–C bond of the phosphinoalkyne and generates the species **224a** and **225** shown in Scheme 117. One product, **224a** (M = W only), results from phosphinoalkyne P–C bond cleavage and *t*-BuC≡C–alkyne coupling: one of the ester CO groups of the DMAD ligates to the group 6 metal.

## Scheme 116. Alkyne–Phosphinoalkyne Coupling Reactions on Cobalt–Molybdenum and –Tungsten Bonds



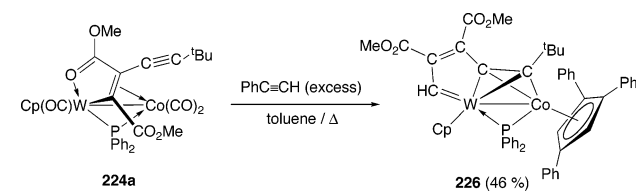
The other complexes, **225** (obtained on Co–Mo and Co–W frameworks), contain new  $\mu$ -hydrocarbyl ligands in which PPh<sub>2</sub> and *t*-BuC≡C fragments have added to the two DMAD acetylenic carbon atoms. X-ray diffraction studies were performed on an example of each class of complex.<sup>194</sup>

## Scheme 117. Cleavage of a Phosphinoalkyne and Coupling of the Fragments with DMAD on Cobalt–Molybdenum and –Tungsten Frameworks



Complex **224a** undergoes a remarkable reaction with excess PhC≡CH to generate **226**, which contains a carbene and a 1,3,4-triphenyl-cyclopentadienyl ligand, derived from the trimerization and bond-cleavage reactions of three PhC≡CH units (Scheme 118). Complex **226** was obtained in 46% yield, and its structure was established by X-ray diffraction.<sup>197</sup>

## Scheme 118. Carbene and Cyclopentadienyl Ligand Formation from PhC≡CH on a Cobalt–Tungsten Center



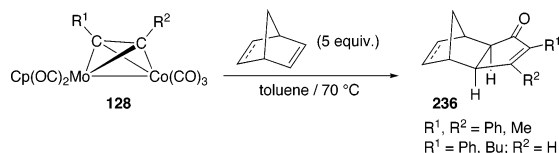
The mixed Fe–Ru diisopropylimine-bridged complex **209a** and its Fe<sub>2</sub> and Ru<sub>2</sub> analogs (Scheme 119) all react with alkynes. In some cases, **209a** is, surprisingly, less reactive than its homobinuclear congeners (see section 3.4.1, Scheme 109).<sup>188,198</sup> The Ru<sub>2</sub> complex adds on an ethyne molecule to give a parallel bridged  $\mu$ -ethyne complex, but it does undergo an alkyne–imine coupling with HC≡CCO<sub>2</sub>Me (section 3.4.6, Scheme 128). The corresponding diiron





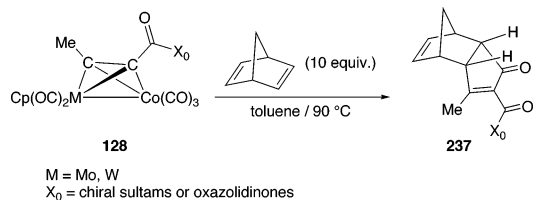
(Scheme 124).<sup>203</sup> The reported yields are higher than those in the dicobalt system. When chiral unsymmetrical alkynes such as menthyl propargyl ether are used, a diastereomeric mixture of Co–Mo  $\mu$ -alkyne complexes are obtained that may be separated chromatographically. The use of a diastereochemically pure Co–Mo complex gave rise to a diastereochemically pure organic product with no sign of the other isomer, in effect giving the asymmetric Pauson–Khand reaction. High levels of stereocontrol can be obtained by taking advantage of the chirality of the dimetal core, in what can be termed an enantiospecific Pauson–Khand reaction.<sup>203,204</sup>

#### Scheme 124. Pauson–Khand Reactions on a Cobalt–Molybdenum Template



*Exo*-fused cyclopentenone adducts are obtained almost exclusively when this reaction is attempted in the dicobalt system. However the cobalt–molybdenum *N*-(2-alkynoyl) derivatives of chiral oxazolidinones or sultams of geometry **128** “show an unprecedented reversal of this stereoselectivity in their reactions with norbornadiene predominantly giving rise to *endo*-fused dicyclopentadienone products **237** in a totally regioselective fashion.”<sup>205</sup> Cobalt–tungsten systems behaved similarly, giving *exo*-fused adducts with “classical” alkynes and *endo*-fused adducts with the *N*-(2-alkynoyl) derivatives. Yields are superior to the Co–Mo systems in most cases (Scheme 125).<sup>206</sup>

#### Scheme 125. Regioselective Ring Fusion Reactions on Cobalt–Molybdenum and –Tungsten Templates

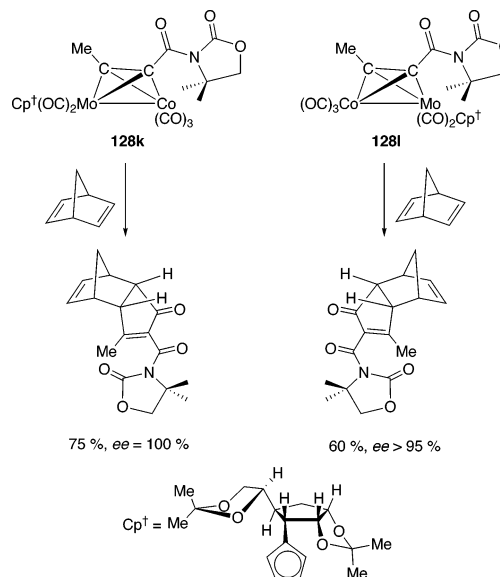


Enantioselective heterobimetallic Pauson–Khand reactions have been reported on a Co–Mo framework by using the chiral-substituted cyclopentadienyl ligands on the molybdenum atoms of the complexes **128k** and **128l** shown in Scheme 126. Both (separated) diastereomers yield organic enones in at least 95% enantiomeric excess.<sup>207</sup>

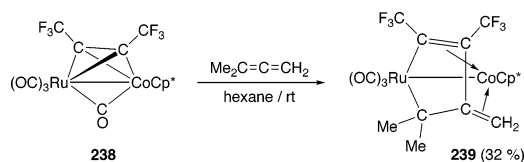
An alkene–alkyne coupling reaction that is not of the Pauson–Khand kind has been reported (Scheme 127). The  $\mu$ -HFB cobalt–ruthenium complex **238** reacted with 1,1-dimethylallene to give **239**. The organic ligand in **239**, formed by coupling the central carbon atom of the allene moiety with the alkyne, is  $(\pi)\eta^4$ -ligated to the cobalt and forms two  $\sigma$ -bonds to the ruthenium atom. The structure of **239** reveals a Co–Ru single bond of 2.6717(17) Å.<sup>208</sup>

Coupling reactions between ligated diazadienes and alkynes have been seen in some iron–ruthenium complexes. In complex **209a** shown in Scheme 128, only one of the diazadiene C=N carbon atoms is bonded to a metal (iron). This complex reacts with DMAD to give two products, a simple alkyne adduct **240** and the more complex **241**, which results from a diazadiene–DMAD coupling reaction. The

#### Scheme 126. Enantioselective Pauson–Khand Chemistry on a Cobalt–Molybdenum Framework

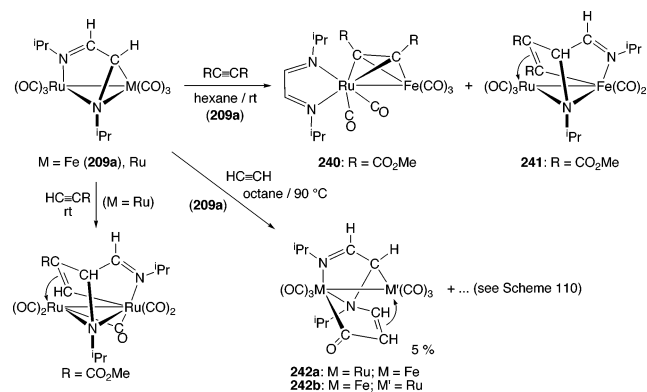


#### Scheme 127. Dimethylallene–Alkyne Coupling on a Cobalt–Ruthenium Bond



relative yields of these species depend on whether the reaction was produced in the presence of UV light; **241** can be the major reaction product under UV irradiation.<sup>198</sup> The DMAD in this complex can be considered to have inserted into the Fe–C bond of the diazadiene as is apparent from its structure.

#### Scheme 128. Alkyne–Diazadiene Coupling on an Iron–Ruthenium Template



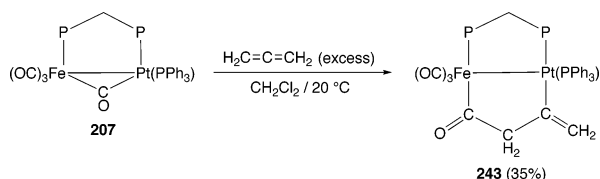
The alkyne  $\text{HC}\equiv\text{CCO}_2\text{Me}$  affords a parallel  $\mu$ -alkyne species with **209a** (see Scheme 119); however, this alkyne reacts with its diruthenium analog to give the Ru<sub>2</sub> equivalent of **241**, but in contrast to Fe–Ru species **241**, which contains only terminal CO ligands, one of the CO ligands in the Ru<sub>2</sub> complex is bridging.<sup>199</sup> This suggests a different electron distribution in the otherwise similar complexes. Ethyne gave primarily ethyne–ethyne coupled products with **209a** (Scheme 119), but trace amounts (~5%) of the diazadiene–ethyne–carbonyl coupled product **242** could be isolated.<sup>198,199</sup>

### 3.5. Alkene–Ligand Coupling

#### 3.5.1. Alkene–Carbonyl Coupling

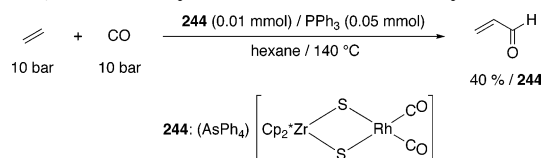
Direct alkene–carbonyl coupling (as opposed to alkene–acyl coupling) is rare on bimetallic frameworks. An example is the reaction of allene with CO on an Fe–Pt framework in the compound **207** to give complex **243** in which the allene has linked up with the carbonyl ligand to give a C(O)–CH<sub>2</sub>–C(=CH<sub>2</sub>)– grouping that bridges the Fe–Pt bond. This reaction is shown in Scheme 129.<sup>209</sup>

**Scheme 129. Coupling of Allene and Coordinated CO on an Iron–Platinum Framework**



In the presence of PPh<sub>3</sub>, the “early–late” anionic sulfido complex [(OC)<sub>2</sub>Rh(μ-S)<sub>2</sub>ZrCp\*<sub>2</sub>]<sup>−</sup> **244** initiates the carbonylation of ethylene at high pressure to give acrolein, as shown in Scheme 130. Addition of triethylorthoformate generates 3,3-diethoxyprop-1-ene in what is now a catalytic reaction.<sup>210</sup>

**Scheme 130. Coupling of Ethylene and CO To Give Acrolein, Mediated by a Rhodium/Zirconium System**



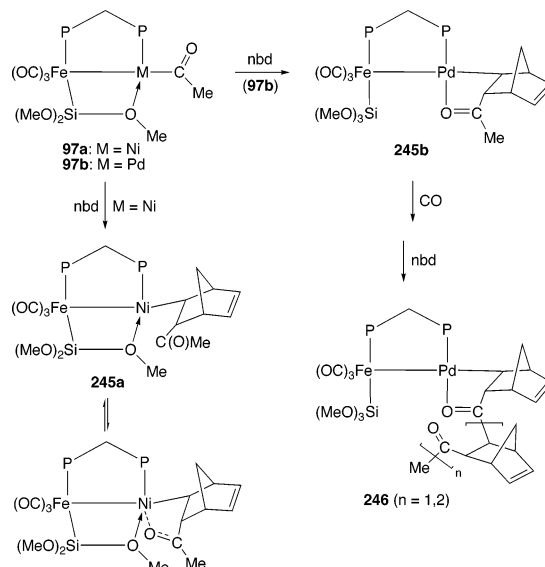
#### 3.5.2. Alkene–Acyl Coupling

Some acyl–alkene coupling reactions are known. These usually have been observed on an Fe–Pd framework, but recent examples on a related Fe–Ni system have been noted. When the μ-dppm iron–palladium complex **97b**, which contains a Pd-bonded acetyl, is treated with norbornadiene, the ligand inserts into the Pd–C(O)CH<sub>3</sub> bond to give the coupled complex **245b** that is now bonded to the palladium atom via the acyl oxygen atom as well as via a norbornadiene carbon. The whole sequence of insertions into the Pd–C bond, starting with carbon monoxide insertion followed by norbornadiene, may be repeated at least two more times to give products **246** (Scheme 131). The reaction is promoted by the hemilabile Si(OMe)<sub>3</sub> ligand, which reversibly forms a (MeO)<sub>2</sub>SiOMe ⇌ Pd bond and generates a vacant coordination site when needed.<sup>117</sup> Similar insertion reactions are observed with ethylene or with methylacrylate<sup>120</sup> and with 7-oxanorbornene or norbornene.<sup>211</sup> The crystal structure of the 7-oxanorbornene insertion product was determined via an X-ray diffraction study.<sup>211</sup> Insertions are also observed with the Fe–Ni complex **97a**. In this case however, a methoxy oxygen atom from a bridging Si(OMe)<sub>3</sub> ligand competes with the acyl oxygen in coordinating to the nickel atom.<sup>119</sup>

#### 3.5.3. Alkene–Alkyl Coupling

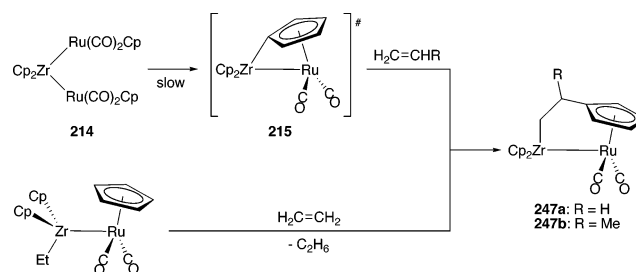
This reaction is similar to acyl–alkene coupling on metal–acyl bonds. It is not commonly reported. The reactive species **215** formed from the trimetallic chain complex **214** (Scheme

**Scheme 131. Acyl–Alkene Coupling Reactions on Iron–Nickel and –Palladium Frameworks**



112) inserts both ethene and propene (regioselectively) into its Zr–C bond to give complexes **247** as shown in Scheme 132. An X-ray diffraction study was undertaken of the ethylene addition product **247a**, and this confirmed that a Ru–Zr bond of 3.064(1) Å was present.<sup>10,192</sup>

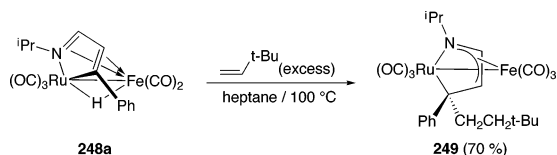
**Scheme 132. Alkene Insertion into a Zirconium–Carbon σ-Bond of a Sterically Strained Early–Late Heterobimetallic Complex**



The related species [Cp(OC)<sub>2</sub>Ru–ZrEtCp<sub>2</sub>] (Ru–Zr) also reacts with ethylene and liberates ethane to give the same complex **247a**.<sup>10</sup>

The azadiene iron–ruthenium complex **248a** shown in Scheme 133 slowly undergoes an unusual reaction with *t*-BuCH=CH<sub>2</sub>. The olefin couples with the phenyl-bonded carbon atom of the ligand and the μ-hydride to form the new aza-allylic complex **249** and a now saturated CPh carbon atom. A mechanism for this reaction is proposed.<sup>212</sup>

**Scheme 133. *t*-Butylethylene–Azadienyl Ligand Coupling on an Iron–Ruthenium Template**

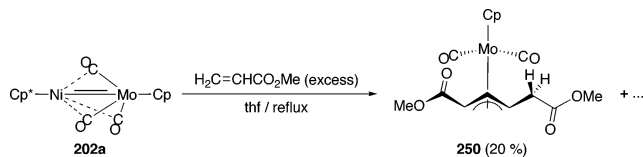


#### 3.5.4. Alkene–Alkene Coupling

This reaction has not been commonly observed and known examples come from one of the author's own results. When the bimetallic unsaturated complex **202a**, which may be considered to contain a Ni=Mo double bond, is refluxed in

thf with methyl acrylate, ( $\text{CH}_2=\text{CHCO}_2\text{Me}$ ), a C–C coupling reaction of the olefin ensues. Complex **250**, which contains a molybdenum atom that is  $\eta^3$ -coordinated to a  $\text{MeO}_2\text{C}-\text{CH}=\text{CH}=\text{CH}-\text{CH}_2-\text{CO}_2\text{Me}$  ligand, is obtained, as shown in Scheme 134. The ligand forms by effective head-to-head coupling of the olefin together with a simultaneous C–H activation and a 1,2-H migration reaction. The alkenes have not strictly dimerized, since the new coupled ligand contains one hydrogen atom less than two methyl acrylate moieties.<sup>213</sup>

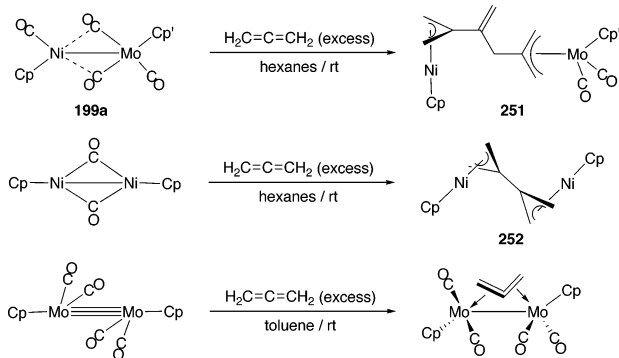
#### Scheme 134. Coupling of Two Alkenes Mediated by an Unsaturated Nickel–Molybdenum Complex



The solid-state structure of **250** was determined unambiguously by an X-ray diffraction study, which revealed that the ligand is *exo*-bonded to the  $\text{Mo}(\text{CO})_2\text{Cp}$  fragment. However  $^1\text{H}$  and  $^{13}\text{C}$  NMR spectroscopy and  $^1\text{H}-^1\text{H}$  and  $^{13}\text{C}-^1\text{H}$  2D NMR correlation spectroscopy indicate that in solution *exo* and *endo* isomers coexist in equilibrium in a 5:2 ratio. No coupled products were ever observed when the molybdenum or nickel dimers were reacted with methyl acrylate, indicating that a mixed-metal system is required for this coupling reaction.<sup>213,214</sup>

Allene trimerizes on the nickel–molybdenum framework present in the complex **199a** to give the  $\mu-\eta^3,\eta^3$ -biallylic  $\text{C}_9\text{H}_{12}$  dianionic ligand, shown in Scheme 135, that straddles the two metals in complex **251**.<sup>215</sup> Two new carbon–carbon bonds are formed in this oligomerization reaction. This reaction contrasts with that of allene with two related homobimetallic dimers: the dinickel complex  $[\text{Ni}(\mu\text{-CO})\text{Cp}]_2$  ( $\text{Ni}-\text{Ni}$ ) reacts very slowly to give a related complex **252**, in which two allenes have coupled to give the biallylic  $\mu-\eta^3,\eta^3$ -2,2'- $\text{C}_6\text{H}_8$  ligand. As in **251**, there is no metal–metal bond present.<sup>215</sup> In contrast, the unsaturated dimolybdenum complex  $[\text{Mo}(\text{CO})_2\text{Cp}]_2$  ( $\text{Mo}\equiv\text{Mo}$ ) adds on a single allene to give the  $\mu-\eta^2,\eta^2$ - $\pi$ -allene complex shown in the scheme.<sup>216,217</sup>

#### Scheme 135. Reactions of Allene with Nickel–Molybdenum and with Related Dinickel and Dimolybdenum Complexes

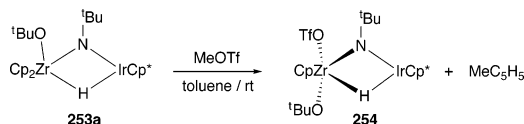


### 3.6. Other Miscellaneous Carbon–Carbon Coupling

This section covers a wide range of different and often unique C–C coupling reactions that are characterized by unsaturation in at least one of the two fragments that are coupling together.

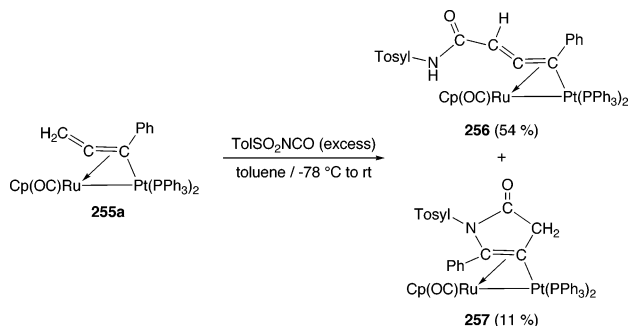
The early–late iridium–zirconium complex **253a** [ $\text{Cp}^*\text{Ir}(\mu\text{-H})(\mu\text{-N-}t\text{-Bu})\text{Zr}(\text{O-}t\text{-Bu})\text{Cp}_2$ ] (no Ir–Zr bond) reacts with methyl triflate to give (free) methylcyclopentadiene and the structurally characterized complex **254** shown in Scheme 136. This reaction is surprising since there are other reactive ligands present in the initial molecule but they are untouched. The lower electron density on the zirconium atom that results from Cp ligand loss is somewhat compensated by increased electron donation from the  $\mu$ -imido ligand. Thus, the Zr–N bond is observably shorter in the product **254** than in a complex of type **253** (with an OTol instead of an O-*t*-Bu group); the reverse is true for the Ir–N bond length.<sup>218</sup>

#### Scheme 136. Elimination of $\text{MeC}_5\text{H}_5$ from an Iridium/Zirconium Bis-cyclopentadienyl Complex on Addition of $\text{MeOSO}_2\text{CF}_3$



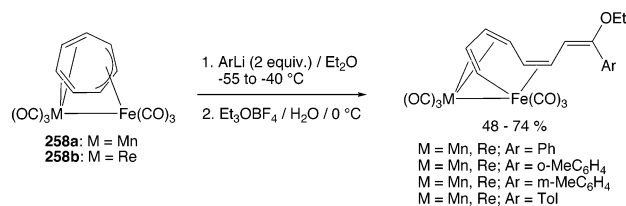
An unusual reaction between the allenyl complex **255a** and tolylsulfonyl isocyanate led to the formal insertion of the organic ligand into one of the two C–H bonds of the allenyl ligand in complex **256**. Another product, **257**, was isolated, which resulted from the cycloaddition of the ligand to the allenyl group. Products **256** and **257** were obtained in a 5:1 ratio. The structures of both species are shown in Scheme 137. When the two platinum-bonded  $\text{PPh}_3$  ligands are replaced with other groups (e.g.,  $\text{Ph}_2\text{P}(\text{CH}_2)_3\text{PPh}_2$  or 2-*t*-BuNC], only cycloaddition products similar to **257** are observed.<sup>219</sup>

#### Scheme 137. Coupling of an Isocyanate Ligand with an Allenyl Group on a Platinum–Ruthenium Framework



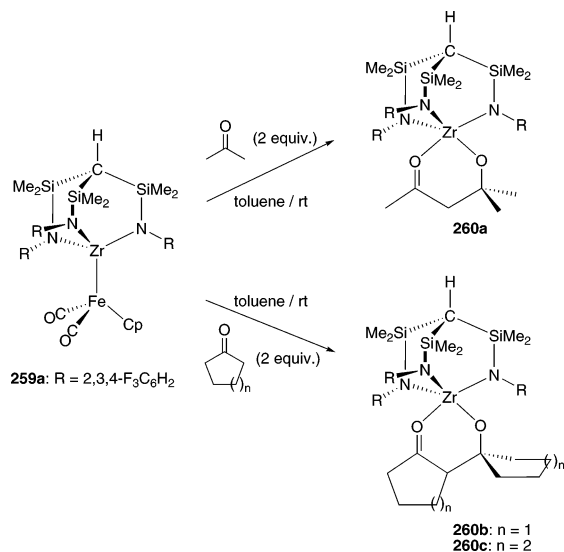
The bridging cycloheptatrienyl ligand in complexes **258** undergoes nucleophilic attack with aryllithium reagents and then electrophilic attack, with  $\text{Et}_3\text{O}^+\text{BF}_4^-$ , to give the ring-opened conjugated  $\mu$ -octatetraene complexes shown in Scheme 138. The structures of some examples of these complexes were established by single-crystal X-ray diffraction studies.<sup>220,221</sup>

#### Scheme 138. Cycloheptatrienyl Ring Opening and Formation of an Octatetraene Complex on Group 7–Iron Complexes



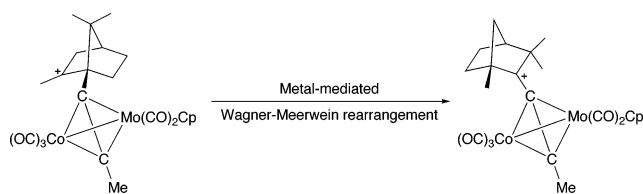
Aldol coupling of ketones has been observed on unsupported iron–zirconium-bonded complexes. Acetone, cyclopentanone, and cyclohexanone all undergo aldol coupling when these  $\alpha$ -H-containing ketones are treated with the iron–zirconium complex **259a** (Scheme 139). The coupled aldols are ligated to the zirconium atom via both oxygen atoms in the products **260**. They thus form stable six-membered rings that are analogous to those found in acetylacetonate complexes.<sup>222</sup>

**Scheme 139. Aldol Coupling of Ketones with  $\alpha$ -Hydrogen Atoms on an Early–Late Heterobimetallic Framework**



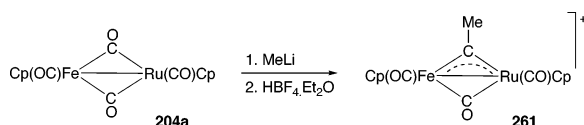
The metal-mediated Wagner–Meerwein rearrangement of a dimetal bonded carbocation has been observed. The bornyl-type cation bonded to a cobalt–molybdenum  $\mu$ -alkyne, whose framework is of type **128**, undergoes this rearrangement to give a fenchyl-type cation (Scheme 140).<sup>223</sup>

**Scheme 140. Wagner–Meerwein Rearrangement on a Cobalt–Molybdenum Bond**



The nucleophilic attack of MeLi on a carbonyl complex normally leads to an acyl anion. Protonation of this species followed by hydroxide-ion loss could lead to a metal carbyne complex. When this reaction sequence is attempted on the Fe–Ru complex **204a**, this is indeed observed (Scheme 141). The resulting red cationic carbyne complex **261** was not isolated.<sup>170,171</sup>

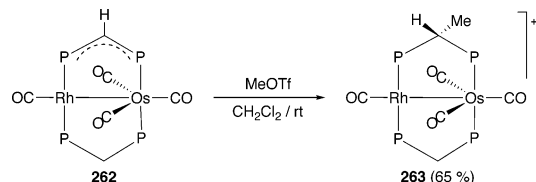
**Scheme 141. Nucleophilic Attack on a Carbonyl Ligand Followed by Protonation To Give a  $\mu$ -Carbyne Complex**



Treatment of the osmium–rhodium complex **262** shown in Scheme 142 with methyltriflate leads to the methylation

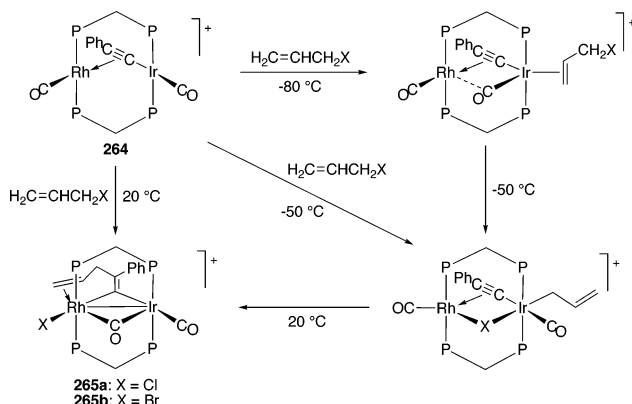
of the unsaturated bridging ligand and to the formation of a methylated derivative of a  $\mu$ -dppm ligand in complex **263**.<sup>224</sup>

**Scheme 142. Carbon–Carbon Bond Formation by Methylation with Methyltriflate on an Osmium–Rhodium Framework**



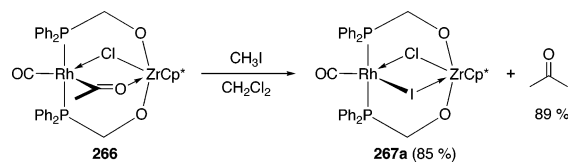
The alkynyl-bridged cationic complex **264** reacts with allyl chloride or bromide to give a substituted  $\mu$ -vinylidene complex **265** in which the allyl group has coupled with the alkynyl ligand (Scheme 143). The reaction progresses sequentially and intermediates have been observed at low temperature. Initial  $\eta^2$ -coordination of the allyl group takes place at  $-80$  °C, followed by oxidative addition of the allyl and the halide groups at  $-50$  °C. Final transformation to the vinylidene complexes **265** takes place at  $20$  °C.<sup>225</sup>

**Scheme 143. Alkynyl–Allyl Coupling on an Iridium–Rhodium Framework**



The  $\mu$ -acetyl group that connects the zirconium and rhodium centers in complex **266** (Scheme 144) is linked to the oxophilic zirconium atom via its oxygen atom. When treated with CH<sub>3</sub>I, acetone and the bis( $\mu$ -halo) complex **267** are formed in a heterobimetallic reductive C–C coupling reaction. The initial  $\mu$ -acetyl complex may also be protonated with HCl. The intermediate rhodium-bonded hydride species that was observed in the <sup>1</sup>H NMR spectrum reductively eliminates acetaldehyde (see Scheme 172). It is noteworthy that none of these early–late heterobimetallic complexes contain metal–metal bonds, and the comment is made that this system “appropriately models a heterogeneous Rh/ZrO<sub>2</sub> interface while avoiding intimate Rh/Zr contact.”<sup>226,227</sup>

**Scheme 144. Methylation of a  $\mu$ -Acetyl Ligand of a Rhodium/Zirconium Complex**



#### 4. Carbon–Carbon Bond Cleavage on Preformed Heterobimetallic Frameworks

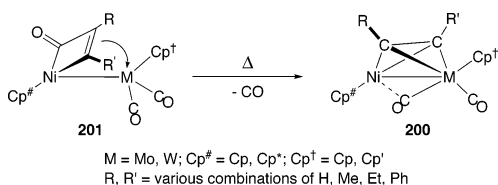
Reported reactions of this type most commonly involve the scission of a C–CO bond in entropy-driven reactions that liberate free carbon monoxide. Many of these reactions

are decarbonylation reactions of metallacyclic species, and these are considered together in section 4.1. Other decarbonylation reactions are classed in section 4.2. [For examples of decarbonylations that occur during protonation reactions, see section 5.1.9].

#### 4.1. Carbon–Carbon Bond Cleavage by Metallacyclic Complex Decarbonylation

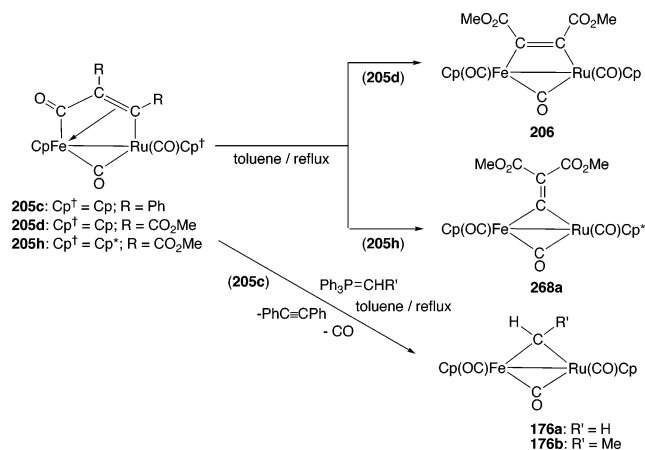
The metallacycles that are formed by coupling of CO with alkynes or with other organic groups often decarbonylate on heating, and this is a common decomposition pathway for these species. Typical examples, from one of the authors' own results, are the general decarbonylation reactions of group 6 nickelacycle complexes **201** to give the  $\mu$ -alkyne complexes **200**, which have a dimetallatetrahedrane geometry, and free CO (Scheme 145). These entropy-driven reactions take place on heating and are facile. The mass spectra of metallacycles **201** show the parent ion as a minor peak: predominant peaks are those with a  $m/e$  ratio that correspond to the  $\mu$ -alkyne complexes, which result from decarbonylation of these metallacycles (see also section 3.4.1, Scheme 105).<sup>46,131,180</sup>

#### Scheme 145. Thermal Decarbonylation of Alkyne–Carbonyl Coupled Metallacycles



The thermal decomposition of the dimetallacyclopentenone complex **205d**, formed by CO–DMAD coupling (section 3.4.1, Scheme 107) afforded the parallel-bonded  $\mu$ -DMAD complex **206**.<sup>170,171</sup> However the similar decomposition of the CpFe–RuCp\* analog **205h** led not to an alkyne but to the  $\mu$ -vinylidene complex **268a** (Scheme 146).<sup>184</sup> Decarbonylation and methylcarboxylate group migration occur concurrently, according to the proposed mechanism, via an intermediate  $\mu$ -DMAD complex.

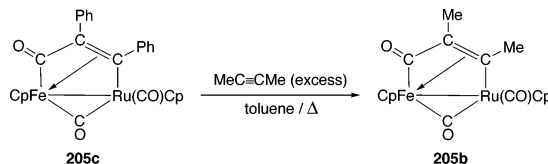
#### Scheme 146. Thermal Decarbonylation of Dimetallacycles on an Iron–Ruthenium Platform



The related Fe–Ru metallacycle **205c** may be transformed into  $\mu$ -CHR (R = H, Me) complexes **176a** and **176b** when treated with the Wittig reagents Ph<sub>3</sub>P=CHR (R = H, Me). Diphenylacetylene and CO are liberated.<sup>170,171</sup>

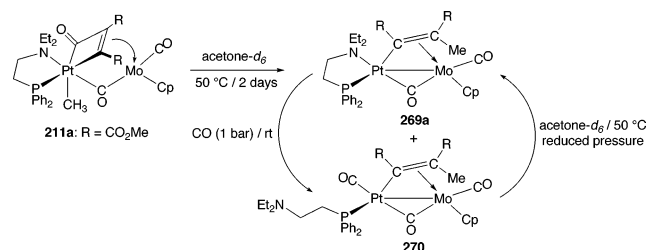
The PhC≡CPh group in the dimetallacycle complex **205c** is smoothly substituted with MeC≡CMe to give free diphenylacetylene and a new metallacycle **205b**, which contains a but-2-yne fragment, by simply heating **205c** in toluene with excess but-2-yne (Scheme 147).<sup>171</sup> (See ref 186 for a related reaction).

#### Scheme 147. Substitution of a PhC≡CPh by a MeC≡CMe Group in a Metallacyclic Species



The decarbonylation of the molybdenum platinacyclobutene complex **211a** shown in Scheme 148<sup>189</sup> also involves a group migration. When **211a** is allowed to stand in acetone-*d*<sub>6</sub> at 50 °C for 2 days, it undergoes a decarbonylation reaction that is accompanied by a methyl group migration. The final product is a  $\mu$ -C(CO<sub>2</sub>Me)=C(CO<sub>2</sub>Me)Me alkenyl complex **269a** whose structure was determined by an X-ray diffraction study. This complex adds CO reversibly. However, **211a** is not reformed, but instead **270** is obtained. In this species, the Et<sub>2</sub>NC<sub>2</sub>H<sub>4</sub>PPh<sub>2</sub> ligand is monodentate with the NEt<sub>2</sub> group no longer coordinated to the platinum atom.<sup>189</sup>

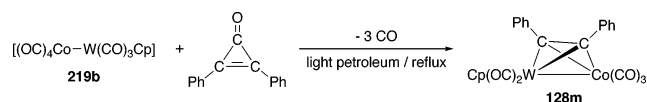
#### Scheme 148. Decarbonylation Accompanied by a Methyl Migration Reaction



#### 4.2. Carbon–Carbon Bond Cleavage by Other Decarbonylation Reactions

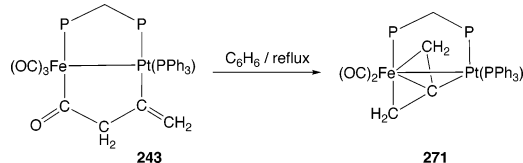
Diphenylcyclopropanone is decarbonylated when it reacts with the cobalt–tungsten complex **219b**. The product is the  $\mu$ -PhC≡CPh complex **128m**, shown in Scheme 149, which is believed to form by ring opening of the organic ligand and coordination of the resulting CPh–CPh–CO group onto the dimetal center, followed by decarbonylation.<sup>138</sup>

#### Scheme 149. Decarbonylation of Diphenylcyclopropanone on a Cobalt–Tungsten Framework



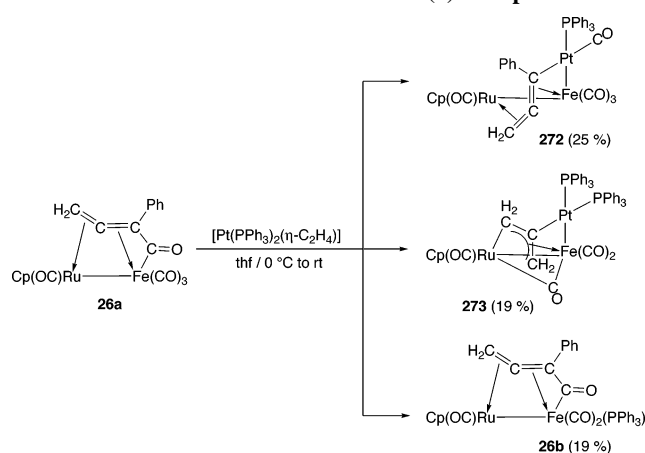
The bridging organic ligand that spans the iron–platinum bond in **243** shown in Scheme 150 is formed by the coupling of allene with a carbonyl ligand (see Scheme 129). When refluxed in benzene, this molecule eliminates CO and forms the allene complex **271** of unusual geometry. The ligand is  $\eta^3$ -coordinated to the iron atom but is also linked, via its central carbon atom, to the platinum. The structure of the closely related methyl-substituted allene complex was established by single-crystal X-ray diffraction.<sup>209</sup>

### Scheme 150. Thermal Decarbonylation of an Allene–CO Coupled Product



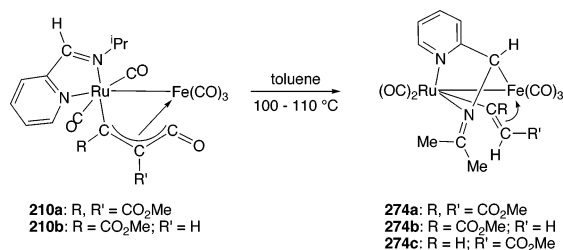
The Fe–Ru-bonded complex **26a** (Scheme 13 and Scheme 151) affords a mixture of di- and trimetallic products when reacted with  $[\text{Pt}(\text{PPh}_3)_2(\eta\text{-C}_2\text{H}_4)]$ . The trimetallic products **272** and **273** contain Ru–Fe–Pt linkages: **272** is an allenyl species, while **273** is a  $\mu$ -dimetallallyl complex, coordinated to a third metal. In these two molecules, the CPh–CO bond originally present has been ruptured. The third product, **26b**, is a  $\text{PPh}_3$ -substituted analog of **26a**.<sup>228</sup>

### Scheme 151. Decarbonylation and Subsequent Reaction of an Unsaturated Hydrocarbonyl Ligand Straddling an Iron–Ruthenium Bond with a Platinum(0) Complex



The thermolysis of the iron–ruthenium 2-pyridylimine propenone complex **210a** (Scheme 152) led to a rearrangement of the imine ligand and to the cleavage of the alkyne–C(O) bond to give the  $\mu$ -alkenyl complex **274a** shown in the scheme. The diimine ligand rearrangement involves a H-transfer reaction from the N-bonded isopropyl carbon atom to what becomes the terminal vinyl carbon. The unsymmetric propenone species **210b** afforded a mixture of alkenyl complexes **274b** and **274c**.<sup>188</sup>

### Scheme 152. Decarbonylation and Rearrangement of a Diimine–Propenone Iron–Ruthenium Complex



## 5. Carbon–Hydrogen Bond Coupling on Preformed Heterobimetallic Frameworks

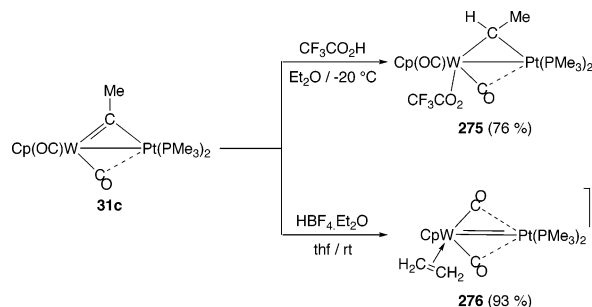
### 5.1. Protonation ( $\text{H}^+$ Addition) Reactions

#### 5.1.1. Proton Addition to Carbynes

Protonation of the alkyldiene carbon atom affords  $\mu$ -alkylidene complexes. These species occasionally rearrange to give

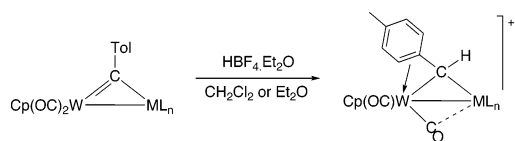
alkene species. Many examples of this reaction come from the group of Stone and co-workers. An early report is the protonation of the platinum–tungsten complex **31c**. The products obtained are a function of the acid used (Scheme 153). With trifluoroacetic acid, a neutral  $\mu$ -alkylidene complex **275** is obtained, in which the TFA group is coordinated to the tungsten atom. In contrast,  $\text{HBF}_4 \cdot \text{Et}_2\text{O}$  afforded the cationic  $\eta\text{-C}_2\text{H}_4$  complex **276** (which is iso-electronic to the  $\text{Pt}=\text{Rh} \eta\text{-C}_2\text{H}_4$  species **46**).<sup>143,144</sup>

### Scheme 153. Protonation of a $\mu$ -CMe Ligand That Spans a Platinum–Tungsten Bond



The protonation of the  $\mu$ -CTol ligands present in a variety of heterobimetallic  $\mu$ -carbyne complexes with W–M bonds ( $\text{M} = \text{Cr}, \text{Co}, \text{Rh}, \text{Pt}$ ) has been achieved with  $\text{HBF}_4 \cdot \text{Et}_2\text{O}$ . In products **9**, **174**, or **278**, the  $\mu$ -CHTol ligand formed is  $\eta^3$ -coordinated to the tungsten atom in what can be considered to be a  $\pi$ -allylic bonding mode (Scheme 154).<sup>62,141,142</sup> The reactions proceed in high yield and are reversible in some cases when hydridic sources are added.<sup>141</sup> Occasionally, there is rotation of the Tol group about the C<sub>carbene</sub>–Tol bond at room temperature on the <sup>1</sup>H NMR time scale. This can be arrested at low temperature.

### Scheme 154. Protonation of $\mu$ -CTol Moieties Affords $\mu\text{-}\eta^1\text{-}\eta^3\text{-CHTol}$ Alkylidene Ligands

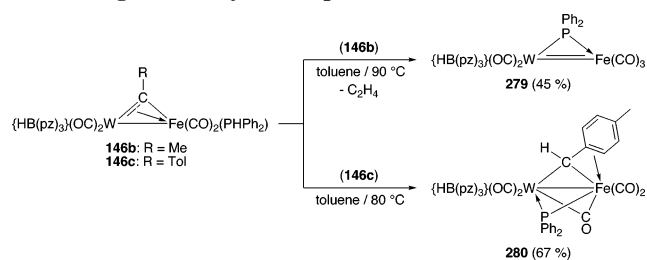


- 31b:**  $\text{ML}_n = \text{Pt}(\text{PMe}_3)_2$   
**31d:**  $\text{ML}_n = \text{Pt}(\text{PMe}_2\text{Ph})_2$   
**31e:**  $\text{ML}_n = \text{Pt}(\text{PMePh}_2)_2$   
**148a:**  $\text{ML}_n = \text{Co}(\text{CO})\text{Cp}^*$   
**148d:**  $\text{ML}_n = \text{Rh}(\text{PMe}_3)(\eta^5\text{-C}_9\text{H}_7)$   
**277:**  $\text{ML}_n = \text{Cr}(\text{CO})(\text{NO})\text{Cp}$   
**9h:**  $\text{ML}_n = \text{Pt}(\text{PMe}_3)_2$  (90 %)  
**9i:**  $\text{ML}_n = \text{Pt}(\text{PMe}_2\text{Ph})_2$  (81 %)  
**9j:**  $\text{ML}_n = \text{Pt}(\text{PMePh}_2)_2$  (87 %)  
**174a:**  $\text{ML}_n = \text{Co}(\text{CO})\text{Cp}^*$  (92 %)  
**174b:**  $\text{ML}_n = \text{Rh}(\text{PMe}_3)(\eta^5\text{-C}_9\text{H}_7)$  (100 %)  
**278:**  $\text{ML}_n = \text{Cr}(\text{CO})(\text{NO})\text{Cp}$  (40 %)

Protonation can also be achieved indirectly via oxidative addition of P–H bonds of  $\text{PPh}_2\text{H}$  ligands and transfer of the hydrogen to the alkyldiene carbon atom. This reaction affords two different products that depend on the nature of the alkyldiene ligand (Scheme 155). When the  $\mu$ -ethylidene complex **146b** is heated, loss of  $\text{C}_2\text{H}_4$  takes place via the presumed formation and decomposition of a  $\mu$ -CHMe alkyldiene complex to give **279**. However, thermolysis of the analogous  $\mu$ -methyltolylidene complex **146c** afforded **280**, which contains a  $\mu\text{-}\eta^1\text{-}\eta^3\text{-CHTol}$  ligand. The lack of  $\beta$ -hydrogen atoms in the ligand and the  $\pi\text{-}\eta^3\text{-benzylic}$  interaction with the iron atom both contribute to the stability of complex **280**.<sup>79</sup>

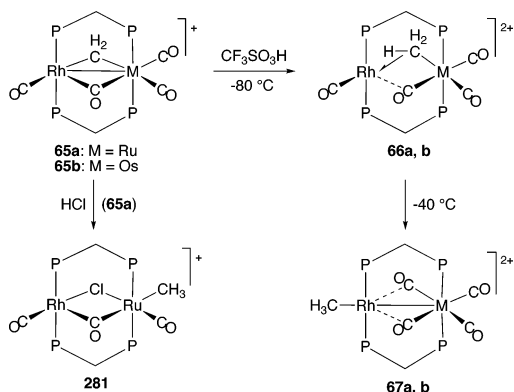
#### 5.1.2. Proton Addition to Carbenes

The protonation of carbene or alkyldiene complexes leads in principle to alkyl species. Frequently these species are

**Scheme 155. Oxidative Addition of P–H Bonds and Hydrogen Addition to the  $\mu$ -Carbyne Carbon of Unsaturated Iron–Tungsten Carbyne Complexes**


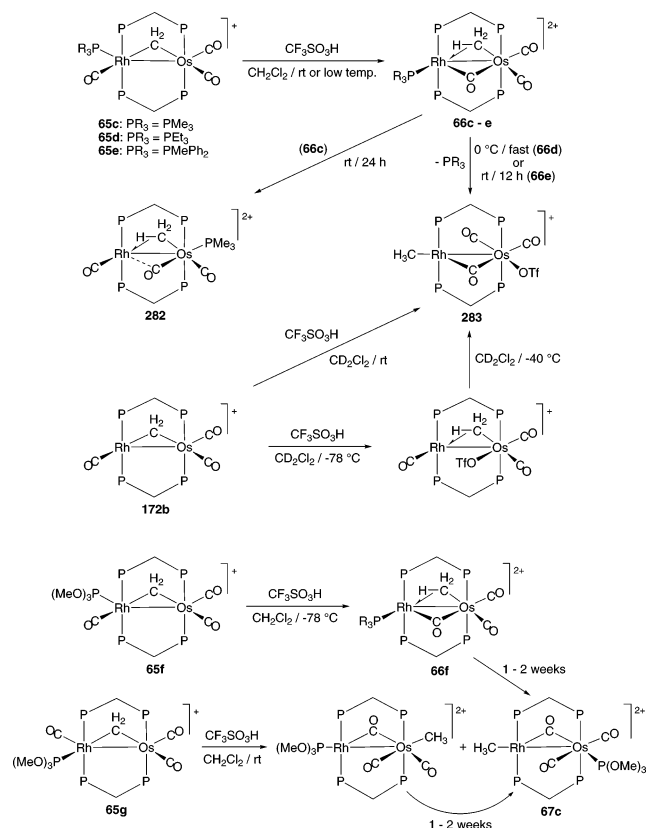
electronically unsaturated, so agostic hydrogen interactions are often seen in such products.

Protonation of the cationic species **65** with triflic acid at  $-80\text{ }^\circ\text{C}$  leads to dications **66** in which the group 8 metal-bonded methyl group undergoes an agostic interaction with the rhodium atom. These complexes are transformed into terminal rhodium-bonded methyl species **67** when the solution is warmed to  $-40\text{ }^\circ\text{C}$  (Scheme 156). Subsequent “CO insertion” leads to  $\mu$ -acetyl complexes. (These reactions have been discussed earlier in section 3.1.1, Scheme 44). Addition of HCl to the Rh–Ru complex **65a** leads, in contrast, to the ruthenium-bonded methyl complex **281**, which also contains a bridging chloride group.<sup>106,107</sup>

**Scheme 156. Protonation of  $\mu$ -Methylene Complexes To Form Methyl Ligands**


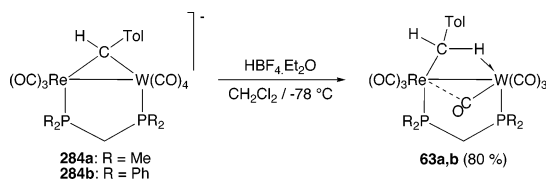
Recently, the protonation of the trialkylphosphine- and trialkylphosphite-substituted rhodium–osmium complexes **65c–g** with HOTf was described. (These complexes are trialkylphosphine- or -phosphite-substituted derivatives of **65b** but the CO ligands are now all terminal). The protonation products of the trialkylphosphine derivatives are the dications **66c–e**, whose structures are similar, but not identical, to the phosphine-free complex **66b**. A Rh–Os bond and a fully bridging CO are now present.

These ligands should stabilize the osmium-bonded methyl group, and the increased electron density thus should lead to more stable agostic complexes. Indeed, a stable agostic bimetallic complex **282** may be isolated following  $\text{PMe}_3$  ligand migration in **66c**. However, with other phosphine ligands, methyl migration onto the rhodium atom takes place, accompanied with phosphine loss and coordination of the triflate anion onto the osmium atom to give compound **283** (Scheme 157). The same complex is also obtained when the unsaturated phosphine-free cation **172b** is protonated with triflic acid. An agostic intermediate was also observed at low temperature.<sup>229</sup>

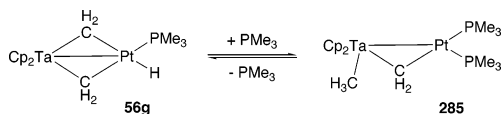
**Scheme 157. Protonation of Rhodium–Osmium  $\mu$ -Methylene Complexes**


The monosubstituted trimethylphosphite complexes exist in two isomeric forms, **65f** and **65g**, with the rhodium-bonded  $\text{P}(\text{OMe})_3$  ligand *cisoid* or *transoid* to the  $\mu$ - $\text{CH}_2$  group. The reactivity of the two isomers toward protonation is different, though the same final product, **67c**, is obtained after 1–2 weeks of reaction (Scheme 157).

The rhenium–group 6 alkylidene complexes  $[(\text{OC})_5\text{M}(\mu\text{-CHTol})\text{Re}(\text{CO})_4]^-$  ( $\text{M}=\text{Re}$ ;  $\text{M} = \text{Cr}, \text{Mo}, \text{W}$ ) decompose when protonated with  $\text{HBF}_4$ . However, clamping the two metals together with  $\mu$ -dmpm or  $\mu$ -dppm ligands stabilizes the system so that the protonation of the complexes **284** at  $-78\text{ }^\circ\text{C}$  affords the 4-methylbenzyl complexes **63** shown in Scheme 158 (see also Scheme 43). NMR and crystallographic data indicate that there are agostic interactions with the tungsten atom in these products [the  $\text{W}\cdots\text{C}$  distance to the  $\text{CH}_2\text{Tol}$  carbon atom is  $2.539(7)\text{ \AA}$ ].<sup>104,105</sup>

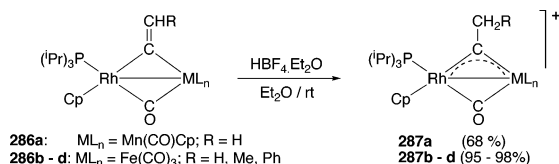
**Scheme 158. Formation of a Rhenium–Tungsten Complex with an Agostic Benzyl Ligand**


In carbene complexes that contain metal hydride ligands, the addition of the hydride to a carbene carbon ligand can occasionally be induced. This is observed when the platinum–tungsten bis( $\mu$ -methylene) complex **56g** is treated with  $\text{PMe}_3$ . The ligand induces a hydride addition to one of the  $\mu$ - $\text{CH}_2$  groups to give the tantalum-bonded methyl complex **285** depicted in Scheme 159. The reaction is reversible.<sup>230</sup>

**Scheme 159.  $\text{PMe}_3$ -Induced Insertion of Hydride Ligand into a Platinum–Methylene Bond**

**5.1.3. Proton Addition to Vinylidenes**

The protonation of  $\mu$ -vinylidene ligands in heterobimetallic complexes leads either to alkenyl or to carbyne complexes, depending on whether the  $\alpha$ - or the  $\beta$ -carbon of the vinylidene group is attacked.

The manganese–rhodium  $\mu$ -vinylidene complex **286a** may be reversibly protonated to give the dark blue cationic carbyne complex **287a** (Scheme 160), which is stable in the solid state. A characteristic carbyne-carbon  $^{13}\text{C}$  NMR chemical shift of  $\delta = 452.7$  ppm is observed for this species. Similar carbyne complexes **287b–d** are observed when the iron–rhodium complexes **286b–d** are treated with  $\text{HBF}_4$ .<sup>231</sup>

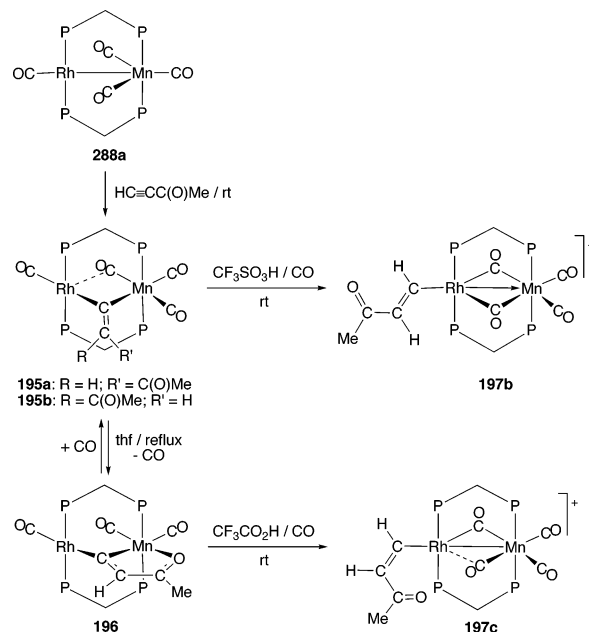
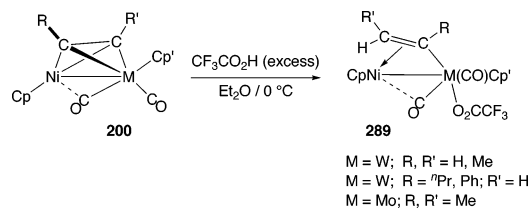
**Scheme 160. Formation of  $\mu$ -Carbyne Complexes by Protonation of  $\mu$ -Vinylidene Complexes**


The  $\mu$ -vinylidene isomers **195** (Scheme 161) can be made by direct reaction of  $[(\text{OC})\text{Rh}(\mu\text{-dppm})_2\text{Mn}(\text{CO})_3]$  ( $\text{Mn}-\text{Rh}$ , **288a**) with  $\text{HC}\equiv\text{CC}(\text{O})\text{Me}$ . When the initial vinylidene mixture **195** is treated with triflic acid, the alkenyl complex **197b** is obtained in a reaction that is accompanied by metal–metal bond formation. The alkenyl ligand is terminally bonded to the rhodium atom in the heterobimetallic complex, and the acetyl ligand is *trans* to the metal. Thermolysis of **195** leads to CO loss, and a new  $\mu$ -vinylidene complex **196** is formed in which the ketone carbonyl functionality is also ligated to the manganese atom. Protonation of this complex affords an alkenyl species **197c** in which the acetyl group is now in a *cis* geometry with respect to the rhodium atom.<sup>178</sup>

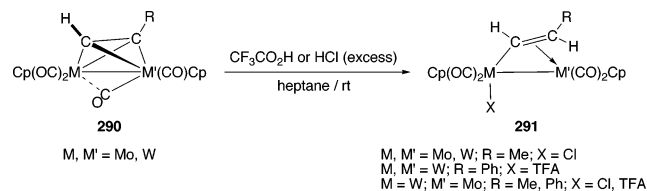
**5.1.4. Proton Addition to Alkynes**

Trifluoroacetic acid has been used to convert a series of  $\mu$ -alkyne nickel–molybdenum and tungsten complexes into their corresponding  $\mu$ - $\eta^1, \eta^2$ -alkenyl derivatives. The protonation of complexes **200** (Scheme 162) proceeds stereospecifically in a Markovnikov manner to afford the alkenyl species **289** of general formula  $[\text{CpNi}\{\mu\text{-}\eta^1(\text{M})\eta^2(\text{Ni})\text{-cis-CR}=\text{CHR}'\}\text{M}(\text{CO})_2(\text{CO}_2\text{CF}_3)\text{Cp}']$  ( $\text{Ni}-\text{M}$ ,  $\text{M} = \text{Mo, W}$ ). Occasionally, the Markovnikov addition product subsequently isomerizes to the anti-Markovnikov isomer. The incoming proton (or deuteron when  $\text{CF}_3\text{CO}_2\text{D}$  is used) is in a *cis* or *syn* orientation with respect to the group 6 metal atom. The stereochemistry was determined by a series of deuterium labeling experiments and by careful study of the  $^1\text{H}-^1\text{H}$  and  $^{183}\text{W}-^1\text{H}$  coupling constants in the  $^1\text{H}$  NMR spectra of the complexes. The structure of the 2-butenyl nickel–tungsten complex of geometry **289** confirmed that the structures proposed on the basis of  $^1\text{H}$  NMR data were correct.<sup>232</sup>

A series of group 6 bimetallic complexes **290** afforded similar  $\mu$ - $\eta^1, \eta^2$ -alkenyl complexes **291** after anti-Markovnikov protonation with  $\text{HCl}$  or  $\text{CF}_3\text{CO}_2\text{H}$  (Scheme 163). In

**Scheme 161. Protonation of  $\mu$ -Vinylidene Complexes Affords Alkenyl Complexes**

**Scheme 162. Stereospecific Protonation of Nickel–Molybdenum and –Tungsten  $\mu$ -Alkyne Complexes**


the mixed-metal case, the tungsten atom is oxidized, and both the alkenyl ligand and the anion ( $\text{Cl}^-$  or  $\text{CF}_3\text{CO}_2^-$ ) are coordinated to it. The molecular structure of  $[\text{Cp}(\text{OC})_2\text{Mo}\{\mu\text{-}\eta^1(\text{W}), \eta^2(\text{Mo})\text{-trans-CH}=\text{CHPh}\}\text{W}(\text{CO})_2\text{ClCp}]$  ( $\text{Mo}-\text{W}$ ) was determined by an X-ray study.<sup>233</sup>

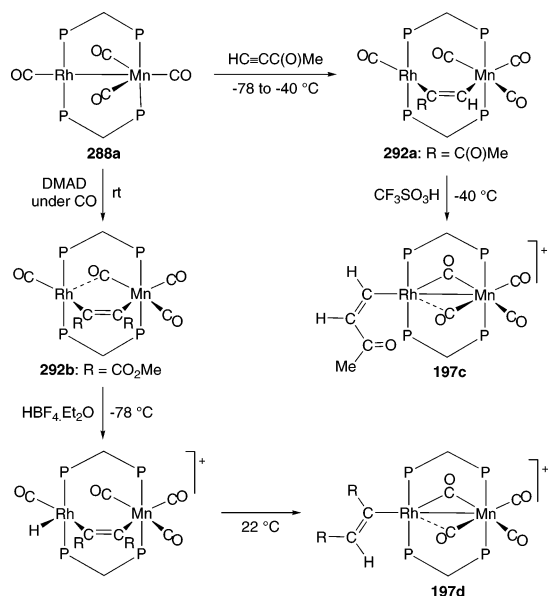
**Scheme 163. Stereospecific Protonation of Group 6  $\mu$ -Alkyne Complexes**


Low temperature addition of  $\text{HC}\equiv\text{CC}(\text{O})\text{Me}$  to the mixed-metal complex **288a** affords the parallel-bridged  $\mu$ -alkyne complex **292a**. This species rearranges to the  $\mu$ -vinylidene mixture **195** shown in Scheme 161 when warmed above  $-22^\circ\text{C}$ , but it may be protonated at low temperature to give the alkenyl complex **197c**, as depicted in Scheme 164.<sup>178</sup> (See section 5.3.1 for protonation followed by alkyne addition). The related parallel-bridged  $\mu$ -DMAD complex **292b** can also be protonated to give the alkenyl complex **197d** in which the two carboxymethyl groups are mutually *cis*. An intermediate rhodium hydride complex is formed during the course of this reaction.<sup>234</sup>

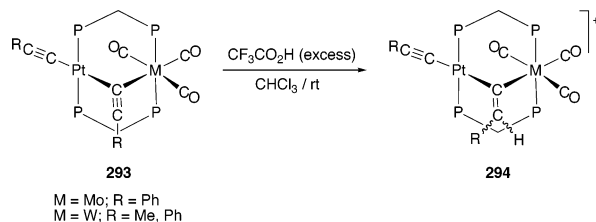
**5.1.5. Proton Addition to Alkynyls**

A series of A-frame group 6–platinum complexes **293** that contain both bridging and terminal acetylde ligands

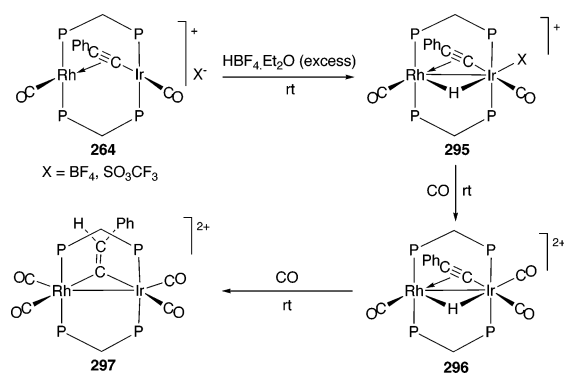


**Scheme 164. Alkenyl Formation from Alkyne Protonation on Manganese–Rhodium Templates**


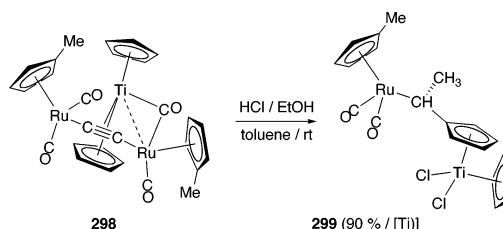
(Scheme 165) all react with trifluoroacetic acid to give  $\mu$ -vinylidene complexes **294**. Only the bridging acetylide ligands are protonated, and despite a Pt–W distance of 3.037(1) Å in one of the starting materials, no metal–metal bonds are believed to be present in the starting materials or products.<sup>235</sup>

**Scheme 165. Preferential Protonation of  $\mu$ -Acetylide Ligands in Bis-acetylide Mixed-Metal Complexes**


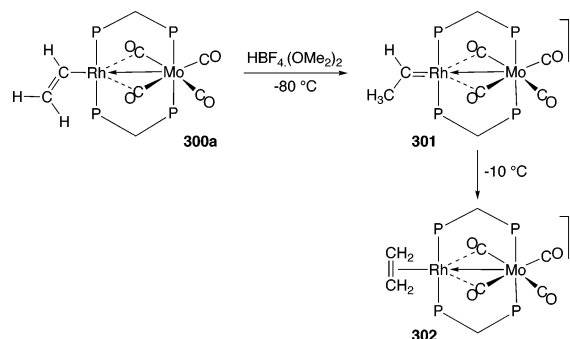
The alkenyl cationic A-frame complex **264** adds on H<sup>+</sup> and forms the bridging hydride complex **295**: the addition is accompanied by metal–metal bond formation and the anion (BF<sub>4</sub><sup>-</sup> or SO<sub>3</sub>CF<sub>3</sub><sup>-</sup>) is also loosely coordinated. Coupling of the acetylide ligand with the hydride is induced by the sequential addition of 2 equiv of CO and yields the dicationic  $\mu$ -vinylidene complex **297** depicted in Scheme 166, via a tricarbonyl intermediate **296**.<sup>225</sup>

**Scheme 166. Conversion of an Alkenyl into a Vinylidene Ligand by Electrophilic (H<sup>+</sup>) Attack on a Rhodium/Iridium Center**


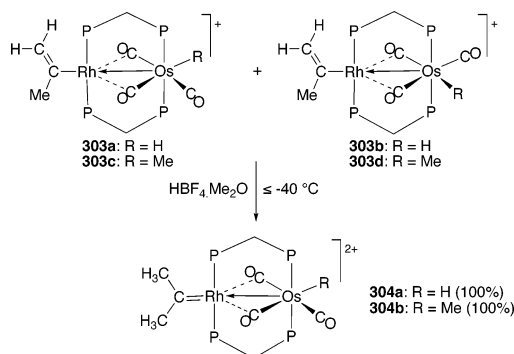
Complex **298** shown in Scheme 167 is best regarded as a dimetalla-alkyne that is  $\pi$ -coordinated to a Cp<sub>2</sub>Ti fragment. This complex reacts in an unprecedented manner with an ethanolic solution of HCl, losing a ruthenium atom and forming multiple C–H bonds and one C–C bond. The final product is the bimetallic Cp-ring-activated titanocene dichloride derivative **299**.<sup>236</sup>

**Scheme 167. Complex Transformation of Dimetalla-alkyne Trimetallic Complex into a Dimetallic Cp-Ring Activated Titanocene Dichloride Derivative**

**5.1.6. Proton Addition to Alkenyls**

The rhodium-bonded terminal vinyl complex [(OC)<sub>4</sub>Mo( $\mu$ -dppm)<sub>2</sub>Rh(CH=CH<sub>2</sub>)] (Mo–Rh, **300a**) may be protonated with HBF<sub>4</sub> at –80 °C to form the rhodium-bonded CHMe alkyldene species **301** shown in Scheme 168. This cation rearranges to the ethylene complex **302** when warmed above –10 °C.<sup>113</sup>

**Scheme 168. Transformation of a  $\eta^1$ -Vinyl into a  $\eta^2$ -Ethene Group on a Molybdenum–Rhodium Template**


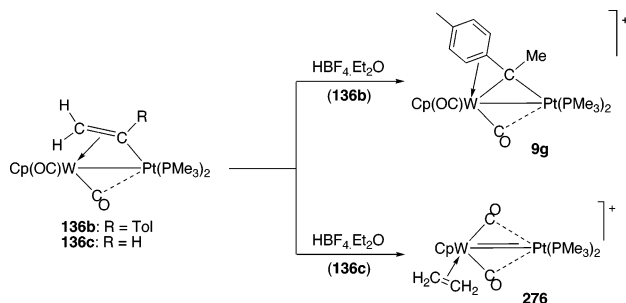
Despite their cationic nature, the mixture of Os–Rh stereoisomeric alkenyl complexes **303a,b** and **303c,d** (Scheme 169) can be protonated with HBF<sub>4</sub>·Me<sub>2</sub>O at low temperature; the molecules are transformed into rhodium-bonded terminal alkyldene dicationic complexes **304**.<sup>114</sup>

**Scheme 169. Protonation of Cationic Alkenyl Complexes to Alkyldene Complexes**


The alkenyl group in complex **136b** is transformed into a  $\mu$ - $\eta^1, \eta^3$ -CHTol group in the complex **9g** when **136b** is

reacted with  $\text{HBF}_4 \cdot \text{Et}_2\text{O}$  (the reaction may be reversed; see Scheme 227, section 6.1.1).<sup>237</sup> The bridging vinyl ligand in the related **136c** is, in contrast, converted into the unsaturated  $\eta$ -ethylene complex **276** under similar conditions (Scheme 170).<sup>143,144</sup>

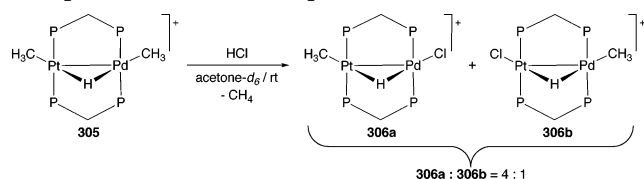
#### Scheme 170. Protonation of Alkenyl Ligands That Span Platinum–Tungsten Bonds



#### 5.1.7. Proton Addition to Alkyls and Acyls

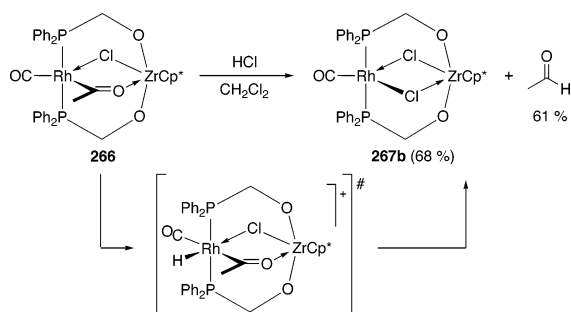
Methane is eliminated when the cationic mixed-metal A-frame complex **305** is treated with HCl in acetone- $d_6$  (Scheme 171). Isomers **306** are formed: the major product **306a** results from Pd–C bond cleavage, but around a fifth of the methane produced comes from Pt–C bond cleavage to give complex **306b**.<sup>238</sup>

#### Scheme 171. Elimination of Methane from an A-frame Group 10 Mixed-Metal Complex



When the  $\mu$ -acetyl group in complex **266** (Scheme 172) is treated with HCl, the intermediate rhodium-bonded hydride species that was observed in the  $^1\text{H}$  NMR spectrum reductively eliminates acetaldehyde and forms **267b**. The related reaction of **266** with MeI to generate acetone has been mentioned earlier (section 3.6, Scheme 144).<sup>226,227</sup>

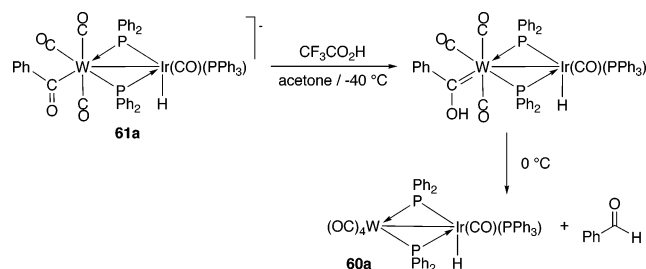
#### Scheme 172. Reductive Elimination of Acetaldehyde by Protonation of a $\mu$ -Acetyl Ligand in a Rhodium/Zirconium Complex



The acyl ligand in the heterobimetallic acyl anion **61a** shown in Scheme 173 (see also section 3.1.1, Scheme 40) may be protonated at the acyl oxygen atom by TFAH at  $-40^\circ\text{C}$  to give a spectroscopically characterized hydroxycarbene moiety that is terminally bonded to the tungsten atom. This

complex undergoes a bimetallic reductive elimination reaction to give benzaldehyde and **60a** when warmed up to  $0^\circ\text{C}$ .<sup>99,100</sup>

#### Scheme 173. Reductive Elimination of Benzaldehyde by Protonation of an Acyl Ligand in an Iridium–Tungsten Complex

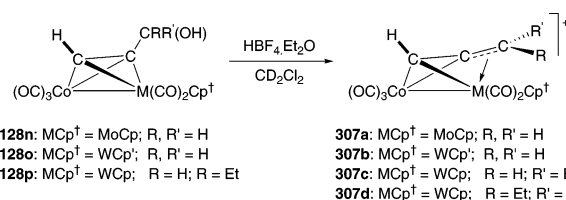


#### 5.1.8. Proton Addition To Generate Heterodimetal-Bound Carbocations

Carbocations have been stabilized on bimetallic frameworks. Heterobimetallic examples are known on both cobalt–molybdenum and cobalt–tungsten frameworks and, more recently, on nickel–molybdenum and nickel–tungsten frameworks. A common synthetic entry to such species is by the protonation of a hydroxy or of an alkoxy group of a  $\mu$ -propargylic alcohol or ether and subsequent loss of water or of an alcohol. The reaction can often be reversed to regenerate a  $\mu$ -alkyne complex by reacting the carbocation with nucleophiles such as hydride, hydroxide, or alkoxide anions. These reactions have been reviewed<sup>19</sup> and are not covered comprehensively here, since they are not strictly hydrocarbyl ligand transformations (C–O bonds are usually broken in these reactions and not C–C or C–H bonds). A few typical examples are detailed.

The first examples of this chemistry in mixed-metal systems were reported for cobalt–molybdenum and –tungsten systems. Protonation of the  $\mu$ -hydroxyalkyne complexes **128n,o** (Scheme 174) affords the carbocationic complexes **307a,b**, respectively. Because there is restricted rotation about the  $\text{C}\equiv\text{CH}_2$  bond in cations **307a,b**, the  $\text{CH}_2$  protons are magnetically inequivalent in their  $^1\text{H}$  NMR spectrum. Protonation of the  $\mu$ - $\text{HC}\equiv\text{CCH}(\text{Et})\text{OH}$  complex **128p** afforded a mixture of non-interconvertible carbocations **307c** and **307d**. All these carbocations are stabilized by interactions with the group 6 metal.<sup>239,240</sup>

#### Scheme 174. Carbocation Formation Following the Protonation of Cobalt–Molybdenum and –Tungsten Hydroxyalkyne Complexes



**128n**:  $\text{MCp}^\dagger = \text{MoCp}$ ; R, R' = H  
**128o**:  $\text{MCp}^\dagger = \text{WCp}$ ; R, R' = H  
**128p**:  $\text{MCp}^\dagger = \text{WCp}$ ; R = H; R' = Et

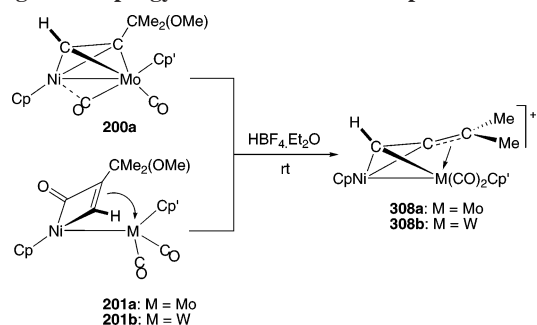
**307a**:  $\text{MCp}^\dagger = \text{MoCp}$ ; R, R' = H  
**307b**:  $\text{MCp}^\dagger = \text{WCp}$ ; R, R' = H  
**307c**:  $\text{MCp}^\dagger = \text{WCp}$ ; R = H; R' = Et  
**307d**:  $\text{MCp}^\dagger = \text{WCp}$ ; R = Et; R' = H

Similar reactions take place with other cobalt–molybdenum  $\mu$ -alkyne species of type **128** with  $\beta$ -hydroxyalkynes;  $\alpha$ - $\text{CF}_3$  propargylium cations are obtained by protonation with  $\text{HBF}_4$  of a  $\mu$ - $n$ - $\text{C}_5\text{H}_{11}\text{C}\equiv\text{CCMe}(\text{CF}_3)\text{OH}$  species (followed by loss of water)<sup>241</sup> and 2-bornyl cations can also be synthesized (without Wagner–Meerwein rearrangements).<sup>242</sup>

Nickel–molybdenum and –tungsten complexes may also be protonated. Addition of  $\text{HBF}_4$  to a  $\alpha$ -methoxyalkyne

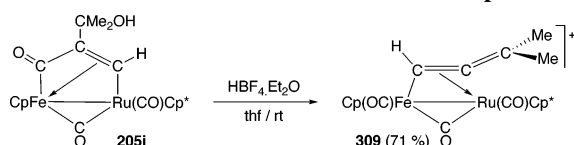
complex **200a** led to methanol loss and to the formation of the bimetallic propargylic cation **308a** shown in Scheme 175. The nickel–tungsten cation **308b** could not be prepared this way, but it (and the Ni–Mo cation **308a**) could be accessed by protonating the related metallacyclic products **201a** and **201b**, which have  $\mu\text{-C(O)-CMe}_2(\text{OMe})\text{-C(H)}$  ligands. The variable-temperature  $^1\text{H}$  NMR spectra of cations **308** demonstrate that in **308a** there is rotation about the  $\text{C}\cdots\text{CMe}_2$  bond. This does not take place in **308b**, presumably because the tungsten interacts more strongly with the cationic center.<sup>181</sup>

#### Scheme 175. Synthesis of Nickel–Molybdenum and –Tungsten Propargylic Carbocationic Complexes



Related species are available in iron–ruthenium systems. The reaction of the dimetallacycle **205i** with  $\text{HBF}_4\cdot\text{Et}_2\text{O}$  affords the cationic species **309** shown in Scheme 176. An X-ray structural determination established that the  $\mu\text{-}\eta^1,\eta^2\text{-allenyl}$  ligand in **309** was  $\sigma$ -bonded to the iron and  $\pi$ -complexed to the ruthenium atom, with an Fe–Ru bond of 2.6831(8) Å. This is slightly longer than what is found in the starting material **205i** [Fe–Ru = 2.6449(7) Å]. Cation **309** is highly fluxional.<sup>184</sup>

#### Scheme 176. Protonation of a Hydroxy Group To Generate a Heterobimetallic Stabilized Carbocationic Complex



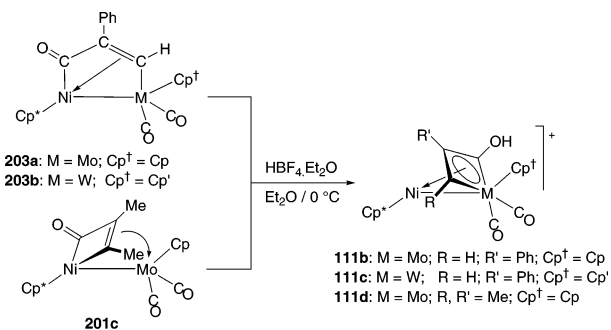
#### 5.1.9. Other Protonations of Hydrocarbyl Ligands

When the nickel–molybdenum and –tungsten complexes **203a** and **203b** (Scheme 177) are reacted with  $\text{HBF}_4\cdot\text{Et}_2\text{O}$ , cationic mixed-metal complexes **111b** and **111c**, which contain molybdena- or tungstenacycle rings are obtained. The transformation of a bimetallic complex that contains a nickelacycle into one that consists of a molybdenacycle ring is also observed when the nickelacyclobutenone complex **201c** is protonated. This ring flip can also be induced by methylation of the metallacycle carbonyl in **201c** by using  $\text{Me}_3\text{O}^+\text{BF}_4^-$  to give **111a** (see Schemes 64 and 72).<sup>46,131</sup>

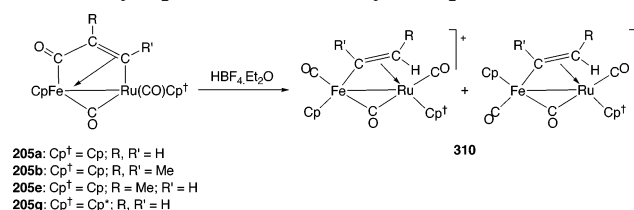
The protonation of various iron–ruthenium complexes **205** leads to CO loss and to the formation of isomeric iron  $\sigma$ -bonded  $\mu$ -alkenyl complexes **310** as shown in Scheme 178. The R and R' groups are always in a *cis* configuration,<sup>170,171</sup> and these reactions mirror those seen in homobimetallic  $\text{Fe}_2$  and  $\text{Ru}_2$  systems.<sup>243</sup> The structure of a  $\mu\text{-CH=CH}_2$  product from the  $\text{CpFe-RuCp}^*$  derivative was determined by X-ray diffraction and shows an Fe–Ru bond of 2.7009(4) Å.<sup>184</sup>

A similar reaction ensues when the iron–platinum dimetallacyclopentenone complexes **208** shown in Scheme 179

#### Scheme 177. Electrophile-Induced Ring Rearrangements in Nickel–Molybdenum and –Tungsten Complexes

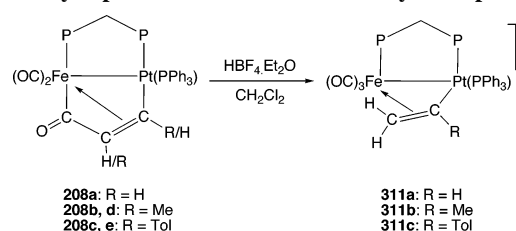


#### Scheme 178. Protonation of Iron–Ruthenium Dimetallacyclopentenones to Alkenyl Complexes



are protonated. The alkenyl complexes **311** obtained have a  $\text{-CR=CH}_2$  regiochemistry irrespective of the arrangement of the R and H groups on the starting dimetallacyclopentenone complex **208**. An X-ray diffraction study of the propenyl complex was carried out and confirmed the proposed platinum  $\sigma$ -bonded structures of these alkenyl complexes.<sup>186</sup>

#### Scheme 179. Protonation of Iron–Platinum Dimetallacyclopentenones To Afford Alkenyl Complexes



The cobalt–tungsten complex **149a** (Scheme 180; see also Scheme 86) is converted into **175**, a complex that can be regarded as either a metalloallyl species or alternatively as a vinyl carbene complex. The structure of the reaction product was established crystallographically and indicates the presence of a Co–W bond of 2.552(1) Å.<sup>141,169</sup>

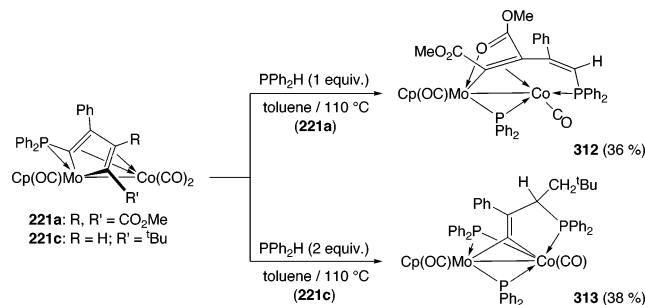
#### Scheme 180. Protonation of a Heterobimetallic Tungstenacyclobutadienyl–Cobalt Complex



The oxidative addition of diphenylphosphine usually generates a  $\mu\text{-PPh}_2$   $\mu$ -hydrido species. Occasionally the hydride ligand adds onto a hydrocarbyl ligand. This kind of reaction is observed in the reaction of complexes **221a** and **221c** shown in Scheme 181 (see also Scheme 116) with  $\text{PPh}_2\text{H}$ . The reaction products depend on the nature of the metallacycle. Complex **312** results from the reaction of the dicarboxymethyl-substituted complex **221a** with 1 equiv of

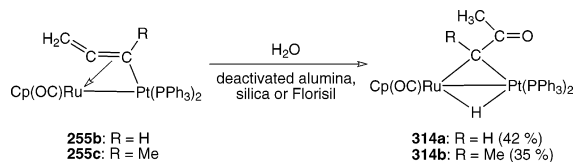
$\text{PPh}_2\text{H}$ . Product **312** is formed by P–H bond cleavage and oxidative addition, followed by C–H bond formation and organic ligand rearrangement. However, the closely related *t*-Bu-substituted derivative **221c** yields the bridging vinylidene derivative **313** when treated with 2 molar equiv of  $\text{PPh}_2\text{H}$ . The same type of mechanism with an additional P–C bond cleavage is envisaged.<sup>195</sup>

#### Scheme 181. Oxidative Addition of $\text{PPh}_2\text{H}$ and Hydrogen Transfer to Metallocyclic Ligands



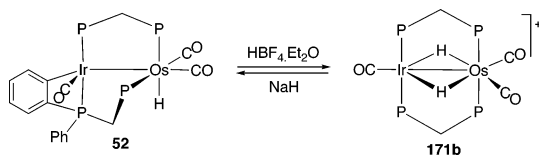
An unusual addition of water to the  $\mu$ -allenyl derivatives **255b** and **255c** occurs in the presence of deactivated chromatographic support materials, such as alumina, silica, or Florisil. Both O–H bonds of the water molecule are broken, and all three atoms add onto the organometallic molecules to afford the bridging alkylidene complexes **314** in which one of the substituents is an acetyl group (Scheme 182). Yields of the product are respectable (ca. 40%), and there are no other products.<sup>244</sup>

#### Scheme 182. Oxidative Addition of Water to a $\mu$ -Allenyl Platinum/Ruthenium Complex



The iridium–osmium complex **52** shown in Scheme 183 contains a cyclometalated species derived from a dppm ligand (see Scheme 32). A  $\mu$ -dppm ligand in complex **171b** is regenerated from **52** when it is protonated with a solution of  $\text{HBF}_4 \cdot \text{Et}_2\text{O}$ . Addition of  $\text{NaH}$  reverses this reaction.<sup>86</sup>

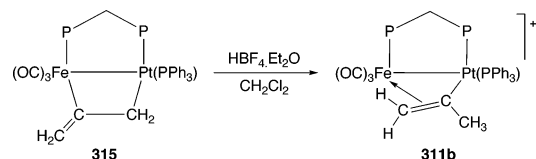
#### Scheme 183. Regeneration of a $\mu$ -dppm Ligand by Protonation of a dppm-Derived Metallocycle



The iron–tungsten parallel-bridged  $\mu$ -allene species **315** is converted into the  $\mu$ -propenyl cationic complex **311b** shown in Scheme 184 when reacted with  $\text{HBF}_4$ . Complex **311b** contains a ligand that is  $\eta^1$ -coordinated to the platinum and  $\eta^2$ -bonded to the iron atom. The same product **311b** is obtained when metallocycles **208b,d** are protonated (see Scheme 179).<sup>209</sup>

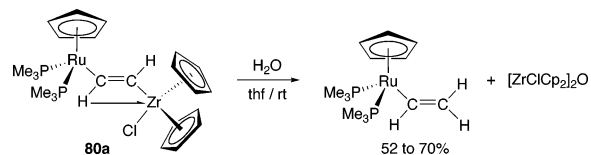
A final example of proton addition is provided by the hydrolysis of complex **80a**. Addition of water cleaves the zirconium–carbon bond of this dimetallaethene complex and affords the monometallic ruthenium vinyl complex [Ru–

#### Scheme 184. Transformation of a $\mu$ -Allene into a $\mu$ -Alkenyl Ligand by Protonation



$(\text{PMe}_3)_2(\text{CH}=\text{CH}_2)\text{Cp}]$  together with  $[(\text{ZrClCp}_2)_2\text{O}]$ , as indicated in Scheme 185.<sup>72</sup>

#### Scheme 185. Formation of a Monometallic Ruthenium Vinyl Complex by Hydrolysis of a Ruthenium/Zirconium Complex

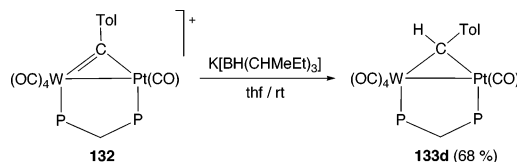


## 5.2. Hydride (H<sup>−</sup>) Addition Reactions

### 5.2.1. Hydride Addition to Carbynes

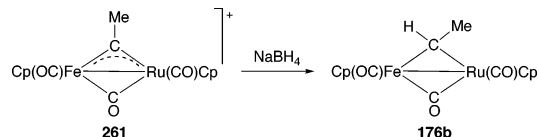
Potassium selectride converts the cationic  $\mu$ -carbyne Pt–W complex **132** into the  $\mu$ -alkylidene species **133d** as shown in Scheme 186 (see also Scheme 77). The reaction was carried out at room temperature and gave a 68% yield of the product.<sup>140</sup>

#### Scheme 186. Conversion of a $\mu$ -Carbyne into a $\mu$ -Carbene Ligand on a Heterobimetallic Center



The addition of sodium borohydride to the cationic alkylidyne complex **261** shown in Scheme 187 transforms the  $\mu$ -alkylidyne ( $\mu$ -CMe) into the  $\mu$ -alkylidene ( $\mu$ -CHMe) ligand found in **176b**. This complex has also been prepared from the reaction of the dimetallacyclopentenone complex **205c** with a phosphorus ylide (see Scheme 146).<sup>170,171</sup>

#### Scheme 187. Addition of Hydride Anion to a $\mu$ -CMe Complex Affords a $\mu$ -CHMe Complex

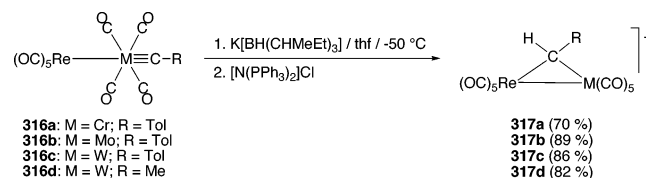


Terminal bimetallic carbyne complexes are also converted to  $\mu$ -alkylidene species when exposed to nucleophilic hydride sources. The group 6–rhenium complexes **316a–c** afford the  $\mu$ -CHTol anionic species **317a–c** when treated with  $\text{K}^+[\text{BH}(\text{CHMeEt})_3]^-$ . These complexes may be isolated as PPN salts. The structure of the Re–W complex **316c** was determined by an X-ray diffraction study. Other nucleophiles ( $\text{Me}^-$ ,  $\text{F}^-$ ,  $\text{OMe}^-$ ,  $\text{NMe}_2^-$ ) do not give isolable products. The related Re–W species **316d** reacts with the selectride anion to give the corresponding  $\mu$ -CHMe species **317d** as shown in Scheme 188.<sup>105</sup>

### 5.2.2. Hydride Addition to Alkenyls and Alkynyls

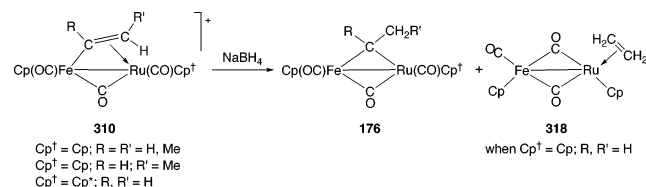
Alkenyl cations can be attacked with hydride sources to give metal alkylidene complexes. This is observed when the

### Scheme 188. Hydric Attack on Terminal Carbyne Bimetallic Complexes Affords $\mu$ -Alkylidene Species



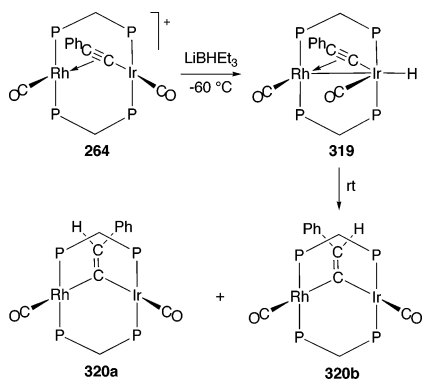
iron–ruthenium  $\mu$ -alkenyl complexes of type **310** shown in Scheme 189 are treated with sodium borohydride. The alkylidene ligands that result from attack on the  $\beta$ -carbon of the alkenyl group adopt a bridging position in the products **176**.<sup>170,171,184</sup> A minor product, the  $\eta^2$ -ethene complex **318** shown in the scheme, was also observed when the RuCp  $\mu$ -CH=CH<sub>2</sub> complex was reacted.<sup>170,171</sup>

### Scheme 189. Hydride Attack of $\mu$ -Alkenyl Ligands on Iron–Ruthenium Complexes



The reaction of **264** with LiBHET<sub>3</sub> at low temperature affords a terminal hydrido complex **319** (Scheme 190). This species rearranges when warmed to room temperature to give isomeric vinylidene complexes **320a** and **320b**.<sup>245</sup>

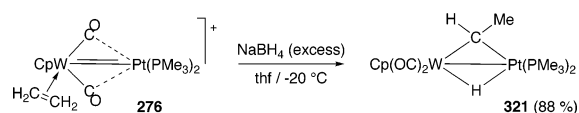
### Scheme 190. Conversion of an Alkynyl Ligand into a Vinylidene Ligand by Hydride Attack on a Rhodium/Iridium Center



### 5.2.3. Hydride Addition to Alkenes

When the unsaturated cationic complex **276** is treated with NaBH<sub>4</sub>, the coordinated ethylene is isomerized into a  $\mu$ -CHMe ligand as a hydride ligand adds to the molecule. The hydride ligand bridges the two metals in the product **321** (Scheme 191).<sup>143,144</sup>

### Scheme 191. Hydride Addition and Conversion of an Ethylene Ligand into a $\mu$ -CHMe Ligand on a Platinum–Tungsten Framework

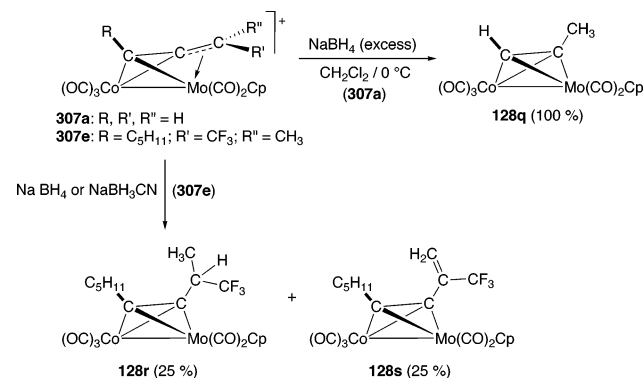


### 5.2.4. Hydride Addition to Carbocations

Carbocations that are stabilized on heterobimetallic templates usually react with sources of hydride anions to afford  $\mu$ -alkyne complexes.

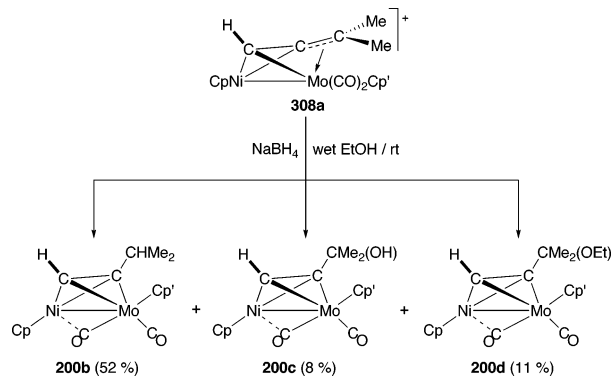
This is observed when the cobalt–molybdenum carbocations **307** (Scheme 192) were treated with hydridic sources.<sup>240,241</sup> In the case of the trifluoromethyl carbocationic species **307e**, a deprotonation reaction to give a different  $\mu$ -alkyne complex **128s** also takes place.<sup>241</sup> All these  $\mu$ -alkyne products have the dimetallatetrahedrane geometries of complexes **128**.

### Scheme 192. Generation of $\mu$ -Alkyne Complexes Following Hydride Attack on Carbocationic Complexes



The nickel–molybdenum carbocationic complex **308a** shown in Scheme 193 reacts similarly with sodium borohydride in wet ethanol to give the  $\mu$ -*i*-PrC≡CH complex **200b**. However side products that result from the addition of hydroxide (**200c**) and of ethoxide ions (**200d**) present in the wet solution to the cationic center were also isolated.<sup>246</sup>

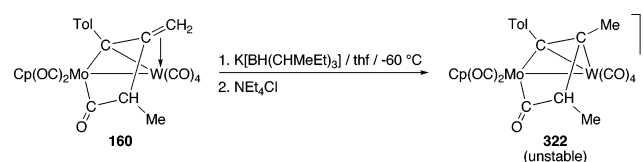
### Scheme 193. Nucleophile Addition to a Nickel–Molybdenum Carbocationic Complex



### 5.2.5. Other Hydride Additions Leading to Carbon–Hydrogen Bond Formation

The exocyclic C=CH<sub>2</sub> group in the heterobimetallic molybdenum metallacycle **160** shown in Scheme 194 is attacked at low temperature by H<sup>-</sup>. The anionic product **322** in which the C=CH<sub>2</sub> group has been transformed into a C–Me group is unstable.<sup>161</sup>

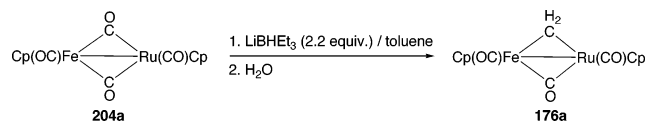
### Scheme 194. Hydride Attack on an Exocyclic C=C Bond in a Metallacyclic Species



The iron–ruthenium analog **204a** of the well-known [M(CO)( $\mu$ -CO)Cp]<sub>2</sub> (M–M, M = Fe, Ru) systems reacts with LiBHET<sub>3</sub>, followed by protonation with water (Scheme

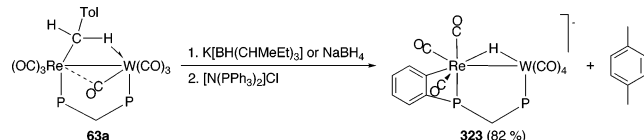
195) to afford the  $\mu$ -methylene complex **176a**.<sup>170,171</sup> This reaction also takes place in the  $\text{Ru}_2$  system.<sup>247</sup>

**Scheme 195. Hydride Attack of a  $\mu$ -CO Ligand Followed by Protonation Affords a  $\mu$ -CH<sub>2</sub> Complex**



In the Re–W complex **63a** shown in Scheme 196 (see also Schemes 43 and 158), which contains a rhenium-bonded  $\text{CH}_2\text{Tol}$  ligand, there is an agostic interaction with the tungsten atom from one of the C–H bonds of the methylene group. When reacted with hydric sources  $[\text{BH}_4^-]$  or  $[\text{BH}(\text{CHMeEt})_3^-]$ , reductive elimination of *p*-xylene is observed, together with cyclometalation of one of the dpmm ligands to give the final product **323**.<sup>105</sup>

**Scheme 196. Nucleophilic Hydride Addition to a Rhenium–Tungsten Alkyl Complex Leads to Reductive Elimination and a Cyclometalation Reaction**



### 5.3. Metal Hydride (M–H) Additions to Hydrocarbyl Ligands

These reactions involve the transfer of a hydrogen atom derived from a metal hydride group onto a hydrocarbyl ligand (hydrometalation reactions).

#### 5.3.1. Metal Hydride Additions to Alkynes and Allenes

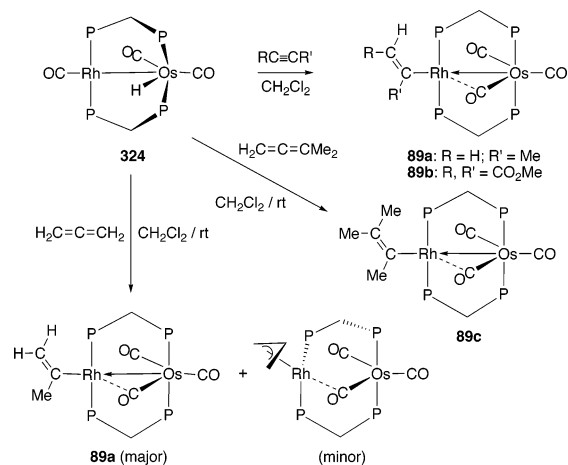
The usual products of metal hydride addition reactions to alkynes are  $\text{CR}=\text{CHR}'$  alkenyl or vinyl complexes ( $\text{R} = \text{R}' = \text{H}$ ), which may be terminal or bridging. The alkyne–hydride coupling reactions to give alkenyl complexes usually proceed regio- and stereoselectively. The most common products find the metal (M) and the hydrogen in the group  $\text{M}-\text{CR}=\text{CHR}$  in a *cis* geometry.

Allenenes often give the same products as the corresponding isomeric alkyne and thus are also treated in this section. Further reaction, rearrangements, or both are sometimes observed with allenenes, and these reactions are more likely to give  $\pi$ -allyl complexes after a C–H coupling reaction than the alkynes under similar reaction conditions.

The reactions of the osmium–rhodium hydrido complex **324** with alkynes and allenenes illustrates some of these points. The reactions of **324** with propyne and with DMAD afford the terminal rhodium-bonded alkenyl complexes **89a** and **89b** regio- and stereospecifically (Scheme 197).<sup>114,224</sup> Complex **89a** is also obtained when **324** is treated with allene, but in this case, a rhodium-bonded  $\pi$ -allyl species is also obtained as a minor product. 1,1-Dimethylallene reacts with **324** to give the 2-methylbutenyl complex **89c** shown in the scheme.<sup>114</sup>

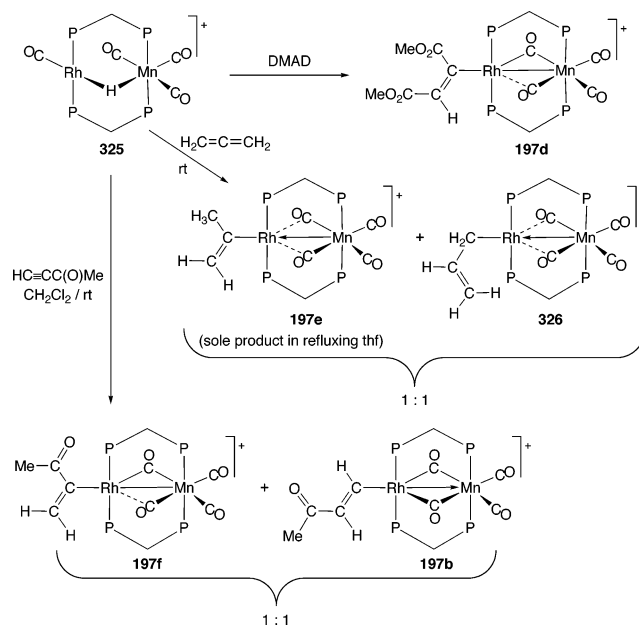
Low-temperature protonation of  $[(\text{OC})\text{Rh}(\mu\text{-dpmm})_2\text{Mn}(\text{CO})_3]$ , **288a**, affords the  $\mu$ -dpmm  $\mu$ -hydride cation **325**. This species reacts with allene at room temperature to give the terminal rhodium-bonded isopropenyl complex **197e** and a  $\sigma$ -(Rh)-bonded allyl species **326** in approximately a 1:1 ratio. Unlike the starting material **325**, complexes **197e** and **326** contain Mn–Rh bonds, as shown in Scheme 198.<sup>234</sup> In

**Scheme 197. Reactions of an Osmium–Rhodium Hydride Complex with Propyne, DMAD, and Allenes**



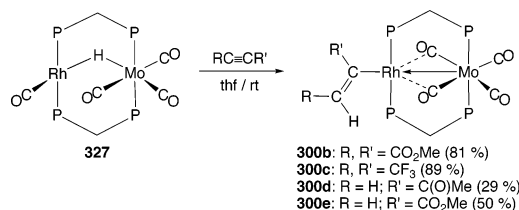
refluxing *thf*, the rhodium-bonded isopropenyl **197e** is obtained exclusively. Complex **325** gives the rhodium-bonded alkenyl complex **197d** as the only product when reacted with DMAD.<sup>234</sup> However a mixture of two alkenyl rhodium-bonded regio-isomers, **197b** and **197f**, are obtained in a 1:1 ratio, with the terminal alkyne  $\text{HC}\equiv\text{CC}(\text{O})\text{Me}$ .<sup>178</sup> [Note that some of the same complexes may be obtained by the protonation of the corresponding alkyne complexes **292**; see section 5.1.4., Scheme 164.<sup>234</sup>]

**Scheme 198. Alkenyl Formation Following Allene– and Alkyne–Hydride Coupling on a Manganese/Rhodium Template**

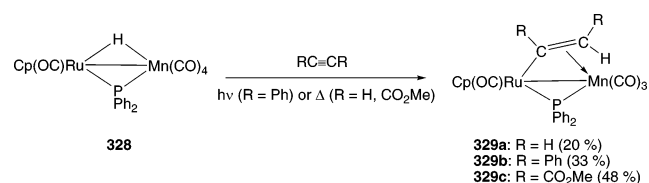


Similar organic transformations to those just discussed take place on a molybdenum/rhodium bimetallic framework. A variety of alkynes formally insert into the Rh–H bond of the dpmm-bridged hydrido complex **327** (Scheme 199) to give the metal–metal-bonded  $\eta^1$ -alkenyl complexes **300**.<sup>113</sup> In each case, the metal and the alkenyl hydrogen atom are in a *cisoid* geometry and terminal rhodium-bonded alkenyl ligands are always observed.

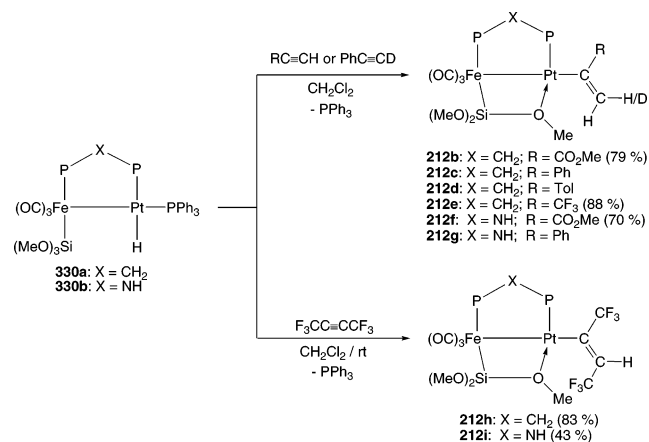
Alkyne addition to heterobimetallic hydride complexes to give alkenyl species is also observed on a manganese–ruthenium template where the two metals are anchored

**Scheme 199. Alkyne Addition to  $\mu$ -Hydride Ligands To Give Terminal Alkenyl Complexes**


together with a  $\mu$ -PPh<sub>2</sub> ligand. When complex **328** is reacted thermally or photolytically with alkynes, complexes **329** with  $\mu$ -*cis*-alkenyl ligands are obtained (Scheme 200).<sup>248</sup>

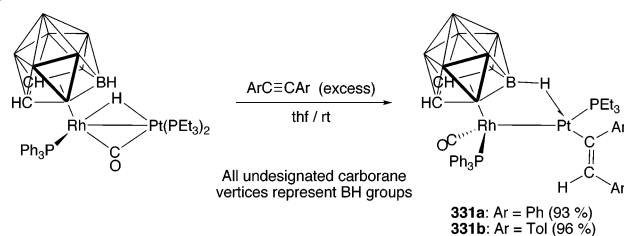
**Scheme 200.  $\mu$ -Alkenyl Formation on a Manganese–Ruthenium Bimetallic Template**


The addition of HC≡CCO<sub>2</sub>Me or of terminal aromatic alkynes ArC≡CH to the iron–platinum species **330** (Scheme 201) leads to similar initial outcomes. Platinum-bonded terminal alkenyl complexes **212** are obtained in what are regioselective hydrometalation reactions. The *cis* addition across the Pt–H bond was demonstrated by using the deuterium-labeled alkyne PhC≡CD.<sup>249</sup> The alkenyl groups in complexes that are derived from aromatic alkynes are slowly transformed into bridging vinylidene complexes, while trimethoxysilane is reductively eliminated (see Scheme 217, section 5.3.3.). The reaction of the Fe–Pt complex **330a** with CF<sub>3</sub>C≡CH afforded a similar product, **212e**, but the perfluoroalkyne HFB led to *trans* (not *cis*) addition across the Pt–H bond to give complexes **212h** and **212i** with **330a** and **330b**, respectively (Scheme 201). Preliminary results show that DMAD appears to give a mixture of isomers with *E* and *Z* stereochemistry. These results indicate that the nature of the alkyne substituents seems to play a crucial role in controlling the stereochemistry of the resultant alkenyl ligand.<sup>250</sup>

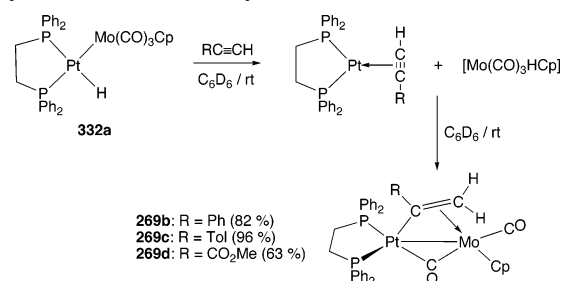
**Scheme 201. Alkyne Addition to Iron–Platinum Hydride Complexes To Give Alkenyl Complexes**


A more complicated but essentially similar reaction is observed when the platinum–rhodium carborane hydride complex shown in Scheme 202 reacts with ArC≡CAr

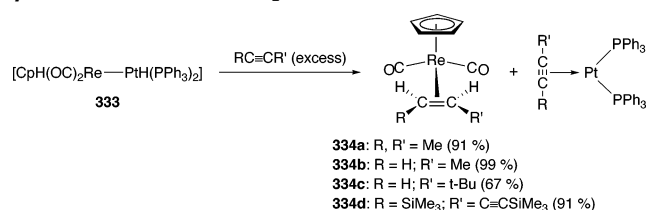
ligands. Terminal platinum-bonded alkenyl complexes **331** with the expected stereochemistry (*H cis* to the Pt atom) ensue. There is an “agostic” B–H interaction from the carborane ligand to the electron-deficient platinum atom.<sup>251</sup>

**Scheme 202. Alkenyl Formation in a Platinum–Rhodium  $\mu$ -Hydride Complex**


The molybdenum–platinum complex **332a** is the Mo–PtH analog of the Mo–PtMe complex **100b**. Complex **332a** reacts sequentially with terminal alkynes. The first products are monometallic: the platinum–alkyne complexes [Pt( $\eta^2$ -RC≡CH)(dppe)] are formed, along with the molybdenum hydride [Mo(CO)<sub>3</sub>HCP], which results from hydride transfer from the platinum to the molybdenum. Both monometallic complexes are observed as intermediates (Scheme 203). The Mo–H bond then adds, in a Markovnikov fashion, across the C≡C bond to give complexes **269b–d**. The reaction stops after the first step when internal alkynes are used.<sup>252</sup>

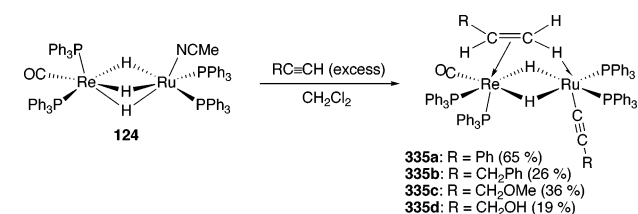
**Scheme 203. Two-Step Alkenyl Formation Starting from a Molybdenum–Platinum Hydride**


The reaction of the platinum–rhenium dihydride complex **333** with alkynes leads to the formation of monometallic rhenium alkene complexes **334** in what is the first stoichiometric hydrogenation of an alkyne to a metal–alkene complex. In the case of 2-butyne, the mechanism is believed to go through an intermediate platinum–rhenium complex, which contains a terminal alkenyl ligand. Subsequent transformations of this species and addition of a second equivalent of alkyne result in the stoichiometric formation of the *cis*-alkene complex **334a** and of the platinum alkyne complex [Pt( $\eta^2$ -MeC≡CMe)(PPh<sub>3</sub>)<sub>2</sub>] (Scheme 204). The reaction is quite general and provides an excellent synthetic entry into pure rhenium–alkene complexes.<sup>253</sup>

**Scheme 204. Stoichiometric Conversion of Alkynes into  $\eta^2$ -Alkene Rhenium Complexes**


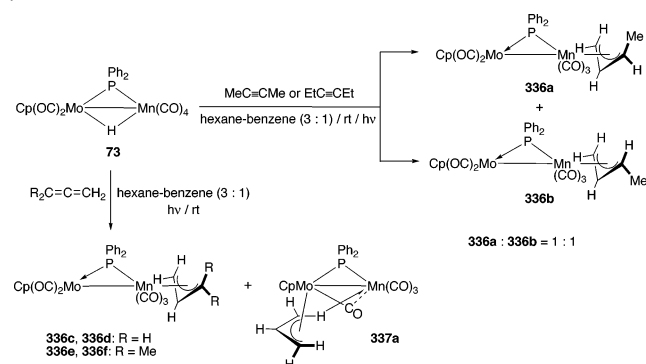
The *tris*  $\mu$ -hydride complex **124** does not afford alkenyl species when treated with a series of terminal alkynes. Instead, unprecedented  $\mu$ -olefin complexes **335** are formed (Scheme 205). The  $\mu$ -alkene moieties in these molecules have  $\pi$ -interactions with the rhenium and agostic  $sp^2$  C–H bond interactions with the ruthenium atom. NMR data provide the best evidence for these interactions: reduced  $J_{CH}$  coupling constants and high field resonances are observed for the agostic hydrogen atom. A single-crystal X-ray diffraction study of the styrene complex **335a** was also obtained. The bonding situation may be “viewed as an arrested migration of a hydrido ligand from...the ruthenium atom onto a bridging  $\eta^1, \eta^2$ -alkenyl group” and “represents the last step of the hydrogenation of an alkyne...at a heterobimetallic center.”<sup>254</sup>

#### Scheme 205. Formation of $\mu$ -Olefin Complexes with Agostic Interactions on a Rhenium–Ruthenium Center



The Mn–Mo complex **73** was reacted with but-1-yne or but-2-yne to give manganese-bonded allylic ligands akin to those seen in diene reactions (discussed in section 5.3.2, Scheme 209). No alkenyl complexes were isolated, but mixtures of *syn*- and *anti*-allyl isomers **336a,b** were obtained in a 1:1 molar ratio (Scheme 206). Alkenyl complexes are proposed as intermediates in the formation of the allylic species, and indeed, the configuration of the allyl complex may depend on the geometry of the intermediate alkenyl species.<sup>255</sup> Similar products **336** are obtained in the reactions of allene and 1,1-dimethylallene with complex **73**; two isomers are obtained in each case, and a molybdenum bonded  $\pi$ -allyl bimetallic complex **337a** is also obtained in low yield with allene. Structures of complexes of types **336** and **337** were reported.<sup>256</sup>

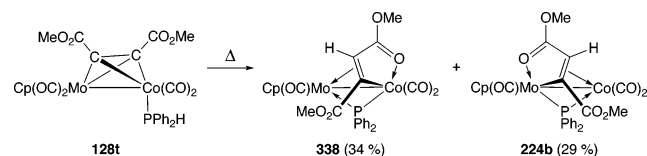
#### Scheme 206. Reactions of a Manganese–Molybdenum $\mu$ -Hydrido Complex with Alkynes and Allenes



When the diphenylphosphine  $\mu$ -alkyne complex **128t** is warmed, oxidative addition of the phosphine to give a  $\mu$ -phosphido ligand takes place, and the phosphine hydrogen atom is transferred to the alkyne. Two isomeric  $\mu$ -alkenyl complexes are produced in close to equimolar amounts: the ligand is  $\sigma$ -bonded to the cobalt atom (via the carbon and by O-donation) and  $\pi$ -bonded to the molybdenum in complex **338**. The situation is reversed in **224b**, in which the molybdenum atom is now  $\sigma$ -bonded to the ligand and the

cobalt atom is  $\pi$ -bonded (Scheme 207).<sup>257</sup> Related reactions are presented in Scheme 181.<sup>195</sup>

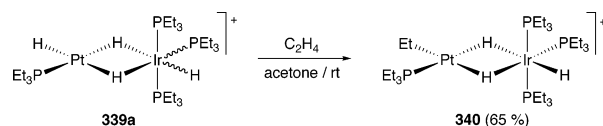
#### Scheme 207. Oxidative Addition of a P–H Bond to a Cobalt–Molybdenum $\mu$ -Alkyne Complex To Give Alkenyl Species



#### 5.3.2. Metal Hydride Additions to Alkenes and Dienes

An early example comes from the reaction of a bimetallic polyhydride complex with ethene. The iridium/platinum cationic species **339a** inserts ethylene into the Pt–H bond to give the Pt– $C_2H_5$  heterobimetallic complex **340** as shown in Scheme 208. (This complex eliminates ethane when treated with a modest pressure of hydrogen; see section 5.4.1, Scheme 218).<sup>258,259</sup>

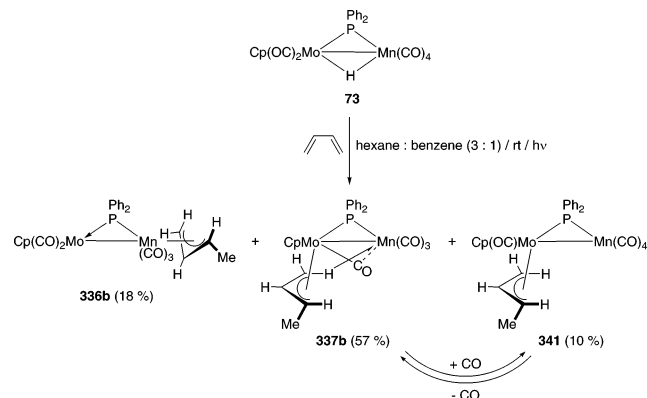
#### Scheme 208. Ethylene Insertion into a Platinum–Hydrogen Bond



Mononuclear metal hydrides add to conjugated dienes to give  $\pi$ -allyl complexes. Similar reactions are observed in the reactions of heterobimetallic hydrides with conjugated dienes, but the additional bonding possibilities of two metal centers leads to a larger array of products. This is illustrated with the reactions of the complex **73** with unsaturated hydrocarbons that has been explored in a series of papers.

Complex **73** reacts with 1,3-butadiene at room temperature and under UV irradiation to afford the manganese-bonded allylic complex **336b** and two molybdenum-bonded  $\pi$ -allylic complexes **337b** and **341**. All these species have Mn–Mo bonds. At  $-20^\circ C$ , complex **341** is the main product, but this species slowly decarbonylates at room temperature to give **337b**, which has an agostic interaction between an allylic hydrogen atom and the electron-deficient manganese atom (Scheme 209). Isoprene reacts similarly except that only analogs of **336b** and **337b** are produced.<sup>256,260</sup> (Reactions of **73** with alkynes and allenes were discussed in section 5.3.1., Scheme 206.)

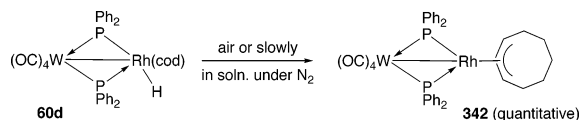
#### Scheme 209. Reactions of a Manganese–Molybdenum $\mu$ -Hydrido Complex with Dienes





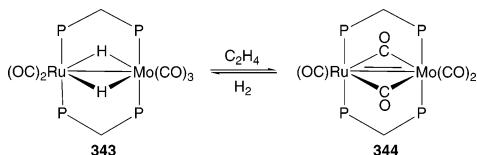
When the rhodium–tungsten 1,5-cod complex **60d** (Scheme 210) is exposed to air or is allowed to stand in solution “under nitrogen for a prolonged period” the hydride spontaneously inserts into one of the olefinic double bonds and affords the  $\eta^3$ -C<sub>8</sub>H<sub>13</sub> (cyclooctenyl) complex **342** shown in the scheme, in what is a reverse  $\beta$ -hydride elimination reaction.<sup>261</sup>

**Scheme 210. Metal Hydride Insertion into a Coordinated 1,5-cod Ligand**



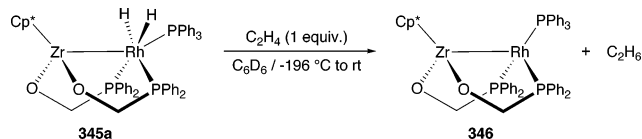
The Mo–Ru  $\mu$ -dihydride complex **343** (Scheme 211) reacts with ethylene to afford an unsaturated mixed-metal complex **344** and (presumably) ethane. This species adds hydrogen at room temperature and regenerates complex **343**.<sup>262</sup>

**Scheme 211. Reaction of a Dihydride with Ethylene To Generate an Unsaturated Molybdenum–Ruthenium Complex**



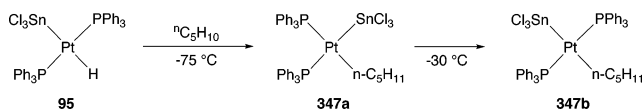
Early–late heterobimetallic complexes with hydride ligands also are capable of hydrogenating ethylene to ethane. The rhodium dihydride zirconium complex **345a** (Scheme 212), whose Rh–Zr bond is spanned by two alkoxydiphenylphosphine ligands, reacts with 1 equiv of ethylene to generate **346**; ethane is liberated.<sup>227</sup>

**Scheme 212. Stoichiometric Hydrogenation of Ethylene to Ethane by an Early–Late Heterobimetallic Complex**



Olefin insertion into the Pt–H bond of *trans*-[(Ph<sub>3</sub>P)<sub>2</sub>Pt(H)–SnCl<sub>3</sub>], **95**, has been observed. This reaction, shown in Scheme 213, has been investigated as a model in olefin hydroformylation by Pt–Sn systems. Addition of pent-1-ene to **95** affords the *cis*-*n*-pentyl complex **347a** at –75 °C. This species isomerizes to the more thermodynamically stable *trans* isomer **347b** at –30 °C, as shown.<sup>116</sup> These reactions have been the subject of theoretical investigations.<sup>263</sup>

**Scheme 213. Pent-1-ene Insertion into the Platinum–Hydrogen Bond of a Platinum–Tin Hydride Complex**



**5.3.3. Metal Hydride Additions to Alkyls**

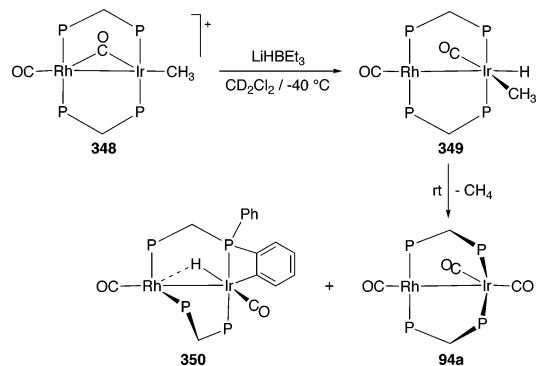
Most reactions of this type involve the reductive coupling of an alkyl group with a metal hydride to give an alkane in a bimetallic reductive elimination reaction. Alkyl hydride

species are observed more often in bimetallic systems than on single metals, since the two groups need not be on the same metal, so reductive elimination is often slower. In some cases, a metal hydride is not observed but is assumed to be an intermediate in the elimination reaction.

Some reactions of heterobimetallic complexes with hydrogen generate metal hydrides, which in turn react further with hydrocarbyl ligands. Reactions of metal hydrides, formed via direct hydrogen addition, with hydrocarbyl ligands are thus presented in section 5.4. Oxidative addition of C–H bonds often leads to subsequent reductive elimination of alkyls. These reactions are discussed in section 6.3.1.

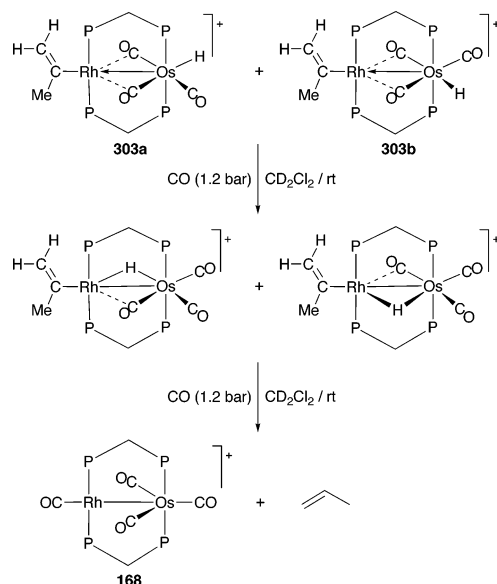
The cation **348** adds a hydride ion to the iridium atom at –40 °C to give the methyl–hydride complex **349** (Scheme 214), which then reductively eliminates methane at ambient temperature to give **94a**. A cyclometalation side reaction from one of the  $\mu$ -dppm *ortho*-C–H bonds gives **350**, an Ir–Rh analog of complex **52**.<sup>264</sup>

**Scheme 214. Reductive Elimination of Methane from a Rhodium–Iridium Methyl Hydride Complex**



Reductive elimination of propene from an isomeric mixture of the propenyl hydride complexes **303a,b** is induced by CO addition (Scheme 215). Propene is eliminated, and complex **168** is obtained via  $\mu$ -hydrido intermediates.<sup>114</sup>

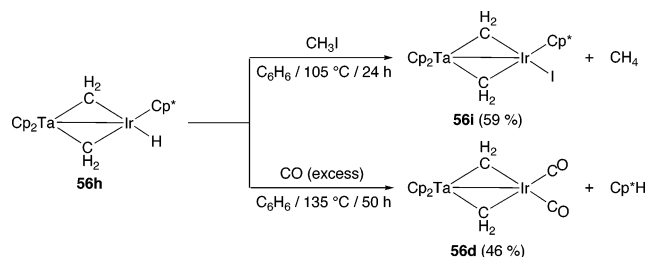
**Scheme 215. Bimetallic Reductive Elimination of Propene Induced by CO Addition**



Methane is liberated when the early–late methylene-bridged complex [Cp<sub>2</sub>Ta( $\mu$ -CH<sub>2</sub>)<sub>2</sub>IrHCp\*] (Ir–Ta) **56h** is heated with iodomethane, and **56i** is generated (Scheme 216).

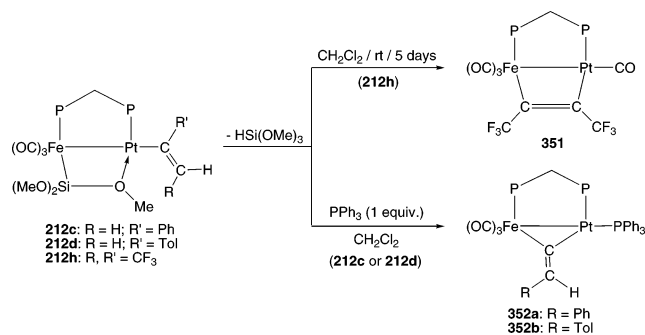
In contrast, the slow reductive elimination of pentamethylcyclopentadiene, Cp\*H, is observed, together with the formation of **56d**, when this complex is heated with excess CO for 50 h at 135 °C.<sup>265</sup>

**Scheme 216. Elimination of CH<sub>4</sub> and of Cp\*H from an Iridium–Tantalum Complex**



Trimethoxysilane forms when complex **212h** is allowed to stand in  $\text{CH}_2\text{Cl}_2$ . The alkenyl group is converted into the parallel  $\mu$ -HFB complex **351** (Scheme 217), whose structure was determined by a single-crystal X-ray diffraction study.<sup>250</sup> Trimethoxysilane is also generated when the alkenyl complexes **212c** and **212d** are treated with triphenylphosphine. The alkenyl ligands are transformed into the  $\mu$ -vinylidene species **352**.<sup>249</sup>

**Scheme 217. Reductive Elimination of Trimethoxysilane from Iron–Platinum Complexes**

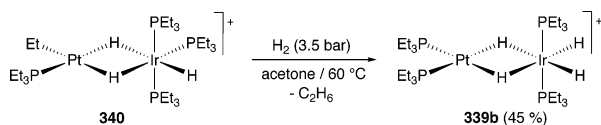


## 5.4. Molecular Hydrogen Addition to Hydrocarbyl Ligands

### 5.4.1. Hydrogen Addition to Alkyls and Acyls

The platinum-bonded ethyl complex **340** in Scheme 218 eliminates ethane when treated with a modest pressure of hydrogen, and generates an isomer, **339b** of the cationic hydride **339a** from which **340** is generated (see section 5.3.2, Scheme 208).<sup>258,259</sup>

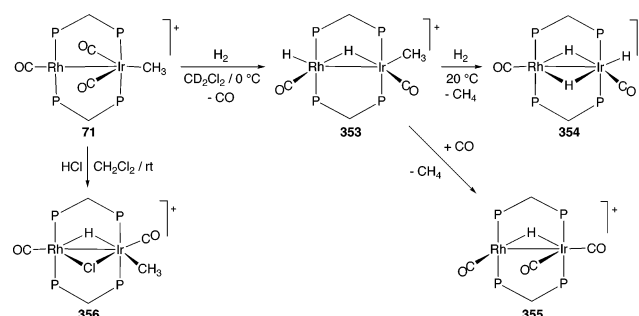
**Scheme 218. Reductive Elimination of Ethane Following Hydrogen Addition to an Iridium/Platinum–Ethyl Complex**



The chemistry of the rhodium–iridium cationic methyl complex **71** toward molecular hydrogen has been investigated. Complex **71** reductively eliminates methane in a two-step process when treated with  $\text{H}_2$  (Scheme 219). First, oxidative addition takes place (accompanied by CO loss) to give a dihydride complex **353**. Methane is then eliminated from **353** when another equivalent of hydrogen is introduced (to give the trihydride complex **354**) or when the dihydride

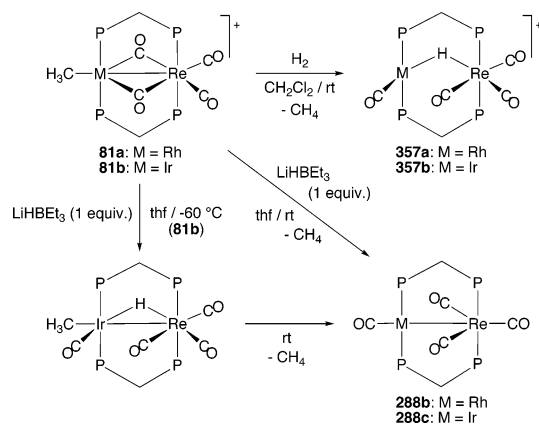
species is exposed to CO (the monohydride complex **355** is formed in this case). Oxidative addition of HCl to **71** is not followed by  $\text{CH}_4$  loss; the hydrido-methyl complex **356** that is formed is stable to reductive elimination.<sup>108,112</sup>

**Scheme 219. Bimetallic Reductive Elimination of CH<sub>4</sub> Following Oxidative Addition of H<sub>2</sub> on an Iridium–Platinum Framework**



Similar reactivity patterns are seen in related rhodium– and iridium–rhenium cationic complexes **81** (Scheme 220). Addition of  $\text{H}_2$  to complexes **81** leads to reductive elimination of methane, metal–metal bond cleavage, and the formation of a  $\mu$ -hydrido ligand that spans the two metals in **357**. Methane is also eliminated when  $\text{H}^-$  is added to the initial cations to give the complexes **288**: an intermediate methyl–hydride complex can be observed at  $-60$  °C in the case of the Ir–Re reaction.<sup>111</sup>

**Scheme 220. Reductive Elimination of Methane from Rhodium– and Iridium–Rhenium Complexes**

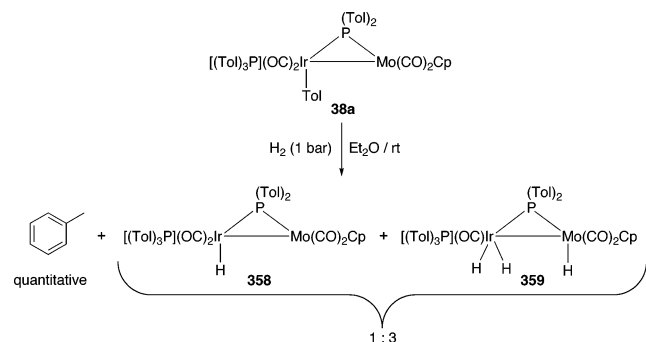
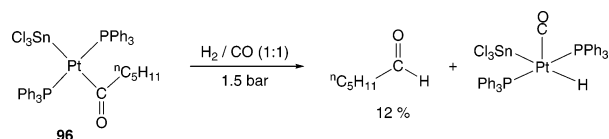


The molybdenum–iridium complex **38a** (first seen in Scheme 19) eliminates toluene when treated with molecular hydrogen. The reaction proceeds via CO loss, oxidative addition of  $\text{H}_2$ , and then reductive elimination of toluene to give a mixture of monohydride **358** and trihydride **359** complexes (Scheme 221).<sup>68</sup>

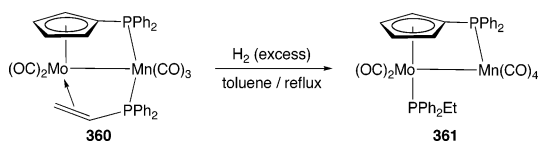
When the Pt–Sn acyl species **96** is treated with hydrogen and CO (1.5 bar), *n*-hexanal was produced in around 12% yield. The main process was loss of pentene to give the platinum–tin carbonyl hydride complex shown in Scheme 222.<sup>116</sup>

### 5.4.2. Hydrogen Addition to Alkenes

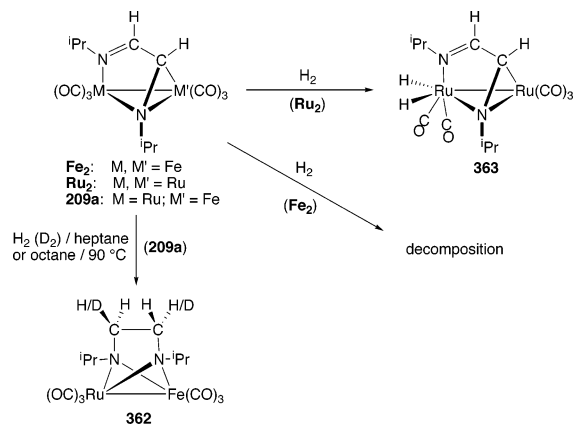
The metals in the manganese–molybdenum complex **360** shown in Scheme 223 are anchored together via a functionalized Cp group and a bridging diphenylvinylphosphine ligand,  $\text{PPh}_2(\text{CH}=\text{CH}_2)$ , whose phosphorus atom is manganese bonded. The complex is robust enough to withstand

**Scheme 221. Reductive Hydrogenation of an Iridium–Molybdenum Tolyl Complex Leading to Toluene**

**Scheme 222. Production of Some Hexanal When a Platinum–Tin Acyl Complex Is Treated with Water Gas**


refluxing toluene. The vinyl group of the phosphine ligand is hydrogenated when exposed to  $H_2$  under these conditions to give a now terminal, molybdenum-bonded  $PPh_2Et$  ligand in the new compound **361**.<sup>266</sup>

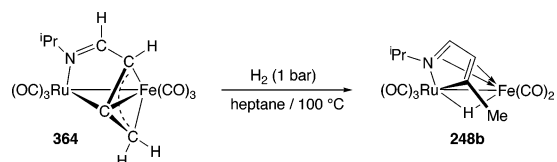
**Scheme 223. Hydrogenation of a Manganese-Bonded Diphenylvinylphosphine Ligand to a Molybdenum-Bonded Ethyldiphenylphosphine Ligand**


The diazadiene ligand in **209a** (see Schemes 109, 119, and 128) is hydrogenated with  $H_2$  in a hydrocarbon solvent at  $90\text{ }^\circ\text{C}$  to give **362**. A deuterium labeling study shows that deuteration gives the *trans*-**362- $d_2$**  complex. The reaction of **209a** is quite different from those of its homobimetallic congeners. The diiron analog of **209a** under similar conditions decomposes with metal–metal-bond cleavage, while the diruthenium complex loses an equivalent of CO and forms a dihydride species **363** (Scheme 224).<sup>199</sup>

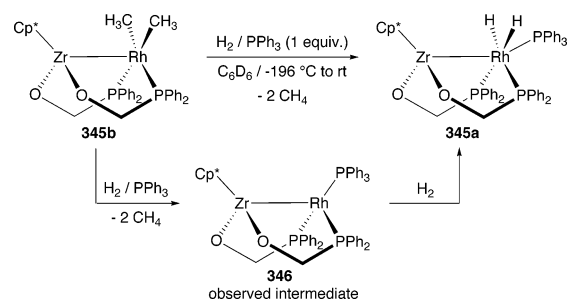
**Scheme 224. Contrasting Behavior of Homo- and Heterobimetallic Group 8 Diimine Complexes with Molecular Hydrogen**


Complex **364** contains an iron- and ruthenium-substituted allylic group linked to an azaalkenyl group. This organic

group is reduced with molecular hydrogen to give the azadiene complex **248b** (Scheme 225).<sup>212</sup>

**Scheme 225. Hydrogenation of an Unsaturated Aza-Ligand Affords an Azadiene  $\mu$ -Hydride Complex**


The strong and very short Rh–Zr bond of 2.444(1) Å found in the dimethylrhodium–zirconium complex **345b**, shown in Scheme 226, suggests that multiple bond character is present. This complex eliminates methane when treated with hydrogen in the presence of  $PPh_3$ . The intermediate product **346** (see also Scheme 212) then oxidatively adds  $H_2$  to form the dihydride **345a**.<sup>227</sup>

**Scheme 226. Reductive Elimination of  $CH_4$  from a Dimethylrhodium–Zirconium Species**


## 6. Carbon–Hydrogen Bond Cleavage on Preformed Heterobimetallic Frameworks

### 6.1. Carbon–Hydrogen Bond Cleavage by Formal Proton ( $H^+$ ) Abstraction

#### 6.1.1. Proton Abstraction from Carbenes

The outcome of reactions of the Pt–W  $\mu$ -alkylidene complexes **9g** and **9h** with hydride sources depends both on the reagent and on the nature of the alkylidene complex. One of the methyl hydrogen atoms of the  $\mu$ -CMe(Tol) ligand in the complex **9g** is abstracted when the complex is stirred with a suspension of NaH (Scheme 227) to generate complex **136b**, which contains a  $\mu$ - $\eta^1(Pt), \eta^2(W)$ -alkenyl ligand.<sup>149</sup> However NaH abstracts the alkylidene proton and generates the neutral carbyne complex **31b** from the  $\mu$ -CHTol complex **9h**. Both complexes **9g** and **9h** add on hydride ligands to give neutral  $\mu$ -hydrido complexes **321** with  $K^+[BH-(CHMeEt)_3]^-$ .<sup>237</sup>

#### 6.1.2. Proton Abstraction from Carbynes

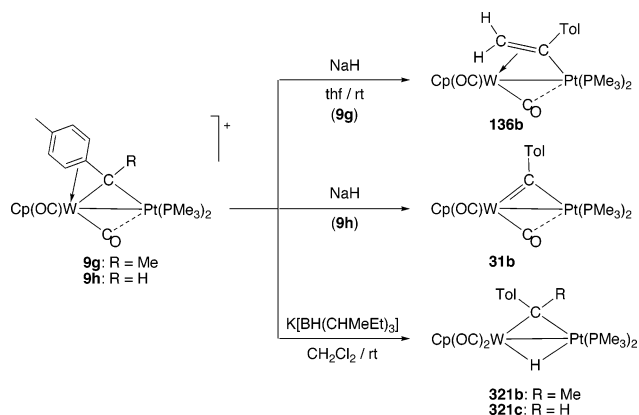
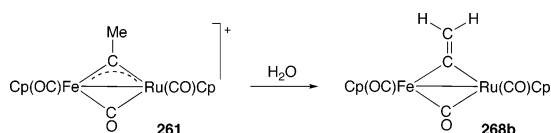
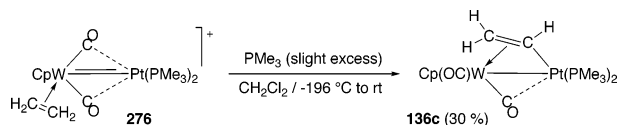
Addition of water to a solution of the  $\mu$ -ethylidyne complex **261** gives the  $\mu$ -vinylidene complex **268b**, following methyl-ligand proton abstraction by water (Scheme 228).<sup>170</sup>

#### 6.1.3. Proton Abstraction from Alkenes

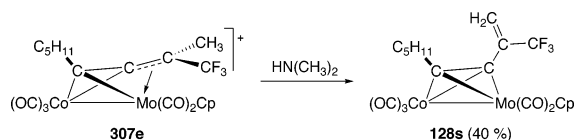
The ethylene ligand in the cationic unsaturated complex **276** shown in Scheme 229 reacts with  $PMe_3$ . Surprisingly the ethene ligand is not substituted with added  $PMe_3$ ; instead the phosphine ligand abstracts a proton and transforms the ethylene into a  $\mu$ -vinyl ligand to give complex **136c**.<sup>143,144</sup>

#### 6.1.4. Proton Abstraction from Methyl Groups in Ligands

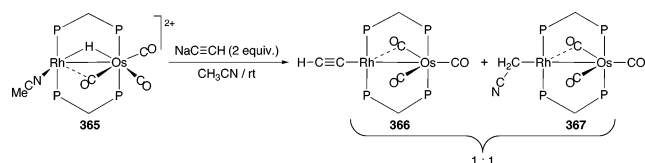
Dimethylamine is able to abstract a proton from the Me group of the carbocationic complex **307e** shown in Scheme

**Scheme 227. Reactions of Platinum–Tungsten  $\mu$ -Alkylidene Complexes with Hydride Sources**

**Scheme 228. Proton Abstraction from a  $\mu$ -Carbyne Complex with Water**

**Scheme 229. Proton Abstraction by  $\text{PMe}_3$  Results in an  $\eta\text{-C}_2\text{H}_4 \Rightarrow \mu\text{-CH=CH}_2$  Conversion**


230. The product is the  $\mu$ -alkyne complex **128s** with an uncoordinated alkene functionality<sup>241</sup> (as seen already in Scheme 192).

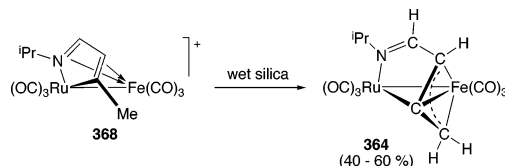
**Scheme 230. Proton Abstraction from a Heterobimetallic Carbocationic Complex**


When the dication **365** is reacted with 2 molar equiv of  $\text{NaC}\equiv\text{CH}$ , a terminal acetylide **366** is formed, together with a second product **367** that contains a new  $\text{CH}_2\text{CN}$  moiety, which is  $\sigma$ -bonded to the rhodium atom (Scheme 231). Complex **367** is formed by base hydrogen abstraction from the methyl group of a coordinated acetonitrile ligand and can be obtained essentially pure in 50–70% yield when 4 equiv of  $\text{NaC}\equiv\text{CH}$  are used.<sup>224</sup> Complexes **366** and **367** are isostructural with the alkenyl and acyl species **89** and **90**.

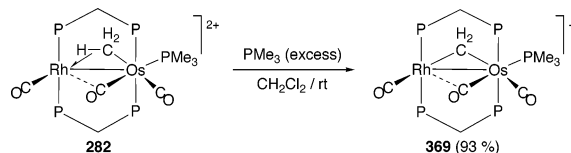
**Scheme 231. Hydrogen Abstraction from a Coordinated Acetonitrile Ligand**


Wet silica abstracts a methyl group proton from the cationic azadiene complex **368** shown in Scheme 232. The structure of the neutral complex **364** was determined by X-ray diffraction. This latter species may be hydrogenated

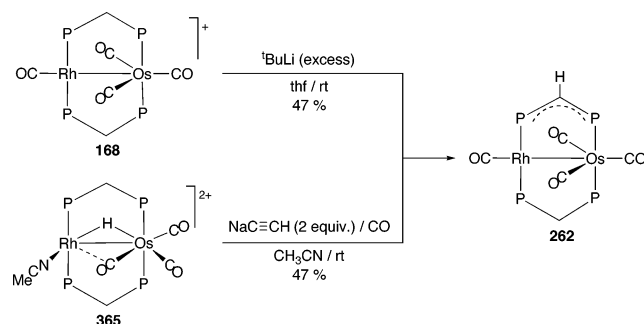
to afford the neutral azadiene iron–ruthenium hydride complex **248b** shown in Scheme 225.<sup>212</sup>

**Scheme 232. Proton Abstraction from a Methyl Group of an Azadienyl Iron–Ruthenium Complex by Wet Silica**


Instead of adding on or substituting a CO ligand in the osmium–rhodium dicationic complex **282** shown in Scheme 233, trimethylphosphine abstracts a proton from the agostic methyl group and affords the  $\mu$ -methylene complex **369**, which is an isomer of **65c**. X-ray diffraction studies established that metal–metal bonds are present in the starting material [ $\text{Os}–\text{Rh} = 2.9177(4)$ ] and in the  $\mu$ -methylene complex [ $2.9246(3)$  Å].<sup>229</sup>

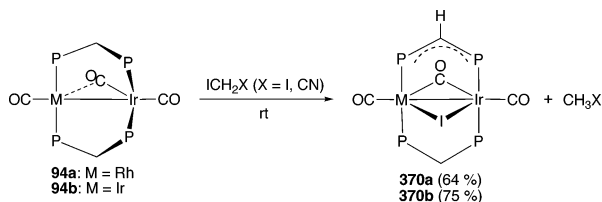
**Scheme 233. Proton Abstraction from an Agostic Methyl Group with  $\text{PMe}_3$  Generates a  $\mu$ -Methylene Complex**

**6.1.5. Proton Abstraction from  $\mu$ -dppm Ligands**

A proton is abstracted from a dppm ligand in the cationic osmium–rhodium complex **168** by  $t\text{-BuLi}$  to give **262** (Scheme 234), which contains an anionic  $\text{Ph}_2\text{P}–\text{CH}–\text{PPh}_2$  bridge. The same species is obtained when complex **365** is reacted with  $\text{NaC}\equiv\text{CH}$  under a CO atmosphere.<sup>224</sup> (See Scheme 142 for the alkylation of **262**.)

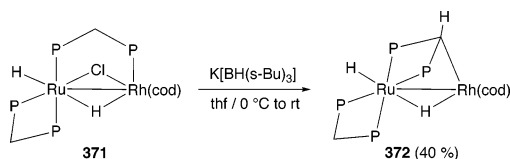
**Scheme 234. Base Abstraction of a Methylene Hydrogen Atom from a  $\mu$ -dppm Ligand in Osmium–Rhodium Complexes**


Complexes **370** with bridging anionic  $\text{PPh}_2\text{CHPPH}_2$  ligands akin to those found in compound **262** (Scheme 234) are generated when diiodomethane or  $\text{ICH}_2\text{CN}$  are added to the  $\mu$ -dppm complexes **94**. Addition of an iodide ligand takes place, and one of the dppm ligand  $\text{CH}_2$  hydrogen atoms is abstracted. The  $\text{CH}_2\text{IX}$  ( $\text{X} = \text{I}, \text{CN}$ ) molecules are transformed into  $\text{CH}_3\text{X}$  (Scheme 235).<sup>267</sup>

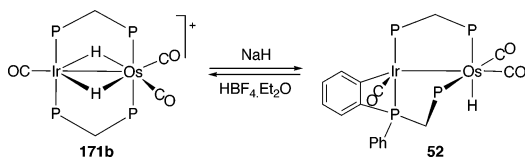
A  $\text{Ph}_2\text{P}–\text{CH}–\text{PPh}_2$  bridge system is also formed when the  $\text{Rh}–\text{Ru}$   $\mu$ -dppm complex **371** (Scheme 236) is reacted with  $\text{K}[\text{BH-}s\text{-Bu}_3]$ . However in this case, the ligand in the product **372** binds to the dimetal system in a different fashion, with both phosphorus atoms bonded to the ruthenium atom

**Scheme 235. Reactions of CH<sub>2</sub>I<sub>2</sub> and CH<sub>2</sub>ICN with Iridium–Rhodium and –Iridium  $\mu$ -dppm Species**


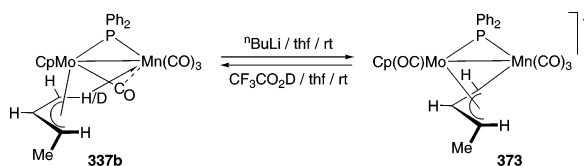
and the methine carbon linked to the rhodium. Complex **372** was characterized structurally.<sup>268,269</sup>

**Scheme 236. Base Abstraction of a Methylene Hydrogen Atom from a  $\mu$ -dppm Ligand in a Rhodium–Ruthenium Complex**


A cyclometalation reaction from a phenyl group of a  $\mu$ -dppm ligand is induced by NaH addition to the  $\mu$ -dppm complex **171b** as shown in Scheme 237. The reaction may be reversed by addition of HBF<sub>4</sub> to the cyclometalated product **52** (Scheme 183).<sup>86</sup>

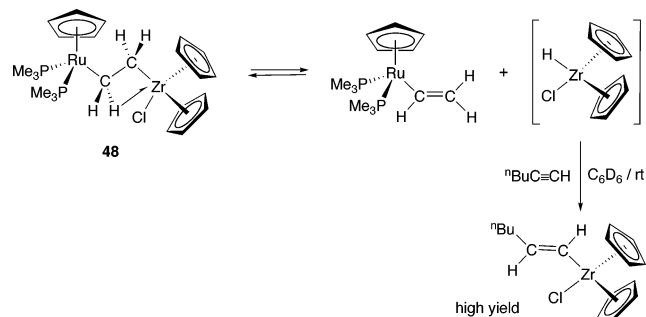
**Scheme 237. Reversible Cyclometalation from a Phenyl Group of a  $\mu$ -dppm Iridium–Osmium Complex**

**6.1.6. Proton Abstraction from a  $\pi$ -Allylic Group**

The electron-deficient complex **337b** has an agostic hydrogen interaction between an *anti*-allylic proton and the manganese atom. This interaction is no longer necessary when the complex reacts with *n*-BuLi, since this base removes a hydrogen atom, and a direct manganese–carbon  $\sigma$ -bond is formed to give the anionic metalloallyl complex **373** (Scheme 238). When deuterio-trifluoroacetic acid is added to this species, the deuterated starting material **337b-d<sub>1</sub>** is reformed. Addition of a variety of electrophiles such as [AuCl(PMe<sub>2</sub>Ph)] to the anionic metalloallyl complex generates new complexes in which electrophilic groups such as Au(PMe<sub>2</sub>Ph) replace the agostic hydrogen atom in **337b**.<sup>270</sup>

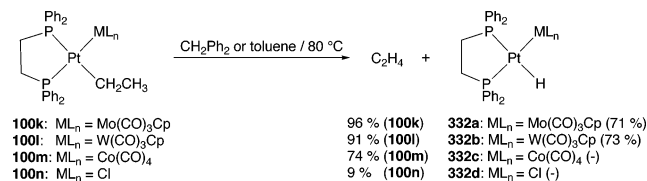
**Scheme 238. Abstraction of an Allylic Agostic Hydrogen Atom with *n*-BuLi**

**6.2. Carbon– $\beta$ -Hydrogen Bond Cleavage by Metal–Hydrogen Abstraction**

Surprisingly few examples are known of this classic elimination reaction in heterobimetallic systems. One example, in which the two metals are not bonded to each other, is provided by the ruthenium/zirconium dimetalla-alkane

complex **48**. This species readily undergoes a  $\beta$ -hydride elimination to afford the ruthenium vinyl species [Ru(PMe<sub>3</sub>)<sub>2</sub>-(CH=CH<sub>2</sub>)Cp] and [Zr(H)ClCp<sub>2</sub>]. The latter complex may be trapped by the addition of an alkyne such as *n*-BuC $\equiv$ CH to give the alkenyl species shown in Scheme 239.<sup>132</sup>

**Scheme 239.  $\beta$ -Hydride Elimination from a Ruthenium/Zirconium Dimetalla-Alkane Complex**


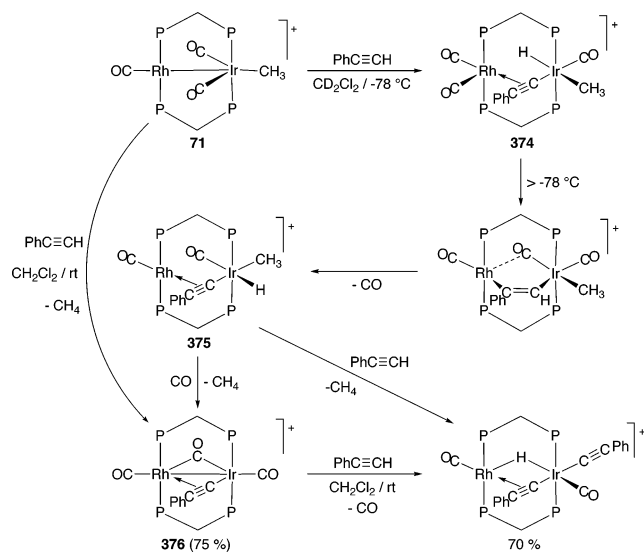
In the examples shown in Scheme 240, the  $\beta$ -hydrogen elimination from the platinum ethyl complexes of type **100** to give complexes **332** takes place at the platinum and is only tangentially affected by the group attached to it. The participation of the second metal is not necessary, but the observed rates of reductive elimination decrease in the order: Pt–Co > Pt–Mo > Pt–W > Pt–Cl. Reactions follow trends in electronegativity of the attached groups, peaking in the electron-withdrawing [(dpe)EtPt–Co(CO)<sub>4</sub>] (Co–Pt) system.<sup>271,272</sup>

**Scheme 240.  $\beta$ -Hydrogen Elimination of Ethylene from Heterobimetallic Ethyl Platinum Complexes**

**6.3. Carbon–Hydrogen Activation by Heterobimetallic Complexes**
**6.3.1. Carbon–Hydrogen Activation of C(sp)–H Bonds**

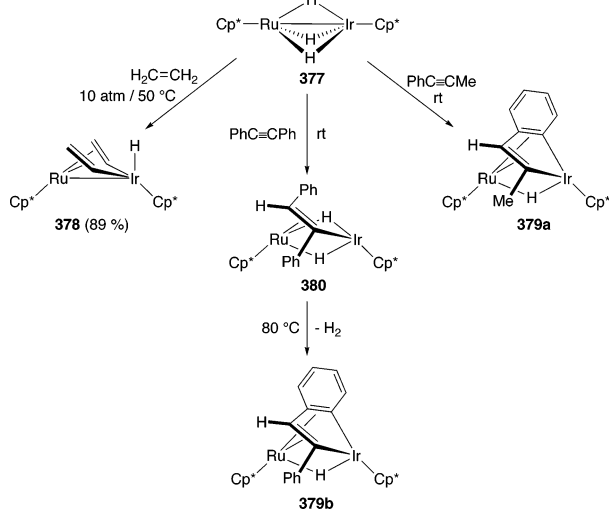
When PhC $\equiv$ CH was reacted with the rhodium–iridium methyl complex **71**, oxidative addition of the alkyne C–H bond ensued at the iridium center at –78 °C to yield **374**. As the reaction mixture was warmed to ambient temperature, a parallel-bridged  $\mu$ -alkyne complex was formed. Carbon monoxide loss followed to give another methyl hydride intermediate complex **375**. Reductive elimination of methane led to the final product, the  $\mu$ -alkynyl complex **376** shown in Scheme 241. Complex **376** itself undergoes C–H bond oxidative addition with PhC $\equiv$ CH to give the bis-alkynyl  $\mu$ -hydrido species shown in the scheme.<sup>191</sup> The latter could also be obtained via elimination of CH<sub>4</sub> by reacting the intermediate methyl hydride **375** with PhC $\equiv$ CH<sup>191</sup> or by reacting the cationic rhodium/iridium  $\mu$ -alkynyl complex **264** (see Scheme 166) with PhC $\equiv$ CH (not shown here).<sup>245</sup>

**6.3.2. Carbon–Hydrogen Activation of C(sp<sup>2</sup>)–H Bonds**

The iridium–ruthenium trihydride **377** reacts with ethylene to afford the divinyl hydride complex **378** (Scheme 242). There is a significant difference in metal–metal bond lengths

**Scheme 241. Activation of Terminal Alkyne C–H Bonds across Iridium–Rhodium Centers**

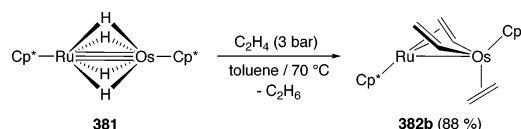
between the starting material [2.4858(4) Å] and the product [2.7313(6) Å].<sup>273</sup>

**Scheme 242. Ethylene and Aromatic Alkyne C–H Activation by an Iridium–Ruthenium Trihydride Complex**

Complex **377** also reacts with some aromatic alkynes. In this case, there is activation of an *ortho*-phenyl C–H bond. The alkyne PhC≡CMe affords the cyclometalated species **379a** also shown in the scheme. A similar product **379b** is obtained from the reaction of PhC≡CPh with **377**. The *trans*-alkenyl intermediate **380** that is formed prior to the reductive elimination of hydrogen and the cyclometalation reaction may be isolated in this case.<sup>273</sup>

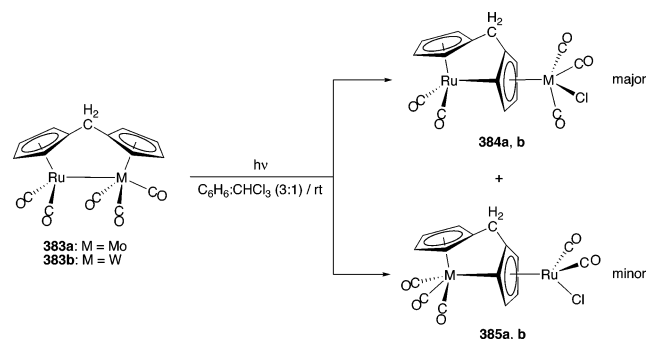
The reaction of the tetrahydrido osmium–ruthenium complex **381** with ethylene is similar to that observed for the just-discussed Ir–Ru  $\mu$ -hydrido species **377**. When **381** is heated under a slight ethylene pressure, ethane is formed, together with complex **382b** (Scheme 243). The Os–Ru bond order goes from triple in the reactant (**381**) to single in the product **382b**. This is corroborated by X-ray crystal data, as the Os–Ru distance changes from 2.4663(5) Å in **381** to 2.7591(10) Å in **382b**.<sup>274</sup>

The activation of cyclopentadienyl-type C–H bonds has been achieved in a number of heterobimetallic complexes

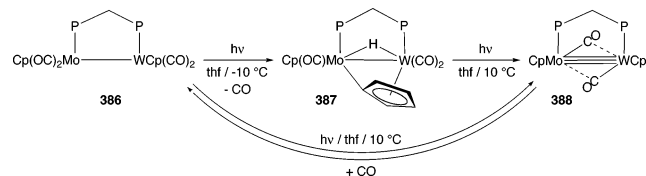
**Scheme 243. Ethylene Activation by an Unsaturated Ruthenium–Osmium Polyhydride Complex**

with Cp ligands or their derivatives. The reactivity of the early–late trimetallic chain complex  $\text{Cp}_2\text{Zr}\{\text{Ru}(\text{CO})_2\text{Cp}\}_2$  **214** toward this kind of reaction has already been discussed (section 3.4.3, Scheme 113, and section 3.5.3, Scheme 132).<sup>10</sup> Other examples follow.

The photolysis of a benzene/chloroform solution of the complexes **383** afforded complexes **384** with  $\mu$ - $\eta^5(M)$ ,  $\eta^1$ ,  $\eta^5$ -(*Ru*)-C<sub>5</sub>H<sub>4</sub>CH<sub>2</sub>C<sub>5</sub>H<sub>3</sub> ligands as the major products (Scheme 244). Isomers **385** with the binding mode of the ligand reversed (i.e.,  $\sigma$ -bonded to the group 6 metal) were isolated as minor products. X-ray diffraction studies of single crystals of each isomer were described.<sup>275</sup>

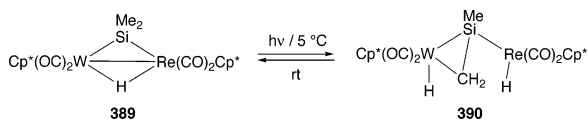
**Scheme 244. Activation of Cyclopentadienyl C–H Bonds in Ruthenium–Group 6 Complexes**

Cyclopentadienyl ligand C–H activation has also been observed in Mo–W complexes. When samples of  $[\text{Cp}(\text{OC})_2\text{Mo}(\mu\text{-dppm})\text{W}(\text{CO})_2\text{Cp}]$  (Mo–W), **386**, are heated, a P–C bond cleavage reaction takes place. However, photolysis at  $-10$  °C led to activation of a tungsten-bonded Cp ligand and to the formation of **387**. This species undergoes further photolytic decarbonylation at  $+10$  °C and regenerates the C<sub>5</sub>H<sub>4</sub>–H bond to give **388**, which contains a Mo≡W bond (Scheme 245).<sup>276</sup> This reaction may be reversed, and if CO is bubbled through a solution of **388**, complex **386** is regenerated. The W<sub>2</sub> analog of **386** also undergoes a reversible C<sub>5</sub>H<sub>4</sub>–H activation,<sup>277,278</sup> but in the Mo<sub>2</sub> system, only P–C bond activation was observed and never C–H activation.<sup>279,280</sup>

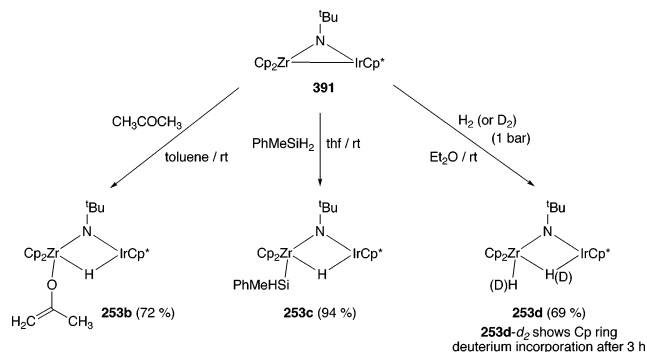
**Scheme 245. Cp Group C–H Activation in a Molybdenum–Tungsten  $\mu$ -dppm Complex**

### 6.3.3. Carbon–Hydrogen Activation of C(sp<sup>3</sup>)–H Bonds

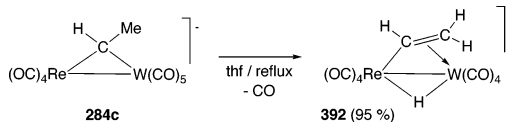
One of the methyl group C–H bonds of the  $\mu$ -SiMe<sub>2</sub> ligand in the  $\mu$ -SiMe<sub>2</sub> complex **389** can be photolytically activated at  $5$  °C. The product is the  $\eta^1(\text{Re})\eta^2(\text{W})$ -silylenyl bridged complex **390** shown in Scheme 246. The complex spontaneously reverts to **389** at room temperature.<sup>281</sup>

**Scheme 246. Activation of a  $\mu$ -SiMe<sub>2</sub> Group in a Tungsten–Rhenium Complex**


Acetone undergoes oxidative addition to the unsaturated iridium–zirconium complex **391** (Scheme 247) to give **253b**. However, acetone effectively reacts in its *enol* form, and it is likely that an O–H bond rather than a C–H bond is activated by the early–late dimetal center.<sup>218</sup> Silanes are also activated (reversibly) by complex **391**: PhMeSiH<sub>2</sub> affords the spectroscopically observed complex **253c** shown in the scheme. Molecules that activate Si–H bonds are often capable of activating molecular hydrogen, and indeed, **391** reacts reversibly with hydrogen or deuterium to give the dihydride or dideuteride complex **253d** (or **253d-d<sub>2</sub>**). There is slow exchange between the Cp ring hydrogen atoms and the added hydrogen: <sup>2</sup>D NMR shows that there is deuterium incorporation in the Cp ring after a 3 h period.

**Scheme 247. Acetone, Silane, Cp C–H, and Molecular Hydrogen Bond Activation by an Iridium–Zirconium Complex**


The anionic rhenium–tungsten ethylidene complex **284c** (Scheme 248) loses an equivalent of CO when the molecule is refluxed in thf. The complex activates one C(sp<sup>3</sup>)–H bond of the ethylidene ligand and rearranges to the  $\mu$ -alkenyl  $\mu$ -hydrido complex **392**.<sup>105</sup>

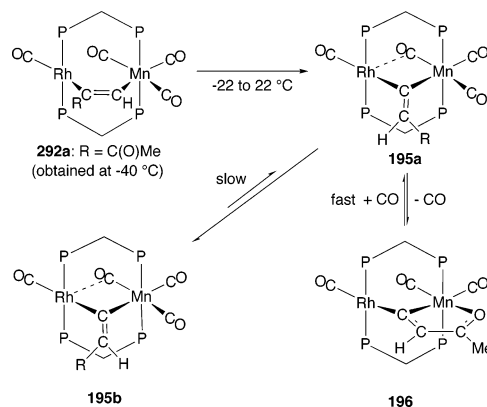
**Scheme 248. Thermal Rearrangement of an Alkylidene Ligand into a Vinyl Hydride Species**

**6.4. Hydrocarbyl Rearrangement Reactions That Lead to Carbon–Hydrogen Bond Cleavage and Concomitant Carbon–Hydrogen Bond Formation**

Some C–H activation reactions result in an initial C–H bond cleavage followed by the formation of a new C–H bond. These varied, and hard to classify, reactions are conveniently collected here. Note that some reactions of this type have already been discussed in sections 3.2.5 (Carbyne–Alkyne Coupling) and 3.3.3 (Carbene–Alkyne Coupling).

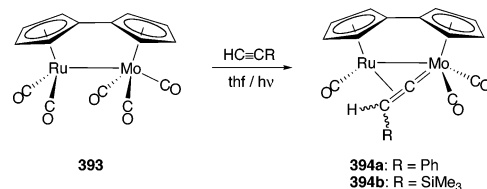
**6.4.1. Hydrocarbyl Rearrangements That Lead to Vinylidenes**

The parallel-bridged alkyne complex **292a** obtained at –40 °C (see Scheme 164) rearranges when warmed to room

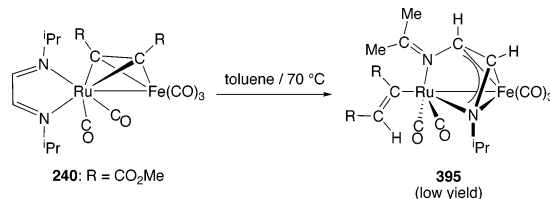
temperature to afford an isomeric mixture of  $\mu$ -vinylidene complexes **195** (Scheme 249).<sup>178</sup> None of these complexes contains Mn–Rh bonds. The reactivities of these species were described earlier (Schemes 104 and 161).

**Scheme 249. Rearrangement of a  $\mu$ -Alkyne Species to Isomeric  $\mu$ -Vinylidene Complexes**


The molybdenum–ruthenium fulvalene complex **393** reacts with the terminal alkynes shown in Scheme 250 to give isomeric  $\mu$ -vinylidene complexes **394** that are  $\sigma/\pi$  bonded to the two metals. Internal alkynes form molybdenum-bonded alkyne complexes. It is believed that the vinylidene complexes are formed from a proton migration reaction from an initially formed terminal alkyne complex, and some experimental evidence supports this view.<sup>282</sup>

**Scheme 250. Reaction of Terminal Alkynes with a Molybdenum–Ruthenium Fulvalene Complex Affords  $\mu$ -Vinylidene Complexes**

**6.4.2. Hydrocarbyl Rearrangements That Lead to Alkenyls**

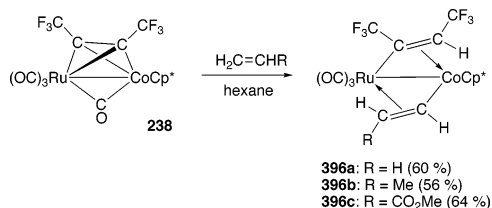
The iron–ruthenium complex **240** (Scheme 251) contains a diisopropyldiimine ligand (specifically *N,N'*-diisopropyl-1,4-diaza-1,3-butadiene) bonded to the ruthenium atom and a DMAD group bridging the metal–metal bond. This complex isomerizes when heated to give a terminal ruthenium-bonded alkenyl complex **395**, in which the diimine ligand is converted into a bridging azaallylic group that spans the two metals as shown.<sup>198</sup>

**Scheme 251. Isomerization of Diisopropyldiimine and DMAD Ligands into Alkenyl and Azaallyl Groups**


The reaction of terminal alkenes RCH=CH<sub>2</sub> with the  $\mu$ -HFB cobalt–ruthenium complex **238** (Scheme 252) leads to an unusual C–H activation reaction. A methylene hydrogen atom from the RCH=CH<sub>2</sub> moiety is transferred

to the  $\mu$ -HFB group and two alkenyl ligands are generated in the new complexes **396**. The alkenyl ligands bridge the bimetallic centers, but the hexafluorobutenyl ligands are  $\sigma$ -bonded to the ruthenium, while the alkene-derived alkenyl ligands are  $\sigma$ -bonded to the cobalt. The structures of two different alkenyl complexes were established by X-ray diffraction and reveal normal Co–Ru distances of ca. 2.60 Å for both complexes.<sup>208</sup>

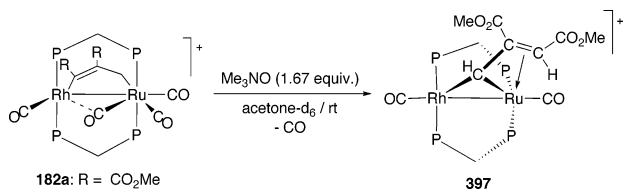
**Scheme 252. Alkene C–H Activation by a  $\mu$ -HFB Cobalt–Ruthenium Complex Leads to the Formation of Two  $\mu$ -Alkenyl Ligands**



**6.4.3. Hydrocarbyl Rearrangements That Lead to Carbenes**

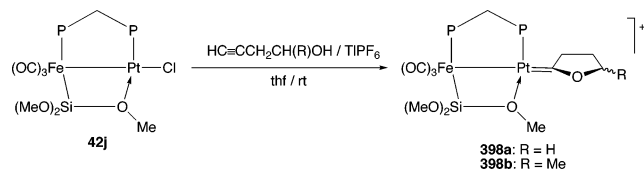
Upon reaction with trimethylamine-*N*-oxide, the cationic rhodium–ruthenium complex **182a** shown in Scheme 253, formed by reacting DMAD with **65a** (Scheme 99), undergoes carbonyl ligand loss accompanied by an internal 1,3-hydrogen shift to afford the vinyl carbene complex **397**. A mechanism that involves hydride formation is proposed.<sup>166,174</sup>

**Scheme 253. Rearrangement of a Rhodium–Ruthenium Dimetallacyclopentene Complex into a Vinyl Carbene Species**



When the hydroxyalkynes HC≡CCH<sub>2</sub>CH(R)OH (R = H, Me) are reacted with the iron–platinum complex **42j** in the presence of TlPF<sub>6</sub>, the Pt–Cl bond is broken, a likely 1–3-proton shift from platinum to carbon occurs, and cyclization of the alkyne takes place. These transformations afford the cationic platinum–bonded carbene complexes **398** (Scheme 254). A mechanism for the formation of the 2-oxacyclopentylidene ligand was proposed.<sup>81</sup>

**Scheme 254. Formation of a Cyclic Carbene Ligand Following a 1,3-Hydrogen Shift from Platinum to Carbon**

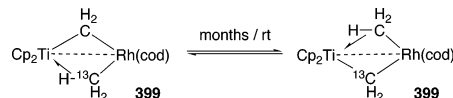


**6.4.4. Hydrogen Scrambling and Hydrogen Exchange Reactions**

There is very slow scrambling between hydrogen atoms of the agostic methyl ligand and those of the bridging methylene group in the rhodium–titanium complex **399** shown in Scheme 255. This reaction represents a well-

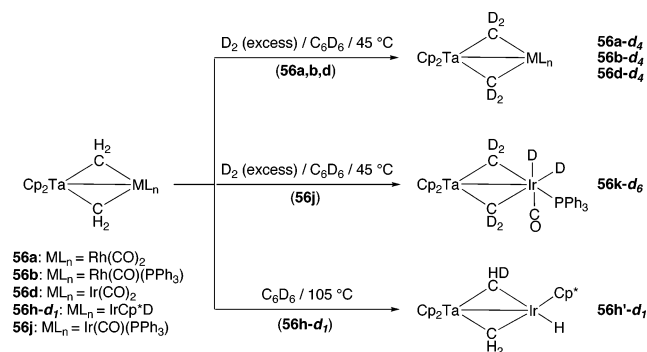
characterized example of a heterobimetallic center activating an alkyl group that contains an agostic hydrogen interaction.<sup>283</sup>

**Scheme 255. Hydrogen Atom Scrambling between an Agostic Methyl Group and a  $\mu$ -Methylene Ligand**



The methylene hydrogen atoms in the tantalum–rhodium and –iridium methylene complexes of class **56** shown in Scheme 256 undergo H/D exchange when the compounds are treated with an excess of diderium. The reaction rate is second order and follows a rate law expressed as rate =  $k[P(H_2)][Ta-M \text{ complex}]$ . For the iridium–tantalum complex **56j**, the H/D exchange is accompanied by oxidative addition of deuterium to give **56k-d<sub>6</sub>**.<sup>94</sup> The related iridium–tantalum bis( $\mu$ -CH<sub>2</sub>) complex **56h-d<sub>1</sub>** undergoes similar scrambling of the deuterium label between the terminal deuteride (hydride) position and the  $\mu$ -CH<sub>2</sub> group hydrogens at 105 °C in a sealed tube in C<sub>6</sub>D<sub>6</sub> (Scheme 256). The reaction may proceed via alkyl (CH<sub>2</sub>D) intermediates.<sup>265</sup>

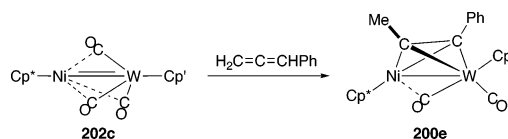
**Scheme 256. Exchange between Hydrogen or Hydride Ligands and  $\mu$ -CH<sub>2</sub> Hydrogen Atoms on Rhodium– and Iridium–Tantalum Frameworks**



**6.4.5. Other Hydrocarbyl Rearrangements**

Phenylallene ligates to the unsaturated nickel–tungsten complex **202c** but is isomerized in the reaction (Scheme 257). The product **200e** contains a  $\mu$ -PhC≡CMe ligand implying that an effective 1,3-hydrogen shift has taken place.<sup>131</sup>

**Scheme 257. Isomerization of Phenylallene on a Nickel–Tungsten Framework**

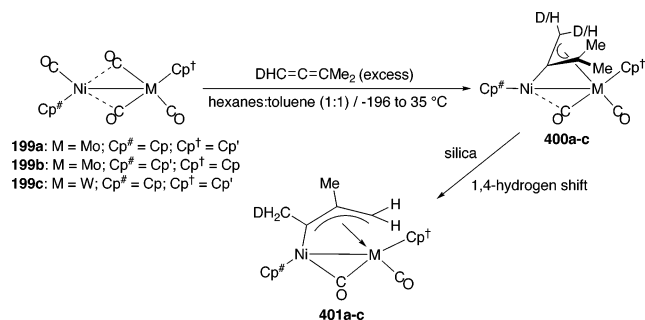


1,1-Dimethylallene reacts with nickel–molybdenum and –tungsten complexes of class **199** to give initial products in which the allene group oxidatively adds to the dimetal center to form 2-nickeloallyl complexes **400**. The central carbon of the dimethylallene is  $\sigma$ -bonded to the nickel atom, while the allylic group is  $\pi$ -coordinated to the group 6 metal (Scheme 258). These complexes isomerize on a silica column to give 1-nickeloallyl complexes **401**. The structure of a representative complex was determined crystallographically. A labeling study, using Me<sub>2</sub>C=C=CHD established that the



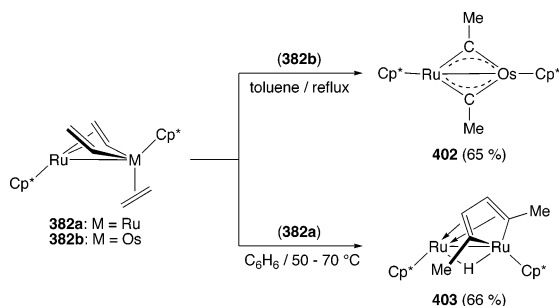
isomerization takes place via a 1,4-hydrogen shift and not a 1,2-methyl shift.<sup>215,284</sup>

**Scheme 258. Oxidative Addition and Isomerization of 1,1-Dimethylallene on Nickel–Molybdenum and –Tungsten Bonds**



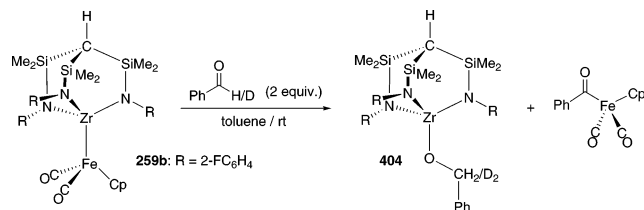
The osmium–ruthenium complex **382b** is slowly transformed into a bis- $\mu$ -CMe complex, **402**, in a double 1,2-hydrogen shift reaction, when refluxed in toluene for 2 days (Scheme 259).<sup>274</sup> This reactivity is in sharp contrast to the reactivity of the Ru<sub>2</sub> analog, **382a**, which affords the metallacyclopentadienyl hydride **403** when heated. This latter species is the result of C–C couplings between the coordinated ethylene and the two vinyl ligands.<sup>285</sup>

**Scheme 259. Transformation of a Bis( $\mu$ -vinyl) into a Bis( $\mu$ -carbyne) Complex**



A Cannizzaro-type disproportionation reaction was observed when the early–late heterobimetallic complex **259b** in Scheme 260 (see also Scheme 139) reacted with benzaldehyde to give **404** and [Fe(CO)<sub>2</sub>(COPh)Cp]. The deuterium-labeled aldehyde PhC(O)D gave a PhCD<sub>2</sub>O–zirconium complex.<sup>222</sup>

**Scheme 260. Cannizzaro-Type Disproportionation on an Iron–Zirconium Bond**

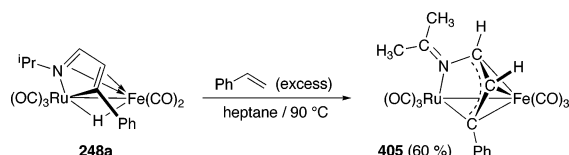


**6.5. Other Carbon–Hydrogen Cleavage Reactions**

Hydrogen abstraction reactions have been reported with diimine ligands. (An example has already been discussed in section 4.2, Scheme 152). When the iron–ruthenium complex **248a** shown in Scheme 261 is heated with styrene or  $\alpha$ -methylstyrene, the latter acts as a hydrogen acceptor for the *i*-Pr methine proton to yield complex **405** with an allylicly bonded ligand depicted in the scheme.<sup>212</sup> Note that

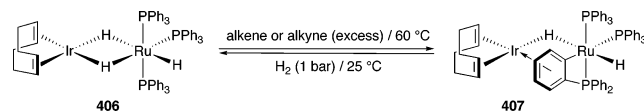
the addition of *t*-BuCH=CH<sub>2</sub> to the complex led not to methine hydrogen abstraction but to abstraction of the hydride ligand and was accompanied by addition of *t*-BuCH<sub>2</sub>-CH<sub>2</sub> to the unsaturated azaligand, as was discussed earlier (section 3.5.3, Scheme 133).<sup>212</sup>

**Scheme 261. Hydrogen Abstraction from a Diimine Complex on Reaction with Styrene**



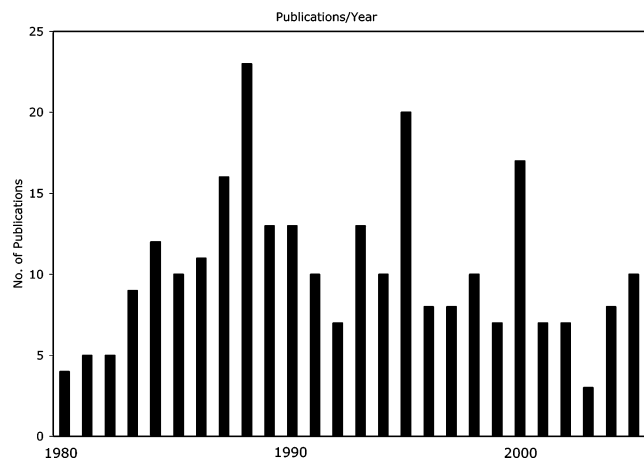
Cyclometalation reactions can be promoted by external reagents. The iridium/ruthenium trihydride complex **406** shown in Scheme 262 reacts with alkynes and with alkenes. Both classes of molecules act as hydrogen acceptors and dehydrogenate the molecule. The resulting unsaturated species then undergoes an *ortho*-metalation reaction with one of the PPh<sub>3</sub> phenyl groups to form **407**. The *ortho*-metalated aromatic ring of **407** is also  $\pi$ -coordinated to the iridium atom. The reaction can be reversed by adding H<sub>2</sub>.<sup>286</sup>

**Scheme 262. Hydrogen Abstraction from a Polyhydride Bimetallic Complex by Alkenes or Alkynes Leads to Orthometalation**



**7. Conclusion**

This review has summarized a wide range of carbon–hydrogen and carbon–carbon bond formation and bond cleavage reactions that have been investigated over the past 25 years. A plot of the number of publications (in the list of referenced articles) as a function of publication date is shown below. This graph is *qualitative*—in most cases the same



article is cited multiple times for different hydrocarbyl ligand transformations, while in other cases, there is only one reaction of interest—but it demonstrates that while research in this field peaked in the late 1980s, there has been a steady stream of manuscripts describing these reactions, and the field remains active.

An analysis of the metals involved in these reactions shows that most transition metals are well represented. Only hafnium, vanadium, and, for radioactivity reasons, technetium

tium, were not involved in any heterobimetallic hydrocarbyl ligand transformation during the last 25 years. In addition, while few examples exist for the metals titanium and niobium, the other metals are well represented. Tungsten (in view of the high stability of its Fischer-type carbene and carbyne complexes), cobalt, and rhodium are particularly well represented.

In order to activate hydrocarbyl ligands, the heterobimetallic center needs to be robust enough not to cleave during the course of the reaction. For a large number of such reactions, the hydrocarbyl ligand bridges the two metals. It thus anchors the two metals together and prevents metal–metal bond rupture. In most cited reactions of heterobimetallic carbene and carbyne complexes, pioneered by Stone and co-workers,<sup>23</sup> these ligands are in bridging positions. Many reactions that involve heterobimetallic alkyne and alkenyl complexes also have these ligands spanning the two metal centers.

In other cases, the metal–metal bond may be reinforced by other bridging species, such as  $\mu$ -dppm ligands, as is seen in most complexes from the group of Cowie.<sup>166</sup> Such  $\mu$ -dppm ligands do not prevent migration of hydrocarbyl ligands from one metal to another and do not extinguish synergistic effects between the two metal centers.

Another way to fortify the metal–metal interaction to prevent metal–metal bond scission is via multiple metal–metal bonding. This approach has been developed by, among others, Suzuki<sup>273,274</sup> in the chemistry of mixed-metal ruthenium–iridium and –osmium complexes and also by the authors of this article, in developing the chemistry of nickel–molybdenum and –tungsten complexes.<sup>46,172,215</sup>

Unsaturation, or easy access to it, is helpful in increasing the reactivity of heterobimetallic complexes and facilitates hydrocarbyl ligand activation. In this review, the vast majority of reactions take place on complexes that exhibit unsaturation, either via a multiple metal–metal bond or, more commonly, via an unsaturated hydrocarbyl ligand. If not present, unsaturation can be generated by lowering the hapticity of a ligand to the metal or by ligand (frequently a metal carbonyl) dissociation.

Another way to introduce electronic unsaturation and, simultaneously, to free up a coordination site at a metal center is to use a hemilabile ligand that coordinates asymmetrically to a metal: an example is provided by the ligand  $\text{Et}_2\text{NC}_2\text{H}_4\text{-PPh}_2$ , with differing coordination aptitudes of the N and the P donor atoms.<sup>125</sup> Hemilabile  $\mu$ -Si(OMe)<sub>3</sub> ligands have also been used as they may coordinate reversibly to a group 10 metal, as necessary.<sup>117,119</sup>

Recent exciting developments in hydrocarbyl ligand transformation include spectacular methylene–alkyne<sup>166,172,174,175</sup> and methylene–alkene coupling reactions<sup>166,173,177</sup> and reports of alkene activation by heterobimetallic complexes.<sup>213,273,274</sup> Developments in early–late heterobimetallic complexes, which take advantage of the oxophilicity of the early metal and hard–soft acid–base properties of the two metals, have also led to unusual activation reactions.<sup>61,92–96</sup> The chemistry of many heterobimetallic combinations toward hydrocarbyl ligand activation remains unexplored, and there remains a great potential for innovative research in this field.

## 8. List of Abbreviations

Bz	benzyl, C <sub>6</sub> H <sub>5</sub> CH <sub>2</sub>
bipy	2,2'-bipyridine

cod	1,5-cyclooctadiene, C <sub>8</sub> H <sub>12</sub>
Cp	$\eta^5$ -cyclopentadienyl, C <sub>5</sub> H <sub>5</sub>
Cp'	$\eta^5$ -methylcyclopentadienyl, C <sub>5</sub> H <sub>4</sub> Me
Cp*	$\eta^5$ -pentamethylcyclopentadienyl, C <sub>5</sub> Me <sub>5</sub>
Cp <sup>†</sup>	any substituted or unsubstituted $\eta^5$ -cyclopentadienyl ligand
Cy	cyclohexyl, <i>cyclo</i> -C <sub>6</sub> H <sub>11</sub>
DMAD	dimethylacetylenedicarboxylate, MeO <sub>2</sub> CC≡CCO <sub>2</sub> Me
dmpm	<i>bis</i> (dimethylphosphino)methane, Me <sub>2</sub> PCH <sub>2</sub> PMe <sub>2</sub>
dppe	1,2- <i>bis</i> (diphenylphosphino)ethane, Ph <sub>2</sub> PCH <sub>2</sub> CH <sub>2</sub> PPh <sub>2</sub>
dppm	<i>bis</i> (diphenylphosphino)methane, Ph <sub>2</sub> PCH <sub>2</sub> PPh <sub>2</sub>
HB(pz) <sub>3</sub>	tris(pyrazolyl)borate
HFB	hexafluorobut-2-yne, CF <sub>3</sub> C≡CCF <sub>3</sub>
phen	1,10-phenanthroline
PPN	bis(triphenylphosphoranylidene)
rt	room temperature
Tf	triflate, CF <sub>3</sub> SO <sub>2</sub> <sup>−</sup>
TFA(H)	trifluoroacetate, CF <sub>3</sub> CO <sub>2</sub> <sup>−</sup> (trifluoroacetic acid, CF <sub>3</sub> -CO <sub>2</sub> H)
thf	tetrahydrofuran
tmeda	N,N,N',N'-tetramethylethylenediamine
Tol	<i>p</i> -tolyl = 4-methylphenyl, 4-CH <sub>3</sub> C <sub>6</sub> H <sub>4</sub> (if not otherwise specified)

## 9. Acknowledgment

We thank the CNRS, the Université Louis Pasteur and the Région Alsace for financial support.

## 10. Addendum

This review covers the period from 1980 to 2005 comprehensively. During the submission and review period of this article, a number of relevant publications have appeared. Selective coverage of some pertinent publications of 2006 are included in this section.

Insertions of two molecules of CO<sub>2</sub> into the tin–hydride bonds of two osmium–tin complexes to give osmium–bisformyl tin complexes was reported.<sup>287</sup> The osmium–tin polyhydride species [H<sub>4</sub>(*i*-Pr<sub>3</sub>P)<sub>2</sub>CIOs–SnPh<sub>3</sub>] reacts, in a complex reaction, with PhC≡CPh to give stilbene, benzene, and [H<sub>3</sub>(*i*-Pr<sub>3</sub>P){Pr<sub>2</sub>PC(Me)=CH<sub>2</sub>}Os–SnClPh<sub>2</sub>].<sup>288</sup> This species in turn affords an osmium-bonded molecular hydrogen Os–Sn complex with both bridging and terminal benzoate ligands when treated with benzoic acid.<sup>289</sup> The monohydride species [Os(CO)<sub>4</sub>(H)(SnPh<sub>3</sub>)] (Os–Sn) reacts with PhC≡CH in the presence of [Pt(*P*-*t*-Bu<sub>3</sub>)<sub>2</sub>] to yield the alkyne insertion trimetallic chain product [(*t*-Bu<sub>3</sub>P)(OC)Pt{ $\mu$ - $\eta^1$ -(*Pt*), $\eta^2$ (*Os*)-*trans*-CH=CHPh}Os(CO)(SnPh<sub>3</sub>)] (Pt–Os–Sn) containing a Pt(*t*-PBu<sub>3</sub>)(CO) group coordinated to the osmium atom and the alkenyl ligand. No reaction with PhC<sub>2</sub>H is observed in the absence of the Pt complex.<sup>290</sup>

New evidence is presented for the participation of heterobimetallic cobalt–rhodium species in the catalytic silylformylation of alkynes by the cluster Co<sub>2</sub>Rh<sub>2</sub>(CO)<sub>12</sub>. DFT calculations and the catalytic cycle presented both suggest that a Co–Rh bimetallic species is required for the addition of a CHO and a SiR<sub>3</sub> group across an alkyne C≡C bond.<sup>291</sup> The smooth reversible insertion of various olefins into M–H bonds of [M(CO)<sub>3</sub>HCp] (M = Mo, W) were catalyzed by [Pd(PPh<sub>3</sub>)<sub>4</sub>] or by [Pd(CH<sub>2</sub>=CHCO<sub>2</sub>Et)(dppe)]; heterobimetallic complexes are implicated, and in some cases, these species were isolated.<sup>292</sup> Aliphatic terminal alkynes have been inserted into the Pt–H bond of the complex [(OC)<sub>3</sub>Fe{Si(OMe)<sub>3</sub>}( $\mu$ -dppm)Pt(PPh<sub>3</sub>)H] (Fe–Pt) to give vinylidenes and dimetallacyclopentenone complexes.<sup>293</sup>

A migratory CO insertion is induced when trialkylphosphines or CO are added to the complexes [Cp<sup>†</sup>(OC)<sub>2</sub>XMo-

$(\text{CH}_2)_n\text{W}(\text{CO})_3\text{Cp}$ ] (various combinations of  $n = 3, 4$ ;  $\text{X} = \text{PMe}_3$  or  $\text{CO}$ ;  $\text{Cp}^\dagger = \text{Cp}, \text{Cp}^*$ ) in coordinating solvents. The products are the molybdenum acyl species  $[\text{Cp}^\dagger(\text{OC})\text{XLMoC}(\text{O})(\text{CH}_2)_n\text{W}(\text{CO})_3\text{Cp}]$  ( $\text{L} = \text{CO}, \text{PMe}_3, \text{PPh}_3$ ).<sup>294</sup> Thermolysis of the related complex  $[\text{Cp}(\text{OC})_2\text{Fe}(\text{CH}_2)_3\text{Mo}(\text{CO})_2(\text{PMe}_3)\text{Cp}]$  afforded cyclopropane and also, via a different decarbonylation pathway, propene and the Fe–Mo complex  $[\text{Cp}(\text{OC})\text{Fe}(\mu\text{-}\eta^1(\text{Fe}), \eta^2(\text{Mo})\text{-CH}_2\text{CH}=\text{CH}_2)(\mu\text{-CO})\text{-Mo}(\text{PMe}_3)(\text{H})\text{Cp}]$  (Fe–Mo).<sup>294</sup>

The reaction of  $[\text{Re}(\text{CO})_5]^-$  with  $[\text{Ru}(\text{dppm})\text{ClCp}^*]$  afforded a complex with a cyclometalated Ph ligand as a side product (25% yield).<sup>295</sup> Isocyanide and alkyne insertions into the Pd–C bonds of various Fe–Pd complexes with  $\mu$ -dppm and iron-bonded  $\text{Si}(\text{OMe})_3$  ligands have been reported, and some products were structurally characterized.<sup>296</sup> The dithiolate Rh–Ru species  $[\text{Cp}^*\text{Rh}(\mu\text{-}1,2\text{-S}_2\text{C}_6\text{H}_4)(\mu\text{-H})\text{RuH}]$  (Rh–Ru) reacts with terminal aryl acetylenes to give alkynyl hydride species via C–H bond activation. Further reactions with alkynes gives metallacycles or six-membered aromatic rings formed by the coupling of three alkynes.<sup>297</sup> Alkynyl–CO coupling reactions are observed when the platinum acetylide  $[\text{Pt}(\text{dppe})\{-\text{C}\equiv\text{C}(3\text{-thiophenyl})\}_2]$  is reacted with  $[\text{Fe}(\text{CO})_5]$ .<sup>298</sup>

The H/D exchange observed when the complexes  $[\text{RuH}(\text{dppm})\text{Cp}^\dagger]$  ( $\text{Cp}^\dagger = \text{Cp}, \text{Cp}^*$ ) and  $[\text{HMn}(\text{CO})_5]$  are mixed at room temperature is believed to proceed via a molecular dihydrogen complex. When the mixture is heated or allowed to stand for more than a week, reaction to form  $[\text{Cp}(\text{OC})\text{-Ru}(\mu\text{-dppm})\text{Mn}(\text{CO})_4]$  (Mn–Ru) ensues. This complex catalyzes the coupling of epoxides with  $\text{CO}_2$  to give cyclic carbonates.<sup>299</sup>

## 11. References

- Naito, S. *J. Chem. Soc., Chem. Commun.* **1985**, 1212.
- Sinfelt, J. H. *Bimetallic Catalysts*; Wiley: New York, 1983.
- Stephan, D. W. *Coord. Chem. Rev.* **1989**, 95, 41.
- Wheatley, N.; Kalck, P. *Chem. Rev.* **1999**, 99, 3379.
- Bruce, M. I. *J. Organomet. Chem.* **1983**, 242, 147.
- Bruce, M. I. *J. Organomet. Chem.* **1985**, 283, 339.
- Chetcuti, M. J. In *Comprehensive Organometallic Chemistry II*; Abel, E. W., Stone, F. G. A., Wilkinson, G., Eds.; Pergamon: Oxford, U.K. 1995; Vol. 10, p 23.
- Gade, L. H. *Angew. Chem., Int. Ed.* **2000**, 39, 2658.
- Bullock, R. M.; Casey, C. P. *Acc. Chem. Res.* **1987**, 20, 167.
- Casey, C. P. *J. Organomet. Chem.* **1990**, 400, 205.
- Braunstein, P.; Knorr, M.; Stern, C. *Coord. Chem. Rev.* **1998**, 178–180, 903.
- Chaudret, B.; Delavaux, B.; Poilblanc, R. *Coord. Chem. Rev.* **1988**, 86, 191.
- Chetcuti, M. J. *J. Cluster Sci.* **1996**, 7, 225.
- Mague, J. T. *J. Cluster Sci.* **1995**, 6, 217.
- Herrmann, W. A. *Adv. Organomet. Chem.* **1982**, 20, 159.
- Puddephatt, R. J. *Polyhedron* **1988**, 7, 767.
- Wojcicki, A. *J. Cluster Sci.* **1993**, 4, 59.
- El Amouri, H.; Gruselle, M. *Chem. Rev.* **1996**, 96, 1077.
- McGlinchey, M. J.; Girard, L.; Ruffolo, R. *Coord. Chem. Rev.* **1995**, 143, 331.
- Bruce, M. I. *Chem. Rev.* **1991**, 91, 197.
- Holton, J.; Lappert, M. F.; Pearce, R.; Yarrow, P. I. *W. Chem. Rev.* **1983**, 83, 135.
- Jeffery, J. C.; Went, M. J. *Polyhedron* **1988**, 7, 775.
- Stone, F. G. A. *Angew. Chem., Int. Ed. Engl.* **1984**, 23, 89.
- Martin-Gil, J.; Howard, J. A. K.; Navarro, R.; Stone, F. G. A. *J. Chem. Soc., Chem. Commun.* **1979**, 1168.
- Orama, O.; Schubert, U.; Kreissl, F. R.; Fischer, E. O. *Z. Naturforsch.* **1980**, 35B, 82.
- Jeffery, J. C.; Ruiz, M. A.; Stone, F. G. A. *J. Organomet. Chem.* **1988**, 355, 231.
- Tang, Y.; Sun, J.; Chen, J. *J. Chem. Soc., Dalton Trans.* **1998**, 4003.
- Tang, Y.-J.; Sun, J.; Chen, J. B. *Organometallics* **1998**, 17, 2945.
- Tang, Y.-J.; Sun, J.; Chen, J. B. *Organometallics* **2000**, 19, 72.
- Chen, J.; Wang, R. *Coord. Chem. Rev.* **2002**, 231, 109.
- Chen, J.; Yu, Y.; Liu, K.; Wu, G.; Zheng, P. *Organometallics* **1993**, 12, 1213.
- Yu, Y.; Chen, J.; Chen, J.; Zheng, P. *J. Chem. Soc., Dalton Trans.* **1996**, 1443.
- Davis, J. H.; Lukehart, C. M.; Sacksteder, L. *Organometallics* **1987**, 6, 50.
- Hart, I. J.; Jeffery, J. C.; Lowry, R. M.; Stone, F. G. A. *Angew. Chem., Int. Ed. Engl.* **1988**, 27, 1703.
- Engel, P. F.; Pfeffer, M.; Fischer, J.; Dedieu, A. *J. Chem. Soc., Chem. Commun.* **1991**, 1274.
- Kläeui, W.; Hamers, H.; Pfeffer, M.; de Cian, A.; Fischer, J. *J. Organomet. Chem.* **1990**, 394, 213.
- Macchioni, A.; Pregnosin, P. S.; Engel, P. F.; Mecking, S.; Pfeffer, M.; Daran, J. C.; Vaissermann, J. *Organometallics* **1995**, 14, 1637.
- Engel, P. F.; Pfeffer, M.; Fischer, J. *Organometallics* **1994**, 13, 4751.
- Lohner, P.; Pfeffer, M.; de Cian, A.; Fischer, J. *C. R. Acad. Sci. Paris, Sér. II c* **1998**, 1, 615.
- Awang, M. R.; Barr, R. D.; Green, M.; Howard, J. A. K.; Marder, T. B.; Stone, F. G. A. *J. Chem. Soc., Dalton Trans.* **1985**, 2009.
- Burn, M. J.; Kiel, G.-Y.; Seils, F.; Takats, J.; Washington, J. *J. Am. Chem. Soc.* **1989**, 111, 6850.
- Takats, J.; Washington, J.; Santarsiero, B. D. *Organometallics* **1994**, 13, 1078.
- Cooke, J.; Takats, J. *J. Am. Chem. Soc.* **1997**, 119, 11088.
- Kiel, G.-Y.; Zhang, Z.; Takats, J.; Jordan, R. B. *Organometallics* **2000**, 19, 2766.
- Otto, H.; Garcia-Alonso, F. J.; Werner, H. *J. Organomet. Chem.* **1986**, 306, C13.
- Chetcuti, M. J.; Grant, B. E.; Fanwick, P. E. *Organometallics* **1996**, 15, 4389.
- Chetcuti, M. J.; Grant, B. E.; Fanwick, P. E. *J. Am. Chem. Soc.* **1989**, 111, 2743.
- Chetcuti, M. J.; Fanwick, P. E.; Grant, B. E. *J. Organomet. Chem.* **2001**, 630, 215.
- Davidson, J. L.; Manojlovic-Muir, L.; Muir, K. W.; Keith, A. N. *J. Chem. Soc., Chem. Commun.* **1980**, 749.
- Davidson, J. L. *J. Chem. Soc., Dalton Trans.* **1983**, 1667.
- Hirpo, W.; Curtis, M. D.; Kampf, J. W. *Organometallics* **1994**, 13, 3360.
- Yáñez, R.; Lugan, N.; Mathieu, R. *Organometallics* **1990**, 9, 2998.
- Chetcuti, M. J.; Fanwick, P. E.; Gordon, J. C. *Inorg. Chem.* **1991**, 30, 4710.
- Farrugia, L. J.; Went, M. J. *J. Chem. Soc., Chem. Commun.* **1987**, 973.
- Scott, I. D.; Smith, D. O.; Went, M. J.; Farrugia, L. J. *J. Chem. Soc., Dalton Trans.* **1989**, 1375.
- Chetcuti, M. J.; DeLiberato, L.; Fanwick, P. E.; Grant, B. E. *Inorg. Chem.* **1990**, 29, 1295.
- Atta, A. M.; Chandler, D. J.; Jones, R. A. *Organometallics* **1987**, 6, 506.
- Rosen, R. P.; Hoke, J. B.; Whittle, R. R.; Geoffroy, G. L.; Hutchison, J. P.; Zubieta, J. A. *Organometallics* **1984**, 3, 846.
- Targos, T. S.; Geoffroy, G. L.; Rheingold, A. R. *J. Organomet. Chem.* **1986**, 299, 223.
- Shuchart, C. E.; Young, G. H.; Wojcicki, A.; Calligaris, M.; Nardin, G. *Organometallics* **1990**, 9, 2417.
- Proulx, G.; Bergman, R. G. *Science* **1993**, 259, 661.
- Jeffery, J. C.; Sambale, C.; Schmidt, M. F.; Stone, F. G. A. *Organometallics* **1982**, 1, 1597.
- Moldes, I.; Ros, J.; Mathieu, R.; Solans, X.; Font-Bardía, M. *J. Chem. Soc., Dalton Trans.* **1987**, 1619.
- Rosenthal, U.; Pulst, S.; Arndt, P.; Ohff, A.; Tillack, A.; Baumann, W.; Kempe, R.; Burlakov, V. V. *Organometallics* **1995**, 14, 2961.
- Renaut, P.; Tainturier, G.; Gautheron, B. *J. Organomet. Chem.* **1978**, 150, C9.
- Longato, B.; Norton, J. R.; Huffman, J. C.; Marsella, J. A.; Caulton, K. G. *J. Am. Chem. Soc.* **1981**, 103, 209.
- Marsella, J. A.; Huffman, J. C.; Caulton, K. G.; Longato, B.; Norton, J. R. *J. Am. Chem. Soc.* **1982**, 104, 6360.
- McFarland, J. M.; Churchill, M. R.; See, R. F.; Lake, C. H.; Atwood, J. D. *Organometallics* **1991**, 10, 3530.
- Cornelissen, C.; Erker, G.; Kehr, G.; Fröhlich, R. *Dalton Trans.* **2004**, 4059.
- Bosch, B. E.; Brümmer, I.; Kunz, K.; Erker, G.; Fröhlich, R.; Kotila, S. *Organometallics* **2000**, 19, 1255.
- Cornelissen, C.; Erker, G.; Kehr, G.; Fröhlich, R. *Organometallics* **2005**, 24, 214.
- Lemke, F. R.; Szalda, D. J.; Bullock, R. M. *J. Am. Chem. Soc.* **1991**, 113, 8466.
- Braunstein, P.; Knorr, M.; Tiripicchio, A.; Tiripicchio Camellini, M. *Angew. Chem., Int. Ed. Engl.* **1989**, 28, 1361.
- Braunstein, P.; Faure, T.; Knorr, M.; Stährfeldt, T.; De Cian, A.; Fischer, J. *Gazz. Chim. Ital.* **1995**, 125, 35.

- (75) Lukehart, C. M.; True, W. R. *Organometallics* **1988**, *7*, 2387.
- (76) Yáñez, R.; Ros, J.; Moldes, I.; Mathieu, R.; Solans, X.; Font-Bardía, M. *J. Chem. Soc., Dalton Trans.* **1990**, 3147.
- (77) Tang, Y.; Sun, J.; Chen, J. *J. Chem. Soc., Dalton Trans.* **1998**, 931.
- (78) Davis, J. H. J.; Lukehart, C. M. *Organometallics* **1984**, *3*, 1763.
- (79) Hoskins, S. V.; James, A. P.; Jeffery, J. C.; Stone, F. G. A. *J. Chem. Soc., Dalton Trans.* **1986**, 1709.
- (80) Afzal, D.; Lukehart, C. M. *Organometallics* **1987**, *6*, 546.
- (81) Braunstein, P.; Faure, T.; Knorr, M.; Balegroune, F.; Grandjean, D. *J. Organomet. Chem.* **1993**, *462*, 271.
- (82) Huang, Y.-H.; Stang, P. J.; Arif, A. M. *J. Am. Chem. Soc.* **1990**, *112*, 5648.
- (83) Stang, P. J.; Huang, Y.-H.; Arif, A. M. *Organometallics* **1992**, *11*, 845.
- (84) Stang, P. J.; Cao, D. *Organometallics* **1993**, *12*, 996.
- (85) Cao, D. H.; Stang, P. J.; Arif, A. M. *Organometallics* **1995**, *14*, 2733.
- (86) Hiltz, R. W.; Franchuk, R. A.; Cowie, M. *Organometallics* **1991**, *10*, 1297.
- (87) Hoxmeier, R.; Deubzer, B.; Kaesz, H. D. *J. Am. Chem. Soc.* **1971**, *93*, 536.
- (88) Pasynskii, A. A.; Skripkin, Y. V.; Kalinnikov, V. T.; Porai-Koshits, M. A.; Antsyshkina, A. S.; Sadikov, G. G.; Ostriko, V. N. *J. Organomet. Chem.* **1980**, *201*, 269.
- (89) Pregosin, P. S.; Togni, A.; Venanzi, L. M. *Angew. Chem., Int. Ed. Engl.* **1981**, *20*, 668.
- (90) Howarth, O. W.; McAteer, C. H.; Moore, P.; Morris, G. E.; Alcock, N. W. *J. Chem. Soc., Dalton Trans.* **1982**, 541.
- (91) Liu, L.-K.; Luh, L.-S.; Wen, Y.-S.; Eke, U. B.; Mesubi, M. A. *Organometallics* **1995**, *14*, 4474.
- (92) Goldberg, K. I.; Bergman, R. J. *J. Am. Chem. Soc.* **1988**, *110*, 4853.
- (93) Hostetler, M. J.; Butts, M. D.; Bergman, R. G. *Inorg. Chim. Acta.* **1992**, *198–200*, 377.
- (94) Hostetler, M. J.; Butts, M. D.; Bergman, R. G. *J. Am. Chem. Soc.* **1993**, *115*, 2743.
- (95) Butts, M. D.; Bergman, R. G. *Organometallics* **1993**, *12*, 4269.
- (96) Butts, M. D.; Bergman, R. G. *Organometallics* **1994**, *13*, 1899.
- (97) Nikonov, G. I.; Lemenovskii, D. A.; Kuzmina, L. G. *J. Organomet. Chem.* **1995**, *496*, 187.
- (98) Mercer, W. C.; Geoffroy, G. L.; Rheingold, A. R. *Organometallics* **1985**, *4*, 1418.
- (99) Breen, M. J.; Geoffroy, G. L.; Rheingold, A. L.; Fultz, W. C. *J. Am. Chem. Soc.* **1983**, *105*, 1069.
- (100) Breen, M. J.; Shulman, P. M.; Geoffroy, G. L.; Rheingold, A. L.; Fultz, W. C. *Organometallics* **1984**, *3*, 782.
- (101) Powell, J.; Couture, C.; Gregg, M. R.; Sawyer, J. F. *Inorg. Chem.* **1989**, *28*, 3437.
- (102) Powell, J.; Couture, C.; Gregg, M. R. *J. Chem. Soc., Chem. Commun.* **1988**, 1208.
- (103) Mercer, W. C.; Whittle, R. R.; Burkhardt, E. W.; Geoffroy, G. L. *Organometallics* **1985**, *4*, 68.
- (104) Jeffery, J. C.; Orpen, A. G.; Robinson, W. T.; Stone, F. G. A.; Went, M. J. *J. Chem. Soc., Chem. Commun.* **1984**, 396.
- (105) Jeffery, J. C.; Orpen, A. G.; Stone, F. G. A.; Went, M. J. *J. Chem. Soc., Dalton Trans.* **1986**, 173.
- (106) Rowsell, B. D.; McDonald, R.; Cowie, M. *Organometallics* **2004**, *23*, 3873.
- (107) Trepanier, S. J.; McDonald, R.; Cowie, M. *Organometallics* **2003**, *22*, 2638.
- (108) Antwi-Nsiah, F. H.; Oke, O.; Cowie, M. *Organometallics* **1996**, *15*, 1042.
- (109) Adatia, T.; Henrick, K.; Horton, A. D.; Mays, M. J.; McPartlin, M. *J. Chem. Soc., Chem. Commun.* **1986**, 1206.
- (110) Coutinho, K. J.; Dickson, R. S.; Fallon, G. D.; Jackson, W. R.; De Simone, T.; Skelton, B. W.; White, A. H. *J. Chem. Soc., Dalton Trans.* **1997**, 3193.
- (111) Antonelli, D. M.; Cowie, M. *Organometallics* **1991**, *10*, 2550.
- (112) Antwi-Nsiah, F.; Cowie, M. *Organometallics* **1992**, *11*, 3157.
- (113) Graham, T. W.; Van Gastel, F.; McDonald, R.; Cowie, M. *Organometallics* **1999**, *18*, 2177.
- (114) Sterenberg, B. T.; McDonald, R.; Cowie, M. *Organometallics* **1997**, *16*, 2297.
- (115) Hiltz, R. W.; Oke, O.; Ferguson, M. J.; McDonald, R.; Cowie, M. *Organometallics* **2005**, *24*, 4393.
- (116) Gomez, M.; Muller, G.; Sainz, D.; Sales, J.; Solans, X. *Organometallics* **1991**, *10*, 4036.
- (117) Braunstein, P.; Knorr, M.; Stahrfeldt, T. *J. Chem. Soc., Chem. Commun.* **1994**, 1913.
- (118) Braunstein, P.; Durand, J.; Kickelbrick, G.; Knorr, M.; Morise, X.; Pugin, R.; Tiripicchio, A.; Ugozzoli, F. *J. Chem. Soc., Dalton Trans.* **1999**, 4175.
- (119) Braunstein, P.; Clerc, G.; Morise, X. *Organometallics* **2001**, *20*, 5036.
- (120) Braunstein, P.; Durand, J.; Knorr, M.; Strohmman, C. *Chem. Commun.* **2001**, 211.
- (121) Knorr, M.; Braunstein, P.; Tiripicchio, A.; Ugozzoli, F. *Organometallics* **1995**, *14*, 4910.
- (122) Fukuoka, A.; Fukagawa, S.; Hirano, M.; Komiya, S. *Chem. Lett.* **1997**, 377.
- (123) Fukuoka, A.; Fukagawa, S.; Hirano, M.; Koga, N.; Komiya, S. *Organometallics* **2001**, *20*, 2065.
- (124) Komine, N.; Hoh, H.; Hirano, M.; Komiya, S. *Organometallics* **2000**, *19*, 5251.
- (125) Tsutsuminai, S.; Komine, N.; Hirano, M.; Komiya, S. *Organometallics* **2003**, *22*, 4238.
- (126) Casey, C. P.; Palermo, R. E.; Rheingold, A. L. *J. Am. Chem. Soc.* **1986**, *108*, 549.
- (127) Lutz, M.; Haukka, M.; Pakkanen, T. A.; Gade, L. H. *Organometallics* **2002**, *21*, 3477.
- (128) Kahn, A. P.; R. B.; Blümel, J.; Vollhardt, K. P. C. *J. Organomet. Chem.* **1994**, *472*, 149.
- (129) Arndt, L. W.; Bancroft, B. T.; Darensbourg, M. Y.; Janzen, C. P.; Kim, C. M.; Reibenspies, K. E.; Varner, K. E.; Youngdahl, K. A. *Organometallics* **1988**, *7*, 1302.
- (130) Garcia, M. E.; Jeffery, J. C.; Sherwood, P.; Stone, F. G. A. *J. Chem. Soc., Dalton Trans.* **1988**, 2443.
- (131) Chetcuti, M. J.; Grant, B. E.; Fanwick, P. E. *Organometallics* **1995**, *14*, 2937.
- (132) Lemke, F. R.; Bullock, R. M. *Organometallics* **1992**, *11*, 4261.
- (133) Onitsuka, K.; Yanai, K.; Takei, F.; Joh, T.; Takahashi, S. *Organometallics* **1994**, *13*, 3862.
- (134) Ogawa, H.; Joh, T.; Takahashi, S. *J. Chem. Soc., Chem. Commun.* **1988**, 561.
- (135) Onitsuka, K.; Ogawa, H.; Joh, T.; Takahashi, S.; Yamamoto, Y.; Yamazaki, H. *J. Chem. Soc., Dalton Trans.* **1991**, 1531.
- (136) Yamada, T.; Tanabe, M.; Osakada, K.; Kim, Y.-J.; Pain, G. N. *Organometallics* **2004**, *23*, 4771.
- (137) He, Z.; Neibecker, D.; Lugan, N.; Mathieu, R. *Organometallics* **1992**, *11*, 817.
- (138) Hart, I. J.; Jardin, A. E.; Jeffery, J. C.; Stone, F. G. A. *J. Organomet. Chem.* **1988**, *341*, 391.
- (139) Howard, J. A. K.; Jeffery, J. C.; Laguna, M.; Navarro, R.; Stone, F. G. A. *J. Chem. Soc., Chem. Commun.* **1979**, 1170.
- (140) Mead, K. A.; Moore, I.; Stone, F. G. A.; Woodward, P. *J. Chem. Soc., Dalton Trans.* **1983**, 2083.
- (141) Jeffery, J. C.; Moore, I.; Razay, H.; Stone, F. G. A. *J. Chem. Soc., Chem. Commun.* **1981**, 1255.
- (142) Jeffery, J. C.; Laurie, J. C. V.; Moore, I.; Razay, H.; Stone, F. G. A. *J. Chem. Soc., Dalton Trans.* **1984**, 1563.
- (143) Awang, M. R.; Jeffery, J. C.; Stone, F. G. A. *J. Chem. Soc., Chem. Commun.* **1983**, 1426.
- (144) Awang, M. R.; Jeffery, J. C.; Stone, F. G. A. *J. Chem. Soc., Dalton Trans.* **1986**, 165.
- (145) Howard, J. A. K.; Jeffery, J. C.; Laguna, M.; Navarro, R.; Stone, F. G. A.; Woodward, P. *J. Chem. Soc., Dalton Trans.* **1981**, 751.
- (146) Garcia, M. E.; Jeffery, J. C.; Sherwood, P.; Stone, F. G. A. *J. Chem. Soc., Chem. Commun.* **1986**, 802.
- (147) Brew, S. A.; Dossett, S. J.; Jeffery, J. C.; Stone, F. G. A. *J. Chem. Soc., Dalton Trans.* **1990**, 3709.
- (148) El Amin, E. A. E.; Jeffery, J. C.; Walters, T. M. *J. Chem. Soc., Chem. Commun.* **1990**, 170.
- (149) Barr, R. D.; Green, M.; Howard, J. A. K.; Marder, T. B.; Moore, I. *J. Chem. Soc., Chem. Commun.* **1983**, 746.
- (150) Garcia, M. E.; Tran-Huy, N. H.; Jeffery, J. C.; Sherwood, P.; Stone, F. G. A. *J. Chem. Soc., Dalton Trans.* **1987**, 2201.
- (151) Delgado, E.; Hein, J.; Jeffery, J. C.; Ratermann, A. L.; Stone, F. G. A. *J. Organomet. Chem.* **1986**, *307*, C23.
- (152) Delgado, E.; Hein, J.; Jeffery, J. C.; Ratermann, A. L.; Stone, F. G. A.; Farrugia, L. J. *J. Chem. Soc., Dalton Trans.* **1987**, 1191.
- (153) Jeffery, J. C.; Mead, K. A.; Razay, H.; Stone, F. G. A.; Went, M. J.; Woodward, P. *J. Chem. Soc., Chem. Commun.* **1981**, 867.
- (154) Jeffery, J. C.; Mead, K. A.; Razay, H.; Stone, F. G. A.; Went, M. J.; Woodward, P. *J. Chem. Soc., Dalton Trans.* **1984**, 1383.
- (155) Green, M.; Howard, J. A. K.; Porter, S. J.; Stone, F. G. A.; Tyler, D. C. *J. Chem. Soc., Dalton Trans.* **1984**, 2553.
- (156) Byrne, P. G.; Ester-Garcia, M.; Jeffery, J. C.; Sherwood, P.; Stone, F. G. A. *J. Chem. Soc., Chem. Commun.* **1987**, 53.
- (157) Garcia, M. E.; Jeffery, J. C.; Sherwood, P.; Stone, F. G. A. *J. Chem. Soc., Dalton Trans.* **1988**, 2431.
- (158) Hein, J.; Jeffery, J. C.; Sherwood, P.; Stone, F. G. A. *J. Chem. Soc., Dalton Trans.* **1987**, 2211.
- (159) Hart, I. J.; Jeffery, J. C.; Grosse-Ophoff, M. J.; Stone, F. G. A. *J. Chem. Soc., Dalton Trans.* **1988**, 1867.
- (160) Hart, I. J.; Stone, F. G. A. *J. Chem. Soc., Dalton Trans.* **1988**, 1899.
- (161) Delgado, E.; Garcia, M. E.; Jeffery, J. C.; Sherwood, P.; Lowry, R. M.; Stone, F. G. A. *J. Chem. Soc., Dalton Trans.* **1988**, 207.
- (162) Hein, J.; Jeffery, J. C.; Marken, F.; Stone, F. G. A. *Polyhedron* **1987**, *6*, 2067.

- (163) Ozawa, F.; Park, J. W.; Mackenzie, P. B.; Schaefer, W. P.; Henling, L. M.; Grubbs, R. H. *J. Am. Chem. Soc.* **1989**, *111*, 1319.
- (164) Trepanier, S. J.; Sterenberg, B. T.; McDonald, R.; Cowie, M. *J. Am. Chem. Soc.* **1999**, *121*, 2613.
- (165) Trepanier, S. J.; Dennett, J. N. L.; Sterenberg, B. T.; McDonald, R.; Cowie, M. *J. Am. Chem. Soc.* **2004**, *126*, 8046.
- (166) Cowie, M. *Can. J. Chem.* **2005**, *83*, 1043.
- (167) Dell'Anna, M. M.; Trepanier, S. J.; McDonald, R.; Cowie, M. *Organometallics* **2001**, *20*, 88.
- (168) Rowsell, B. D.; Trepanier, S. J.; Lam, R.; McDonald, R.; Cowie, M. *Organometallics* **2002**, *21*, 3228.
- (169) Jeffery, J. C.; Moore, I.; Razay, H.; Stone, F. G. A. *J. Chem. Soc., Dalton Trans.* **1984**, 1581.
- (170) Gracey, B. P.; Knox, S. A. R.; Macpherson, K. A.; Orpen, A. G.; Stobart, S. R. *J. Organomet. Chem.* **1984**, *272*, C45.
- (171) Gracey, B. P.; Knox, S. A. R.; Macpherson, K. A.; Orpen, A. G.; Stobart, S. R. *J. Chem. Soc., Dalton Trans.* **1985**, 1935.
- (172) Chetcuti, M. J.; Grant, B. E.; Fanwick, P. E. *Organometallics* **1990**, *9*, 1345.
- (173) Chetcuti, M. J.; Grant, B. E.; Fanwick, P. E. *Organometallics* **1991**, *10*, 3003.
- (174) Rowsell, B. D.; McDonald, R.; Ferguson, M. J.; Cowie, M. *Organometallics* **2003**, *22*, 2944.
- (175) Wigginton, J. R.; Chokshi, A.; Graham, T. W.; McDonald, R.; Ferguson, M. J.; Cowie, M. *Organometallics* **2005**, *24*, 6398.
- (176) Girard, L.; Baird, M. C.; Chetcuti, M. J.; McGlinchey, M. J. *J. Organomet. Chem.* **1994**, *478*, 179.
- (177) Chokshi, A.; Rowsell, B. D.; Trepanier, S. J.; Ferguson, M. J.; Cowie, M.; Calhorda, M. J. *Organometallics* **2004**, *23*, 4759.
- (178) Wang, L.-S.; Cowie, M. *Organometallics* **1995**, *14*, 2374.
- (179) Azar, M. C.; Chetcuti, M. J.; Eigenbrot, C.; Green, K. A. *J. Am. Chem. Soc.* **1985**, *107*, 7209.
- (180) Chetcuti, M. J.; Eigenbrot, C.; Green, K. A. *Organometallics* **1987**, *6*, 2298.
- (181) Chetcuti, M. J.; McDonald, S. R. *Organometallics* **2002**, *21*, 3162.
- (182) Chetcuti, M. J.; Green, K. A. *Organometallics* **1988**, *7*, 2450.
- (183) Chetcuti, M. J.; Grant, P. E.; Fanwick, P. E.; Geselbracht, M. J.; Stacy, A. M. *Organometallics* **1990**, *9*, 1343.
- (184) Dennett, J. N. L.; Knox, S. A. R.; Anderson, K. M.; Charmant, J. P. H.; Orpen, A. G. *Dalton Trans.* **2005**, 63.
- (185) Fontaine, X. L. R.; Jacobsen, G. B.; Shaw, B. L.; Thornton-Pett, M. *J. Chem. Soc., Chem. Commun.* **1987**, 662.
- (186) Fontaine, X. L. R.; Jacobsen, G. B.; Shaw, B. L.; Thornton-Pett, M. *J. Chem. Soc., Dalton Trans.* **1988**, 741.
- (187) Muller, F.; van Koten, G.; Kraakman, M. J. A.; Vrieze, K.; Heijdenryk, D.; Zoutberg, M. C. *Organometallics* **1989**, *8*, 1331.
- (188) Kraakman, M. J. A.; de Koning, T. C.; de Lange, P. P. M.; Vrieze, K.; Kooijman, H.; Spek, A. L. *Inorg. Chim. Acta* **1993**, *203*, 145.
- (189) Tsutsuminai, S.; Komine, N.; Hirano, M.; Komiya, S. *Organometallics* **2004**, *23*, 44.
- (190) Knorr, M.; Strohmman, C.; Braunstein, P. *Organometallics* **1996**, *15*, 5653.
- (191) Antwi-Nsiah, F. H.; Oke, O.; Cowie, M. *Organometallics* **1996**, *15*, 506.
- (192) Casey, C. P.; Palermo, R. E.; Jordan, R. F.; Rheingold, A. L. *J. Am. Chem. Soc.* **1985**, *107*, 4597.
- (193) Hong, F.-E.; Lue, I.-R.; Lo, S.-C.; Lin, C.-C. *J. Organomet. Chem.* **1995**, *495*, 97.
- (194) Davies, J. E.; Mays, M. J.; Raithby, P. R.; Sarveswaran, K.; Shields, G. P. *J. Organomet. Chem.* **1999**, *573*, 180.
- (195) Davies, J. E.; Mays, M. J.; Raithby, P. R.; Sarveswaran, K.; Solan, G. A. *J. Chem. Soc., Dalton Trans.* **2000**, 3331.
- (196) Davies, J. E.; Mays, M. J.; Raithby, P. R.; Sarveswarana, K.; Solan, G. A. *J. Chem. Soc., Dalton Trans.* **2001**, 1269.
- (197) Davies, J. E.; Mays, M. J.; Raithby, P. R.; Sarveswaran, K.; Solan, G. A. *Chem. Commun.* **2000**, 1313.
- (198) Muller, F.; van Koten, G.; Kraakman, M. J. A.; Vrieze, K.; Zoet, R.; Duineveld, D.; Heijdenryk, D.; Stam, C. H.; Zoutberg, M. C. *Organometallics* **1989**, *8*, 982.
- (199) Elsevier, C. J.; Muller, F.; Vrieze, K.; Zoet, R. *New J. Chem.* **1988**, *12*, 571.
- (200) Dossett, S. J.; Hart, I. J.; Pilotti, M. U.; Stone, F. G. A. *J. Chem. Soc., Dalton Trans.* **1991**, 511.
- (201) Adams, R. D.; Huang, M. *Organometallics* **1995**, *14*, 2887.
- (202) Jeffery, J. C.; Parrott, M. J.; Stone, F. G. A. *J. Chem. Soc., Dalton Trans.* **1988**, 3017.
- (203) Rutherford, D. T.; Christie, S. D. R. *Tetrahedron Lett.* **1998**, *39*, 9805.
- (204) Fletcher, A. J.; Rutherford, D. T.; Christie, S. D. R. *Synlett* **2000**, 1040.
- (205) Rios, R.; Pericàs, M. A.; Moyano, A.; Maestro, M. A.; Mahía, J. *Org. Lett.* **2002**, *4*, 1205.
- (206) Rios, R.; Pericàs, M. A.; Moyano, A. *Tetrahedron Lett.* **2002**, *43*, 4903.
- (207) Rios, R.; Paredes, S.; Pericàs, M. A.; Moyano, A. *J. Organomet. Chem.* **2005**, *690*, 358.
- (208) Dennett, J. N. L.; Jacke, J.; Nilsson, G.; Rosborough, A.; Ferguson, M. J.; Wang, M.; McDonald, R.; Takats, J. *Organometallics* **2004**, *23*, 4478.
- (209) Fontaine, X. L. R.; Jacobsen, G. B.; Shaw, B. L.; Thornton-Pett, M. *J. Chem. Soc., Dalton Trans.* **1988**, 1185.
- (210) Kalck, P.; Serra, C.; Mached, C.; Broussier, R.; Gautheron, B.; Delmas, G.; Trouvé, G.; Kubicki, M. *Organometallics* **1993**, *12*, 1021.
- (211) Braunstein, P.; Cossy, J.; Knorr, M.; Strohmman, C.; Vogel, P. *New J. Chem.* **1999**, *23*, 1215.
- (212) Beers, O. C. P.; Elsevier, C. J.; Smeets, W. J. J.; Spek, A. L. *Organometallics* **1993**, *12*, 3199.
- (213) Braunstein, P.; Chetcuti, M. J.; Welter, R. *Chem. Commun.* **2001**, 2508.
- (214) Chetcuti, M. J., Braunstein, P. Unpublished results.
- (215) Chetcuti, M. J.; Fanwick, P. E.; McDonald, S. R.; Rath, N. N. *Organometallics* **1991**, *10*, 1551.
- (216) Chisholm, M. H.; Rankel, L. A.; Bailey, W. I. J.; Cotton, F. A.; Murillo, C. A. *J. Am. Chem. Soc.* **1977**, *99*, 1261.
- (217) Bailey, W. I. J.; Chisholm, M. H.; Cotton, F. A.; Murillo, C. A.; Rankel, L. A. *J. Am. Chem. Soc.* **1978**, *100*, 802.
- (218) Baranger, A. M.; Bergman, R. G. *J. Am. Chem. Soc.* **1994**, *116*, 3822.
- (219) Willis, R. R.; Calligaris, M.; Faleschini, P.; Gallucci, J. C.; Wojcicki, A. *J. Organomet. Chem.* **2000**, *593–594*, 465.
- (220) Wang, B.; Li, R.; Sun, J.; Chen, J. *Chem. Commun.* **1998**, 631.
- (221) Xiaon, N.; Zhang, S.; Qiu, Z.; Li, R.; Wang, B.; Xu, Q.; Sun, J.; Chen, J.; Rager, M. N. *Organometallics* **2002**, *21*, 3709.
- (222) Gade, L. H.; Memmler, H.; Kauper, U.; Schneider, A.; Fabre, S.; Bezougli, I.; Lutz, M.; Galka, C. H.; Scowen, I. J.; McPartlin, M. *Chem.—Eur. J.* **2000**, *6*, 692.
- (223) Kondratenko, M.; El Hafa, H.; Gruselle, M.; Vaissermann, J.; Jaouen, G.; McGlinchey, M. J. *J. Am. Chem. Soc.* **1995**, *117*, 6907.
- (224) Sterenberg, B. T.; Hiltz, R. W.; Moro, G.; McDonald, R.; Cowie, M. *J. Am. Chem. Soc.* **1995**, *117*, 245.
- (225) George, D. S. A.; Hiltz, R. W.; McDonald, R.; Cowie, M. *Organometallics* **1999**, *18*, 5330.
- (226) Ferguson, G. S.; Wolczanski, P. T. *J. Am. Chem. Soc.* **1986**, *108*, 8293.
- (227) Ferguson, G. S.; Wolczanski, P. T.; Parkanyi, L.; Zonneville, M. C. *Organometallics* **1988**, *7*, 1967.
- (228) Willis, R. R.; Shuchart, C. E.; Wojcicki, A.; Rheingold, A. L.; Haggerty, B. S. *Organometallics* **2000**, *19*, 3179.
- (229) Wigginton, J. R.; Trepanier, S. J.; McDonald, R.; Ferguson, M. J.; Cowie, M. *Organometallics* **2005**, *24*, 6194.
- (230) Jacobsen, E. N.; Goldberg, K. I.; Bergman, R. J. *J. Am. Chem. Soc.* **1988**, *110*, 3706.
- (231) Werner, H.; Garcia Alonso, F. J.; Otto, H.; Peters, K.; von Schnering, H. G. *Chem. Ber.* **1988**, *121*, 1565.
- (232) Chetcuti, M. J.; Gordon, J. C.; Green, K. A.; Fanwick, P. E.; Morgenstern, D. *Organometallics* **1989**, *8*, 1790.
- (233) Acum, G. A.; Mays, M. J.; Raithby, P. R.; Solan, G. A. *J. Organomet. Chem.* **1995**, *492*, 65.
- (234) Wang, L.-S.; Cowie, M. *Can. J. Chem.* **1995**, *73*, 1058.
- (235) Blagg, A.; Hutton, A. T.; Pringle, P. G.; Shaw, B. L. *J. Chem. Soc., Dalton Trans.* **1984**, 1815.
- (236) Griffith, C. S.; Koutsantonis, G. A.; Skelton, B. W.; White, A. H. *Angew. Chem. Int. Ed.* **2005**, *43*, 3038.
- (237) Jeffery, J. C.; Moore, I.; Stone, F. G. A. *J. Chem. Soc., Dalton Trans.* **1984**, 1571.
- (238) Xu, C.; Anderson, G. K. *Organometallics* **1996**, *15*, 1760.
- (239) D'Agostino, M. F.; Frampton, C. S.; McGlinchey, M. J. *J. Organomet. Chem.* **1990**, *394*, 145.
- (240) Gruselle, M.; Kondratenko, M. A.; El Amouri, H.; Vaissermann, J. *Organometallics* **1995**, *14*, 5242.
- (241) Kondratenko, M. A.; Malézieux, B.; Gruselle, M.; Bonnet-Delpon, D.; Bégue, J. P. *J. Organomet. Chem.* **1995**, *487*, C15.
- (242) Gruselle, M.; El Hafa, H.; Nikolski, M.; Jaouen, G.; Vaissermann, J.; Li, L.; McGlinchey, M. J. *Organometallics* **1993**, *12*, 4917.
- (243) Dyke, A. F.; Knox, S. A. R.; Morris, N. J.; Naish, P. J. *J. Chem. Soc., Dalton Trans.* **1983**, 1417.
- (244) Shuchart, C. E.; Willis, R. R.; Wojcicki, A.; Rheingold, A. L.; Haggerty, B. S. *Inorg. Chim. Acta* **2000**, *307*, 1.
- (245) George, D. S. A.; McDonald, R.; Cowie, M. *Organometallics* **1998**, *17*, 2553.
- (246) Chetcuti, M. J.; McDonald, S. R. *J. Organomet. Chem.* **2004**, *689*, 1882.
- (247) Bercaw, J. E.; Berry, D. H. Unpublished results.
- (248) Caffyn, A. J. M.; Mays, M. J.; Raithby, P. R. *J. Chem. Soc., Dalton Trans.* **1992**, 515.
- (249) Knorr, M.; Strohmman, C. *Eur. J. Inorg. Chem.* **2000**, 241.
- (250) Knorr, M.; Jourdain, I.; Villafañe, F.; Strohmman, C. *J. Organomet. Chem.* **2005**, *690*, 1456.

- (251) Goldberg, J. E.; Howard, J. A. K.; Müller, H.; Pilotti, M. U.; Stone, F. G. A. *J. Chem. Soc., Dalton Trans.* **1990**, 3055.
- (252) Yasuda, T.; Fukuoka, A.; Hirano, M.; Komiya, S. *Chem. Lett.* **1998**, 29.
- (253) Casey, C. P.; Rutter, E. W., Jr. *J. Am. Chem. Soc.* **1989**, *111*, 8917.
- (254) He, Z.; Plasseraud, L.; Moldes, I.; Dahan, F.; Neibecker, D.; Etienne, M.; Mathieu, R. *Angew. Chem., Int. Ed. Engl.* **1995**, *34*, 916.
- (255) Horton, A. D.; Kembball, A. C.; Mays, M. J. *J. Chem. Soc., Dalton Trans.* **1988**, 2953.
- (256) Hay, C. M.; Horton, A. D.; Mays, M. J.; Raithby, P. R. *Polyhedron* **1988**, *7*, 987.
- (257) Martín, A.; Mays, M. J.; Raithby, P. R.; Solan, G. A. *J. Chem. Soc., Dalton Trans.* **1993**, 1431.
- (258) Immirzi, A.; Musco, A.; Pregnosin, P. S.; Venanzi, L. M. *Angew. Chem., Int. Ed. Engl.* **1980**, *19*, 721.
- (259) Boron, P.; Musco, A.; Venanzi, L. M. *Inorg. Chem.* **1982**, *21*, 4192.
- (260) Horton, A. D.; Mays, M. J.; Raithby, P. R. *J. Chem. Soc., Chem. Commun.* **1985**, 247.
- (261) Shulman, P. M.; Burkhardt, E. D.; Lundquist, E. G.; Pilato, R. S.; Geoffroy, G. L.; Rheingold, A. L. *Organometallics* **1987**, *6*, 101.
- (262) Chaudret, B.; Dahan, F.; Sabo, S. *Organometallics* **1985**, *4*, 1490.
- (263) Rocha, W. R.; De Almeida, W. B. *Organometallics* **1998**, *17*, 1961.
- (264) Oke, O.; McDonald, R.; Cowie, M. *Organometallics* **1999**, *18*, 1629.
- (265) Butts, M. D.; Bergman, R. G. *Organometallics* **1994**, *13*, 2668.
- (266) Doyle, M. J.; Duckworth, T. J.; Manojlovic-Muir, L.; Mays, M. J.; Raithby, P. R.; Robertson, F. J. *J. Chem. Soc., Dalton Trans.* **1992**, 2703.
- (267) Torkelson, J. R.; Oke, O.; Muritu, J.; McDonald, R.; Cowie, M. *Organometallics* **2000**, *19*, 854.
- (268) Ben Laarab, H.; Chaudret, B.; Dahan, F.; Poilblanc, R. *J. Organomet. Chem.* **1987**, *320*, C51.
- (269) Ben Laarab, H.; Chaudret, B.; Delavaux, B.; Dahan, F.; Poilblanc, R.; Taylor, N. J. *New J. Chem.* **1988**, *12*, 435.
- (270) Horton, A. D.; Mays, M. J.; McPartlin, M. *J. Chem. Soc., Chem. Commun.* **1987**, 424.
- (271) Fukuoka, A.; Sugiura, T.; Yasuda, T.; Taguchi, T.; Hirano, M.; Komiya, S. *Chem. Lett.* **1997**, 329.
- (272) Komiya, S.; Yasuda, T.; Fukuoka, A.; Hirano, M. *J. Mol. Catal. A: Chem.* **2000**, *159*, 63.
- (273) Shima, T.; Suzuki, H. *Organometallics* **2000**, *19*, 2420.
- (274) Shima, T.; Suzuki, H. *Organometallics* **2005**, *24*, 3939.
- (275) Bitterwolf, T. E.; Saygh, A. A.; Shade, J. E.; Rheingold, A. L.; Yap, G. P. A.; Lable-Sands, L. M. *Inorg. Chim. Acta* **2000**, *300–302*, 800.
- (276) Alvarez, C.; García, M. E.; Riera, V.; Ruiz, M. A. *Organometallics* **1997**, *16*, 1378.
- (277) Alvarez, M. A.; Garcia, M. E.; Riera, V.; Ruiz, M. A.; Bois, C.; Jeannin, Y. *J. Am. Chem. Soc.* **1993**, *115*, 3786.
- (278) Alvarez, M. A.; Garcia, M. E.; Riera, V.; Ruiz, M. A.; Falvello, L. R.; Bois, C. *Organometallics* **1997**, *16*, 354.
- (279) Garcia, G.; Garcia, M. E.; Melon, S.; Riera, V.; Ruiz, M. A.; Villafañe, F. *Organometallics* **1997**, *16*, 624.
- (280) Riera, V.; Ruiz, M. A.; Villafañe, F.; Bois, C.; Jeannin, Y. *J. Organomet. Chem.* **1989**, *375*, C23.
- (281) Sakaba, H.; Ishida, K.; Horino, H. *Chem. Lett.* **1998**, 149.
- (282) Boese, R.; Huffman, M. A.; Vollhardt, K. P. C. *Angew. Chem., Int. Ed. Engl.* **1991**, *30*, 1463.
- (283) Park, J. W.; Mackenzie, P. B.; Schaefer, W. P.; Grubbs, R. H. *J. Am. Chem. Soc.* **1986**, *108*, 6402.
- (284) Chetcuti, M. J.; McDonald, S. R.; Rath, N. P. *Organometallics* **1989**, *8*, 2077.
- (285) Suzuki, H.; Omori, H.; Dong, H. L.; Yoshida, Y.; Fukushima, M.; Tanaka, M.; Moro-oka, Y. *Organometallics* **1994**, *13*, 1129.
- (286) Poulton, J. T.; Folting, K.; Caulton, K. G. *Organometallics* **1992**, *11*, 1364.
- (287) Albertin, G.; Antoniutti, S.; Bacchi, A.; Bortoluzzi, M.; Pelizzi, G.; Zanardo, G. *Organometallics* **2006**, *25*, 4235.
- (288) Esteruelas, M. A.; Lledós, A.; Maseras, F.; Oliván, M.; Oñate, E.; Tajada, R. M. A.; Tomàs, M. *Organometallics* **2003**, *22*, 2087.
- (289) Equillor, B.; Esteruelas, M. A.; Oliván, M. *Organometallics* **2006**, *25*, 4691.
- (290) Adams, R. D.; Captain, B.; Zhu, L. *J. Am. Chem. Soc.* **2006**, *128*, 13672.
- (291) Yoshikai, N.; Yamanaka, M.; Ojima, I.; Morokuma, K.; Nakamura, E. *Organometallics* **2006**, *25*, 3867.
- (292) Kuramoto, A.; Nakanishi, K.; Kawabata, T.; Komine, N.; Hirano, M.; Komiya, S. *Organometallics* **2006**, *25*, 311.
- (293) Jourdain, I.; Vieille-Petit, L.; Clement, S.; Knorr, M.; Villafañe, F.; Strohmman, C. *Inorg. Chem. Commun.* **2006**, *8*, 127.
- (294) Changamu, E. O.; Friedrich, H. B.; Onani, M. O.; Rademeyer, M. J. *Organomet. Chem.* **2006**, *691*, 4615.
- (295) Ye, S.; Leong, W. K. *J. Organomet. Chem.* **2006**, *691*, 1216.
- (296) Knorr, M.; Jourdain, I.; Braunstein, P.; Strohmman, C.; Tiripicchio, A.; Ugolozzi, F. *Dalton Trans.* **2006**, 5248.
- (297) Takemoto, S.; Shimadzu, D.; Kamikawa, K.; Matsuzaka, H.; Nomura, R. *Organometallics* **2006**, *25*, 982.
- (298) Yamazaki, S.; Taira, Z.; Yonemura, T.; Deeming, A. J. *Organometallics* **2006**, *25*, 849.
- (299) Man, M. L.; Lam, K. C.; Sit, W. N.; Ng, S. M.; Zhou, Z.; Lin, Z.; Lau, C. P. *Chem.—Eur. J.* **2006**, *12*, 1004.

CR940270Y